

**CHARACTERIZATION OF THE INTERACTION
BETWEEN ACETYLCHOLINESTERASE AND LAMININ:
A TEMPLATE FOR DISCOVERING REDUNDANCY**

CHRISNA SWART

**Dissertation presented for the degree of Doctor of Philosophy in
Medical Sciences (Medical Biochemistry)
at Stellenbosch University**



Project supervisor: Dr Glynis Johnson

March 2012

Declaration

By submitting this dissertation electronically, I declare that the entirety of the work contained therein is my own, original work, that I am the sole author thereof (save to the extent explicitly otherwise stated), that reproduction and publication thereof by Stellenbosch University will not infringe any third party rights and that I have not previously in its entirety or in part submitted it for obtaining any qualification.

Signature:

Date:

"

"

"

"

"

"

"

"

"

"

"

"

"

"

"

Eqr { tki j vÍ "4234"Ugmgpdquej "Wpkxgtukv{

Cm'tki j w'tgugtxgf

Abstract

Apart from its primary function in the synaptic hydrolysis of acetylcholine, acetylcholinesterase (AChE) has been shown through *in vitro* demonstrations to be able to promote various non-cholinergic functions, including cell adhesion and neurite outgrowth, differentiation, and amyloidosis. AChE was also shown to bind to mouse laminin-111 *in vitro* by an electrostatic mechanism. Previous results suggest that the site on AChE recognised by certain monoclonal antibodies (MAbs) might be critical for differentiation. These MAbs were found to inhibit both laminin binding and cell adhesion in neuroblastoma cells. In this study, the structure and characteristics of this site were investigated, using the AChE-laminin interaction as a template as well as a detailed epitope analysis of the MAbs. The interaction sites of AChE and laminin were investigated using phage display, modelling and docking, synthetic peptides, enzyme linked immunosorbent assays (ELISAs) and conformational interaction site mapping. Docking of AChE with the single-chain variable fragments (scFvs) produced from the phage display showed the major recognition motifs to be the ⁹⁰Arg-Glu-Leu-Ser-Glu-Asp motif, the ⁴⁰Pro-Pro-Met-Gly sequence, and the ⁵⁹Val-Val-Asp-Ala-Thr-Thr (human) motif. Mouse AChE was found to interact with the basic structures Val²⁷¹⁸-Arg-Lys-Arg-Leu²⁷²²; Tyr²⁷³⁸-Tyr²⁷³⁹, Tyr²⁷⁸⁹-Ile-Lys-Arg-Lys²⁷⁹³; and Val²⁸¹⁷-Glu-Arg-Lys²⁸²⁰, on the α 1 G4 domain of laminin. ELISAs using synthetic peptides confirmed the involvement of the AG-73 site (2719-2729). This site overlaps with laminin's heparin-binding site. Docking showed the major component of the interaction site on AChE to be the acidic Arg⁹⁰-Glu-Leu-Ser-Glu-Asp⁹⁵ (omega loop), and also involving the Pro⁴⁰-Pro-Val⁴², Arg⁴⁶ (linked to Glu⁹⁴ by a salt bridge) and the hexapeptide Asp⁶¹ Ala-Thr-Thr-Phe-Gln⁶⁶. Epitope analysis showed the MAb's major recognition site to be the sequence Pro⁴⁰-Pro-Met-Gly-Pro-Arg-Arg-Phe⁴⁸ (human AChE). The MAbs also reacted with the proline-rich sequences Pro⁷⁸-Gly-Phe-Glu-Gly-Thr-Glu⁸⁴ and Pro⁸⁸-Asn-Arg-Glu-Leu-Ser-Glu-Asp⁹⁵. These results define the interaction sites involved in the AChE-laminin interaction and suggest that the interaction plays a role in cell adhesion.

Despite the *in vitro* demonstrations of the importance of AChE's non-classical functions, the AChE knockout survives. Results from this study suggest the possibility of functional redundancy between AChE and other molecules in early development. Using these *in vitro* findings that AChE is able to bind laminin-111, information on the interaction sites, as well as results from the monoclonal antibody (MAb) epitope analysis, the idea of redundancy was investigated. Docking and bioinformatics techniques were used to investigate structurally similar molecules that have comparable spatiotemporal expression patterns in the embryonic nervous system. AChE has been shown to be involved in the pathogenesis of Alzheimer's disease, thus molecules associated with brain function and neurodegeneration were also investigated. Molecules with which AChE could be possibly redundant are syndecans, glypicans, perlecan, neuroligins and the low-density lipoprotein receptors and their variants. AChE was observed to dock with growth arrest-specific protein 6 (Gas6) as well as apolipoprotein E3 (ApoE-3) at the same site as the laminin interaction. The AChE interaction site was shown to resemble the apolipoprotein-binding site on the low density lipoprotein receptor, and related molecules, including the low density lipoprotein receptor-related molecule (LRP) and the sortilin-related receptor (SORL1). These molecules, along with apoE, are associated with Alzheimer's disease. Resemblances to the triggering receptor on myeloid cells (TREM1) were also suggested; this is interesting as AChE has been implicated in both haematopoiesis and haematopoietic cancers. Coimmunoprecipitation results, applied to investigate alternative ligands for AChE, confirmed the AChE-laminin interaction in neuroblastoma cells, and also suggested the existence of other binding partners.

In conclusion, characterisation of the AChE-laminin interaction sites and investigation of structurally similar sites in other molecules suggests a role for AChE in the stabilization of the basement membrane of developing neural cells and provides a feasible explanation for the survival of the knockout mouse. Furthermore, the demonstrated similarity of the AChE interaction site to sites on molecules, notably the low density lipoprotein receptor family and SORL1 and their apolipoprotein ligands that are implicated in the pathology of Alzheimer's disease, as well as the possible link to haematopoietic differentiation and cancers, warrants further investigation.

Opsomming

Talle *in vitro* studies wys dat die ensiem asetiëlcholinesterase (AChE), behalwe vir sy klassieke rol in die hidrolise van asetiëlcholien (ACh), 'n aantal nie-cholinerge rolle vertolk insluitend in sel adhesie, in die uitgroei van neurietes, in differensiering, asook in amyloidosis. Dit is vooraf gewys dat AChE, met behulp van elektrostatische meganismes, *in vitro* met muis laminin-111 kan bind. Dit word verneem dat die area op AChE wat herken word deur monoklonale teenliggaampies (MAbs), moontlik 'n kritiese area is met betrekking tot differensiasie. Dieselfde MAbs is gevind om beide die laminin-interaksie, sowel as sel adhesie van neuroblastoma selle, te inhibeer. In hierdie projek word die struktuur en eienskappe van die betrokke kritiese areas ondersoek deur die AChE-laminin interaksie te gebruik as sjabloon. 'n Gedetailleerde analise van die teenliggaam epitooop het ook geskied. Met behulp van faag vertoon, modellering en hegting, sintetiese peptiede, ensiem-gekoppelde immunosorbent toetse (ELISAs) en konformasie interaksie area kartering, is die betrokke interaksie areas bestudeer. Hegting van enkel-ketting variërende fragment (scFv) volgordes, verkry vanaf die vaag vertoon, aan AChE dui dat die hoof herkennings motiewe die ⁹⁰Arg-Glu-Leu-Ser-Glu-Asp motief, die ⁴⁰Pro-Pro-Met-Gly volgorde, en die ⁵⁹Val-Val-Asp-Ala-Thr-Thr (mens) motief is. 'n Interaksie tussen muis AChE en die $\alpha 1$ G4 domein van laminin is gevind. Die interaksie betrek die basiese structure: Val²⁷¹⁸-Arg-Lys-Arg-Leu²⁷²²; Tyr²⁷³⁸-Tyr²⁷³⁹, Tyr²⁷⁸⁹-Ile-Lys-Arg-Lys²⁷⁹³; en Val²⁸¹⁷-Glu-Arg-Lys²⁸²⁰. Die betrokkenheid van die AG-73 (2719-2729) area by hierdie interaksie is bevestig met ELISA eksperimente wat sintetiese peptiede inkorporeer. Die AG-73 area oorvleuel die heparin interaksie area op laminin. Hegtings eksperimente wys dat die hoof komponent van die interaksie area op AChE die suur volgorde Arg⁹⁰-Glu-Leu-Ser-Glu-Asp⁹⁵ op die omega-lus is. Die interaksie betrek ook die Pro⁴⁰-Pro-Val⁴², Arg⁴⁶ (gekoppel aan Glu⁹⁴ deur 'n sout-brug) en die heksapeptied Asp⁶¹ Ala-Thr-Thr-Phe-Gln⁶⁶ motiewe. Analise van die MAb epitooop wys die hoof erkennings area as volgorde Pro⁴⁰-Pro-Met-Gly-Pro-Arg-Arg-Phe⁴⁸ (mens AChE). Die MAbs blyk ook gunstig te wees teenoor prolien-ryke volgordes soos Pro⁷⁸-Gly-Phe-Glu-Gly-Thr-

Glu⁸⁴ en Pro⁸⁸-Asn-Arg-Glu-Leu-Ser-Glu-Asp⁹⁵. Die areas betrokke by die AChE-laminin interaksie is dus gedefinieer en 'n moontlike rol vir hierdie interaksie in sel adhesie word voorgestel.

Die noodsaaklikheid van AChE se nie-klassieke funksies word bevraagteken na die oorlewing van die AChE uitklop-muis. Resultate hier dui op die moontlikheid van funksionele oortolligheid as verduideliking hiervan, spesifiek met betrekking tot molekules betrokke in vroeë ontwikkeling asook in die proses van neurale agteruitgang. Deur gebruik te maak van die *in vitro* demonstrasies van die AChE-laminin interaksie, informasie verkry ten opsigte van die betrokke interaksie areas, asook resultate verkry vanaf die monoklonale teenliggaam (MAb) epitooptoonanalise, word die idee van funksionele oortolligheid ondersoek. Hegtings- en bioinformatika-tegnieke is gebruik om molekules met soortgelyke strukture en uitdrukkingspatrone in die embrioniese sensuweestelsels te ondersoek. Ko-immunopresipitasie-tegnieke is gebruik om so moontlike alternatiewe ligande vir AChE te ondersoek. Moontlike funksionele oortolligheid van AChE met die volgende molekules is gevind: syndecan; glypican; perlecan; neuroligin; asook die lae-digtheid lipoproteïen (LDL) reseptore en hul variante. Hegting van AChE met 'growth arrest-specific' proteïen 6 (Gas6) en die apolipoproteïen E3 (apoE3) is gedemonstreer en gevind om dieselfde area as die laminin interaksie te betrek. Die betrokke interaksiearea op AChE het ooreenstemminge met die apolipoproteïen interaksiearea op die LDL reseptor asook met verwante molekules soos die lae-digtheid lipoproteïen reseptor-geassosieerde molekule (LRP) en die sortilin-geassosieerde reseptor (SORL1). Hierdie molekules, insluitend apoE, speel beduidende rolle in die patologie van Alzheimer se siekte. Ooreenkomste tussen AChE en die verwekkingsreseptor op myeloïde selle (TREM1) is ook voorgestel, die interaksie is van belang siende dat AChE voorheen geassosieer is met beide haematopoïese en haematopoïetiese kankers. Ko-immunopresipitasie resultate bevestig die AChE-laminin interaksie en dui op die moontlike teenwoordigheid van alternatiewe ligande vir AChE *in vivo*.

In konklusie, karakterisering van die AChE-laminin interaksie areas, gepaard met identifisering van struktureel ooreenstemmende areas in ander molekules, dui op 'n rol vir AChE in die stabilisering van die basale membraan en verskaf dus 'n geldige verduideliking vir die oorlewing van die AChE uitklop-muis. Die ooreenstemming van die AChE interaksie area met areas op ander molekules (spesifiek geassosieer met Alzheimer se siekte), asook die moontlike assosiasie van AChE met haematopoietiese differensiering en kanker, lê die grondslag vir verdere ondersoeke.

Publications

Part of the work in this thesis has been published:

Johnson G, Swart C, Moore SW (2008). Interaction of acetylcholinesterase with the G4 domain of the laminin alpha1-chain. *Biochem J* **411**: 507-514.

Johnson G, Swart C, Moore SW (2008). Non-enzymatic developmental functions of acetylcholinesterase--the question of redundancy. *FEBS J* **275**: 5129-5138.

Acknowledgements

The studies reported in this thesis would not have been possible without the contribution of many individuals. I am indebted to my promoter, Dr. Glynis Johnson for all the support, encouragement and guidance throughout my post-graduate studies. I am thankful to the University of Stellenbosch and the Department of Biomedical Sciences, along with the head of our department, Prof. Paul Van Helden, for providing the infrastructure and facilities to complete this study. I am forever grateful to Cecil, my family and friends for supporting me and encouraging me during difficult times. I am thankful to my fellow colleagues in the department for always being available when I needed them.

List of Figures

Figure 1	Components of Synaptic neurotransmission	4
Figure 2	Hydrolysis cascade	4
Figure 3	Primary structure of cholinesterases	10
Figure 4	The secondary structure of AChE	11
Figure 5	The 3D structure of TcAChE	12
Figure 6	The active site gorge of AChE	13
Figure 7	Structure of TcAChE	13
Figure 8	Mouse AChE (PDB code 1J06) showing the PAS and associated omega loops	15
Figure 9	AChE isoforms	17
Figure 10	AChE associates with ColQ and PRiMA	20
Figure 11	Alternative splicing of molecular forms of AChE	21
Figure 12	Structures of PAS-binding inhibitors	27
Figure 13	Cell adhesion molecules homologous to AChE	36
Figure 14	The temporal relationship of the developmental expression of AChE and BChE	46
Figure 15	Laminin molecule	59
Figure 16	The structure of mouse AChE molecule (1J06.pdb).	73
Figure 17	Whole molecule binding between AChE and laminin	107
Figure 18	Binding of the controls BSA and IgG to laminin-111	107
Figure 19	The effects of NaCl on the binding of AChE to laminin	108
Figure 20	Effects of AChE inhibitors on AChE-laminin binding	109
Figure 21	Position on mouse AChE (1J06.pdb) of the peptides used in this study	110
Figure 22	AChE peptides binding to laminin	111
Figure 23	Coimmunoprecipitation	112
Figure 24	Sample A: Anti-AChE Ab used for detection	113
Figure 25	Sample A: Anti-laminin Ab used for detection	115
Figure 26	Sample L: Anti-laminin Ab used for detection	116

Figure 27	Sample L: Anti-AChE Ab used for detection	117
Figure 28	Position on mouse AChE (1J06.pdb) of the principle MAb recognition motifs	120
Figure 29	Sequences of clone no.7 and clone no. 21	122
Figure 30	Sequence alignment of clone no. 7 and clone no. 21	122
Figure 31	3D modelling of sequences 7 and 12	124
Figure 32.	Residues on scFv sequence 7 that interact with AChE in the docking simulations	125
Figure 33	Residues on scFv sequence 21 that interact with AChE in the docking simulations	125
Figure 34	ScFv sequence 7 model docking with AChE (1J06.pdb)	126
Figure 35	ScFv sequence 21 model docking with AChE (1J06.pdb)	126
Figure 36	AChE structure (1J06.pdb) showing the position of the Arg 46-Glu 94 salt bridge	133
Figure 37	Comparison of mouse and human AChE (residues 40-96), <i>Torpedo</i> AChE (residues 38-94), and the human BChE sequence (residues 36-92)	134
Figure 38	Sequence alignment of laminin $\alpha 1$ and $\alpha 2$	139
Figure 39	Docking of mouse AChE (1J06.pdb) with mouse laminin $\alpha 2$ G4 and G5 domains (1DYK.pdb)	140
Figure 40	The G4 and G5 domains of the laminin molecule showing the AG-73 interaction site	141
Figure 41	Binding of AChE to the AG-73 laminin peptide	142
Figure 42	Effects of NaCl on AChE-AG-73 binding	143
Figure 43	Effects of AChE inhibitors on AChE binding to AG-73	143
Figure 44	Competition between AChE and heparan sulfate for binding laminin-111	144
Figure 45	Docking of AChE (PDB code 1J06) and laminin (PDB code 2JD4)	147
Figure 46	Sequence alignment of neuroligins 1-4, AChE and BChE	154
Figure 47	Docking of AChE with Gas6	156

Figure 48	Docking of AChE with apolipoprotein E3	157
------------------	---	------------

List of Tables

Table 1	Comparison of AChE and BChE	32
Table 2	Peptide sequences	76
Table 3	Grouping of the antibody clones based on their amino acid sequences	121
Table 4	BLAST results for sequence no. 7	127
Table 5	BLAST results for sequence no. 21	128
Table 6	Sequence 21 BLAST-hits	129
Table 7	ScFv control BLAST	130
Table 8	ScFv antigen alignments with AChE	131
Table 9	Recognition of motifs by MAb	134
Table 10	HSPGs in the developing nervous system	150

List of Abbreviations

%	percentage
°C	degrees Celsius
3D	three dimensional
μ	micro
Å	angstrom
Aβ	beta amyloid
Ab	antibody
ABTS	2,2'-azino-bis(3-ethylbenzothiazoline-6-sulphonic acid)
ACh	acetylcholine
AChE	acetylcholinesterase
AChR	acetylcholine-receptor
AD	Alzheimer's disease
A-form	asymmetric-form
Ag	antigen
AML	acute myeloid leukemia
AMP	dibutyl cyclic-adenosine monophosphate
Apo (-A, -E, -J)	apolipoprotein (-A, -E, -J)
APP	amyloid precursor protein
ASG	active site gorge
ATP	adenosine triphosphate
BACE	β-secretase
BCh	butyrylcholine
BChE	butyrylcholinesterase
BLAST	basic local alignment search tool
BM	basement membrane
BNHS	biotin (long-arm) N Hydroxysuccinimide ester
BW284c51	1,5 bis [4-allyldimethyl ammonium

	phenyl] pentane-3-one dibromide
Ca ²⁺	calcium
CAM	cell adhesion molecule
CAS	catalytic anionic subsite
Cdc2	cell division control protein 2
CDR	complimentary determining region
CH	constant heavy domain
ChAT	choline acetyltransferase
ChE	cholinesterase
CJD	Creutzfeldt-Jacob disease
CL	constant light domain
CLAM	cholinesterase domain protein
CLiPS™	Chemically Linked Peptides on Scaffolds
CNS	central nervous system
CO ₂	carbon dioxide
Co-IP	coimmunoprecipitation
ColQ	acetylcholinesterase-associated collagen
CRAC	cholesterol recognition amino acid consensus
CsCl	caesium chloride
C-terminal	At the COOH-terminus of the protein
C-terminus	COOH-terminus of the protein
dH ₂ O	distilled water
DMF	dimethylformamide
DMSO	dimethyl sulfoxide
DNA	deoxyribonucleic acid
DRG	dorsal root ganglion
DS	Down's syndrome
DTT	dithiothreitol
ECM	extracellular matrix
E.coli	Escherichia coli

EDTA	ethylenediaminetetraacetic acid
EEG	electroencephalogram
ELISA	enzyme-linked immunosorbent assay
EMEM	Eagle's Minimum Essential Medium
Ep-tube	Eppendorf tube
FCS	fetal calf serum
FGF	fibroblast growth factor
FGFR	fibroblast growth factor receptor
g	gram
G4/5	globular domain 4/5
GAG	glycosaminoglycan
Gas6	growth arrest-specific protein 6
GF	growth factor
G-form	globular-form
GPCR	G-protein coupled receptor
GPI	glycophosphatidylinositol
G-protein	guanine nucleotide-binding proteins
GTP	guanosine triphosphate
HCl	hydrogen chloride
HDL	high density lipoprotein
H ₂ O	water
H ₂ O ₂	hydrogen peroxide
HPLC	high-performance liquid chromatography
HS	heparan sulfate
HSP70	70 kilodalton heat shock protein
HSPG	heparan sulfate proteoglycan
IgG	immunoglobulin
IKACh	inward-rectifying potassium channel
IL (-1, -2)	interleukin (-1, -2)
IPTG	isopropyl-beta-D-thiogalactopyranoside

Iso-OMPA	tetraisopropylpyrophosphoramidate
KCl	potassium chloride
kDa	kilo Dalton
KH ₂ PO ₄	potassium dihydrogen phosphate
K ₂ HPO ₄	potassium hydrogen phosphate
L	liter
LB	Luria-Bertani bacterial growing medium
LB agar	Luria-Bertani bacterial growth agarose
LDL	low density lipoprotein
LDLR	low density lipoprotein repeats
LG (-4, -5)	laminin globular domain (-4, -5)
M	molar
mM	millimolar
MAb	monoclonal antibody
mAChR	muscarinic acetylcholine receptor
MDS	myelodysplastic syndrome
mg	milligram
Mg ²⁺	magnesium
MgSO ₄	magnesium sulfate
min	minutes
ml	milliliter
mRNA	messenger ribonucleic acid
m/v	mass/volume
MuSK	muscle specific kinase
N2α	neuroblastoma cells
nAChR	nicotinic acetylcholine receptor
NaCl	sodium chloride
NaF	sodium fluoride
NaHCO ₃	sodium bicarbonate
Na ₂ HPO ₄	sodium monohydrogen phosphate
NaN ₃	sodium azide

NaOH	sodium hydroxide
Na ₃ VO ₄	sodium vanadate
NCBI	National Centre for Biotechnology Information
ng	nanogram
NL (-1, -2)	neuroligin (-1, -2)
N-linked	nitrogen-linked
nM	nanomolar
NMJ	neuromuscular junction
NMR	nuclear magnetic resonance
N-terminal	at the NH ₂ -terminus of a protein
N-terminus	NH ₂ terminus of a protein
OD	optical density
PAS	peripheral anionic site
PAGE	polyacrylamide gel electrophoresis
PBS	phosphate buffered saline
PCR	polymerase chain reaction
PD	Parkinson's disease
PDB-code	proteindatabase-code
PEG	polyethylene glycol
PG	proteoglycan
pH	potentia hydrogenii
pI	isoelectric point
pmol	picomol
PMSF	phenylmethanesulfonylfluoride
PnO	pontine reticular formation
PRAD	proline-rich attachment domains
PRiMA	proline-rich membrane anchor
PrP	prion protein
PS	peptide sequence
RAP	receptor-associated protein

RBC	red blood cell
REM	rapid eye movement
rHuAChE	recombinant human accetylcholinesterase
RNA	ribonucleic acid
rpm	rotations per minute
RT	room temperature
SDS	sodium dodecyl sulfate
ScFv	single chain variable fragment
sec	seconds
SORL1	sortilin-related receptor
SOS	Son of Sevenless protein
TBS	Tris-buffered saline
<i>Tc</i>	<i>Torpedo</i>
TEMED	N,N,N',N' – tetramethylethylenediamine
TM	transmembrane
TMB	3,3',5,5' tetramethylbenzidine liquid substrate system for membranes
Tris-HCl	Tris-hydrogen chloride
v/v	volume/volume
VAcHT	vesicular acetylcholine transporter
VH	variable heavy domain
VL	variable light domain
Vps110	vacuolar protein sorting-10
w/w	mass/mass
Wnt	wingless-type murine-mammary-tumour virus integrated site

Table of contents

Declaration	II
Abstract	III
Opsomming	V
Publications	VIII
Acknowledgements	IX
List of Figures	X
List of Tables	XII
List of Abbreviations	XIII
Table of contents	XIX
Declaration	II
Abstract	III
Opsomming	V
Publications	VIII
Acknowledgements	IX
List of Figures	X
List of Tables	XII
List of Abbreviations	XIII
Table of contents	XIX

1. Introduction and Literature Review	1
1.1 Historical Aspects	1
1.2 The Cholinergic System.....	2
1.2.1 Components and Neurotransmission	2
1.2.2 Acetylcholine Receptors	5
1.3 Acetylcholinesterase	6
1.3.1 Evolution, Phylogeny and Distribution.....	6
1.3.2 AChE Structure.....	7
1.3.2.1 Gene and Transcription.....	7
1.3.2.2 Gene Expression and Activation.....	8
1.3.2.3 Primary, Secondary and Tertiary Structure	9
1.3.2.3 Quaternary Structure	16
1.3.2.4 Post Translational Modifications	18
1.3.2.4.1 Anchorage of AChE in the basal lamina and cell membrane	22
1.3.3 Catalysis in AChE.....	23
1.3.4 Inhibitors	26
1.4 Butyrylcholinesterase.....	29
1.5 Cholinesterase-Domain Proteins (CLAMS)	33
1.6 Non-Classical Role for AChE.....	36
1.6.1 Indications of Alternative Functions.....	36
1.6.1.1 The non-neuronal cholinergic system and non-classical distribution of ACh and AChE	37
1.6.2 Non-classical Functions Related to Development and Differentiation.....	43

1.6.2.1 Neurogenesis.....	43
1.6.2.2 Developmental Expression of Acetylcholinesterase.....	45
1.6.2.3 Cell Adhesion.....	46
1.6.2.4 Neuritogenesis.....	47
1.6.2.5 AChE complexation and the identification of potential AChE ligands....	51
1.6.2.6 The role of electrostatics in AChE-mediated cell adhesion and neurite outgrowth	52
1.6.3 Non-Classical Role in Degeneration.....	52
1.6.3.1 Amyloid & Fibril Formation.....	53
1.6.3.2 Acetylcholinesterase and Neurodegenerative Disorders: Alzheimer’s Disease	54
1.6.4 Acetylcholinesterase and Cancer	56
1.7 The Basement Membrane: Importance of Laminin	58
1.8 Work leading up to the thesis.....	60
1.8.1 Non-Classical AChE Binding Partners and Binding Sites	60
1.8.1 The AChE Knockout and Functional Redundancy.....	61
1.9 Aims of the Thesis	63
2. Materials and Methods	65
2.1 Materials	65
2.1.1 Instruments.....	65
2.1.2 Reagents/Chemicals.....	66
2.1.3 Consumables	69
2.1.4 Proteins	70
2.1.5 Primary antibodies	70
2.1.6 Secondary antibodies	70
2.1.7 Kits.....	70
2.1.8 Antibodies	71
2.1.9 Biotinylation	73
2.1.10 General buffers and solutions	74
2.2 Methods.....	75
2.2.1 ELISA	75
2.2.2 Phage display	79
2.2.2.1 Affinity selection	84
2.2.2.2 Micropanning.....	89
2.2.2.3 Antibody phage display	90
2.2.3 Peptide array/microarray.....	92
2.2.4 Bioinformatics.....	93
2.2.4.1 Homology modelling	93
2.2.4.2 Protein-protein docking	94
2.2.4.3 Identification of Motifs.....	95
2.2.4.4 Other Bioinformatics Methods	96
2.2.5 Coimmunoprecipitation	97
2.2.5.1 Cell culturing	98

2.2.5.2 Coimmunoprecipitation	99
2.2.5.3 SDS-PAGE	101
2.2.5.4 Western blotting.....	103
3. Results	106
3.1 Demonstrating the interaction between AChE and laminin-111	106
3.1.1 Whole molecule binding: ELISA.....	106
3.1.2 AChE peptides binding to laminin: ELISA	109
3.1.3 Demonstration of the interaction between AChE and laminin: Co-IP	111
3.2 Definition and characterization of the binding sites involved in the AChE-laminin interaction	119
3.2.1 Phage display using peptide libraries.....	119
3.2.2 Phage display using antibody libraries	120
3.2.3 Conformational epitope mapping of adhesion-inhibiting anti-AChE MAb: Peptide Arrays.....	132
3.2.4 Identification of potential binding sites on laminin α 1 through sequence analysis.....	136
3.2.5 Docking with laminin α 2, and identification of AG-73 as likely site.....	138
3.2.5 In vitro binding of the PAS of AChE to AG-73	140
3.2.7 AChE competing with heparan sulfate for binding to laminin-111 and AG-73	144
3.2.8 Docking of AChE and laminin α 1: Identification of interaction sites on both AChE and laminin.....	145
3.3 Functional Redundancy	148
3.3.1 In neural development.....	148
3.3.1.1 Clues from the laminin site.....	148
3.3.1.2 Clues from the AChE site	152
3.3.1.2.1 Homologous proteins	152
3.3.1.2.2 Searches for similar motifs in other proteins	154
3.3.1.2.3 The LDL receptor pentapeptide DGSDE.....	156
3.3.2 Potentially redundant molecules in Neurodegeneration: Alzheimer's disease	158
3.3.2.1 Searches for the ELSEED motif.....	158
3.3.2.2 Searches for the DGSDE motif.....	159
4. Discussion	162
4.1 Defining the interaction between AChE and laminin.....	165
4.2 The question of redundancy.....	171
4.3 Conclusions.....	178
5. Bibliography	180

1. Introduction and Literature Review

1.1 Historical Aspects

As early as the 1900s scientists already had a clear idea of the human nervous system and how it works. They identified that individual cells called neurons form the basis of this system and that these cells communicate with one another via electrical messengers. The mechanisms underlying the travelling of these messengers between two adjacent cells, however, were still unknown (Dellon & Dellon, 1993; Moreno & Tharp, 2007; Changeux & Edelman, 2005). In 1904 a young Cambridge undergraduate, Thomas R. Elliott, proposed that a chemical compound, today called a neurotransmitter, was responsible for carrying the message from one cell to another. Even though Elliott originally postulated that adrenaline might be the substance liberated when the nervous stimulus reaches the periphery, his work intrigued another scientist and friend of his, Henry Dale (Elliott, 1904). Nearly two decades after Elliott's hypothesis, a German scientist, Otto Loewi in collaboration with Dale, went on to identify the compound responsible as acetylcholine (ACh) (Loewi & Navratil, 1926). In 1936, Loewi and Dale were awarded the Nobel Prize in Physiology or Medicine "for *their discoveries relating to the chemical transmission of nerve impulses*" ("The Nobel Prize in Physiology or Medicine 1936". Nobelprize.org. 28 Mar 2011 http://nobelprize.org/nobel_prizes/medicine/laureates/1936/).

Dale had already postulated the existence of cholinesterases (ChEs) back in 1914 (Dale 1914). In 1932, Stedman and colleagues observed that horse serum had a "splitting" effect on ACh. Their experiments demonstrated that there is an enzyme present in the blood-serum of horses which hydrolyses both acetyl- and butyryl-choline. The name "choline-esterase" was suggested for this enzyme (Stedman *et al.*, 1932). Later studies by Mendel and Rudney, however, showed that the serum contained two enzymes capable of hydrolyzing ACh (Mendel & Rudney, 1943). Today the term 'cholinesterase' is used to define a family of enzymes that specifically catalyze the hydrolysis of choline esters. Even though both of the enzymes documented by Mendel and colleagues belong to the class serine hydrolases, they are distinguished by their specificities towards substrates

and inhibitors. The term Acetylcholinesterase (AChE) was assigned to the enzyme capable of hydrolyzing ACh, the smallest member of the choline ester series, faster than any other choline ester. AChE was found primarily in neural synapses and blood; the latter is therefore also known as red blood cell (RBC) or erythrocyte cholinesterase. Similarly, Butyrylcholinesterase (BChE) was defined by its capacity to hydrolyze other choline esters, including the larger BCh, as well. The enzyme commission recommended in 1964 the term AChE (Acetylcholine Acetylhydrolase; EC 3.1.1.7) for a 'true' and 'specific' cholinesterase. The less specific BChE (Acylcholine Acylhydrolase; EC 3.1.1.8), was termed simply "cholinesterase" or "pseudocholinesterase". A 53% identity between AChE and BChE was revealed through sequence analysis indicating a very strong homology between the two enzymes (Schumacher *et al.*, 1986; Lockridge *et al.*, 1987). Mutagenesis of only a few amino acids can convert AChE into a BChE-like enzyme (Harel *et al.*, 1992; Vellom *et al.*, 1993; reviewed in Legay, 2000). In practical terms, such as assays, the two enzymes are distinguished by their reaction with different inhibitors: AChE is specifically inhibited by BW284c51 (1,5-bis [4-allyldimethylammoniumphenyl] pentan-3-one dibromide), and BChE by the organophosphate iso-OMPA (tetra [monoisopropyl] pyrophosphortetramide) (Luo *et al.*, 2006).

1.2 The Cholinergic System

1.2.1 Components and Neurotransmission

The main physiological function of AChE, i.e. the hydrolysis of the neurotransmitter ACh at cholinergic synapses and neuromuscular junctions, is a rapid process occurring within one millisecond after ACh's release. This reaction allows for precise temporal control of muscle contraction (Rosenberry *et al.*, 1975). In the central nervous system, synapses of the basal forebrain and brain stem complexes are all cholinergic, while in the peripheral nervous system, the entire parasympathetic nervous system, all neuromuscular junctions, and the preganglionic neurons of the sympathetic nervous system are also cholinergic. In the peripheral nervous system, ACh has effects that include contraction of

smooth muscles (Hurwitz *et al.*, 1967), dilation of blood vessels (Furgott & Zawadzki, 1990), increased glandular secretions (e.g. Jin *et al.*, 1992), and slowing of heart rate (Loewi & Navratil, 1926).

The molecular components of the cholinergic system include: ACh, the neurotransmitter; choline acetyltransferase (ChAT), the enzyme responsible for ACh synthesis; the acetylcholine receptors (AChR, both muscarinic and nicotinic; see section 1.2.2) which bind ACh and generate the signal, and AChE, the enzyme responsible for the breakdown of ACh, thus controlling the duration of the signal (Figure 1 show the components involved in cholinergic neurotransmission). This system also contains another component called the vesicular acetylcholine transporter (VAChT) which is a neurotransmitter transporter responsible for loading ACh into secretory organelles in neurons making it available for secretion (Erickson & Varoqui, 2000). The action of AChE in hydrolyzing the neurotransmitter is necessary to limit the duration of post-synaptic AChR activation.

Like all neurotransmitters, ACh can elicit either an excitory or inhibitory response, depending on the receptor to which it binds. Even though there is still many unanswered questions on how exactly ACh elicits a nerve impulse, the basic mechanism has been determined. By binding to its target receptor, ACh transfers its chemical signal. It is important that this binding is reversible in order for the nerve impulse to be terminated. It was found that immediately after binding, the ACh molecule is hydrolyzed i.e. breaking the ester bond by addition of H₂O, ending the nerve impulse and hence enabling the two separate compounds, choline and acetate, to form new ACh and the nerve impulse-cascade to continue (Figure 2) (Changeux & Edelstein, 2005).

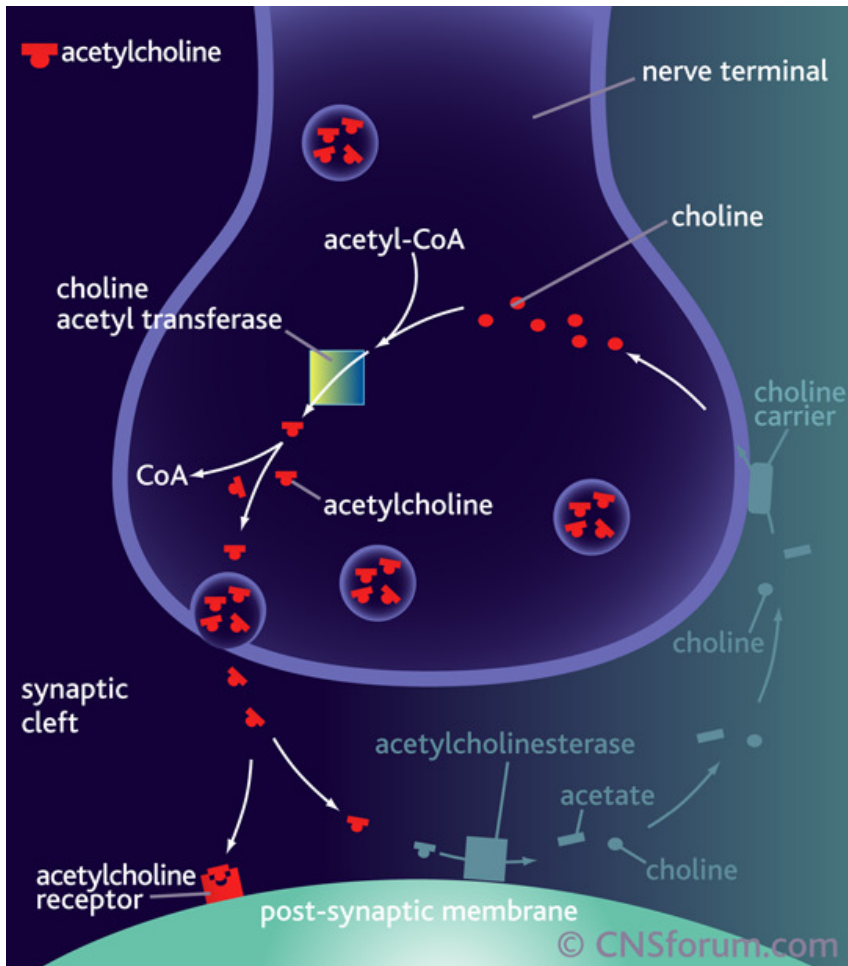


Figure 1. Components of synaptic neurotransmission. (Katzung, 2001; Hardman *et al.*, 2001).

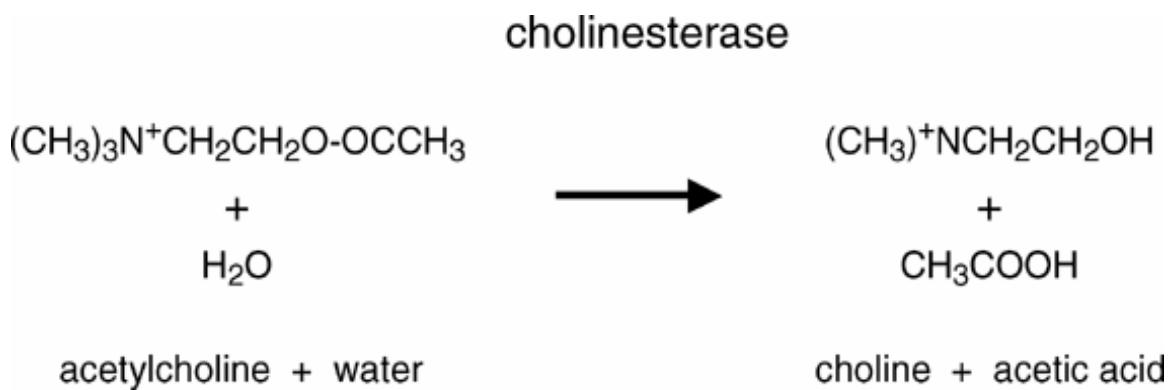


Figure 2. Hydrolysis cascade. AChE catalyses the hydrolysis of ACh (Wilson & Henderson, 2007)

1.2.2 Acetylcholine Receptors

As mentioned above, there are two types of ACh receptors (AChR) that bind ACh and transmit its signal: muscarinic AChRs (mAChRs) and nicotinic AChRs (nAChRs). Muscarinic receptors, primarily abundant in the central nervous system (CNS), are characterised through their interaction with an H₂O soluble toxin derived from a mushroom (*Amanita muscaria*) called muscarin (reviewed in Brann *et al.*, 1993). mAChRs form part of the G-protein coupled receptors (GPCRs), also known as seven transmembrane domain receptors, 7TM receptors, heptahelical receptors, serpentine receptors, and G protein-linked receptors. GPCRs comprise a large and diverse protein family of transmembrane receptors whose primary function is to transduce extracellular stimuli into intracellular signals by using a second messenger cascade system. This system involves the increase of intracellular calcium to transmit signals inside the cells, thus mediating a slow metabolic response (King *et al.*, 2003; Kroeze *et al.*, 2003). Estimates of the exact size of the GPCR superfamily vary. Fredriksson *et al.* (2003) listed over 800 during an analysis of the GPCRs in the human genome. This large-scale systematic phylogenetic analysis included the majority of GPCRs in the human genome and resulted in the classification of GPCRs into five families (*Glutamate*, *Rhodopsin*, *Adhesion*, *Frizzled/Taste 2*, and *Secretin*) (Fredriksson *et al.*, 2003). ACh-receptor binding induces a conformational change within the receptor leading it to associate with the activation of an intracellular G protein. G proteins are composed of three subunits: α , β , and γ . Receptor activation of these protein requires a dual mechanism that involves guanine nucleotide exchange and changes in subunit conformation, and result in G proteins acting as enzymes catalyzing downstream intracellular events (Lee *et al.*, 1992). An inhibitory postsynaptic potential is created where activation of the G protein decreases the probability of postsynaptic neuronal firing (Destexhe & Sejnowski, 1995). mAChRs are involved in a large number of physiological functions in the human body, including contraction of smooth muscles, heart rate and force and the release of neurotransmitters (reviewed in Brann *et al.*, 1993).

Nicotinic receptors (reviewed in Takacs *et al.*, 2001), characterised through their interaction with nicotine in tobacco, function as ligand-gated ion channels mediating fast synaptic transmission of the neurotransmitter by forming pores in the cells plasma membranes. nAChRs can be either neuronal or muscle type. The muscle-type nAChRs are localised at neuromuscular junctions (NMJs) where an electrical impulse from a neuron to a muscle cell signals contraction of the muscle. These muscle tone regulatory functions of these receptors make them targets for muscle relaxants. There are many types of neuronal nAChRs located at synapses between neurons as in the CNS where they are involved in learning and memory, arousal, reward, motor control, analgesia and cognitive function. Once two ACh molecules bound to and activated the receptor, a conformational change occurs resulting in the formation of an ion pore producing a rapid increase in the cellular membrane permeability of sodium and calcium ions. This results in the excitation and depolarisation of the muscle cell producing muscular contraction. The influx of calcium ions affects the release of neurotransmitters. The ACh binding site on the nicotinic receptor is a target for a variety of neurotoxins. These neurotoxins include a family of polypeptides found in certain snake venoms called α -neurotoxins (e.g. erabutoxin) which serve as antagonists for the ACh binding site (reviewed in: Endo & Tamiya, 1987; Menez, 1991). Upon binding to the nAChR, the neurotoxin prevents the binding of ACh which reversibly blocks the opening of the ion channel and formation of a pore preventing cations from passing through. This could result in neuromuscular inhibition of the envenomated species (Karlin, 1993).

1.3 Acetylcholinesterase

1.3.1 Evolution, Phylogeny and Distribution

AChE is a type B carboxylesterase belonging to the α/β hydrolase fold protein superfamily. This group is defined by a common structural homology and the subfamily includes the cholinesterases (EC 3.1.1.7; EC 3.1.1.8), cholinesterase-domain proteins (CLAMS), carboxylesterases (EC 3.1.1.1), non-specific esterase and lipases (EC 3.1.1.3) (Holmquist, 2000). Although many of these proteins show little sequence homology,

conservation of the topology suggests that they diverged from a common ancestor (Ollis *et al.*, 1992). The carboxylesterases and the cholinesterases on the other hand, are sequentially related. The cholinesterases are specialised carboxylesterases and have evolved from carboxylesterases (Shibata *et al.*, 1993). Carboxylesterases are found in eubacteria, protozoans, fungi and metazoans. They are not seen in either plants or archeabacteria (Pezzementi *et al.*, 2010).

AChE is found in vertebrate nervous, muscular and haematopoietic systems and AChE-like enzymes are also found in many invertebrate groups (Grisaru *et al.*, 1999). AChE-like proteins have been reported in algae (Raineri & Modenesi, 1986), *Paramecium* (Corrado *et al.*, 1999), and the slime mould, *Dictyostelium*, where it was found to promote aggregation (Rubino *et al.*, 1989). Examination of these sequences, however, indicates that these enzymes are not true cholinesterases (Johnson *et al.*, unpublished). True cholinesterases, as defined by the presence of the choline-binding site (mammalian numbering: Trp 86, Tyr 133, Glu 202 and Phe 337) (Sussman *et al.*, 1991), are first seen in the nervous tissue of the Platyhelminthes. Cnidarians, which do have primitive nervous systems, do not have cholinesterases. Presumably, the ACh hydrolysis function is accomplished by carboxylesterases in these animals. Observations of AChEs non-neuronal distribution gave rise to the idea that AChE may have other functions apart from its traditional cholinergic role and will be discussed in more depth in sections to follow (see section 1.6).

1.3.2 AChE Structure

1.3.2.1 Gene and Transcription

Through the techniques of fluorescent *in situ* hybridization coupled with selective polymerase chain reaction (PCR), the human AChE gene was found to reside on chromosome 7q22 (Ehrlich *et al.*, 1992). The AChE gene is activated by cholinergic neurotransmission, suggesting a feedback mechanism where neurotransmission possibly leads to increased AChE protein formation as well as accelerated degradation of ACh at

cholinergic synapses (Nitsch *et al.*, 1998). Increased synthesis of ACh leads to increased stimulation of AChR, which leads to increased expression of AChE (Choi *et al.*, 2003). Cholinesterases are synthesized into the endoplasmic reticulum, processed, transported through the secretory pathway, and then targeted to their final destination. The primary translation product contains an N-terminal secretion signal. This is cleaved in the mature protein. The N-terminal signal is followed by a small C-terminal region and the catalytic domain (Massoulié *et al.*, 1999). Early genetic linkage studies suggested that, for the human AChE gene, allelic variants at a single locus exists (Coates & Simpson, 1971). The core of human AChE, common to all variants, consists of 543 amino acids. These amino acids are encoded by exons E2, E3 and E4 of the AChE gene. Exon E1 is a non-coding exon (Soreq *et al.*, 1990). At post-transcriptional level, alternative splicing of the remaining two exons (E5 and E6) give rise to different C-terminal regions generating alternative AChE mRNA species (Li *et al.*, 1993). The different splice variants, together with the association of AChE catalytic subunits with additional domains and proteins, result in an array of oligomeric forms. These oligomeric forms are broadly grouped into globular and asymmetric forms (Massoulié, 2002). The different molecular forms are discussed in more detail in section 1.3.2.3.

1.3.2.2 Gene Expression and Activation

Neurons, hematopoietic cells and muscle cells have been the main focus in unfolding the molecular mechanisms underlying the regulation of AChE gene expression (Angus *et al.*, 2001; Luo *et al.*, 1994; Tung *et al.*, 2004; Soreq & Seidman, 2001). Post-transcriptional regulatory mechanisms seem to play an important role in the induction of AChE expression by stabilizing existing transcripts in all the molecular forms (Chan *et al.*, 1998; Coleman & Taylor, 1996; Deschenes-Furry *et al.*, 2003; Luo *et al.*, 1994). Transcriptional activation of the AChE gene in *Torpedo*, mouse, rat and human have, on the other hand, been reported to be regulated by several regulatory elements within the AChE promoter (Angus *et al.*, 2001; Ben Aziz-Aloya *et al.*, 1993; Chan *et al.*, 1999; Ekstrom *et al.*, 1993; Mutero *et al.*, 1995; Siow *et al.*, 2002). During the differentiation of myoblasts into myotubes, the elevation of intracellular Ca^{2+} seemed to increase AChE

transcript levels. This suggested that transient increases of intracellular Ca^{2+} may be critical for the commitment of AChE expression during myogenesis (Luo *et al.*, 1994). With the use of chick or mouse myotubes expressing promoter-reporter constructs from genes of AChE, the pathway to activation of the AChE gene was shown to involve protein kinase C and once again, intracellular Ca^{2+} . At the neuromuscular junctions of vertebrates, adenosine triphosphate (ATP) is known to stabilize ACh in the synaptic vesicles and is co-released with it. It seems that ATP acts via the ATP receptor to stimulate AChE expression, which is mediated by protein kinase C and intracellular Ca^{2+} release (Choi *et al.*, 2003).

Amyloid precursor protein (APP) was reported to increase AChE activity in p19 embryonic carcinoma and retina cells via a calcium influx mechanism (Melo *et al.*, 2003; Sberna *et al.*, 1997). Apoptosis in various cell types, including non-nervous, non-muscle and non-hematopoietic systems, was found to induce AChE expression, suggesting a novel role for AChE in apoptosis (Zhang *et al.*, 2002). Calcium is an important second messenger and plays significant roles in the modulation of intracellular processes such as apoptosis (Demaurex & Distelhorst, 2003; Groenendyk *et al.*, 2003). Ca^{2+} overload has been suggested as the final pathway of all types of cell death (Rizzuto *et al.*, 2003). Studies show that cytosolic Ca^{2+} plays a key role in AChE regulation during apoptosis (Zhu *et al.*, 2007). It is thus safe to conclude that calcium is an important mediator in the regulation of AChE expression and its role in other processes involving AChE will be discussed in later sections.

1.3.2.3 Primary, Secondary and Tertiary Structure

The primary structure of several cholinesterases is shown in Figure 3. As mentioned above, AChE belongs to the α/β hydrolase fold protein superfamily. These proteins contain a β -sheet internal scaffold of several β -strands supporting an array of helices and loops (Figure 4) (Sussman & Silman, 1992). In addition to the sequence homology, other common features of carboxylesterases and cholinesterases are a Ser-His-Glu catalytic triad (Figure 5), characteristically located at the bottom of a deep gorge, and the so-called

carboxylesterase type B signature 2, the EDCLYLN motif, which surrounds a Cys residue involved in disulphide bonding. The sequence immediately surrounding the active site Ser is conserved in the family, and is described by ProSite pattern PS00122 (carboxylesterase type B serine active site; consensus pattern F-[GR]-G-x(4)-[LIVH]-x-[LIV]-x-G-x-S-[STAG]-G, where the single “S” is the active Ser). The carboxylesterase type B signature 2 is described by ProSite pattern PS00941, [EDA]-[DG]-C-L-[YTF]-[HVT]-[DNS]-[LIV]-[LIVFYW]-x-[PQR] (Sigrist *et al.*, 2010).

		*
T. californica AChE	.(64).PNN C QQY...(91).SED C LYL..(197).FGES S AGG	
Bovine AChE	.(66).QSV C YQY...(93).SED C LYL..(200).FGES S AGA	
Human AChE	.(66).QSV C YQY...(93).SED C LYL..(200).FGES S AGA	
Human BChE	.(62).ANS C CQN...(89).SED C LYL..(195).FGES S AGA	
C. rugosa lipase	.(57).GPS C MQQ...(94).SED C LTI..(206).FGES S AGS	
G. candidum lipase	.(58).SPAC C MQL..(102).NED C LYL..(214).FGES S AGA	
		*
T. californica AChE	(251).NLN CNLNSDEELIH C LR..(324).NKDE G SF	
Bovine AChE	(254).LVG C PPGGAGGNDTELVA C LRA..(331).VKDE G SY	
Human AChE	(254).LVG C PPGGTGGNDTELVA C LRT..(331).VKDE G SY	
Human BChE	(249).LTG CSRENETEII C LRN..(322).NKDE G TA	
C. rugosa lipase	(265).NAG CGSASDKLA C LRG..(338).QNDE G TF	
G. candidum lipase	(273).YAG C ...DTSASANDTLE C LR..(351).QEDE G TA	
		*
T. californica AChE	(399).NV I CPLM..(437).GV I HGYE..(518).VQ M CVFW	
Bovine AChE	(406).NV V CPVA..(444).GV P HGYE..(526).AQ A CAFW	
Human AChE	(406).NV V CPVA..(444).GV P HGYE..(526).AQ A CAFW	
Human BChE	(397).NF I CPAL..(435).GV M HGYE..(517).AQ Q CRFW	
C. rugosa lipase	(414).G F TLARR..(446).G T FHSND..(520).AG Y DALF	
G. candidum lipase	(427).L F QSPRR..(460).G T F H GNE..(531).EG I SNFE	

Figure 3. Primary structure of cholinesterases. The partial α/β hydrolase fold sequences are numbered from the amino terminus of the mature protein. Commonly conserved residues are highlighted in bold and include those of the catalytic triad (marked by asterisks) and the cysteines involved in intra-subunit disulphide bonds (http://www.weizmann.ac.il/sb/faculty_pages/Sussman/kurt/fig6.html).

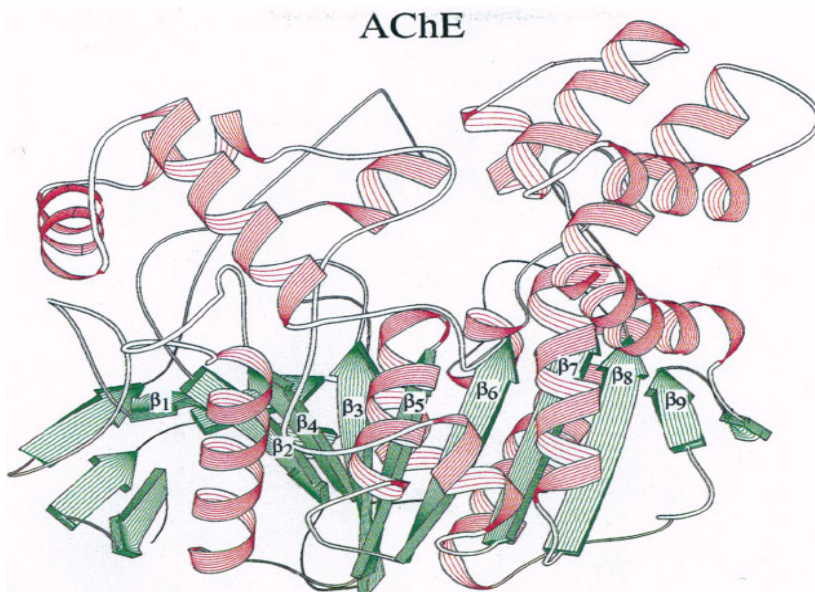


Figure 4. The secondary structure of AChE. The β -sheets are shown in green and the α -helices in red (Ripoll *et al.*, 1992).

AChE itself is a large (~68-kDa) single domain protein containing the characteristic hydrolase fold (Abram *et al.*, 1989; Wasserman *et al.*, 1993). When the crystal structure for *Torpedo californica* (*Tc*) AChE was revealed (Sussman *et al.*, 1991) the active centre was shown to be buried at the bottom of a narrow gorge, about 20Å deep, lined with conserved aromatic residues (Figure 6). This gorge was termed the active site gorge (ASG) and the entire gorge lining as well as its periphery seems to be involved in the catalytic reaction. The ASG is only ~5Å wide at a bottleneck formed by van der Waals surfaces of Tyr 121 and Phe 330 (residue numbers refer to *Tc*AChE sequence). The diameter of the quaternary choline moiety was found to be 6.4Å. It seems that substantial breathing motion of the gorge is required for sufficient substrate and product trafficking (Colletier *et al.*, 2006). Seeing as AChE is one of the most efficient enzymes known, with an impressive turnover number, it might seem counter-intuitive to have the active site located deep within the enzyme. But these structures have been strongly conserved throughout all life forms and thus clearly have a selective advantage. It is likely that the confinement of the substrate in a relatively small space and surrounded almost entirely by the enzyme allows for exact positioning and stabilization (Harel *et al.*, 1996). See section 1.3.3 for details on catalysis.

Several specific subsites have been identified within the gorge; the numbering used corresponds to *TcAChE* numbering followed by mammalian (human and mouse) AChE numbering in brackets (Figures 5 & 7). These sites include the actual active or acylation site (Ser 200 (203), His 440 (447) and Glu 327 (334)), a hydrophobic or choline-binding subsite (also called the anionic site; Trp 84, Phe 330, Tyr 130 and Glu 199 (mammalian: Trp 86, Tyr 337, Tyr 133 and Glu 202)) which binds and stabilizes the choline moiety of the substrate, the acyl pocket (Phe 288 (295) and Phe 290 (297)) and the oxyanion hole (Gly 118 (121), Gly 119 (122), Ala 201 (204)) involved in the stabilization of the substrate transition state (Sussman *et al.*, 1991; Sussman & Silman, 1996; Shafferman *et al.*, 2005). An additional anionic site (the peripheral site or peripheral anionic site (PAS; Tyr 70 (72), Asp 72 (74), Tyr 121 (124), Trp 279 (286) and Tyr 334 (341)) surrounds the rim of the gorge, on the molecule's surface. The PAS is a secondary substrate binding site lying approximately 20Å distant from the active site itself, and binds ACh as the first step in the catalytic pathway (Hosea *et al.*, 1996; Mallender *et al.*, 2000). This site allosterically modulates catalysis and is also the main binding site for specific inhibitory compounds (see section 1.3.4 for details on AChE inhibitors) (Radic *et al.* 1991).

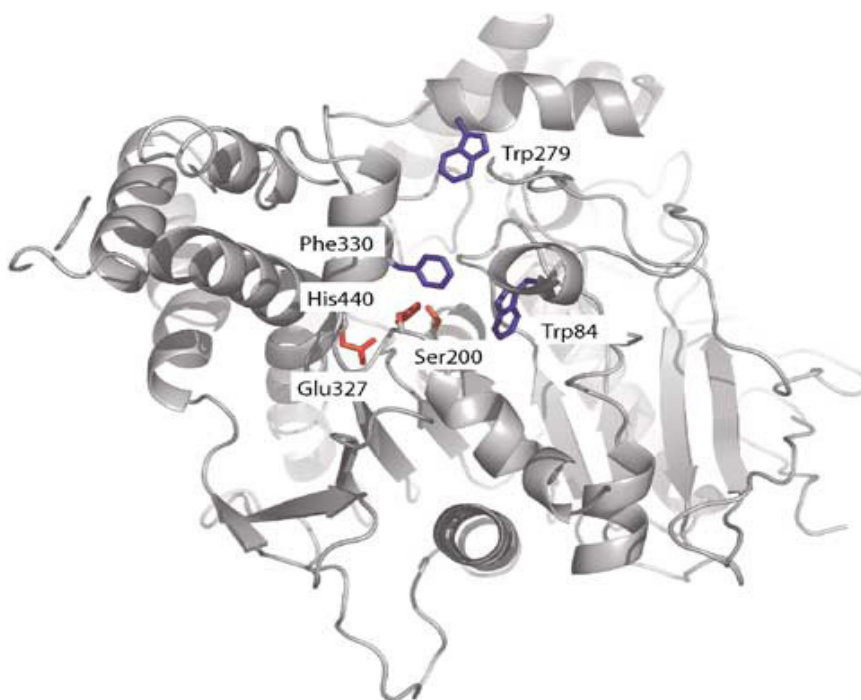


Figure 5. The 3D structure of TcAChE. The catalytic triad is highlighted in red, Trp 84 in the catalytic anionic subsite (CAS; choline binding subsite), Trp 279 at the PAS, and the bottleneck residue Phe 330 in blue (residue numbers refer to *TcAChE*) (Colletier *et al.*, 2006).

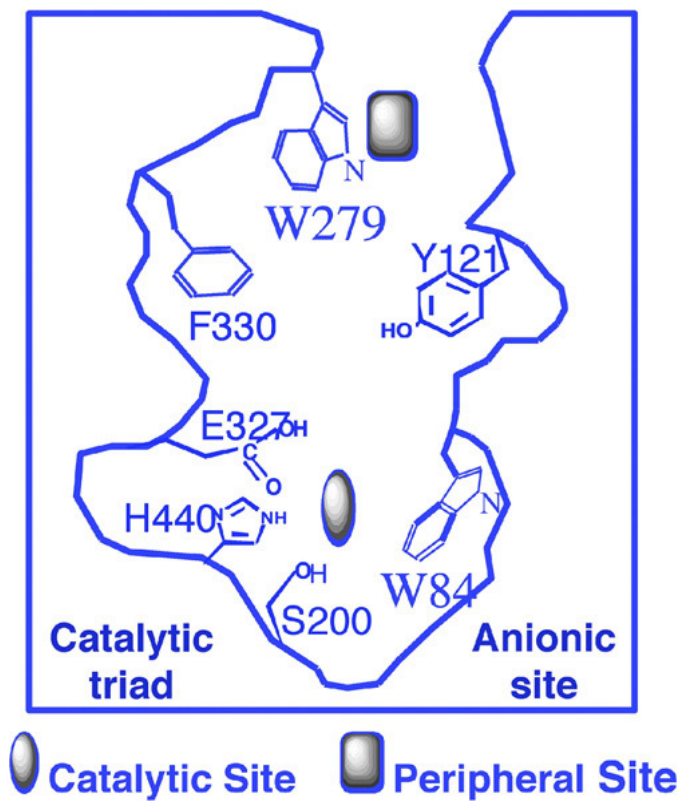


Figure 6. The active site gorge of AChE. A cross-section through the ASG of *TcAChE*, showing the residues involved in the CAS, PAS and the catalytic triad (Silman & Sussman, 2008).

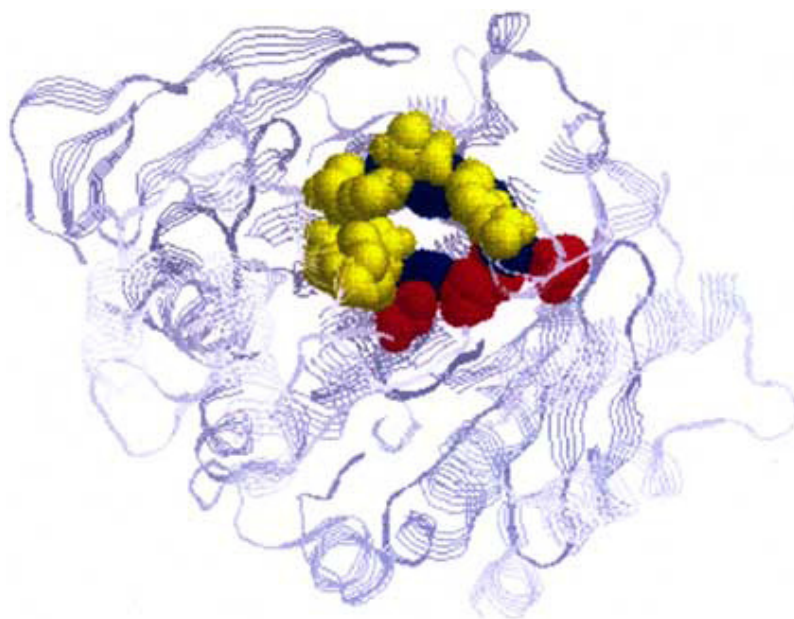


Figure 7. Structure of TcAChE. The different subsites are shown: the active site (in red), the choline-binding site (in blue) and the PAS (in yellow) (Johnson & Moore, 2006).

There are a number of surface loops associated with the PAS (Figure 8) which incorporate several of its residues. The Cys residue (Cys 96), which is part of the carboxylesterase type B signature 2 motif (described above), forms a disulphide bond with Cys 69 (Barak *et al.*, 1995). The residues between them form a large omega loop. Omega loops are non-regular secondary structures found in globular proteins. They are characterized by a polypeptide chain that follows a loop-shaped course in three-dimensional space and are so-called because it forms the shape of the Greek upper-case Ω , with the two Cys residues forming the link at the base (Fetrow, 1995). Structural homology is found between AChE Cys 69-Cys 96 loop and the lid loop that seizes substrate in neutral lipases. This structural element is conserved throughout the esterase/lipase family (Cygler *et al.*, 1993). Two of the PAS residues (Tyr 70 (72) and Asp 72 (74)) lie on the Cys 69-Cys 96 omega loop. Trp 84 (86), the major component of the anionic choline-binding subsite near the base of the gorge, lies on the latter section of this loop. A section of the loop thus runs between the PAS at the rim of the gorge, and the bottom of the gorge, and these residues form part of the gorge lining (Sussman *et al.*, 1991). The high aromatic content of the active site gorge and the PAS specifically is a remarkable feature of AChE and it is the aromatic residues contained within the gorge lining that contributes to its flexibility. It was found that even in the absence of ligand, AChE can assume different conformations (Xu *et al.*, 2008).

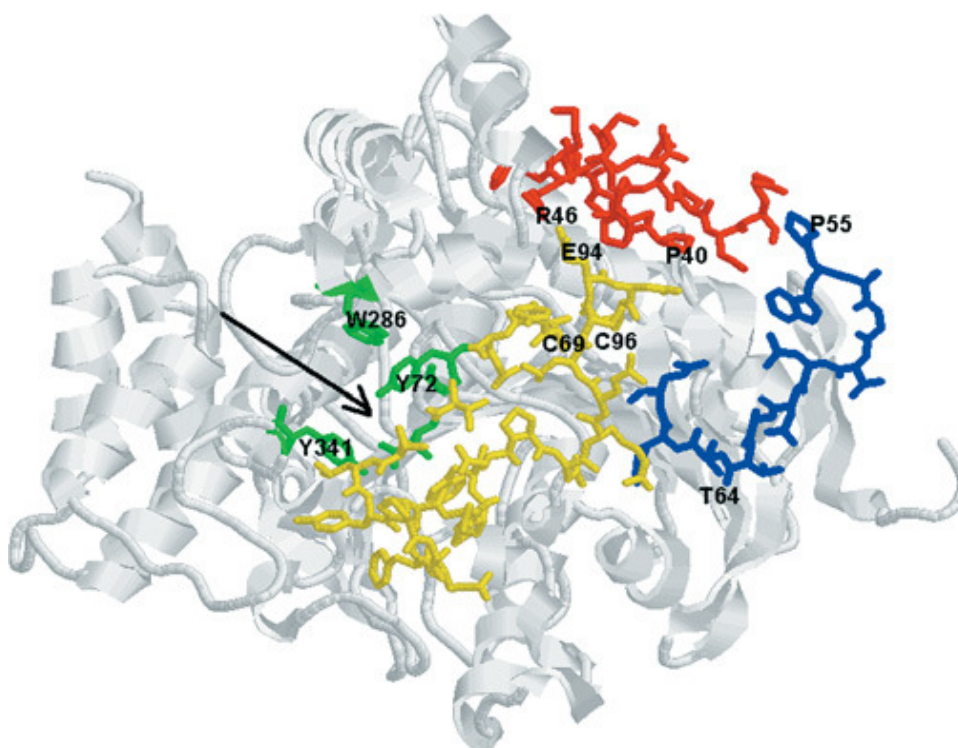


Figure 8. Mouse AChE (PDB code 1J06) showing the PAS and associated omega loops. One of the two catalytic subunits is shown. The arrow indicates the opening of the ASG. PAS residues (Tyr 72, Asp 74, Tyr 124, Trp 286 and Tyr 341) are shown in green with the omega loop (Cys 69-Cys 96) in yellow apart from the two PAS residues, Tyr 72 and Asp 74 which are in green. The sequences 40-54 are shown in red and 55-66 in blue (Johnson *et al.*, 2008).

When the 3D structure of *TcAChE* was examined, the enzyme showed a marked asymmetric spatial distribution of charged residues. These residues are segregated into a ‘northern’ negative hemisphere (where the mouth of the gorge is taken as the northern pole) and a ‘southern’ positive one. This electrostatic pattern gives rise to the strong negative dipole moment found in AChE, running more or less parallel to the direction of the active site gorge (Ripoll *et al.* 1993; Porschke *et al.* 1996). The asymmetric distribution of surface potentials contributes directly to the steering of the positively charged ACh towards the active site (Antosiewicz *et al.*, 1996). There are seven acidic residues near the opening of the gorge. These residues directly contribute to this dipole moment. See section 1.3.3 for details on the role of the dipole moment in catalysis.

1.3.2.3 Quaternary Structure

As mentioned above, alternative splicing of the AChE gene generate alternative molecular forms. Even though these molecular forms, sometimes called size-isomers, are identical in catalytic properties, their subunit assembly, hydrodynamic behavior, ionic or hydrophobic interactions, and modes of cell surface associations differ substantially (Massoulié *et al.*, 1993; Massoulié & Toutant, 1988; Taylor, 1991). These molecular forms are (Figure 9):

(a) AChE-T/ AChE-S: Splicing of exons E1-E2-E3-E4-E6 results in a 40 amino acid peptide at the C-terminal end of the catalytic domain. This form is an amphipathic protein and contains cysteine, which allows for dimerisation and the formation of higher order AChE oligomers. It also contains seven aromatic residues, including three tryptophans, organized in an amphiphilic α -helix, with these residues forming a hydrophobic cluster, and which allow for interaction with the membrane-anchoring proteins ColQ and hydrophobic Proline Rich Membrane Anchor (PRiMA) (Massoulié, 2002). This transcript, called AChE-T (for tailed) by Massoulié (Massoulié, 2002) and AChE-S (for synaptic) by Soreq (Soreq *et al.*, 2010), is the major AChE splice variant, and the form predominating in synapses and neuromuscular junctions. It is also the principal form in brain and muscle tissue (Grisaru *et al.*, 1999; Seidman *et al.*, 1995).

(b) AChE-H/ AChE-E: The second molecular variant is produced by splicing exons E1-E2-E3-E4-E5-E6 producing a 43 amino acid peptide at the C-terminus. This peptide is cleaved after residue 14 of E5 (residue 557 from the N-terminus) and is linked to glycosylphosphatidylinositol (GPI), which allows for membrane association. These AChE isoforms, called AChE-H (for hydrophobic) and AChE-E (for erythrocyte) are found in *Torpedo* muscle and the erythrocyte membrane of mammals (Massoulié *et al.*, 1999; Massoulié, 2002).

(c) AChE-R: This third major AChE specie is formed by continuous transcription through intron 14 to yield E1-E2-E3-E4-I4-E5-E6 and produces a hydrophilic 26 amino

acid C-terminal peptide that lacks cysteine, and thus remains monomeric. This “readthrough” form, expressed in embryonic and tumour cells, is also induced in response to AChE inhibition and stress (Grisaru *et al.*, 1999; Karpel *et al.*, 1994, Karpel *et al.*, 1996). AChE-R RNA is also significantly less stable than the AChE-S isoform (Chan *et al.*, 1998). A shift in the splicing pattern of AChE is often seen as a result of its transcriptional activation. This can lead to the accumulation of this rare AChE variant. AChE-R mRNA levels measured after 30 minutes of confined swim stress, for example, was shown to be considerably increased compared to normal levels. The same result presented after exposure to anti-AChEs or acetylcholine analogues (Soreq & Seidman, 2001).

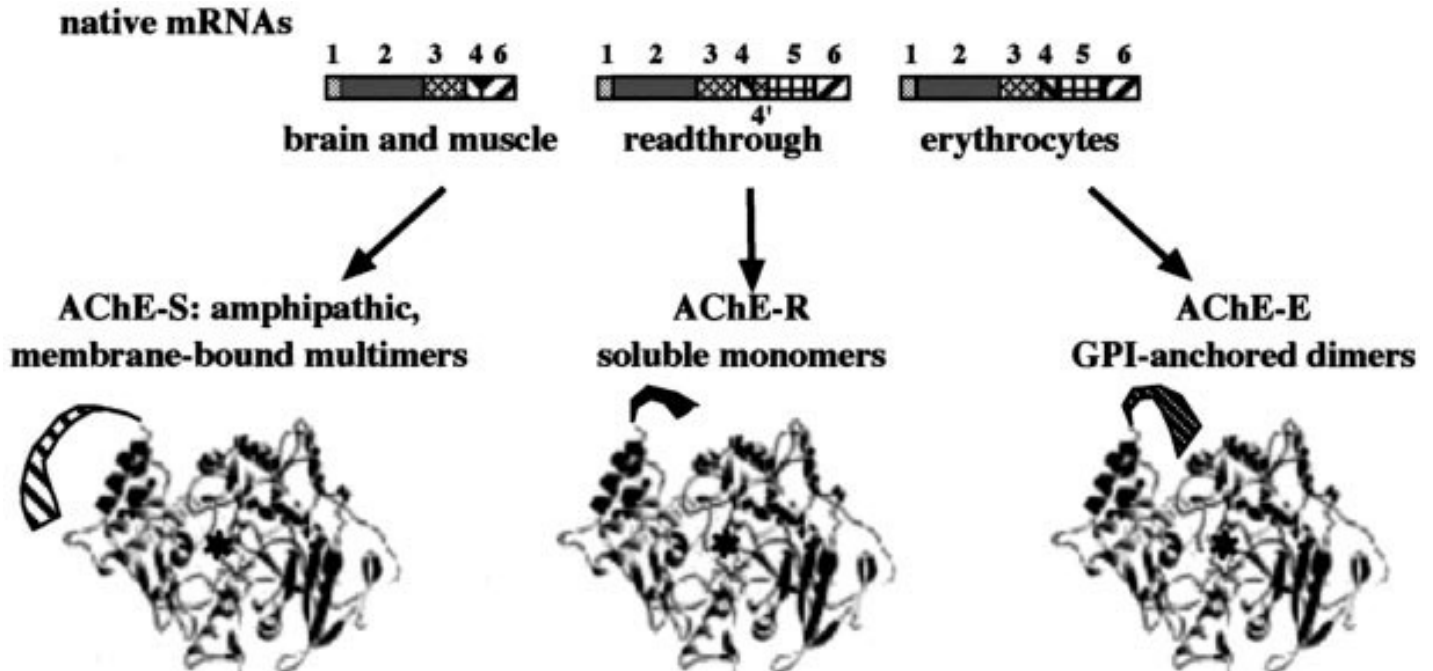


Figure 9. AChE isoforms (Grisaru *et al.*, 1999)

Apart from these three major AChE molecular forms, a fourth form exists. This form is also called AChE-S, but here the S stands for ‘snake’ or ‘soluble’ as it is found in Elapid snakes (*Bungaris*, *Naja*, etc.) only. These snakes possess a high level of secreted and

soluble monomeric AChE in their venoms. Through partial peptide sequencing, Cousins *et al.* showed that this AChE form is very closely homologous to other AChEs, but it has not been found in significant levels in other tissues. Gene analysis of the AChE-S form revealed the absence of an H exon and the presence of a T exon, which is expressed in the snake muscle. It also contains a novel S exon which encodes the C-terminal of the venom enzyme. AChE's role in the snake venom is unclear as AChE does not reinforce toxicity and is also a non-toxic entity by itself (Cousin *et al.*, 1996; Cousin *et al.*, 1998; Massoulié *et al.*, 1999).

1.3.2.4 Post Translational Modifications

During biosynthesis, cholinesterases are transferred into the endoplasmic reticulum because of their N-terminal secretory signal peptide. Here, in addition to alternative splicing, they are subjected to various post translational modifications in the secretory pathway. These modifications include oligomerization, association with membrane-anchoring proteins and glycosylation, further producing even more variations of the molecule (Massoulié *et al.*, 2005). Different post-transcriptional modifications and quaternary associations are determined by the H and T C-terminal peptides. Cysteine residues of the C-terminal peptide of AChE-H transcripts may form intercatenary disulfide bonds and contain signals for cleavage and the addition of GPI. These residues allow for the formation of mature GPI-anchored amphiphilic dimers. Likewise, the AChE-T peptide contains a free cysteine located near its C terminus and this peptide allows for a variety of quaternary associations (Massoulié *et al.*, 1993; Sussman *et al.*, 1991). Dimers of both AChE-H and -T peptides may further associate to produce tetramers (dimers of dimers).

As mentioned, AChE-T is mostly expressed in mammalian cholinergic tissues where the C-terminal 40-residue peptide allows the formation of AChE-T tetramers (Massoulé *et al.*, 2005; Massoulé & Bon, 2006). Heteromeric complexes assemble around structural proteins where complexes containing collagen ColQ are attached to the basal lamina at NMJs and complexes containing proline-rich membrane anchor (PRiMA) are anchored in

cell membranes (Gennari *et al.*, 1987; Inestrosa *et al.*, 1987; Krejci *et al.*, 1997; Feng *et al.*, 1999; Perrier *et al.*, 2002). It was shown that the T-peptide forms an amphiphilic α -helix with a sector containing the seven aromatic residues conserved in all vertebrate ChEs (Bon *et al.*, 2004). These aromatic residues play an important role in the association of four T-peptides with proline-rich motifs found in the N-terminal regions of ColQ and PRiMA called proline-rich attachment domains (PRADs) (Perrier *et al.*, 2002; Bon *et al.*, 1997; Belbeoc'h *et al.*, 2004). Interactions with ColQ seem to be mostly dependant on the T-peptide as addition of this peptide at the C-terminus of foreign proteins was found to enable these proteins to form tetramers associated with ColQ (Bon *et al.*, 1997). The PRAD motif of ColQ is preceded by a pair of adjacent cysteines which can form disulfide-like bonds with the C-terminal cysteines of the two T-peptides, where the remaining two T-peptides are disulfide-linked to each other. It was shown that the disulfide bonds between the PRAD and the T-peptides could only form when the cysteines were located at opposite extremities (Bon *et al.*, 2004). ColQ and PRiMA differ in the lengths of their proline-rich motifs. ColQ contains 10 and PRiMA 15 residues. They also differ markedly in the number of prolines in their PRADs (8 in ColQ, 14 in PRiMA) (Noureddine *et al.*, 2007). The numbers and dispositions of cysteines in ColQ and PRiMA are also very different which may lead to different organization of complexes. It was reported that the two PRADs of ColQ and PRiMA differ in their interaction with AChE-T subunits. Very few heavy dimers in the complexes formed with the PRiMA PRADs were found. In certain complexes it was shown that all four AChE-T subunits appeared to be disulfide-linked to PRiMA, whereas in others, they were associated only in pairs (light dimers). Mutation of the last aromatic residue in the T-peptide was shown to differently affect the formation of complexes with the PRADs of ColQ and PRiMA. The quaternary organization of AChE-T tetramers with ColQ and PRiMA thus appear to be somewhat different (Noureddine *et al.*, 2008). Figure 10 shows the N-terminal sequences of human ColQ and PRiMA containing the PRADs, as well as the organization of the disulfide bonds between the T-peptides and ColQ, along with a schematic model of the AChE collagen-tailed molecule.

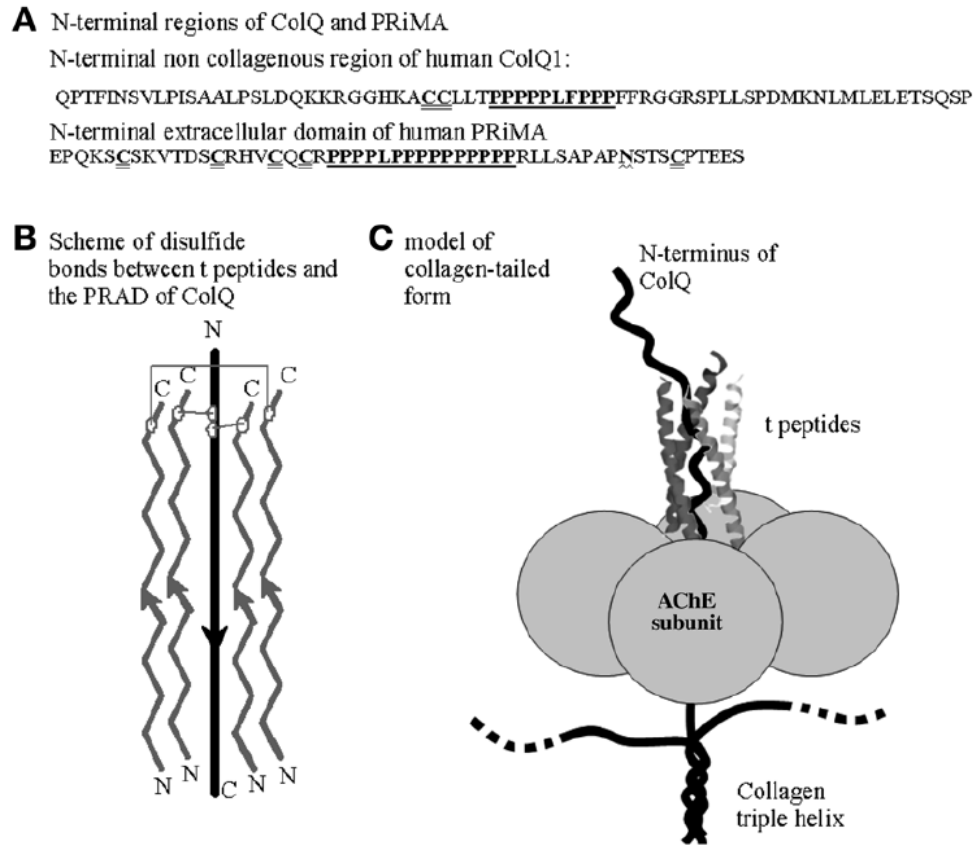


Fig 10. (A) The sequences of the N-terminal regions of human ColQ and PRiMA, containing the PRADs, are shown. The PRAD segment is underlined and cysteines contained within the sequence are doubly underlined. A potential N-glycosylation site is also indicated. (B) The organization of disulfide bonds between the four T-peptides and ColQ. (C) A schematic model of an AChE collagen-tailed molecule: the Figure shows only one AChE tetramer attached to one of the three collagen ColQ subunits (Massoulé & Bon, 2006; modified from Dvir *et al.*, 2004).

The presence or absence of the collagen ColQ tail is used to characterize the different molecular forms of AChE. Isoforms lacking the ColQ tail are termed globular (G) forms. Globular forms constitute a heterogeneous group, which can be subdivided into monomers (G1), dimers (G2) and tetramers (G4) (Figure 11) (Massoulié *et al.*, 1992; Massoulié *et al.*, 1993). G1 is largely intracellular and appears to be a precursor form of G4 (Lazar & Vigny, 1980). These G forms can be amphiphilic or nonamphiphilic and they represent the major fraction of AChE in most vertebrate tissues (Toutant & Massoulié, 1987; Massoulié & Toutant, 1988). If there is no association with GPI or PRiMA, these forms are hydrophilic. Hydrophilic G isoforms are frequently found in

embryonic development, and they may be precursors of the more complex forms. Amphiphilic isoforms include amphiphilic dimers, usually GPI-linked, as found in the erythrocyte membrane, and amphiphilic tetramers, linked to PRiMA, which appear during differentiation in the embryo and are the predominant form in the synapses of the CNS of the adult (Bon *et al.*, 1991; Bon *et al.*, 1988a; Bon *et al.*, 1988b).

ColQ-linked isoforms are also known as asymmetric or A forms, because of the appearance conferred by the addition of the tail (Figure 11). Asymmetric forms predominate in neuromuscular junctions, and include tetramers (A4), octamers (A8), consisting of two tetramers linked to ColQ, and, most commonly, dodecamers (A12), consisting of three tetramers linked to ColQ (Massoulié *et al.*, 1992b; Massoulié *et al.*, 1993). It has been suggested that, although the functional significance of these AChE polymorphisms are still elusive, it allows the placement of catalytically active subunits in distinct cell types and sub cellular locations to perform site-specific functions. In mammals, for example, glycopospholipid-linked dimers are found preferentially in hematopoietic tissue whereas asymmetric forms are exclusively expressed in differentiated muscle and neuronal cells (Chan *et al.*, 1998).

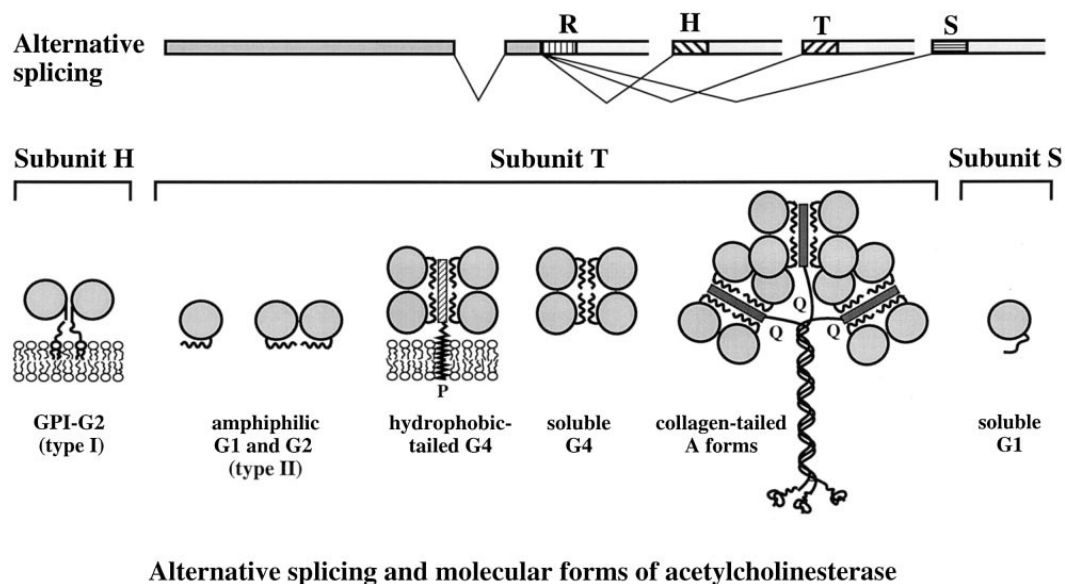


Figure 11. Alternative splicing of molecular forms of AChE (Krejci, 1998)

Yet more variation is conferred by differences in glycosylation. Post translational glycosylation can have multiple effects on the transport of proteins towards the cell surface, their biological activity, their stabilization and also functional conformation (Chu *et al.*, 1978; Gibson *et al.*, 1979; Dubé *et al.*, 1988; Matzuk *et al.*, 1989; Semenkovich *et al.*, 1990). ChEs are multimeric glycosylated ectoenzymes displaying several potential glycosylation signals, although, the number and location are not conserved throughout the ChE family (Velan *et al.*, 1993). For example, human BChE has nine potential sites where human AChE has only three N-linked glycosylation sites: Asn 265, Asn 350, Asn 464 (Lockridge *et al.*, 1987; Prody *et al.*, 1987; Soreq *et al.*, 1990; Velan *et al.*, 1993). Mouse and rat AChE also contain three where foetal bovine AChE has five (Rachinsky *et al.*, 1990; Legay *et al.*, 1993; Kronman *et al.*, 1995). The three glycosylation sites in human AChE are conserved in all mammalian ChEs sequenced to date (Gentry & Doctor, 1991). Site-directed mutagenesis analysis of these three sites showed that all three glycosylation signals are utilized but not all the secreted molecules are fully glycosylated. It was also found that glycosylation at all three sites is important for effective biosynthesis and secretion and glycosylation mutants presented impaired stability reflected in their increased susceptibility to heat inactivation (Velan *et al.*, 1993).

In pathology, several neurodegenerative disorders, such as Alzheimer's disease (AD) and Creutzfeldt-Jakob disease (CJD), have been found to cause characteristic alterations in the glycosylation patterns of certain brain proteins (Saez-Valero *et al.*, 1999). Mutations of the AChE gene have also been linked to certain cancers. A more in depth discussion on these topics follows.

1.3.2.4.1 Anchorage of AChE in the basal lamina and cell membrane

In the neuromuscular junction, AChE is anchored in the basal lamina by ColQ. ColQ binds to the heparan sulfate proteoglycan perlecan, which in turn binds to the dystroglycan complex through α -dystroglycan (Peng *et al.*, 1999). ColQ also binds to MuSK, forming a ternary complex of AChE/ColQ, perlecan and MuSK (Cartaud *et al.*,

2004). These interactions result in clustering of AChE, and the formation of scaffolds through which AChR can be clustered by activation of the MuSK.

During development of the nervous system, and in the adult central nervous system, the predominant isoform is the amphiphilic G4, which is anchored in the cell membrane by PRiMA. PRiMA contains a number of domains: an extracellular domain, which contains the PRAD, a transmembrane domain, and a cytoplasmic domain (Perrier *et al.*, 2002). PRiMA is targeted to membrane rafts, possibly by its CRAC (cholesterol recognition/interaction amino acid consensus) motif located at the C-terminus (Xie *et al.*, 2010). PRiMA-linked AChE in fibroblasts and astrocytes is also reported to co-localise with perlecan (Anderson *et al.*, 2008).

1.3.3 Catalysis in AChE

High speed action is a prerequisite of any enzyme functioning in the nervous system. AChE is thought to be one of the fastest enzymes and its turnover number is of special interest. The entire course of signal transmission at the neuromuscular junction i.e. the release of ACh, its diffusion across the synaptic cleft, its reversible interaction with the AChR and, finally, hydrolysis by AChE, occurs within milliseconds. This rapid process must, therefore, be tightly integrated both spatially and temporally (Scholl & Scheiffele, 2003; Bourne *et al.*, 2003). AChE has an unusually high turnover number especially for a serine hydrolase, operating at a rate close to that of diffusion (Quinn, 1987; Scholl & Scheiffele, 2003). According to Wilson and Harrison (1961) the turnover number for AChE at 25°C, a pH of 7.0 and ACh level of $2.5 \times 10^{-3} \text{M}$, was found to be $7.4 \times 10^5 \text{min}^{-1}$. The importance of rapid cholinergic transmission is also underlined by the magnitude of AChE's $k_{\text{cat}}/K_{\text{M}}$, $\approx 10^9 \text{M}^{-1} \cdot \text{s}^{-1}$ (Nolte *et al.*, 1980; Radic *et al.*, 1992), which ranks as one of the highest catalytic efficiencies known (Fersht, 1985). In vertebrates, because of their intelligence and quick movements, selective pressure has driven AChE to become an almost 'perfect enzyme' (Quinn, 1987).

It was originally suggested, through kinetic studies, that the substrate might be attracted to the active site by a large number of negative charges in the vicinity (Nolte *et al.*, 1980). This notion was later disproved by the crystal structure characterization of AChE (Sussman *et al.*, 1991). Theoretical calculations indicated the presence of a large, permanent dipole moment which may guide the substrate to the gorge (Ripoll *et al.*, 1993; Tan *et al.*, 1993). Mutagenesis of the seven acidic residues near the opening of the gorge was found to adversely affect AChE's catalytic efficiency (Shafferman *et al.*, 1994; Zhou *et al.*, 1998). Because of the position of the active site at the bottom of a gorge, the substrate has to be guided down the gorge as rapidly and efficiently as possible. Choline esters such as ACh, are positively charged and thus electrostatically attracted towards the opening of the gorge and the negative charge surrounding the PAS (Felder *et al.*, 1997; Silman & Sussman, 2008). Even though the importance of the electrostatic guidance mechanism in accelerating the binding of cationic ligands is unquestioned, a lot of controversy over the contribution of the dipole moment to the high turnover rate exist (Shafferman *et al.*, 1994; Antosiewicz *et al.*, 1995). Antosiewicz *et al.* (1996) showed that in AChE, there is an electrostatic steering of substrate present where the effects of electrostatics were observed mainly in the area above the entrance to the gorge. The charge distribution seems to become more important as the ligand moves down the gorge. It was stated that neither the enzyme's total charge, nor its dipole moment, can fully account for this electrostatic steering of ligand to the active site. It appears that there is no simple correlation between the rate constants and electrostatic aspects such as net charge and dipole moment. It is evident that higher moments of the enzyme's charge distribution are also important. That being said, electrostatic steering does exist, as indicated by the fact that the hydrolysis and encounter rate constants for cationic substrate are substantially larger than those for neutral substrate (Antosiewicz *et al.*, 1996).

Apart from the dipole moment, other factors also contribute towards enzyme function. Choline esters also contain a quaternary ammonium group. Quaternary ammonium groups interact with aromatic rings and seeing as the gorge is lined with a number of aromatic residues, the substrate thus interact with their side chains as it heads down the

gorge (Xu *et al.*, 2008). As mentioned these aromatic residues also contribute to the flexibility of the gorge in order to accommodate substrates larger than the gorge itself.

The first step in the catalytic pathway is the binding of the substrate to the PAS of the AChE molecule. The PAS enhances catalytic efficiency by 'trapping' the substrate on its way to the catalytic site or active centre (Mallender *et al.*, 2000; Hosea *et al.*, 1996). Trp 286 (numbering from here on refers to mammalian unless otherwise stated) in the PAS is especially important in the binding of cationic ligands (Ordentlich *et al.*, 1993; Bourne *et al.*, 2003). It has been shown that substrate binding at the PAS triggers a conformational change that is transmitted allosterically to the acylation site (De Ferrari *et al.*, 2001a). A relay of cation- π interactions with Trp 86, Phe 295 and Tyr 341 assist in movement down the gorge (Branduardi *et al.*, 2005). The fourteen aromatic residues within the gorge are involved in this relay system (Sussman *et al.*, 1991). When ACh reaches the base of the gorge, it binds to the choline-binding site. Trp 86 is the major component of this site, interacting with the quaternary ammonium of the choline moiety by cation- π interactions (Sussman *et al.*, 1991). This binding positions the ACh molecule optimally for nucleophilic attack on the vulnerable ester bond by the Ser (Ser 203) of the acylation site (Eastman *et al.*, 1995). In the reaction, His 447 acts as a general acid-base catalyst, accepting or donating a proton. It is possible that the acidic residue of the triad, Glu 334, functions by forming a temporary salt bridge with the His (Dodson & Wlodawer, 1998). The oxyanion hole and the acyl pocket are involved in stabilization of the transient and fragile transition state. The acyl pocket is responsible for substrate selectivity by preventing access of larger members of the choline ester series and the oxyanion hole provides hydrogen bond donors that stabilize the tetrahedral transition state of the substrate (Ordentlich *et al.*, 1998). Finally, the molecule is stabilised by cation- π interactions with Trp 86 in the active centre.

An intriguing feature of AChE reactivity is the modulation of catalytic activity following ligand binding to the PAS (Changeux, 1966; Hucho *et al.*, 1991). The concentration of neurotransmitter and other charged species, such as Ca^{2+} , Mg^{2+} and Na^+ , fluctuate in the synaptic cleft. Such catalytic activity modulation can play a significant role in adjusting

to these fluctuations (Berman & Nowak, 1992). Opposite to Michaelis-Menten kinetics, when substrate concentration is at a high, a reduction in turnover i.e. substrate inhibition is seen. This is a consequence of substrate binding to the PAS (Radic, 1991; Aldridge & Reiner, 1969). A number of reasons could account for this, including physical blocking of the gorge entrance preventing access of additional substrate molecules; charge repulsion between molecules or even an allosteric interaction between the active and peripheral sites could occur involving conformational changes in the enzyme molecule (Taylor *et al.*, 1994).

1.3.4 Inhibitors

Cholinergic nerves control cognition and fast skeletal muscles. AChE is an important mediator in these functions and thus essential for life. It is for this reason that AChE is targeted by a variety of anti-cholinesterases and inhibitors. Some of these inhibitors remain of value as medical agents contributing in drug development for the treatment of diseases such as Alzheimer's disease, *myasthenia gravis* and glaucoma. Other inhibitors target AChE as toxins such as insecticides and snake venoms and some anti-cholinesterases even possess potential for insidious use as chemical warfare agents (Soreq & Seidman, 2001; Pope *et al.*, 2005).

The inhibition of AChE by anti-cholinesterases, such as insecticides, results in the accumulation of ACh at the synaptic terminals and subsequent overstimulation of postsynaptic cells leading to death (e.g. Ecobichon, 1991). Many of these, such as carbamates and organophosphates, bind irreversibly and competitively to the active or acylation site serine. Other inhibitors, for example edrophonium, bind to the anionic (hydrophobic subsite) site. Yet other inhibitors, for example, BW284c51 (1.5-bis(4-allyldimethylammoniumphenyl)-pentan-3-one dibromide), propidium iodide and fasciculin 2 from green mamba snake venom, bind to the PAS (Figure 12 show the different structures of PAS binding inhibitors). This inhibition is non-competitive, and is a result of allosteric modulation. Inhibitors that bind to the hydrophobic subsite within the gorge, as well as others binding non-competitively at the PAS, also exist. Competition of

substrate for binding with ligand specific for the PAS as well as site-directed mutagenesis studies show that the sites controlling substrate inhibition and inhibitor binding, overlap (Radic *et al.*, 1991; Marchot *et al.*, 1993; Shafferman *et al.*, 1992).

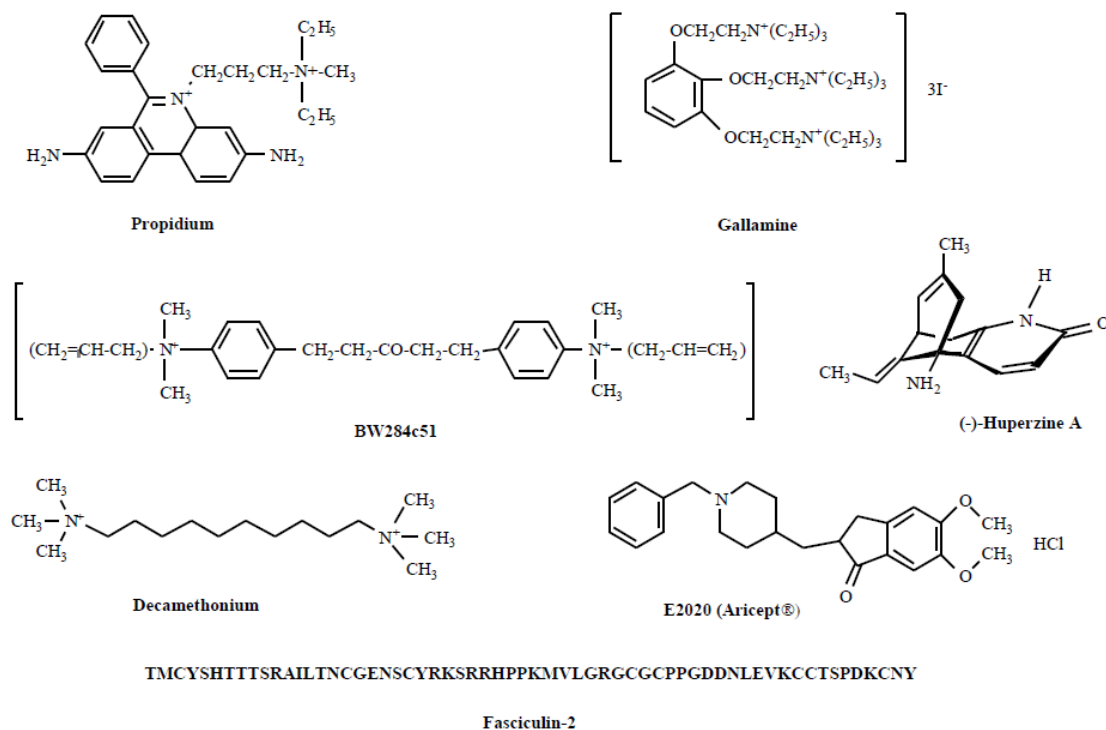


Figure 12. Structures of PAS-binding inhibitors (Johnson & Moore, 2006)

Compounds binding directly to the PAS include quaternary inhibitors, such as gallamine, that have structures resembling the quaternary ammonium group of ACh and thus bind in the same manner as ACh. Bisquaternary inhibitors are long thin molecules with quaternary ammonium groups on each end. These inhibitors include BW284c51, decamethonium and E2020 (Aricept), and span both the anionic site and the PAS. Here Tyr 72, Tyr 124 and Trp 286 participate in this binding (Vellom *et al.*, 1993; Kryger *et al.*, 1998; Felder *et al.*, 2002). A small cationic inhibitor called propidium binds to a pocket formed by the aromatic residues of the PAS centered around Trp 286 where as various parts of the (-)-huperzine A molecule bind to the anionic site and the PAS (Dvir *et al.*, 2002).

A 61 amino acid peptide from mamba venom called fasciculin-2, is a member of the 3 loop toxin family that also include the α -bungarotoxin and the cardiotoxins. Fasciculin-2 is evolved to have a binding site that is highly specific for the PAS and thus show a high affinity and selectivity for AChE (Radić *et al.*, 1994). This inhibitor blocks substrate access by inserting one of the loops into the gorge entrance while another loop binds to the 69-96 omega loop (Harel *et al.*, 1995; Bourne *et al.*, 1995). The residues of the 275-305 loop on the opposite end of the gorge is also included and Van der Waals contacts are made with the PAS tyrosine residues (Tyr 72, Tyr 124 and Tyr 341) by loop II of the fasciculin molecule which is also packed against Trp 286.

PAS-binding inhibitors inhibit partly by steric hindrance of the gorge entrance, for example fasciculin-2 that obscures approximately 200\AA^2 of the AChE surface after binding (Bourne *et al.*, 1995), and partly by allosteric modulation binding of structures within the gorge, in particular Trp 86 (Eastman *et al.*, 1995; Barak *et al.*, 1995). An example of this is where the mutation of Trp 86 reduces the ability of propidium to inhibit AChE (Ordentlich *et al.*, 1993). This occurrence suggests coupling between this residue and the PAS (Johnson & Moore, 2006).

The toxic effects of anti-cholinesterases such as insecticides have been studied in adult as well as young animal models and the sensitivity seems to be age-related. Young animals seem to be generally more susceptible to the lethal effects of these compounds (Brodeur & DuBois, 1963; Lu *et al.*, 1965; Benke & Murphy, 1975; Harbison, 1975). Species-related differences in susceptibility can be partially explained by a differential sensitivity in AChE (e.g. Johnson & Wallace, 1987). Gagne and Brodeur hypothesized that this may also explain the increased sensitivity in younger rats vs. adult rats (Gagne & Brodeur, 1972). This hypothesis makes sense when taking into account the many changes that occur during development of the nervous system (Benjamins & McKhann, 1981). The age-related differences in sensitivity in rat brain AChE to two carbamates (aldicarb and carbaryl), as well as to the activated oxons of two organophosphorus (chlorpyrifos-oxon and malaoxon; active metabolites of chlorpyrifos and malathion, respectively)

insecticides were investigated. Results showed that AChE in young and adult brain differs mostly in its specific activity while kinetics and sensitivity to anti-cholinesterase insecticides are not different (Mortenson *et al.*, 1998).

AChE-directed insecticides are facing increased resistance among target species leading to a resurgence of disease vectors, insects destructive to agriculture, and residential pets. The concern for human toxicity from current compounds is also growing (e.g. Pang *et al.*, 2009; Polsinelli *et al.*, 2010). Many disease-transmitting insect and agricultural pests contain two AChE genes, AP and AO (reviewed in Polsinelli *et al.*, 2010). Reports showed the presence of a free cysteine residue at the entrance to the active site of AP-AChE. This was seen in lower organisms but not at that of AO-AChE and AChEs from mammals, fish or birds (Pang, 2006; Pang *et al.*, 2009). A small Cys-targeting molecule that irreversibly inhibits all AChE activity was recently extracted from aphids (Pang *et al.*, 2009). Identical exposure to human AChE had no effect. These findings provide insight into the development of human-safe insecticides.

1.4 Butyrylcholinesterase

As mentioned above, AChE is very closely related to BChE with a sequence identity of 50% (Harel *et al.*, 1992). These two enzymes have been distinguished by their substrate specificity. AChE hydrolyzes acetylcholine much faster, and is much less active towards butyrylcholine, whereas BChE displays similar activity towards the two substrates (Mendel & Rudney, 1943; Chatonnet & Lockridge, 1989). BChE is also able to act upon a more diverse and larger set of substrates, as the narrow groove of the gorge, as well as the dimensions of the acyl pocket, limit entry of larger molecules to the AChE active site. A number of choline esters are subject to hydrolysis by BChE, a few of which include ACh, BCh, propionylcholine as well as benzoylcholine (Layer, 1991).

In muscle fibers, BChE is also concentrated at the neuromuscular junction (Jedrzejczyk *et al.*, 1984; Kasprzak & Salpeter, 1985). It was shown that during the development and regeneration of myofibres *in vivo*, the accumulation at synaptic sites of AChRs, AChE,

and BChE, are all triggered by the same molecule. This molecule was shown to be similar, if not identical, to an aggregating factor previously identified in *Torpedo* electric organ (Wallace, 1986). During the development of chicken skeletal muscle, the amounts and forms of AChE change in parallel with those of BChE (Lyles *et al.*, 1979). BChE activity was found to be very high during the developmental stage prior to hatching. Localization of AChE and BChE during this stage is unclear, but an identical location is implied by the fact that subunits of both participate in the same asymmetric forms (Tsim *et al.*, 1988).

In the nervous system, most research on the brain cholinergic system has been devoted to AChE, where BChE has been viewed as a non-specific, non-essential enzyme almost interfering with studies on AChE (Darvesh *et al.*, 2003; Silver, 1974). This view was changed by observations that BChE could have more specific functions in this context. Expression of BChE in distinct populations of neurons has been reported, as well as its role in co-regulating cholinergic neurotransmission (Friede, 1967; Tago *et al.*, 1992; Darvesh & Hopkins, 2003; Darvesh *et al.*, 1998; Mesulam *et al.*, 2002). BChE also seems to be involved in the development of the nervous system (Robertson & Mostamand, 1988; Layer, 1991; Dubovy & Haninec, 1990; Kostovic & Goldman-Rakic, 1983). Before the onset of synaptogenesis in the chicken neural tube, AChE and BChE are expressed in a mutually exclusive manner (Layer, 1983). In early embryonic neural development, prior to synaptogenesis, BChE is diffusely distributed along the ventricular layer in the developing neural tube (Layer, 1995). Here, BChE seem to precede and influence AChE expression. A functional role for BChE in the regulation of cell proliferation and the onset of differentiation during early neuronal development, independent of its enzymatic activity, has been reported (Layer 1983; 1991; Mack & Robitzki, 2000).

Comparing the catalytic machinery of BChE to that of AChE, it is apparent that they differ in a number of ways, all of which contribute to its reduced specificity. First of all, the PAS is largely absent, and, within the gorge, the acyl pocket is larger due to the replacement of both of the Phe residues (Phe 295 and Phe 297 in AChE) with Leu and

Val (Masson *et al.*, 1999; Harel *et al.*, 1992; Vellom *et al.*, 1993). The larger acyl pocket enables accommodation of the larger substrates in BChEs. The number of aromatic residues in the BChE gorge is reduced from AChE's 14 to 8 in BChE (Jbilo *et al.*, 1994). BChE also lacks the negative dipole moment seen in AChE (Botti *et al.*, 1998).

Kaplan *et al.* (2001) showed human AChE to be eight times faster than BChE (AChE: $K_m=140\mu\text{M}$ & $k_{\text{cat}}= 4 \times 10^5/\text{min}$; BChE: $K_M= 40\mu\text{M}$ & $k_{\text{cat}}= 0.5 \times 10^5/\text{min}$). Although BChE is not as fast as AChE, it still is a fast enzyme in its own right. A number of factors contribute towards the differences in catalytic prowess between these two enzymes. Even though no direct evidence exists, differences in charge distribution, specifically the lack of the dipole moment in BChE, could account for the reduction in the efficiency of BChE in comparison with AChE. Another contributing factor could be the reduction in the number of aromatic residues in BChE. Both these factors are responsible for the steering of substrate down the gorge. It seems that the fundamental part of the catalytic machinery is the same in both AChE and BChE (i.e. the active site and the choline-binding site which functions in positioning the substrate). This would account for the fact that they are both good enzymes. The differences lie in the 'modulatory' parts of the catalytic apparatus that contribute directly to efficiency and turnover.

The 'modulatory' differences in AChE and BChE are most likely due to the differences in function between the two enzymes. Although the specific function of BChE have yet to be determined, BChE have been shown to play a major role in detoxification where it scavenges organophosphates and other inhibitory compounds (Nicolet *et al.*, 2003). It is thus useful for BChE to be able to accommodate a variety of substrates, hence the more versatile acyl pocket. AChE and BChE also seem to play different roles in the NMJ. AChE is very fast but is inhibited at higher substrate concentrations, while BChE is less fast but is also activated at higher substrate concentrations. BChE may thus function as both protector and backup for AChE. In the AChE knockout mouse, for example, BChE was observed to have taken over the synaptic functions of AChE (Xie *et al.*, 2000).

There is suggestive evidence that BChE may play a role in regulating the expression of AChE (Koelle *et al.*, 1976; Layer *et al.*, 1992). Despite the high level of homology between AChE and BChE, they are encoded by different genes, located on different chromosomes (Soreq *et al.*, 1987; Arpagaus *et al.*, 1990; Gaughan *et al.*, 1991). BChE is thought to have originated by gene duplication and seem to occur in different phylogenetic lineages (McClellan *et al.*, 1998). In mammals, these two enzymes are each encoded by a single gene: AChE at 7q22, and BChE at 3q26.1-q26.2 (Getman *et al.*, 1992). The duplication of the ancestral BChE gene most probably occurred before the split of cartilaginous fish but after the divergence of jawless fish as BChE is found in *Torpedo*, birds and mammals, but not in hagfish or lamprey (Pezzimenti *et al.*, 1998). Table 1 is a summarized comparison between the two ChEs.

Table 1. Comparison of AChE and BChE.

	ACETYLCHOLINESTERASE (AChE): E.C. 3.1.1.7	BUTYRYLCHOLINESTERASE (BChE): E.C. 3.1.1.8
Gene location	7q22	3q26.1-q26.2
Substrates subject to hydrolysis	ACh	ACh, BCh, propionylcholine, benzoylcholine
Specific inhibitor	BW284C51 (1,5 bis [4-allyldimethyl ammonium phenyl] pentane-3-one dibromide)	Iso-OMPA (tetra [monoisopropyl] pyrophosphortetramide)
Catalytic machinery	PAS present; 14 aromatic residues in the gorge; narrow acyl pocket; high turnover number; dipole moment	PAS largely absent; 8 aromatic residues in the gorge; larger acyl pocket; lower turnover number; no dipole moment

1.5 Cholinesterase-Domain Proteins (CLAMS)

AChE is sequentially homologous to a number of other proteins, collectively known as the cholinesterase-domain proteins (Krejci *et al.*, 1991). These proteins appear to have lost their enzyme function secondarily, and the majority functions as cell adhesion molecules particularly during neural developments. For this reason, they have been termed the “CLAMS” (Cholinesterase-Like Adhesion Molecules) (Gilbert & Auld, 2005). The CLAMS include the invertebrate proteins neurotactin, gliotactin and glutactin, and the neuroligins. Gliotactin is found in nematodes and arthropods; neurotactin and glutactin is found only in insects, and neuroligin is found in many invertebrate and vertebrate species (noted through sequence/genome analysis – unpublished observations). The vertebrate protein thyroglobulin is the only cholinesterase-domain protein that is not a cell adhesion molecule. Botti *et al.* (1998) described a consistent ring-shaped pattern of negative charge surrounding the gorge entrance that was apparent in CLAMs as well as ChEs that mediated cell adhesion (see below), namely, neuroligin, neurotactin, glutactin and AChE. The motif was not apparent in BChE, which does not mediate cell adhesion. These molecules were therefore termed the “electrotactins” (Botti *et al.*, 1998).

Thyroglobulin was the first AChE-homolog to be identified. This protein is the precursor of the thyroid hormones and contains an AChE-like sequence at its carboxyl end (MacPhee-Quigley *et al.*, 1986). A 28% amino acid identity extending over 544 residues and involving over 90% of the AChE sequence, but only the C-terminal portion of the much larger thyroglobulin, was found (Swillens *et al.*, 1986). When the hydropathy profiles of the homologous regions were determined, a striking resemblance suggested that these regions in both proteins adopt a similar three-dimensional structure. AChE and thyroglobulin are both known to interact with the cell membrane and it is because of this that it was suggested that the AChE-like domain of thyroglobulin is involved in the binding (Swillens *et al.*, 1986). These predictions speculate that thyroglobulin may have evolved from a copy of the AChE gene and are consistent with the hypothesized common evolutionary origin of the nervous and endocrine systems in vertebrate stating that both evolved to support intracellular communication (Chatonnet & Lockridge, 1989).

Thyroglobulin is the only homologous molecule that is not neural, but thyroid is derived from the neural crest in the embryo indicating a possible link.

Glutactin, a strongly anionic sulfated glycoprotein, is an important component of *Drosophila* embryonic basement membranes. Even though glutactin contains a signal peptide and an N-terminal domain strongly resembling thyroglobulin, AChE as well as other serines esterases, it lacks the essential serine residue of the catalytic triad found in the AChEs. The presence of glutactin at several basement membrane sites suggests that it might be a component of the extracellular matrix. In *Drosophila*, glutactin also functions as a cell adhesion molecule (Olson *et al.*, 1990).

Gliotactin, another transmembrane protein, is expressed by peripheral glia of *Drosophila* where it is involved in the formation of the blood-brain barrier. The extracellular domain of gliotactin contains sequence similarities with members of the serine esterase family. The catalytic triad is missing indicating a structural function for the serine esterase domain (Auld *et al.*, 1995).

The neuroligins (isoforms 1-4) are found in vertebrates and invertebrates and constitutes a multigenic family of mammalian brain-specific AChE-homologous proteins. Through alternative splicing, these proteins are subject to considerable heterogeneity and they have been suggested to exert overlapping functions in mediating recognition processes between neurons (Ichtchenko *et al.*, 1996). Neuroligins, sharing 34% residue identity with AChE, are involved in synaptogenesis and they can trigger de novo formation of pre-synaptic structures through their interaction with β -neurexins in the post-synaptic membrane (Scheiffele *et al.*, 2000; Rao *et al.*, 2000; Biederer & Stagi, 2009). Their expression in non-neuronal cells has been found to induce synaptic vesicle clustering as well as pre-synaptic differentiation in adjacent axons. These actions were prevented by addition of the extracellular domain of β -neurexin (Scheiffele *et al.*, 2000). Neuroligins bind to β -neurexin through their extracellular AChE-like domains (Ichtchenko *et al.*, 1996); it is thus presumed that AChE may also be able to bind β -neurexin (Soreq & Seidman, 2001). However, AChE cannot substitute for the extracellular domain of

neuroligin (Comoletti *et al.*, 2010). Neuroligin-neurexin connections may also play an important role in interneuronal recognition pathways where they could possibly regulate axonal pathfinding and plasticity. In development, cross-talk between AChE and neurexins have been suggested in experiments where overexpression of mice bearing the human AChE transgene was found to suppress neurexin I β production in embryonic transgenic mouse motor neurons (Andres *et al.*, 1997). Neuroligin 1 (NL-1) and neuroligin 2 (NL-2) are involved in excitatory and inhibitory synapses, respectively (Chubykin *et al.*, 2005). Mutations in neuroligin-3 and neuroligin-4 have been associated with autism (Jamain *et al.*, 2003).

Neurotactin is a transmembrane cell adhesion molecule and it has been observed that a substitution of its extracellular domain with *Torpedo* AChE also promotes cell adhesion (Darboux *et al.*, 1996). In *Drosophila*, it has been described as a glycoprotein expressed in neuronal and epithelial tissues during embryonic and larval stages. The heterophilic adhesive properties of neurotactin indicate a role in interneuronal interactions. Structural analysis of neurotactin show that the extracellular domain is comprised of an N-terminal region, a catalytically inactive AChE-like domain consisting of a gorge with a three-dimensional structure almost identical to that of AChE, a short hydrophobic transmembrane region as well as less conserved intracellular C-terminal region (Hortsch *et al.*, 1990; Darboux *et al.*, 1996). CAMs homologous to AChE are shown in Figure 13.

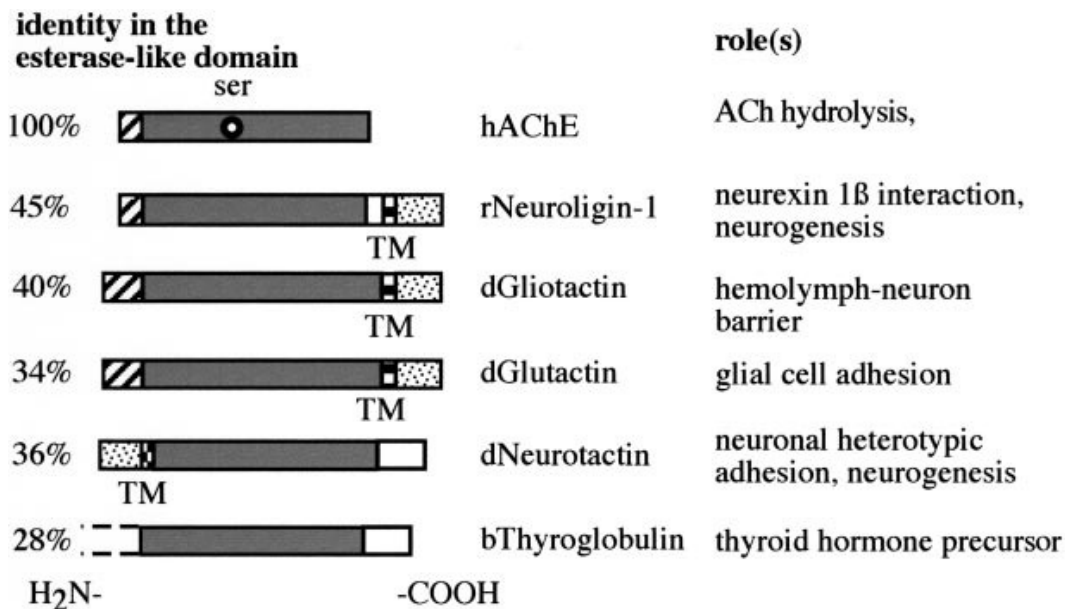


Figure 13. Cell adhesion molecules homologous to AChE. On the basis of amino acid sequences, AChE-like proteins have been identified. These include rat (r) neuroigin, *Drosophila* (d) gliotactin, neurotactin and glutactin as well as the bovine (b) thyroglobulin. Represented are the percentage sequence identities of the AChE-like regions, signal peptide domains, transmembrane sequences (TM, patterned) and the position of the active site serine (Ser, circle) (<http://www.ensam.inra.fr/cholinesterase>; Grisaru *et al.*, 1999).

1.6 Non-Classical Role for AChE

1.6.1 Indications of Alternative Functions

From early on in the study of AChE, certain facts surrounding this enzyme raised speculations of it functioning in ways separate to its classical, cholinergic function. The wide distribution of AChE throughout the human body, for instance, as well as its apparent abundance in most living organisms, hint that although hydrolysis of ACh is its main function, it very likely is not its only function. The term “non-classical” may be defined as any function outside that of ACh hydrolysis in the synapse and neuromuscular junction. Such a non-classical function may be either enzymatic or non-enzymatic. The former could involve hydrolysis of ACh or another substrate in a non-synaptic context, or enzymatic functions of a different type; the latter, functions that may be mediated by a

structural site, such as signaling functions resulting from interaction with other proteins or molecules, or even phosphorylation.

Distribution, solubility, as well as functional effects, form the basis of these non-classical speculations. The idea that AChE may have functions outside of ACh hydrolysis was originally suggested by histochemical observations showing the presence of AChE in early embryonic development prior to synaptogenesis (Drews, 1975). Both AChE and BChE have also been described in various tissues during development as the evident presence of BChE in some embryonic cells. In this context it has been shown that BChE can be replaced by AChE, suggesting a role as an embryonic cholinesterase (Chatonnet & Lockridge, 1989). It is also apparent that not all AChE activity is localized with its presumed substrate, ACh (Silver, 1974; Massoulié & Bon, 1982; Eckenstein & Sofroniew, 1983). High concentrations of AChE activity have been found in erythrocytes (Ott *et al.*, 1982), platelets, megakaryocytes (Paulus *et al.*, 1981) and plasma (Small *et al.*, 1987). AChE presence has also been observed in developing avian cartilage (Layer, 1990) and developing oocytes and sperm (Malingier *et al.*, 1989; Soreq *et al.*, 1990; Sastry *et al.*, 1981).

1.6.1.1 The non-neuronal cholinergic system and non-classical distribution of ACh and AChE

From the beginning of life, cholinergic communication and regulation has been established in primitive uni- and multicellular organisms (Wessler *et al.*, 1999, 2001, 2003; Horiuchi *et al.*, 2003). The cholinergic components are even found in a variety of living systems that lack nervous systems. ACh is a phylogenetically ancient molecule, and its presence, together with its receptors, has been detected in plants, fungi, bacteria, protozoa as well as in all living animals (Horiuchi *et al.*, 2003). The specific function of ACh in fungi and lower invertebrates are still unknown. In plants ACh has been implicated in the regulation of differentiation, phytochrome-mediated processes, as well as ion water transport (Hartmann & Kilbinger, 1974a, 1974b; Jaffe, 1970; Raineri & Modenesi, 1986; Smallman & Maneckjee, 1981; Wessler *et al.*, 2001). The expression of

AChRs (both muscarinic and nicotinic) in mammalian cells, along with the ubiquitous synthesis of ACh, gives an indication of the complexity of biological systems. Single non-neuronal cells use the same receptor subtypes and signal-transduction pathways as cholinergic neurons to communicate among each other and to maintain organ homeostasis (reviewed in Wessler & Kirkpatrick, 2008). Although the functions of these non-neuronal systems are very poorly understood, the widespread synthesis of ACh in non-neuronal cells have been the focus of many reviews over the last decade (Sastry and Sadavongvivad, 1978; Grando, 1997; Wessler *et al.*, 1998, 1999, 2001, 2003, 2008; Kawashima and Fujii, 2000, 2004; Eglon, 2006; Grando *et al.*, 2006, 2007; Kurzen *et al.*, 2007).

Evidence for ACh synthesis is provided by positive anti-ChAT immunoreactivity, ChAT enzyme activity and ACh content. Originally the most widely used method for identifying cell bodies of cholinergic neurons relied on AChE histochemistry. However, it was later questioned whether AChE has a legitimate role as a specific marker for cholinergic neurons alone as it is also found in different populations of monoaminergic neurons and non-neuronal structures (Rossier, 1977; Butcher, 1978; Fibiger, 1982). It seems that even in the nervous system, AChE activity is not always associated with cholinergic neurons or their terminals. Even though most cholinergic neurons contain AChE activity, many non-cholinergic neurons show AChE activity (Small, 1990). Today, antibodies directed against ChAT offers a more specific immunohistochemical method for identifying cholinergic cell bodies (e.g. Mesulam *et al.*, 1983; Kimura *et al.*, 1981).

The vast majority of human non-neuronal cells seem to demonstrate ACh. Examples include: cells of the kidney, urogenital tract, placenta, glandular tissue, and eye; as well as epithelial, endothelial, and mesenchymal cells (reviewed in Wessler & Kirkpatrick, 2008; Grando, 1997). Schlereth and colleagues documented the release of non-neuronal ACh in human skin in 2006 as the first evidence of *in vivo* release of non-neuronal ACh from human tissue (Schlereth *et al.*, 2006). Embryonic stem cells in mice also synthesize considerable amounts of ACh (Paraoanu *et al.*, 2007) and the release of non-neuronal ACh was shown in isolated tissue such as human placenta and tumor cells (Sastry &

Krishnamurty, 1978; Wessler *et al.*, 2001; Song *et al.*, 2003). More examples can be seen in lymphocytes (Kawashima & Fujii, 2004), as well as in transformed cells and haematopoietic precursors (Wessler *et al.*, 1998; Grando, 2003). ACh is also expressed in non-neuronal brain cells and tissues where it is synthesized in a wide variety of non-neuronal cells such as mesothelial, meninges, blood vessels, immune cells, as well as glia, muscle fibres and parenchymal cells. These groups are presumably cholinceptive (Eckenstein & Sofroniew, 1983; Mesulam, 1988a; Mesulam *et al.*, 1984).

Outside the nervous system, AChE expression has been reported in several cell types, including haematopoietic cells (Soreq & Seidman, 2001), osteoblasts (Genever *et al.*, 1999), endothelial cells (Carvalho *et al.*, 2005) and apoptotic cells (Zang *et al.*, 2002). Within the adult human brain, AChE have been found in areas that lack cholinergic innervations and its distribution in tissue with no corresponding ACh or ChAT has been puzzling biochemists for years (Karczmar, 1969; Silver 1974; Layer & Willbold, 1995). An example is the high concentrations of AChE found in the cerebellum, a brain area containing very few cholinergic synapses. In several brain regions there is a disparity between levels of AChE and ChAT (Silver, 1974) which can be visualized in neurons and compared directly to AChE (Levey *et al.*, 1983; Cuello & Sofroniew, 1985). First evidence of a soluble, secreted form of AChE was identified many years ago during experimental work performed in the adrenal medulla (Chubb & Smith, 1975). Soon after, it was shown that a similar phenomena occurs in the central nervous system (CNS) where AChE can be detected in the cerebrospinal fluid (Chubb *et al.*, 1976). It seemed that, because the levels of AChE in the cerebrospinal fluid were dramatically reduced after an electrolytic lesion of the substantia nigra, that this region must be one of the main origins of the secreted form (Greenfield & Smith, 1979). It was later reported that in the substantia nigra, AChE is secreted from dendrites of non-cholinergic, dopaminergic neurons where AChE appears to extend local neurotrophic effects, thus activating neurons known to respond to dopamine and not AChE (Llinas & Greenfield, 1987; Webb & Greenfield, 1992).

AChE expression has been reported within the cortical pyramidal neurons of the rat brain where it contributes to their maturation and establishment of synaptic connection (Geula *et al.*, 1993). During post-natal development, as shown in the rat brain, non-cholinergic expression of AChE occurs. Here it is expressed in the form of transient activity within certain fibers and terminals in the somatosensory visual and auditory cortices as well as in a large population of cortical pyramidal neurons (Kristt, 1979; Kristt & Waldman, 1982; Robertson *et al.*, 1991; Robertson *et al.*, 1985). The origins of these AChE-rich fiber systems are thalamic neurons which themselves seem to express AChE transiently during postnatal development (Kristt, 1983; Kristt & Waldman, 1981; Robertson, 1987; Robertson, 1988; Robertson *et al.*, 1991). See section 1.6.2.2 for details on the developmental expression of AChE.

Non-neuronal ACh is released from cells, such as epithelial and endothelial cells, and binds to n- and mAChRs and neighbouring cells. Here ACh acts via paracrine, autocrine and juxtacrine mechanisms as a local cell signalling molecule or cytotransmitter controlling multiple cell functions such as proliferation, differentiation, apoptosis, secretion, cytoskeleton organization, lateral migration, ciliary activity, cell-cell contact and immune functions (Grando, 1997; Wessler *et al.*, 1998, 1999, 2003; Kawashima & Fujii, 2000; Grando *et al.*, 2003). Most cell types lacking cholinergic innervation express n- and mAChRs that are part of this autocrine and paracrine regulatory loop. ACh seems to play an intermediary role in the interactions of non-neuronal cells with the external environment, hormones, growth factors, cytokines and also the neural system. These factors can, on the other hand, affect the expression and function of the non-neuronal cholinergic system (reviewed in Wessler & Kirkpatrick, 2008). During signal transduction, additional endogenous compounds are able to stimulate cholinergic receptors too (e.g. Raufman *et al.*, 2003; Alexander *et al.*, 2006), enabling cells to receive input from hormone-like pathways as well as local pathways. These endogenous allosteric modulators play an essential role as sophisticated tools to fine-tune the cholinergic input to a cell. An example is the allosteric modulation of the neuronal $\alpha 4$ subtype receptor through progesterone (Valera *et al.*, 1992).

A wide variety of modulatory functions have been associated with ACh. ACh have been shown to be involved in central respiratory control (Burton *et al.*, 1994; Gillis *et al.*, 1988; Metz, 1958; Murakoshi *et al.*, 1985; Nattie & Li, 1990; Weinstock *et al.*, 1981). Central cholinergic mechanisms contribute to respiratory failure caused by organophosphate poisoning (Lotti, 1991). Both *in vivo* and *in vitro* demonstrations showed that perturbations of ACh synthesis, release, degradation, or activation of AChRs in the brain stem result in perturbations of respiratory pattern (Foutz *et al.*, 1987; Gillis *et al.*, 1988; Nattie & Li, 1990; Burton *et al.*, 1994; Monteau *et al.*, 1990; Murakoshi *et al.*, 1985). ACh release has also been implicated in the modulation of sleep and wakefulness. The pontine reticular formation (PnO) contains an oral component that contributes to the generation of cortical electroencephalogram (EEG) activation and rapid eye movement (REM) sleep (Lydic & Baghdoyan, 2005; Steriade & McCarley, 2005). ACh present in the PnO was found to promote REM sleep (Lydic & Baghdoyan, 2008). Blocking degradation of ACh thus activates the EEG and enhances REM sleep. A role for ACh in the modulation of ion channels has been postulated (e.g. Hevron *et al.*, 1986; Renaudon *et al.*, 1997). An example is the activation of the inward-rectifying potassium channel (IKACH) via the release of ACh from the vagus nerve onto pacemaker cells in the heart (Wickman & Clapham, 1995). ACh, through binding to mAChRs, acts via G-proteins to activate the IKACH channel (Corey *et al.*, 1998). This activation results in an increase of K^+ ions flowing out of the cell and causes the cell to hyperpolarize (Morris & Malbon, 1999). Neurons in hyperpolarized states cannot fire action potentials and this leads to slowing of heartbeat. More examples of modulatory roles for ACh has been demonstrated in the synaptic mechanisms in the cerebral cortex (Krnjevic, 2004), as well as in impulsive action via nAChRs in rats (Tsutsui-Kimura *et al.*, 2010).

A large body of evidence indicates that all elements of the cholinergic system (ChAT and ACh synthesis, AChE, release mechanisms, receptors), functionally expressed independent of cholinergic innervations, can modify and even control phenotypic cell functions (reviewed in Wessler & Kirkpatrick, 2008). Detailed analysis of the regulatory role for non-neuronal ACh have been established for the epidermis by the investigation of intact skin, wound healing and cultured keratinocytes using different techniques such as

knockout mice, antisense RNA and selective agonists and antagonists (Grando *et al.*, 1995, 2006; Chernyavsky *et al.*, 2003, 2004, 2005; Kurzen *et al.*, 2004, 2007). AChE expression was previously shown in fibroblasts and astrocytes (Thullbery *et al.*, 2005), two cell types that play critical roles in wound healing. Anderson *et al.* (2008) investigated the distribution and function of AChE in these cells and reported that fibroblasts and astrocytes express high levels of AChE that co-migrates with recombinant AChE, but contains very little catalytic activity. Elevation of AChE expression was found to increase fibroblast wound healing where addition of anti-AChE antibodies were shown to slow it down. It was reported that AChE surface patches co-localise with amyloid precursor protein (APP) and the extracellular matrix protein, perlecan (independent of α -dystroglycan). It was concluded that cell surface AChE may contribute to a generalized mechanism for polarized membrane protrusion and migration in all adherent cells (Anderson *et al.*, 2008). Studies also show that one of the major nAChR subunits, nAChR α 7, exhibits an essential role in the cholinergic anti-inflammatory pathway (Metz & Tracey, 2005). Although the human skin is not innervated by parasympathetic systems, it prominently expresses distinct nAChR subunits such as nAChR α 7. These subunits are involved in physiological and physiopathological processes such as keratinocyte adhesion, migration, differentiation and apoptosis (Arredondo *et al.*, 2002; Zia *et al.*, 2000; Grando *et al.*, 1995, Chernyavsky *et al.*, 2004). A recent study demonstrated that nAChR α 7 is time-dependantly expressed in distinct cell types, which may be closely involved in inflammatory response and the repair process in wound healing (Fan *et al.*, 2011).

Morphogenetic properties for ACh have also been well documented. In particular, a role for ACh in the promotion of proliferation and suppression of neurite outgrowth, the morphological indicator of differentiation in primitive neural cells, has been proposed (e.g. Biagioni *et al.*, 2000). AChE, by hydrolysing and thus removing ACh, may thus indirectly act as a promoter of neurite outgrowth. Evidence suggests that AChE does, in fact, function in this way (Behra *et al.*, 2002). This AChE function could be classified as non-classical, but enzymatic. A large body of evidence also show non-enzymatic

morphoregulatory effects for AChE on neurons and will be discussed in depth in section 1.6.2.

In the late 1980s, both trypsin-like and carboxypeptidase-like activity was observed in association with AChE. These activities supported the hypothesis that AChE may have a role as a neuropeptide processing enzyme postulated to function in regulating growth and development (Small, 1988; Small, 1990). However, these activities were found to be due to contaminating enzymes (Checler & Vincent, 1989).

Aryl acylamidase activity has also been linked with AChE (Jayanthi *et al.*, 1992). This activity is high during early brain development in the chick, and has also been observed in association with BChE activity (Boopathy & Layer, 2004; Montenegro *et al.*, 2008). The strong association of the activity with both cholinesterases suggests that it may play a role, as yet undetermined, in early development.

1.6.2 Non-classical Functions Related to Development and Differentiation

1.6.2.1 Neurogenesis

During early development, neuronal navigation is essential for establishing the cellular organization and specific nerve connections in the nervous system (Kandel *et al.*, 2000; Sane *et al.*, 2000). The complexity of the decision necessary to specify multiple cell types and to determine their axonal connections is a striking feature of neural development. Morphogenesis requires the directed migration of neural cell precursors to designated locations in the nervous system as well as the guidance of axon growth cones to their synaptic targets (Song & Poo, 2001). Evidence indicates that both forms of navigation depend on common guidance molecules, surface receptors and signal transduction pathways; thus linking receptor activation to cytoskeletal reorganization (Song & Poo, 2001; Hatten, 1999; Mueller, 1999; Tessier-Lavigne & Goodman, 1996). The dorsal margin of the neural tube produces neural crest cells that migrate over long distances and along specific routes to form sensory, autonomic and enteric ganglia in the peripheral

nervous system (Le Douarin *et al.*, 1994). Once their destination is reached, each neuron develops dendrites and a single long axon extending along specific routes to reach prospective synaptic partners (Goodman & Tessier-Lavigne, 1997). Synapse formation requires interaction between pre- and postsynaptic cells to establish connections and so, the formation of a network. Cells that fail to make connections undergo apoptosis or cell death. Apoptosis is a highly complex process involving cell adhesion molecules (CAMs) (e.g. Dransfield *et al.*, 1995), signaling molecules (e.g. Graham *et al.*, 2002), cytokines (e.g. Lotem & Sachs, 1999) as well as growth factors (e.g. Wolff *et al.*, 2007). Thus, there are two phases during development of the nervous system: the migratory phase and the synaptogenic phase, involving the formation of the synaptic network.

Early histochemical studies confirmed the presence of ChE activity during early development in the sea urchin, the amphibian, and the chick and rat brain. It was found that ChE appears in every embryonic blastema at a very early stage of development, independent of innervations. It was interesting to note that this ChE presence disappears from the cells after they have assembled into definite organ structures. ChE thus play a role in embryonic development and its presence in differentiating cells during a limited phase of development is termed “embryonic cholinesterase”. Further observations that ChE is found in cells engaged in morphogenetic movements, led to the belief that the enzyme is involved in the regulation of cellular movements during development (Drews, 1975).

The distribution of ChE activity in neuroepithelial, neural crest, somite, and ectodermal cells was investigated in a comparative, cytochemical study using chick and mouse embryos. Nonspecific staining in these tissues during neurulation showed similar distribution in the two species. AChE staining, however, was found to be absent in the mouse where the only cells showing the presence of this enzyme at these stages of development are blood cells. According to these reports, AChE staining appear later in the brain in neural tissues as well as in some migratory neural crest cells. Although AChE distribution differences in these two species indicate that the timing of the first appearance of AChE is unrelated to neuroepithelial morphogenesis or to neural crest

motility, the correlation between nonspecific cholinesterases and morphogenetic movements is also supported by these findings (Martins-Green & Erickson, 1988).

1.6.2.2 Developmental Expression of Acetylcholinesterase

Analysis of the developmental expression of AChE during neuronal differentiation from a pluripotent stem cell showed that retinoic acid is able to induce differentiation of embryoid bodies into neurons and glia. Undifferentiated stem cells showed no AChE activity, but commitment to a neuronal pathway resulted in increased levels of AChE mRNA, production of a tetrameric form of the enzyme as well as secretion of AChE into the culture medium (Coleman & Taylor, 1996). AChE thus seems to be expressed on the surface of migrating developing neural crest cells. At this point, expression is limited to a hydrophilic tetramer that is secreted into the extracellular matrix. When these cells reach their destinations and adhere and differentiate, AChE expression reaches very high levels and shifts to a membrane associated tetramer. This isoform is anchored in the cell membrane by a post-translationally attached hydrophobic domain rather than association by a glycopospholipid tail. Seeing as no change in the transcription rate of the AChE gene was detected during the course of differentiation, it was suggested that transcription takes place during very early stages of development. Figure 14 shows the temporal relationship of the expression of AChE and BChE to the final stages of cell proliferation, the onset of differentiation and neurite outgrowth.

It was concluded that an early event in neuronal differentiation is the stabilization of mRNA leading to expression of the secreted form of AChE. The transition from secretion of the tetrameric form to its localization on the cell membrane is an important step associated with neurite outgrowth (Coleman & Taylor, 1996). AChE expression in the developing vertebrate brain interestingly corresponds temporally with the major period of axon elongation and pathfinding (Hanneman & Westerfield, 1989; Layer, 1991; Ross *et al.*, 1992; Schlaggar *et al.*, 1993).

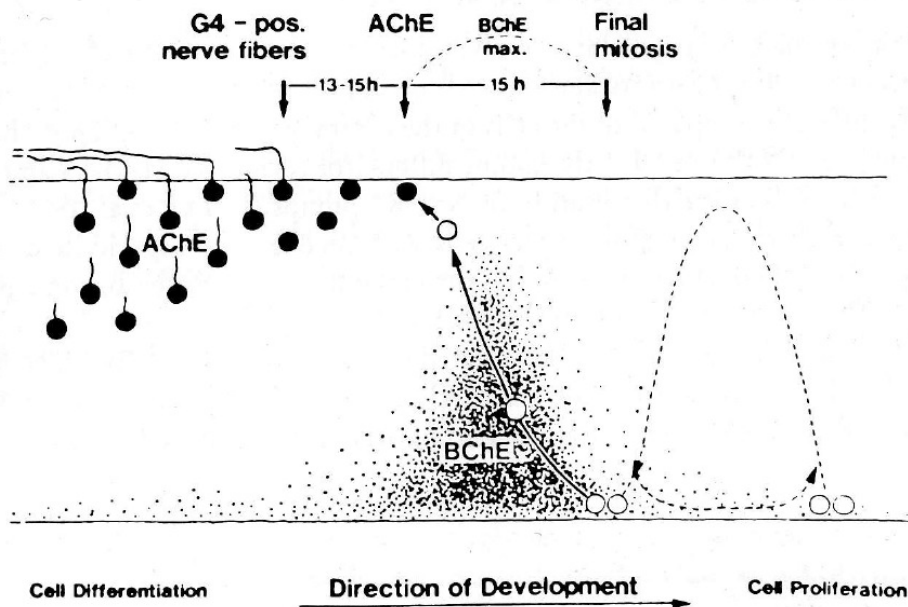


Figure 14. The temporal relationship of the developmental expression of AChE and BChE. BChE is especially expressed during the final stages of mitosis and the onset of differentiation. 13-15 hours after AChE expression is initialized in the cells, G4 positive fibers begin to emanate from the cell bodies and grow toward targets (Layer & Willbold, 1995).

1.6.2.3 Cell Adhesion

It used to be thought that CAMs were simply involved in the anchoring of cells to the extracellular matrix. Recently, however, it has been found that cell adhesion is key to the developmental process and that certain cell surface adhesion molecules play an important part in neuronal navigation (Walsh & Doherty, 1997). During neural development, neural cell adhesion molecules nucleate and maintain groups of cells at key sites (reviewed in Crossin & Krushel, 2000). Cell adhesion impacts on dynamic processes such as intracellular signaling (e.g. Povlsen *et al.*, 2003) and gene expression (e.g. Mahoney *et al.*, 2001), leading to cell migration (Huveneers & Danen, 2009), proliferation (e.g. Fernandez-Vidal *et al.*, 2006), differentiation (e.g. Shin *et al.*, 2002) and survival. Prevention of adhesion suppresses cell growth and induces apoptotic cell death (Boudreau *et al.*, 1995). It seems that these molecules are all active in neural development

(Holmquist, 2000) and their ChE-like domain has been found to be able to act as a protein-protein interaction domain. AChE, being sequentially related to a number of non-enzymatic cell adhesion and signaling molecules (e.g. *Drosophila* glutactin, neurotactin, gliotactin as well as the mammalian neuroligins), may also engage in protein-protein interactions (Paraoanu & Layer, 2008). Although the importance of the electrostatic potential of AChE is disputed (Shafferman *et al.*, 1994), it is also well known that electrostatic interactions can facilitate target recognition via protein-complex formation. Seeing as all the ChE-like adhesion molecules display similar electrostatic characteristics, it strongly supports the notion that AChE can function as a CAM (Botti *et al.*, 1998; Shafferman *et al.*, 1994).

1.6.2.4 Neuritogenesis

Neurotransmitters have long been associated with non-classical functions related to neural differentiation. Some examples include studies showing how glutamate, serotonin and dopamine influence neurite outgrowth in culture (Mattson, 1988; Lipton & Kater, 1989). Many studies have demonstrated that the expression of AChE during early development can be closely correlated with the major phase of neurite outgrowth (Layer *et al.*, 1988; 1992; Layer, 1991; Layer & Kaulich, 1991; Robertson, 1987; Robertson *et al.*, 1988; Robertson & Yu, 1993; Small *et al.*, 1992). It was observed that the expression of AChE is a very early step in postmitotic neurons (Layer & Sporns, 1987), occurring prior to neurotrophic processes in brain tissues, cultured spheroids (Layer *et al.*, 1988; Weikert *et al.*, 1990) and non-cholinergic neurons in the rat thalamus (Kristt, 1989). Cell adhesion is also a major mechanism to direct neurite outgrowth. Given that AChE may function as a cell adhesion molecule, a role for AChE in neuritogenesis is not unlikely.

In 1993, Layer *et al.* (1993) provided the first direct evidence for a role of AChE in regulating neuritic growth. It was shown that neurite growth can be modified *in vitro* by some anti-ChEs. The catalytic- and peripheral anionic-site blocking inhibitor, BW284c51, was found to decrease neurite outgrowth. On the other hand, echothiopate, an inhibitor that blocks only the esterase activity, had no effect on neurite outgrowth,

indicating that this non-classical role is not the result of enzyme activity. A secondary site on cholinesterase molecules may be responsible for these adhesive functions (Layer *et al.*, 1993). Addition of fasciculin 2, a potent blocker of the peripheral site alone, induced a similar reduction in neurite growth (de La Escalera *et al.*, 1990), indicating the PAS as a possible site of interest associated with these functions.

Various other studies (e.g. Small *et al.*, 1995; Keymer *et al.*, 1998; Anderson and Key 1999) have also noted similar effects of AChE inhibitors on neurite outgrowth in neural cells. The same pattern, that is, inhibition of neurite outgrowth by PAS-binding inhibitors such as BW284c51 and fasciculin 2, but not with active site inhibitors such as ecothiophate or eserine, was observed throughout.

Addition of AChE or pre-coating plates with AChE also induces neurite sprouting. Bataillé *et al.* (1998) showed that addition of purified AChE to the culture medium of embryonic spinal rat motoneurons affected neurite growth. It was reported that when AChE was added, the surface as well as the total length of the neurites and axons were increased. Several other studies, in particular, Jones *et al.* (1995), using dopaminergic neurons, Munoz *et al.* (1999), using rat spinal cord neurons, Olivera *et al.* (2003), using hippocampal neurons, and Srivatsan and Peretz (1997), in *Aplysia* (a marine mollusc) used similar methods, and obtained similar results. All these studies indicated a role for AChE in the promotion of neurite outgrowth, and suggested that this role was non-enzymatic, although Bataille *et al.* (1998) observed some slight effects (slight decrease in the number of primary neurites as well as a decrease in the spreading index during the first three days in culture) after addition of the active site inhibitor ecothiophate. In contrast with Layer (1993), this study shows the possible involvement of both catalytic and non-catalytic mechanisms, but suggesting significant involvement of the PAS. Given that ACh can act as a suppressor of neurite outgrowth (e.g. Biagioni *et al.*, 2000), and that AChE has been shown to indirectly enhance neurite outgrowth by hydrolyzing (removing) ACh (Behra *et al.*, 2002), these results could be indicative of this catalytic non-classical function of AChE. On the other hand, AChE active site inhibitors, in

particular the organophosphates, are able to induce neurotoxicity by mechanisms other than AChE inhibition (reviewed in Costa, 2006).

Other studies have investigated AChE-mediated neurite outgrowth using different neural cell types cultured on a coating of AChE, rather than adding the AChE to the culture medium. These include Small *et al.* (1995) using isolated chick sympathetic neurons, and Johnson and Moore (2000) using human neuroblastoma cells. Similar effects on neurite outgrowth were seen. Small *et al.* (1995), however, noted that these effects seemed dependant upon the presence of substratum-bound heparan sulfate proteoglycans (HSPG).

Although experiments using inhibitors or the external addition of AChE to the culture medium or to the substratum demonstrate a possible morphogenetic role for AChE, studies in which the levels of AChE are changed within the neuron itself are more definitive. The effects of cell transfection with AChE cDNA has been reported by a number of authors: Karpel *et al.* (1996) using rat glioma cells, Koenigsberger *et al.* (1997), Sharma *et al.* (2001) and De Jaco *et al.* (2002), all using various neuroblastoma cell lines. All observed a correlation between AChE overexpression and increased neurite outgrowth. Lev-Lehman *et al.* (2000) described excessive neurite outgrowth in transgenic mice that overexpressed AChE in motoneurons.

Several studies have investigated the possible differential effects of the AChE splice variants on neurite outgrowth. Karpel *et al.* (1996), using transfection of rat glioma cells, observed that, while the most prevalent E6 splice variant (synaptic/tailed AChE) promoted neurite outgrowth, the less common stress-related readthrough form (AChE-R) did not. Promotion of neurite outgrowth was observed to be unrelated to catalysis but not the readthrough form (AChE-R). Sternfeld *et al.* (1998), likewise, showed a dominant role for the E6-derived AChE-T in neurite outgrowth, and also confirmed that the process was non-enzymatic. As the splice variants differ at their C-termini, it would be logical to conclude that the C-terminus is directly involved in the neurite outgrowth process. However, it should also be borne in mind that factors such as differences in

oligomerisation and possibly in conformation between the different variants may play a part as well. De Jaco *et al.* (2002), however, did not observe differences between the splice variants in their ability to promote neurite outgrowth.

The evidence concerning the effects of oligomerisation on cell adhesion and neurite outgrowth is relatively scanty and somewhat conflicting. Day and Greenfield (2002) suggested that only AChE monomers were involved. On the other hand, the isoforms associated with migration and differentiation, and hence with cell adhesion and neurite outgrowth, are tetramers (e.g. Layer & Willbold, 1995; Johnson & Moore, 2000), both the secreted hydrophilic G4 and, later, the membrane-associated G4. In the crystal structure of the mouse tetramer, Bourne *et al.* (1999) observed that the PAS is obscured in two of the four catalytic domains, so that, if the PAS is indeed involved in promoting these processes, the overall efficacy of the molecule would be compromised.

Treatment of cells with anti-AChE antibodies was observed to have an inhibitory effect on neurite outgrowth. Sharma and Bigbee (1998) and Sharma *et al.* (2001) used a polyclonal anti-AChE antibody, and Johnson and Moore (2000) used a variety of monoclonal antibodies, several of which were known to recognise the PAS specifically. These PAS-binding antibodies were also found to affect the adhesion of neuroblastoma cells to the substratum: antibody treatment resulted in the cells rounding up, floating, and subsequently dying, an observation consistent with the concept of anoikis (cell death as result of loss of cell adhesion). The deleterious effects of anti-AChE antibodies on neural cells suggest that AChE is necessary for cell survival, adhesion and neurite outgrowth.

The consistent effects of PAS-binding inhibitors, such as BW284c51 and fasciculin 2, as well as the effects of PAS-reacting monoclonal antibodies, strongly suggest involvement of the PAS in AChE-mediated cell adhesion and neurite outgrowth. The involvement of the PAS in the adhesion-mediating and neurite outgrowth-promoting processes was confirmed (Johnson & Moore, 1999). On the other hand, Greenfield *et al.* (2008), present evidence for the involvement of C-terminal peptides in both neurite outgrowth and apoptosis.

1.6.2.5 AChE complexation and the identification of potential AChE ligands

There are two sites on the AChE molecule that appear to be particularly responsive to ligand binding and complex formation. One of these is obviously the C-terminal T-peptide which is responsible for oligomerisation and the association of AChE with the anchoring proteins ColQ and PRiMA. Interestingly, the T-peptide aligns with the amyloid precursor protein (APP), in particular, the region of APP that cleaves to form the amyloid beta-peptide (Greenfield & Vaux, 2002), which is primarily responsible for the formation of senile plaques in Alzheimer's disease. Furthermore, Cottingham *et al.* (2002; 2003) have shown that isolated AChE T-peptides are themselves capable of forming amyloid-like fibrils. Greenfield's group (e.g. Day & Greenfield, 2002) has shown that a peptide derived from the T-peptide is capable of promoting neurite outgrowth at low concentrations, and apoptosis in higher concentrations, with the involvement of the nAChR.

In the neuromuscular junction, AChE associates with heparan sulfate proteoglycans (particularly perlecan) in the basal lamina. This interaction is mediated, not through a part of the AChE protein, but by ColQ. Interestingly, Anderson *et al.* (2008) observed an association of AChE with both APP and perlecan in the cell membranes of fibroblasts and astrocytes (where it would not normally be anchored by ColQ), forming an apparently novel signalling complex that might contribute to membrane protrusion and cell migration.

AChE has been observed to bind a number of ligands at the PAS. These include the amyloid beta-peptide, laminin-111, collagen IV, the prion protein and fibronectin. The amyloid beta-peptide was observed to bind a hydrophobic loop containing the PAS residue W286 (residues 274-308, *Torpedo* numbering; De Ferrari *et al.*, 2001). Interestingly, a very recent article (Dinamarca *et al.*, 2011) has shown that the AChE homologue neuroligin-1, is also capable of binding the amyloid- β peptide. Johnson and Moore (2003) observed binding of AChE to the extracellular matrix proteins laminin-111 and collagen IV. The binding to laminin was later localised to the laminin α 1 chain

(Johnson *et al.* 2008a and this thesis); Paraoanu and Layer (2005), however, observed binding to domain IV of the $\beta 1$ chain. Interactions of AChE with the prion protein (Clos *et al.* 2006) and fibronectin (Giordano *et al.* 2006), also apparently mediated by the PAS, as shown by the blocking effects of PAS-binding inhibitors, have also been observed. Bigbee and Sharma (2004), using a blot overlay technique, identified potential AChE ligands of MW 200, 110, 35 and 33 kDa, respectively. These proteins were not identified.

1.6.2.6 The role of electrostatics in AChE-mediated cell adhesion and neurite outgrowth

The PAS, as its name indicates, is anionic in nature. Botti *et al.* (1998) have described a characteristic ring-shaped motif of negative charge surrounding the entrance to the active site gorge. This motif is apparent in AChE, as well as in the CLAMS neuroligin, gliotactin, neurotactin, and glutactin, all of which have been observed to mediate cell adhesion, but not in BChE, which does not. On this basis, they, as described above, termed these proteins “electrotactins”, as electrostatics appeared likely to play a major role in the adhesion process. The role of electrostatics in AChE-mediated cell adhesion and neurite outgrowth has been confirmed by Johnson and Moore (2003) and Bigbee and Sharma (2004).

1.6.3 Non-Classical Role in Degeneration

Disorders such as Alzheimer’s , Parkinson’s, Creutzfeldt-Jacob disease, and other diseases such as Lewy body dementia and Guam syndrome, are all mostly characterized by the progressive loss of cognition due to degeneration of cholinergic neurons in the basal forebrain. Although these disorders are all distinct, they share an underlying common neurodegenerative mechanism (Calne *et al.*, 1986; Greenfield And Vaux, 2002).

1.6.3.1 Amyloid & Fibril Formation

Protein misfolding underlies an array of debilitating human diseases called conformational diseases (Fersht, 1999). Proteins can often convert from their normally soluble forms to insoluble fibrils or plaques called amyloids (as introduced by Virchow (1851), meaning “starch-like”), which accumulate in a variety of organs, affecting normal functioning thereof (Tan & Pepys, 1994; Kelly, 1998; Lansbury, 1999; Perutz, 1999). These fibrils are typically 60-100Å in diameter and exhibit a characteristic apple-green birefringence when stained with the dye Congo Red (Sipe, 1994; Kelly, 1996). Aggregation of amyloid is an important process in a wide variety of abnormal diseases including Alzheimer’s and Parkinson’s disease (AD & PD), type II diabetes, the transmissible spongiform encephalopathies, amyloidotic polyneuropathies and a range of less familiar conditions such as fatal familial insomnia (Tan & Pepys, 1994; Fink, 1998).

In Alzheimer’s disease, the key component of extracellular plaques is the 40-42 residue A β peptide that is produced by endoproteolytic cleavage of the amyloid protein precursor (APP) (Evin *et al.*, 1994). Aggregation (fibril formation) of the peptide has been shown to be mediated by a multi-step nucleation-dependant polymerization process that is critically dependant on pH and ionic strength (Snyder *et al.*, 1994). Amyloid fibrils have been found to associate with plasma and extracellular matrix molecules to form amyloid deposits that invade the extracellular space (Tan & Pepys, 1994; Merlini & Bellotti, 2003).

The structure of A β enables it to bind to a variety of biomolecules such as lipids, proteins and proteoglycans as well as to interact with the cellular membrane. It has been observed to bind to apoE, amongst other lipoproteins. ApoE is found in an array of amyloid deposits such as A β in AD, prion in Creutzfeldt-Jakob disease as well as in light chain amyloidosis. It seems to co-localize in all amyloid deposits and is found to specifically interact with fibrils *in vitro* (Namda *et al.*, 1991). The apoE4 allele is a risk factor for late-onset AD.

Several constituents normally present in the ECM are also found in neuritic plaques including proteoglycans, perlecan, collagen IV, entactin, fibronectin, nidogen, AChE and BChE (Inestrosa, 1988; Brandan & Inestrosa, 1993). During amyloidosis, the major basement membrane components (collagen, entactin, laminin, perlecan) codeposit both spatially and temporally with A β (Ancsin, 1999). Even though laminin was found to bind A β , it seems to be a potent inhibitor of A β fibril formation (Castillo *et al.*, 2000).

1.6.3.2 Acetylcholinesterase and Neurodegenerative Disorders: Alzheimer's Disease

The cholinergic aspects of this disease involve synaptic and neuronal loss particularly of targeted cholinergic neurons in the basal forebrain, an area concerned with memory and cognition (Whitehouse *et al.*, 1982). Dystrophic neurons contain AChE and they are incorporated in the peripheral area of senile plaques and stain positive for phosphorylated tau (Kasa *et al.*, 2003).

AChE seems to be the common feature shared by the different neuronal groups in which lesions occur (Smith & Cuello, 1984). AD brains show neurochemical changes that include loss of AChE and ChAT activity associated with cortical cholinergic axons and cholinceptive neurons. Therapeutic interventions to treat the characteristic loss of memory and cognitive deficits associated with AD are AChE inhibitors, which, in fact, are the only drugs approved for the treatment of Alzheimer's symptoms. BChE activity, on the other hand, is found to increase in AD (Perry, 1980). This increase in activity could possibly be a method of compensation for the loss of AChE activity.

It seems that most areas of the brain susceptible to plaque and tangle formation are highly AChE and BChE positive (Hirano & Zimmerman, 1962; Ishii, 1966; Ishino & Otsuko, 1975; Kemper, 1984; Mesulam *et al.*, 1984; Smith & Couello, 1984; McDuff & Sumi, 1985), and both proteins are associated with the plaques. Reports show that the cytotoxicity of amyloid complexes increase as the concentration of AChE increase (Munoz & Inestrosa, 1999). The association of BChE with amyloid plaques seems to correspond with when A β deposits assume the compact β -sheet conformation, suggesting

that BChE may participate in the transformation of A β from a benign to the malignant form found in neurodegeneration (Guillozet *et al.*, 1997).

Although the impact of disturbed cholinergic innervation on plaque formation has been documented (Price *et al.*, 1982), the deposition of AChE seems to be unrelated to cholinergic neuron degeneration. Plaque-associated AChE differs from uncomplexed AChE in its reaction with inhibitors (Mesulam *et al.*, 1987; Geula & Mesulam, 1989). The enzymatic properties of tangle and plaque-associated AChE diverge from the AChE of normal axons or cell bodies. Another possible explanation is that binding to amyloid blocks or affects the sites to which the PAS-binding inhibitors bind.

The *in vivo* colocalization of AChE and A β was recreated *in vitro* to investigate whether these actions occur and if so, how they influence the process leading to amyloid deposition (Inestrosa *et al.*, 1996). It was reported that bovine brain AChE, as well as the human and mouse recombinant enzyme, accelerated amyloid formation independent of the subunit array of the enzyme. This action was not affected by the active site inhibitor edrophonium, but addition of the PAS ligand, propidium, did show an effect. On the other hand, BChE, lacking the peripheral site, did not affect amyloid formation. From this study it seems that AChE may play a role in accelerating A β formation and function in amyloid deposition (Inestrosa *et al.*, 1996).

Through the process of complex formation with growing fibrils, AChE has been shown to promote the aggregation of A β -peptide. This process was found to be resistant to high ionic strength treatment suggesting that hydrophobic interactions play a role in stabilizing the complex (Alvarez *et al.*, 1997). Reyes and colleagues (1997) observed that a PAS-reacting monoclonal antibody inhibited AChE induction of amyloid formation. De Ferrari *et al.* 2001b, using protein docking and synthetic peptides, identified the amyloid-binding site on AChE. This was found to be the hydrophobic peptide 274-308, which incorporates the PAS residue W286.

Much of the current research on AChE and AD is concerned with the discovery and development of new AChE inhibitors, in particular, inhibitors that are capable of addressing both the cholinergic deficit and amyloid formation. Such inhibitors would bind simultaneously to the active site, to inactivate and address the cholinergic deficit, and to the PAS, to block the AChE-A β -peptide interaction and thus control amyloidosis (for reviews on this topic see Castro & Martinez, 2006; Munoz-Torrero *et al.*, 2008; Galdeano *et al.*, 2010). On the basic research side, Garcia-Ayllon *et al.* (2011) have suggested the possibility that the amyloid beta-peptide and P-tau interact through AChE, and Dinamarca *et al.* (2011) have shown that neuroligin (the CLAM AChE homologue) is also capable of interacting with the amyloid beta-peptide and promoting amyloidosis.

1.6.4 Acetylcholinesterase and Cancer

A role for ChEs in tumorigenesis has been proposed. It seems that both the AChE and BChE genes are amplified, mutated or expressed in a variety of human tumor types (Montenegro *et al.*, 2005; 2006; Perry *et al.*, 2002; Vidal, 2005; Zakut *et al.*, 1990; Lapidot-Lifson *et al.*, 1989). As a very broad generalization, the patterns of amplification and expression follow those observed during neural development, with an association of BChE with proliferation and AChE with differentiation. However, there are numerous variations on this pattern. It may be that the amplification and expression of the ChEs in neoplasia is dependent upon the specific tissue from which the tumour was derived. These genes are located within regions subject to non-random chromosomal abnormalities associated with myelodysplastic syndromes (MDS) and acute myeloid leukemia (AML) (Kere *et al.*, 1989a, 1989b; Kere, 1989). Deletions of the AChE locus is associated with MDS and AML, reinforcing the possibility that AChE may play a role as a myeloid suppressor gene (Stephenson *et al.*, 1996). A study investigating amplifications and deletions in the AChE and BChE genes in sporadic breast tumor cells found tumor malignancy grade to be positively correlated to the number of alterations of the BChE gene, and tumor size to be significantly higher when the AChE gene was amplified (Bernardi *et al.*, 2010). Furthermore, translocations in 7q22 were shown to define a critical region associated with uterine leiomyomas (Sargent *et al.*, 1994).

The consensus peptide motif S/T-P-X-Z, which is found in many substrates of cell division control protein 2 or cdc2-related protein kinases, is also present in both AChE and BChE. Cdc2 kinases are master regulators of G2/M transition during the eukaryotic cell cycle and its phosphorylation activity has been linked to a variety of cell cycle abnormalities that could be involved in cancer formation (e.g. Hosoya *et al.*, 1994; Furukawa *et al.*, 2000). Soreq and colleagues proposed the possibility that phosphorylation by cdc2-related kinases may be the molecular mechanism linking cholinesterases with tumor cell proliferation (Grifman *et al.*, 1997). Organophosphorus compounds have been known to induce tumorigenic risks (Soreq & Zakut, 1993; Brown *et al.*, 1991).

The haematopoietic effects of AChE have also been postulated (Kawashima & Fujii, 2003a, 2003b). These effects include reduction in proliferation of multipotent stem cells committed to erythropoiesis, megakaryocytopoiesis and macrophage production, and promotion of apoptosis in their progeny (Soreq *et al.*, 1994). Constitutional rearrangements of 7q22 have also been found to lead to haematopoietic malignancies (Forrest & Lee, 2002), affects that are reportedly attributed to the non-catalytic properties of AChE-R (Grisaru *et al.*, 2001; Deutsch *et al.*, 2002). AChE-R has been shown to interact with protein kinase C in glioblastoma cells where it elicits a cellular signal transduction response that promotes tumorigenesis (Perry *et al.*, 2004).

Alterations in CAM expression have been shown to be significant in the development of tumors, specifically in the regulation of proliferation and apoptosis, cellular motility and invasion, as well as the cell surface localization of metalloproteinase angiogenesis (reviewed Varner & Cheresch, 1996). Our own as well as other evidence show that AChE is able to promote cell adhesion and differentiation in immature and malignant neural cells (Layer & Wilbold, 1995).

1.7 The Basement Membrane: Importance of Laminin

Basement membranes (BM) consist of thin sheets of highly specialized ECM molecules. They are present at the epithelial/mesenchymal interface of most tissue surrounding muscle, peripheral nerve fibers as well as fat cells. Components of the BM are able to regulate biological activities such as cell growth, differentiation and migration and they have been found to influence tissue development and repair (Couchman & Woods, 1993; Aumailley & Krieg, 1996; Timpl, 1996; Aumailley & Gayraud, 1998). Laminins, entactin-1/nidogen-1, collagen IV and HSPGs are contained within all BMs (Fitch & Lisenmayer, 1994; Timpl & Brown, 1996). The electron dense region of the BM, called the lamina densa, predominantly consists of polymeric networks of collagen and laminin integrated by crosslinkers like nidogen and perlecan (Ghohestani *et al.*, 2001). Assembly of the BM depends on the polymerization of two independent networks. The first type of assembly involves collagen IV, which becomes covalently stabilized (Yurchenco & Schittny, 1990). The second type involves polymerization of laminin, and this assembly is non-covalent and calcium-dependant. These two networks are connected by entactin (Yurchenco *et al.*, 1992).

Laminin proteins are large (400-900 kDa), four armed, heterotrimeric glycoproteins that are composed of various combinations of α , β , and γ chains (Figure 15; Miner & Yurchenco, 2004). The four arms consist of three shorter arms that can bind other laminin molecules forming sheets, and one longer arm that can bind to cells and thus help anchor the actual organs to the membrane. There are 16 known laminins in mammals and these proteins play a significant role in BM architecture and function (Aumailley *et al.*, 2005; reviewed Tzu & Marinkovich, 2008). Laminins bind cells via high affinity receptors and mediate attachment, migration and organization of cells into tissue during development by interacting with other ECM components (Nurcombe *et al.*, 1989; Tzu & Marinkovich, 2008). During embryogenesis, laminin-111, previously called laminin-1 (Aumailley *et al.*, 2005), is the first synthesized component of the BM and plays an important role in embryonic development (Miner *et al.*, 1997; Aumailley *et al.*, 2000; Colognato & Yurchenco, 2000). Serum IgG anti-laminin-111 autoantibodies have been associated with recurrent first-trimester miscarriages and studies reported a significant association of these antibodies with endometriosis in infertile patients. It seems that the presence of

anti-laminin autoantibodies results in abortion (Inagaki *et al.*, 2003, 2001, 2005). The ability of laminin-111 to promote migration of neural crest cells enables the preferential migration of these cells along the basal lamina. The interaction of neural crest cells with laminin-111 involves two major cell binding domains that are both recognized by the $\alpha1\beta1$ integrin and it was found that $\alpha1\beta1$ integrin is able to elicit different cellular responses depending on the laminin-111 domain it interacts with (Desban & Duband, 1997).

Laminin is able to self-assemble into a polymer via a reversible, entropy-driven and calcium facilitated process, *in vitro*. This self-assembly is dependant upon the short-arm globular domains (Yurchenco *et al.*, 1992). Polymerisation was shown to require the interaction of all three ligands, one from each short arm, through calcium activated assembly (Yurchenco & Cheng, 1993). Ligands identified for laminin include nidogen (entactin), fibulin, thrombospondin, HSPG (heparin), perlecan, agrin, and collagen IV (Tzu & Marinkovich, 2008; Chen *et al.*, 1999; Schneider *et al.*, 2006; Mecham, 1991). The induction of AChR clustering is an important step during the development of the neuromuscular junction (Fertuck & Salpeter, 1976). Laminin is able to induce AChR clustering; however, it was found that laminin-111 induces AChR clustering by a pathway independent of that used by neural agrin (Sugiyama *et al.*, 1997).

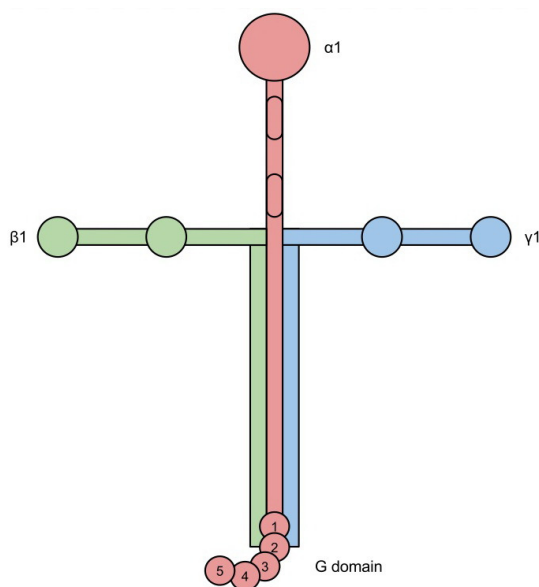


Figure 15. Laminin molecule. Structure of the laminin-111 molecule showing the $\alpha1$ chain, containing the G binding domains; the $\beta1$ and $\gamma1$ chains.

Laminin is induced by brain injury and colocalizes with $A\beta$ -deposits in AD brains (Engel, 1992; Liesi *et al.*, 1984, 1989;

Murtomaki *et al.*, 1992). Through a binding site on the α chain, laminin is able to bind A β with relatively high affinity (Castillo *et al.*, 2000), and its binding with APP has also been reported (Koo *et al.*, 1993). It was found that laminin is able to inhibit the formation of amyloid fibrils (Bronfman *et al.*, 1996; Castillo *et al.*, 2000). Related findings suggest that laminin may be effective as a therapeutic agent in AD (Monji *et al.*, 1998).

1.8 Work leading up to the thesis

1.8.1 Non-Classical AChE Binding Partners and Binding Sites

Interactions of AChE with a number of proteins and peptides have been reported. Our own as well as other evidence show that AChE is able to interact with laminin-111, (Johnson & Moore, 2003; Paraoanu & Layer, 2004). AChE is also able to interact with collagen IV and this interaction, along with the laminin-111 interaction, was shown to involve electrostatic mechanisms associated with the PAS (Johnson & Moore, 2003). By use of the yeast two-hybrid method, Paraoanu and Layer (2004) identified an interaction between the globular IV (G4) domain of laminin chain β 1 and the amino acids 240-503 of mouse AChE. Results suggested that through this interaction, AChE is able to exert changes in adhesion signalling pathways (Paraoanu & Layer, 2004). AChE was shown to modulate neurite outgrowth through interactions with fibronectin (Giordano *et al.*, 2007). Associations of asymmetric AChE with glycosaminoglycans and fibronectin have also been suggested to bind AChE to the basal lamina (Massoulie & Bon, 1982). Interactions of AChE with the nicotinic ACh receptor (Greenfield *et al.*, 2004) as well as with A β (De Ferrari *et al.*, 2001b) have been reported. Pera *et al.* (2006) identified that AChE is able to bind and initiate the aggregation of prion protein (PrP) (Pera *et al.*, 2006). The collagen tail of the asymmetric forms of AChE has been found to bind heparin, supporting the proposed concept that the asymmetric AChE forms are immobilized on the synaptic basal lamina via interactions with heparin-like molecules probably related to HSPGs (Brandan

& Inestrosa, 1984). Bigbee and Sharma (2004) observed an association of AChE with four as yet unidentified proteins of MW 200, 100, 35 and 33 kDa, respectively.

Studies have shown that the AChE site that mediates cell adhesion is localized to the PAS (Johnson & Moore, 1999; Munoz *et al.*, 1999; Olivera *et al.*, 2003). Johnson and Moore (2004) have recently identified the site more precisely using synthetic peptides. The site was defined as a discontinuous (conformational) structure involving the participation of residues from a number of surface loops in the area of the PAS. Its most striking characteristic is its strong negative charge (supporting the “electrotactin” characterization) and its high degree of flexibility, caused by movement of the loops (Johnson & Moore, 2004).

Greenfield and colleagues also proposed an important role for the C-terminal peptide of AChE. It was reported that this site promotes outgrowth of neurites in low concentrations and apoptosis in higher concentrations (Day & Greenfield, 2003). The C-terminal peptide seems to interact with the nicotinic AChE receptors (Greenfield *et al.*, 2004; Zbarsky *et al.*, 2004). This peptide also shares sequence similarities with APP (Greenfield & Vaux, 2002) and have been found to be amyloidogenic (Cottingham *et al.*, 2003). The physiological relevance of this peptide, as well as Greenfield’s proposal that monomers alone promote non-classical functions, could possibly need some revision as it is located in the part of the AChE sequence involved in oligomerisation.

1.8.1 The AChE Knockout and Functional Redundancy

Although the *in vitro* evidence, particularly the studies using anti-AChE antibodies which induced apoptosis in treated cells, suggests that AChE is essential for the survival and normal development of neural precursors, the AChE knockout mouse survives. Investigation showed that BChE compensates for the lack of AChE in cholinergic synapses and neuromuscular junctions, taking over its synaptic function (Xie *et al.*, 2000). However, BChE has not generally been observed to promote non-cholinergic cell adhesion (Johnson & Moore, 2000; Mack & Robitzki, 2000), and so is unlikely to replace

AChE in this context. Nevertheless, the knockout has severe developmental abnormalities: it is largely immobile, with defects in muscle structure and function (Vignaud *et al.*, 2008), it requires a liquid diet in order to survive, has significant behavioural abnormalities, and has nervous system defects, in particular, in the development of the eye (Bytyqi *et al.*, 2004). Abnormalities associated with eye development, in particular, suggest the presence of non-classical functions, and that AChE is indispensable in this context.

Another *in vivo* study using catalytically inactive, but otherwise structurally intact, AChE in the zebrafish showed little evidence for non-cholinergic developmental functions as the zebrafish does not have compensating BChE. AChE activity was found to be necessary for development and maintenance of the axial muscle apparatus as well as for survival of primary sensory neurons, providing evidence of cholinergic non-classical functions (Behra *et al.*, 2002).

Cousin *et al.* (2005) published a highly critical paper on the non-classical functions of AChE stating that neither the invertebrate (*C. elegans*, *D. melanogaster*) nor the vertebrate models (zebrafish and mouse) provide strong enough evidence in favor of these functions. It was proposed that in all aspects so far studied, *in vivo*, the loss of function of AChE in these systems is responsible for the appearance of several phenotypes and that these phenotypes can be explained by an excess of the undergraded substrate, ACh, resulting in loss of function and pathological alterations. Furthermore, the observed phenotypes could solely be a consequence of the lack of AChE catalytic activity in the mutants as none of them appears to require the postulated adhesive or other non-catalytic functions (Cousin *et al.*, 2005).

An obvious discrepancy exists between the *in vivo* evidence of the knockouts and the documented interactions and effects *in vitro*. Presuming that AChE is indeed capable of producing said effects *in vitro*, a possible explanation, reconciling both sides of the debate, could be that of functional redundancy. The number of knockouts reported with no associated phenotype suggests that redundancy is fairly common in higher organisms.

Redundancy seems to appear more frequently in proteins expressed in developmental, rather than ‘housekeeping,’ context, possibly because these proteins tend to be expressed in precise spatiotemporal pattern with a relatively smaller margin for error. Here redundancy may promote robustness by providing a back-up or fail-safe device. The fact remains that AChE is evolved almost perfectly to fulfil another function (ACh hydrolysis), and it may be that the adhesion function may have developed fortuitously as a back-up for a critical interaction.

1.9 Aims of the Thesis

The overall aim of this thesis was the characterisation of the AChE-laminin interaction, relating specifically to both cell adhesion and neurite outgrowth in neural development, and amyloidosis in neurodegeneration. A further problem that was addressed was the apparent discrepancy between the evidence suggesting the importance and necessity of AChE for neural development, and the largely normal phenotype of the AChE knockout mouse. The hypothesis that AChE in its non-classical role as a cell adhesion molecule is functionally redundant was proposed.

Specific Aims:

1. Demonstration of the interaction between AChE and laminin-111 (using ELISA and Co-IP);
2. Definition and characterisation of the laminin-binding site on AChE (using phage display, peptide array, molecular modelling and docking);
3. Definition and characterisation of the AChE-binding site on laminin-111 (using phage display, molecular modelling and docking);
4. Identification of molecules that are expressed during the migration and differentiation of neural precursors and also the Alzheimer’s-affected brain, which structurally mimic characteristics of the AChE-laminin interaction, and thus with which this interaction may show functional redundancy (using bioinformatics).

2. Materials and Methods

2.1 Materials

2.1.1 Instruments

Autoclave: Speedy autoclave HL-340	HLMC Co., Taipei, Taiwan
Balances: Sartorius Weighing Instrument	Cape Scientific, Cape Town, SA
Cell culture hood: Bio-Flow	Hospital & Lab Solutions, Cape Town, SA
Centrifuge: Sorvall® RC-5B Refrigerated Superspeed Centrifuge	Du Pont Instruments, West Virginia, USA
Centrifuge: Eppendorf Centrifuge 5417R	Merck, Germiston, SA
Dounce homogeniser	Cole-Parmer, Vernon Hills, USA
Electrophoresis tank/SDS gel tank: Mini-PROTEAN® Tetracell	BioRad Laboratories Ltd., Johannesburg, SA
Electrophoresis and blotting power supply	Consort E844, Belgium
Hägar HB2 Dry Block Heater	Hägar Designs HB2, Wildernis, SA
Incubator for neuroblastoma cells (CO ₂)	Thermo Electron Corp., Ohio, USA
Laminar flow hood: Class II Biohazard	VividAir, Durban, SA
Magnetic stirring plates	FMH Instruments, Lasec, SA
Multipipette	Nichipet EX, Nichiryo, Japan
Microscope	Nikon, SA
Oak Ridge centrifuge tubes	Nalgene Centrifuge Ware, USA
pH meter: Orion 3star porTable	Thermo Scientific, Johannerburg, SA
Pipettes	Gilson Pipetman, Middleton, Wisconsin, USA
Pipetting device: Pipetteboy	Integra Biosciences, Zürich, Switzerland
Polyallomer SW41 tube	Beckman Coulter, Cape Town, SA
Rocker: 25	MainLab Services, Labnet, Cape Town, SA
Spectrophotometer: Ultraspec	LKB Biochrom, Cambridge, UK

Vortex	VELP Scientifica, Usmate, Italy
Waterbaths: Labcon	MainLab Services, Cape Town, SA
Western blotting tank: Mini Trans-Blot® Cell	BioRad Laboratories Ltd., Johannesburg, SA

2.1.2 Reagents/Chemicals

ABTS (2,2'-azino-bis(3-ethylbenzthiazoline-6-sulphonic acid))	Sigma, St Louis, Missouri, USA
Acrylamide/Bis solution	BioRad Laboratories Ltd., Johannesburg, SA
Agar bacteriological (Bacto agar)	Merck, Darmstadt, Germany
Ammonium persulfate	Sigma, St Louis, Missouri, USA
BSA (Albumin, bovine serum)	Sigma, St Louis, Missouri, USA
Bacto-tryptone	Sigma, St Louis, Missouri, USA
Biotin, NHS (N Hydroxysuccinimido ester)	Sigma, St Louis, Missouri, USA
Bromophenol blue	Sigma, St Louis, Missouri, USA
Butanol	Sigma, St Louis, Missouri, USA
BW284c51 (1,5-bis [4-allyldimethylammoniumphenyl] pentan-3-one dibromide)	Sigma, St Louis, Missouri, USA
Chloroform	Merck, Darmstadt, Germany
DMF (N,N-Dimethylformamide)	Fluka Chemika, Johannesburg, SA
DMSO (Dimethyl sulfoxide)	Fluka Chemika, Johannesburg, SA
DTT (Dithiothreitol)	Fluka Chemika, Johannesburg, SA
EDTA (Ethylenediaminetetraacetic acid)	Sigma, St Louis, Missouri, USA
EMEM (Eagle's minimum essential medium): HyClone	Thermo Scientific, Waltham, Massachusetts, USA
FCS (Fetal calf serum)	Biowhitaker, Lonza Walkersville Inc., Walkersville, Maryland, USA
Gallamine triethiodide	Sigma, St Louis, Missouri, USA

Gelatin	Sigma, St Louis, Missouri, USA
L-Glutamine	Sigma, St Louis, Missouri, USA
Glycerol	Sigma, St Louis, Missouri, USA
Glycine	Merck, Darmstadt, Germany
HCL	Merck, Wadeville, SA
Hydrogen peroxide (H ₂ O ₂)	Sigma, St Louis, Missouri, USA
Imperial™ protein stain	Pierce, Rockford, Illinois, USA
IPTG (Isopropyl β-D-1-thiogalactopyranoside)	Merck, Darmstadt, Germany
Isopropanol	Sigma, St Louis, Missouri, USA
Kanamycin	Fluka Chemika-Biochemika, Johannesburg, SA
KCL	Merck, Darmstadt, Germany
KH ₂ PO ₄	Merck, Darmstadt, Germany
K ₂ HPO ₄	Merck, Darmstadt, Germany
D(+) – Maltose monohydrate	Fluka Chemika-Biochemika, Johannesburg, SA
β-Mercaptoethanol	Research Organics, Inc., Cleveland, Ohio, USA
Methanol	Sigma, Schnelldorf, Germany
MgSO ₄	BDH Laboratories Supplies, Kampala, Uganda
NaCl	Fluka, Chemika-Biochemika, Johannesburg, SA
NaF	Sigma, St Louis, Missouri, USA
NaHCO ₃	Sigma, St Louis, Missouri, USA
Na ₂ HPO ₄	Merck, Darmstadt, Germany
NaN ₃	Sigma, St Louis, Missouri, USA
NaOH	Sigma, St Louis, Missouri, USA
Na ₃ VO ₄	Sigma, St Louis, Missouri, USA

NP40	Sigma, St Louis, Missouri, USA
NZ amine A	Sigma, St Louis, Missouri, USA
PEG8000	Sigma, St Louis, Missouri, USA
Penicillin/Streptomycin	Biowhitaker, Lonza Walkersville Inc., Walkersville, Maryland, USA
Phenol red	Sigma, St Louis, Missouri, USA
PMSF (phenylmethanesulfonylfluoride)	Sigma, St Louis, Missouri, USA
Poly-L-lysine	Sigma, St Louis, Missouri, USA
PI (Propidium iodide)	Sigma, St Louis, Missouri, USA
Protease inhibitor cocktail	Sigma, St Louis, Missouri, USA
Protein A - sepharose	Sigma, St Louis, Missouri, USA
Pyridostigmine bromide (reversible cholinesterase inhibitor)	Sigma, St Louis, Missouri, USA
Sarkosyl (sodium lauroyl sarcosinate)	Sigma, St Louis, Missouri, USA
SDS (Sodium dodecyl sulfate)	BDH Laboratories Supplies, Kampala, Uganda
Streptavidin from Streptomyces avidinii	Sigma, St Louis, Missouri, USA
Streptavidin-peroxidase conjugate	Sigma, St Louis, Missouri, USA
Spectra™ multicolour broad range protein ladder	Fermentas, Glen Burnie, Maryland, USA
TEMED (N,N,N',N' – tetramethylethylenediamine)	USB® Corporation, Cleveland, Ohio, USA
Tetracycline	Fluka Chemika-Biochemika, Johannesburg, SA
TMB (3,3',5,5' tetramethylbenzidine liquid substrate system for membranes)	Sigma, St Louis, Missouri, USA
Trizma base	Merck, Darmstadt, Germany
Triton X100	Sigma, St Louis, Missouri, USA
Trypsine/Versene	Biowhitaker, Lonza Walkersville Inc., Walkersville, Maryland, USA

Tween 20	Fluka Chemika, Johannesburg, SA
Yeast extract	Merck, Darmstadt, Germany

2.1.3 Consumables

Blotting filter paper, mini transblot	BioRad, BioRad Laboratories Ltd., Johannesburg, SA
Cellstar tissue culture flasks	Greiner Bio-One, Germany
Centricon 30kDa ultrafilter	Amicon, Millipore, St. Charles, Missouri, USA
Disposable filter unit	Lasec, Cape Town, SA
Disposable nitrile examination gloves	Hi-Care, Kolkata, India
Eppendorf tubes (1ml, 1.5ml, 2ml)	Quality Scientific Plastics (QSP), Whitehead Scientific, Cape Town, SA
Immobilon-P transfer membrane	Millipore, St. Charles, Missouri, USA
Microtiter plates/ELISA plates	Costar, Corning Inc., NY, USA
Parafilm	Lasec, Cape Town, SA
Petridishes (35mm, 90mm)	Lasec, Cape Town, SA
Pipettes (1ml, 5ml, 10ml, 25ml)	Lasec, Cape Town, SA
Pipette tips	Lasec, Cape Town, SA
Plastic tubes, sterile, 15ml: Cellstar	Greiner Bio-One, Frickenhausen, Germany
Plastic tubes, sterile, 50ml: Polypropelene Conicol tubes	Becton Dickinson Labware, NJ, USA
Slide-A-Lyzer	Pierce, Rockford, Illinois, USA
Snakeskin® pleated dialysis tubing	Pierce, Rockford, Illinois, USA
Syringes	Promex, Johannesburg, SA
24-well plates	Greiner Bio-One, Frickenhausen Germany

2.1.4 Proteins

AChE, amphiphilic from human erythrocytes	Sigma, St Louis, Missouri, USA
AChE, recombinant, from human	Sigma, St Louis, Missouri, USA
Laminin, from Engelbreth-Holm-Swarm murine sarcoma	Sigma, St Louis, Missouri, USA
Non-specific anti-human IgG (biotinylated)	Sigma, St Louis, Missouri, USA

2.1.5 Primary antibodies

Anti-AChE, produced in goat, polyclonal, 100µg/200µl	Sigma, St Louis, Missouri, USA
Anti-laminin, rabbit, produced in rabbit, polyclonal, 1mg/ml	Sigma, St Louis, Missouri, USA

2.1.6 Secondary antibodies

Anti-goat IgG (whole molecule)-biotin, produced in rabbit, conjugated, 0.2-2 mg/ml	Sigma, St. Louis, Missouri, USA
Anti-rabbit (whole molecule)-biotin, produced in goat, polyclonal, solution in 0.01 M PBS pH 7.4, containing 15 mM sodium azide	Sigma, St Louis, Missouri, USA

2.1.7 Kits

Phage display peptide library kit	New England BioLabs® Inc., Ipswich, Massachusetts, USA
Wizard® genomic DNA purification kit	Promega, Madison, Wisconsin, USA

2.1.8 Antibodies

Prior to the work described in this thesis, a network of idiotypic (Ab1), anti-idiotypic (Ab2) and anti-anti-idiotypic (Ab3) antibodies was developed. The initial monoclonal Ab (MAb), E8, was raised in Balb/c mice against human erythrocyte AChE (Sigma). This MAb was found to have esterolytic activity (Johnson & Moore, 1995). Subsequently, two more catalytic MAbs (C2 and 43B4C) were raised against the same antigen (Johnson & Moore, 2000). Fusions and cloning of these Ab1s were performed according to standard protocols (Harlow & Lane, 1988). SDS/PAGE confirmed the purity of the Ag and the Abs were screened against both erythrocyte and recombinant human AChE. No significant differences in reactivity were observed. Purification of Abs was done by Protein A-Sepharose 4B affinity chromatography using low-salt buffers, according to standard protocols (Harlow & Lane, 1988). Another MAb, E12C8, was raised against *Torpedo* AChE and also block cell adhesion. MAb E12C8 was a gift from the Walter Reed Army Institute (Washington, DC, USA). It was observed that all three MAbs were able to block the ability of cultured neuroblastoma cells to adhere to the substratum. Neuroblastoma cells (cell line N2 α) are normally flattened and adherent. If the MAbs were added to the cells at the time of plating, the cells remained in suspension without adhering, and subsequently died. When the MAbs were added to already adherent cells, the cells rounded up, floated, and subsequently died. This effect was dose-dependent. It was concluded that these MAbs were interfering with an AChE-mediated cell adhesion process.

The MAbs showed very similar enzyme kinetics (Johnson & Moore, 2000) and this, together with the similarity of their effects on cells (quantitated by both the timing and percentage of adhesion loss) suggested that they recognised a common epitope on AChE. It was found, using competition ELISA and fluorometry, that the MAbs competed with the PAS-binding inhibitors propidium, gallamine, BW284c51 and fasciculin-2, which indicated that this epitope lay at or near the PAS. The results also confirm the association of AChE's adhesion-mediating ability with the PAS. Subsequent work showed that the

MABs blocked the interaction between AChE and laminin-111. It was therefore concluded that the MABs' epitope and the laminin-interaction site on AChE have structural features in common, and are possibly identical. Two more anti-AChE Abs, 9H and AE-2, appeared to bind near the PAS but did not inhibit cell adhesion or laminin binding. These were used as controls. MAB 9H was raised in our laboratory and MAB AE-2 was also a gift from the Walter Reed Army Institute (Washington, DC, USA).

Anti-idiotypic (Ab2) MABs were raised against the original catalytic and adhesion-inhibiting MAB, MAB E8. Several of these Ab2s were found to be capable of promoting neurite outgrowth in neuroblastoma cells, and also of binding to laminin-111, suggesting that their idiotope was mimicking the adhesion-mediating site on AChE (Johnson & Moore, 2004). These Ab2s were not catalytic. Anti-anti-idiotypic (Ab3) MABs were similarly raised against an Ab2. These were 13B9F and 13B9C. These Ab3s resembled the original MAB E8 in being both catalytic and adhesion-inhibiting.

While the Ab1s showed both relatively similar enzyme kinetics and adhesion-inhibiting ability, more variation was seen among the Ab2s and Ab3s. Thus, it was thought that the Abs, especially as they are not exactly similar to AChE or its binding partner(s), would provide a "variation on a theme" that might prove useful in determining the relative importance of specific aspects on the adhesion-mediating site, both on AChE and on its interaction partner(s). A further consideration is the "localisation" of the site of interest on the Ab to a very specific area, namely the complementarity-determining regions (CDRs). A moderately-sized protein such as AChE could conceivably have a number of interaction sites; the C-terminal region, in particular, is noted for its ability to interact with membrane anchoring proteins and structures, which would confuse the issue. This consideration would apply even more to laminin, which is a very large molecule with a multiplicity of interaction sites.

2.1.9 Biotinylation

The resultant number of biotins per AChE molecule was not determined; however, previous results from the laboratory had shown that biotinylation had no significant effect on AChE's enzyme activity, inhibitor binding (inhibitors pyridostigmine, edrophonium BW284c51 and propidium), nor was MAb-AChE binding affected. These results suggest two things: firstly, as both BW284c51 and propidium are cationic PAS-binding compounds, this suggests that the charge of the PAS has not been significantly affected; it also suggests that steric hindrance effects are not significant. The MAb binding to AChE is also not affected, suggesting that the epitope is not restricted by biotinylation.

AChE (human and mouse) contains 10 Lys residues (K23, K53, K332, K348, K470, K495, K538, K554, K568 and K576). Of these, only 3 lie on the gorge opening "face" of the molecule (Figure 16). These 3 residues are K23, K53 and K348. The others all lie away from this region, largely in AChE's C-terminal domain; 4 lie in the distal part of the domain in the T-peptide oligomerisation domain. A high concentration of acidic residues (Asp and Glu) on the gorge opening "face" is also found. Because of this high concentration of acidic charge, the neutralisation of several positively charged residues may not have a drastic effect on the overall charge distribution. The experimental results support this. The biotinylated peptides used in this study were biotinylated at the NH₂ terminal only.

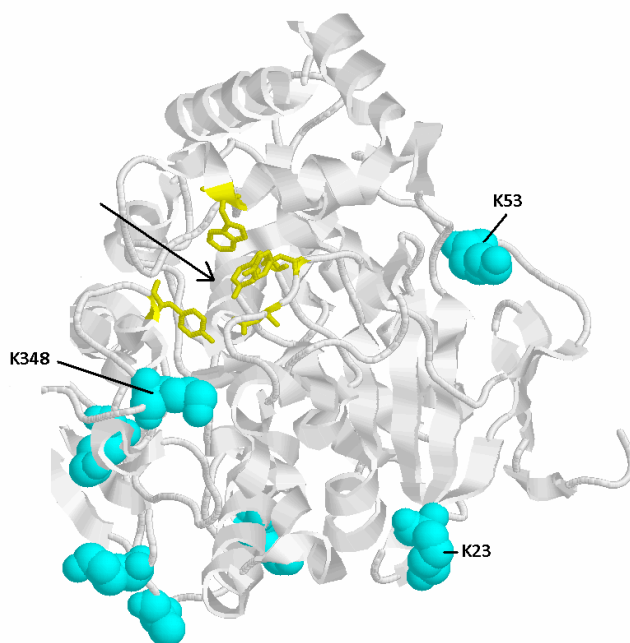


Figure 16. The structure of mouse AChE molecule (1J06.pdb). The three Lys residues at the gorge opening are colored in cyan. The PAS residues are shown in yellow. The arrow shows the entrance to the ASG.

2.1.10 General buffers and solutions

Phosphate buffered saline (PBS): A 10X stock solution was made up by dissolving 80g of NaCl, 2.0g of KCl, 14.4g of Na₂HPO₄ and 2.4g of KH₂PO₄ in 800ml of dH₂O. The pH was adjusted to 7.4 after which the volume was increased to 1L with additional dH₂O. The solution was sterilised by autoclaving and stored at room temperature (RT). A 1X working solution was made up by adding 100ml of the 10X stock solution to 900ml of dH₂O.

PBS/Tween (wash buffer): Tween 20 was added to a 1X PBS solution to give a final concentration of 1% (v/v). The solution was stored at RT.

PEG/NaCl precipitation buffer: 110g of PEG 8000 and 116.9g of NaCl were added to 475ml of dH₂O and the mixture was stirred and heated to 65°C until solute dissolved. The solution was stored at 4°C.

Tris-buffered saline (TBS) 1X solution: 8g of NaCl, 0.2g of KCl and 3g of Trizma base was dissolved in 800ml of dH₂O. 0.015g of phenol red was added as a pH control. The pH was adjusted to 7.4 with HCl, until the red colour cleared. The total volume was increased to 1L with addition of dH₂O. The solution was sterilised by autoclaving and stored at RT.

TBS/Tween (wash buffer): Tween 20 was added to a TBS solution at a final concentration of 0.5% (v/v). The solution was stored at RT.

2.2 Methods

2.2.1 ELISA

Enzyme-linked immunosorbent assay (ELISA) is a powerful method of determining the presence as well as concentration of a particular protein in a sample. In “direct ELISA”, the antigen-containing sample is immobilised on a polystyrene microtitre plate and a specific antibody coupled to an enzyme (usually horseradish peroxidase or alkaline phosphatase) is added. The bound antibody is then detected by the addition of substrate together with a colour reagent that develops according to the amount of enzyme/antibody bound. There are a number of variations on this technique. In the “indirect” ELISA, both a primary (anti-antigen) and a secondary (anti-primary antibody) antibody are used. The secondary antibody may be coupled to the enzyme, or, as is frequently used, coupled to biotin. In the latter situation, an additional step using an avidin-enzyme complex is included. The use of the secondary antibody, as well as the biotin-avidin step, help to augment the final signal obtained.

In the “sandwich” ELISA (also called the “capture” ELISA), the microtitre plate is coated with primary antibody, instead of the antigen. This antibody coating “captures” the antigen in the sample. This is followed by incubation with primary and secondary antibodies, as above. As with the indirect ELISA, this additional step helps to augment the final signal.

A fourth type of ELISA is the “competition” or “competitive” ELISA. In a competitive ELISA used to quantitate antigen in a sample, the sample is incubated beforehand with the antibody to produce an antigen-antibody complex. The complex is then added to a microtitre plate which is coated with the antigen. The two “antigens” (antigen in the sample and antigen on the plate) thus compete for antibody binding. As a result, the higher the concentration of the antigen in the sample, the lower will be the final signal, as this is a measure of the amount of coated antigen that binds to the antibody. Competitive ELISAs are useful for the detection of antigen in crude samples.

In this thesis, several types of ELISA were used: indirect, sandwich, and a variation of the competitive ELISA described above.

AChE synthetic peptides: Peptides corresponding to the following sequences of human AChE were synthesised by Bio-Synthesis Inc, Lewisville, Texas, USA, except for peptides 37-53 and 340-353 which were synthesised by PepMetrics:

Table 2. Peptide sequences

Residue	Corresponding region	Sequence
28-53 (or 37-53)	Surface loop adjacent to the PAS	ISAFGLGIPFAEPPMGPRRFLPPEPKKP
55-66	Surface loop adjacent to the PAS	PWSGVVDATTFQ
69-96	Omega loop	CYQYVDTYPGFEGTEMWNP NRELSEDC
275-290	Part of large loop on the opposite side of the PAS and including PAS residue W286	RPAQVLVNHEWHVLP
340-353	Including PAS residue Y341	VYGAPGFSKDNESL

Peptides were purified by HPLC to > 95% purity and lyophilised. Lyophilised peptides were dissolved in double distilled water at a concentration of 2mg/ml, and frozen in aliquots. Aliquots that had been thawed were used immediately and not refrozen.

Purified erythrocyte AChE was used in all assays.

Peptides binding to laminin: Binding proteins, AChE and BSA, were biotinylated by the method of Bhakdi *et al* (1989) using the N-hydroxysuccinimide biotin ester. Biotinylation had no significant effect on AChE's enzyme activity and MAb-AChE binding was also unaffected. The binding of biotinylated BSA and non-specific anti-human IgG served as controls. Biotinylated non-specific anti-human IgG was used as its pI (5.4) is very close to that of AChE (pI 5.3) and BSA (pI 4.7) was used as a neutral control unlikely to bind. 96-well microtiter plates were pre-coated with 5µg/ml poly-L-lysine in water (50µl per well) and incubated for 1 h at RT. After incubation, the plates were washed twice with 1X PBS and a laminin of 100µg/ml in 1X PBS, were added. The plates were covered and left to incubate for 2 h at RT. The remainder of the binding sites in the coated wells were then blocked by adding 200µl of 1% BSA/PBS blocking buffer. The plates were covered and left to incubate for 2 hours at RT. After blocking, 50µl/well of the biotinylated proteins were added at dilutions of 0-35 nM and the plates were incubated for 4 h at RT. The amount of biotinylated protein bound was probed with streptavidin-peroxidase and H₂O₂/ABTS, and the absorbance was measured at 405nm. Binding data was analysed by nonlinear regression using SigmaPlot™.

Parallel experiments using non-poly-L-lysine coated microtiter plates were run to allow for differences in peptide acidity and hydrophobicity. Here the peptides were dissolved in 50mM NaHCO₃ (pH 9.0) and incubated overnight at 4°C before blocking. Non-specific binding was determined in the absence of peptide coating, and these values were subtracted from readings.

Laminin synthetic peptide: An unbiotinylated version of the laminin peptide, AG-73, Arg²⁷¹⁹-Lys-Arg-Leu-Gln-Val-Gln-Val-Ser-Ile-Arg-Thr²⁷³⁰ (mouse sequence, Swiss-Prot accession number NP_032506), along with a scrambled version, Leu-Gln-Ile-Thr-Arg-Ser-Arg-Gln-Arg-Val-Lys-Leu, were obtained from PepMetric Technologies (Vancouver, British Columbia, Canada). The free N-terminal amines of the peptides alone were biotinylated. The peptides underwent HPLC purification to >95% purity and lyophilised. The lyophilised peptides were dissolved in double distilled water at a

concentration of 2mg/ml and frozen in aliquots. Thawed aliquots were used immediately and not refrozen.

Proteins binding to laminin peptides: AChE and BSA were biotinylated as above. Recombinant human AChE was used in this assay, instead of the erythrocyte AChE species against which the MAbs were raised (no significant differences in reactivity of the MAbs towards the two species was observed). Biotinylated non-specific anti-human IgG and BSA was used as controls (reasons mentioned above). Proteins and peptides were absorbed on high-binding microtiter plates in 50mM NaHCO₃ (pH 9.0) overnight at 4°C. The concentrations used were 10µg/ml for proteins and 20µg/ml for peptides. After incubation, the plates were washed with washing buffer (0.2% Tween 20 in 1X PBS) and blocked with 1% BSA/PBS blocking buffer for 2 h at RT. Serial dilutions of biotinylated proteins or peptides were added (0-20µg/ml) and incubated for 4 h at RT. Bound biotinylated proteins was probed with streptavidin-peroxidase and H₂O₂/ABTS. Absorbance was measured at 405nm. Non-specific binding was determined in the absence of absorbed protein or peptide and the binding data was analysed by nonlinear regression by SigmaPlot™.

Whole molecule binding of AChE and laminin: Binding proteins, AChE and BSA, were biotinylated as above. Laminin was diluted to 10µg/ml working dilution in 50mM NaHCO₃ (pH 8.0). The plates were coated with 10µg/ml of laminin. The plates were blocked with PBS/BSA and washed as above. Biotinylated AChE was added at serial dilutions of 20, 10, 5, 2.5, 1.25, 0.625, 0.312, and 0.156µg/ml. The amount of biotinylated protein bound was probed with streptavidin-peroxidase and H₂O₂/ABTS and the absorbance was measured at 405nm. Binding data was analysed by nonlinear regression using Prism 5. The controls BSA and anti-human IgG, as well as AChE, were added at concentrations of 0.00, 0.625, 1.25, 2.5, 5, and 10µg/ml and binding was observed as above.

Competition ELISA: The microtiter plates were coated as above. Biotinylated AChE or laminin (20µg/ml) was pre-incubated with various concentrations of either the AG-73

peptide or its scrambled version. Incubation proceeded for 1 h at RT before adding the protein mixtures to the pre-coated plates. Bound proteins were detected as above. Due to similarities in the AChE-laminin binding site and the heparin-laminin binding site, the question of whether AChE competes with heparan sulfate in binding to laminin, was put under investigation. Microtiter plates were coated with 10µg/ml laminin-111, blocked, and washed as above. Serial dilutions of AChE (0-20µg/ml; 0-286nM) were added together with 10µg/ml heparan sulfate and binding was determined as above.

Inhibitors: PAS-binding inhibitors, propidium and gallamine, as well as active-site binding inhibitor, pyridostigmine, were used at concentrations of 0-500µM. Prior to addition to microtiter plates, inhibitors were incubated with 20µg/ml (286nM) biotinylated AChE (biotinylation had no significant effect on its reaction with the inhibitors) for 1 h at RT. The amount of biotinylated AChE bound was probed and measured as above.

Effects of NaCl: The effect of the salt concentration of the buffer on the binding of AChE and laminin, as well as on the binding of AChE and AG-73, was investigated. The different buffer NaCl concentrations used were: 500nM, 250nM, 125nM and 62.5nM. Protein binding was probed and measured as above.

2.2.2 Phage display

Often in molecular biology one requires information on the binding partners of molecules. This may be needed, for example, in identifying a ligand for a particular receptor or characterising antigen-antibody or enzyme-substrate or enzyme-inhibitor interactions. In the earlier days of molecular biology, candidate molecules would have to be purified or synthesised, and their binding to the molecule of interest determined and analysed. This is a very time-consuming and laborious process.

There are a number of methods that are used to investigate protein-protein interactions. The two major approaches are the yeast two-hybrid system and phage display. Mass

spectrometry may also be used, but is not common, probably due to availability of the equipment that is required. In this thesis, phage display was chosen over yeast two-hybrid. In yeast two-hybrid, the protein of interest is expressed in yeast cells. A mammalian protein must be able to fold correctly and exist in a stable state inside the yeast cell. Furthermore, posttranslational modifications, such as disulfide bonding, glycosylation and phosphorylation, may not occur at all, or may occur inappropriately, in the yeast (Van Crielinge & Beyaert, 1999). Previous results from the laboratory had localised the adhesion-mediating site of AChE to the PAS area. This area is associated strongly with the Cys 69-Cys 96 omega loop, and thus dependent on correct disulfide bond formation. The PAS as well as AChE's catalytic activity are very sensitive to conformational changes (Shi *et al*, 2003), and previous results (unpublished) have indicated that imperfectly glycosylated AChE has reduced catalytic activity, attributed to altered conformation.

Phage display, introduced by Smith (1985), is a way of greatly speeding up the process of ligand identification. Genes encoding peptides or proteins can be introduced into the genome of filamentous bacteriophage in such a way that the gene product is expressed ("displayed") on the bacteriophage surface as a fusion product of a phage coat protein. Phage expressing these peptides or proteins can then be incubated with the receptor molecule of interest and their ability to bind determined. The phage binders can be used to infect bacterial cells, and thus amplified. Because of the link between phenotype (the "displayed" peptide or protein) and genotype, the DNA of the binders can be sequenced and the peptide sequence of the peptide or protein determined.

Phage libraries of up to 10^{10} different sequences can be developed, allowing for rapid screening of potential binding partners. The most commonly used phage is filamentous phage and phagemid (based on M13, fl or fd). T7 (Houshmand *et al*, 1999) and lambda (Mikawa *et al*, 1996) phage have also been used. Phage display is a robust method and is probably the most commonly used *in vitro* technique for the selection of peptide and protein binders. Initially, it was used for peptides and epitope mapping (e.g. Scott & Smith, 1990), and subsequently for antibody identification, hormone affinity optimisation

(Lowman & Wells, 1993) and for identifying the binding partners for many proteins (e.g. Bradbury & Marks, 2004 for review).

Proteins and Abs: Phage display selection was performed against AChE and the three MAbs E8, C2, and 43B4C.

Phage display libraries: Random peptide libraries of filamentous phage in the Type 88 Vector f88-4 was used (obtained from Professor George Smith of the University of Missouri; protocols available at: <http://www.biosci.missouri.edu/smithgp/PhageDisplayWebsite/PhageDisplayWebsiteIndex.html>), specifically the f88-4/CysO library. This library contained 5.6×10^8 primary clones and has a DNA size of 9267 bases. The concentration of physical particles was 1.48×10^{14} virions/ml and the approximate infectivity 10.7%. The Cys-linked library was used because the peptides displayed on the phage surface are Cys-Cys linked, these were more likely to yield information about nonlinear recognition sites. The peptides used were thus linear peptides that were cyclized.

Blocking buffer: The buffer contained 0.1M NaHCO₃, 5mg/ml dialyzed BSA, 0.1µg/ml streptavidin and 0.02% NaN₃. 1.26g of NaHCO₃, 0.75g of dialyzed BSA, 1µl of a 5mg/ml streptavidin solution and 0.03g of NaN₃ were dissolved in dH₂O to give a final volume of 150ml. The solution was filter sterilized and stored at 4°C. The buffer was re-used until it showed evidence of microbial growth or accumulation of insoluble matter.

TTDBA: 0.2g of BSA and 0.2g NaN₃ were dissolved in ~200ml TBS/Tween to a final concentration of 1mg/ml and 0.02% (m/v), respectively. Solution was stored at RT.

Elution buffer: The buffer contained 0.1N HCl (pH adjusted to 2.2 with glycine) and 1mg/ml BSA. The glycine.HCl buffer was made and adjusted as a 4X stock, filter sterilized, and stored at RT. The glycine.HCl buffer, along with the other components, was made up in autoclaved water and was filter sterilized. The solution was stored at 4°C.

Bacterial strain: E. coli bacterial strain K91Blukan (obtained from Professor George Smith of the University of Missouri).

LB medium (1X): 10g of bacto-tryptone, 5g of NaCl and 5g of yeast extract were added to 800ml of dH₂O and the pH was adjusted to 7.0 with NaOH after which the volume was increased to 1L with additional dH₂O. The mixture was autoclaved and stored at RT.

LB agar plates: Bacto agar was added as 15g/L to the 1X LB medium described above and autoclaved. Once mixture had cooled to about 50°C, the antibiotics (tetracycline and/or kanamycin) were added for antibiotic-resistance selection. The solution was poured onto petri-dishes (85mm) and left at RT to allow agar to solidify. The solid plates were sealed and stored at 4°C.

NZY medium (1X): 10g of NZ amine A, 5g of yeast extract and 5g of NaCl was dissolved in 1L of dH₂O and the pH was adjusted to 7.5 with NaOH. The solution was autoclaved and stored at RT.

NZY agar plates: 15g of bacto-agar was added to the NZY medium and the solution was autoclaved. Once solution had cooled down to about 50°C, tetracycline and kanamycin was added at concentrations of 40µg/ml and 100µg/ml respectively. The solution was poured onto petri-dishes and left at RT to solidify after which the plates were sealed and stored at 4°C.

Terrific broth: 12g of bacto-tryptone, 24g of yeast extract and 4ml of glycerol were dissolved in 900ml of dH₂O. 90-ml portions in 125-ml polypropylene bottles were autoclaved. When cooled, 10ml of separately autoclaved potassium phosphate buffer (containing 0.17M KH₂PO₄ and 0.72M K₂HPO₄: 2.31g of KH₂PO₄ (anhydrous) and 12.54g of K₂HPO₄ (anhydrous) were dissolved in 90ml of dH₂O, volume was adjusted to 100ml and buffer was autoclaved) was added to each bottle.

Tetracycline stock solution, 20mg/ml: 40ml glycerol was autoclaved in a 100ml bottle. After the glycerol cooled down, 40ml of a 40mg/ml tetracycline solution filter sterilised in water, was added to it. The solution was mixed thoroughly and stored at -20°C, away from light

Kanamycin stock solution, 100mg/ml: Kanamycin sulphate was dissolved in dH₂O to a final concentration of 80mg/ml. The pH was adjusted to 6-8 with NaOH or HCl where necessary. The solution was autoclaved, filter sterilized using a syringe and disposable filters, and stored at 4°C.

Preparation of starved cells: K91BluKan cells were grown by shaking at 37°C in 20ml NZY medium to log phase (OD₆₀₀ ~0.45). The cells were then incubated with gentle shaking for an additional 5min, to allow any sheared F pili to regenerate. Cells were centrifuged in a 50ml tube at 2.5 Krpm for 10 min at 4°C. Cells were then gently resuspended in 20ml 80mM NaCl. Resuspended cells were then poured into a sterile 125ml flask and shook gently at 37°C for 45 min. The centrifuging step was repeated after which the cells were resuspended gently in 1ml cold NAP buffer (80mM NaCl, 50mM NH₄H₂PO₄ pH 7 with NH₄OH). The concentration of viable cells was ~5 x 10⁹ml and cells remained infectible for 3-5 days.

Preparation of terrific broth cultures: A few ml of NZY medium was inoculated with K91Blukan cells and left to shake overnight at 37°C. 100µl of this overnight culture was used to inoculate 10ml of *terrific broth* in a 125-ml flask and allowed to shake vigorously at 37°C. Once culture became turbid, OD₆₀₀ of 1/10 dilutions were read until 1/10 dilution reached 0.1-0.2 on the spectrophotometer after which the shaking was slowed down to allow sheared F-pili to regenerate. Cells were used within 1 h and the concentration of viable cells was ~5 x 10⁹ml.

Protein biotinylation: (see section 2.1.9) AChE and the mAbs were biotinylated to enable biotin/avidin-detection. Biotin (long-arm) N Hydroxysuccinimide ester (BNHS) reacts with amino groups in proteins. Biotin was dissolved in DMF at a final

concentration of 25mg/ml and was prepared prior to use. AChE was dissolved in sodium bicarbonate at a concentration of 2mg/ml. AChE was biotinylated by adding 1/10th of the protein weight biotin and incubating at room temperature for 2 h, stirring occasionally. The biotinylated protein was then dialyzed against three changes of 2L of 1X TBS buffer

2.2.2.1 Affinity selection

One-Step selection: In one-step selection phage, contained in the library, are captured by a biotinylated selector (AChE, MAbs) that has been pre-immobilized on the surface of a streptavidin-coated petri dish. 35mm petri dishes were coated with 400µl 10µg/ml streptavidin in 0.1M NaHCO₃ for at least 1 h at RT. The solution was aspirated out and dishes were filled to the brim with blocking buffer and allowed to sit with the lid off for 2 h at RT. The blocking solution was poured off and the dishes were washed five times with TBS/Tween. 10µg of the biotinylated receptor (bAChE), diluted in 400µl TTDBA buffer, was added and the petri dishes were allowed to react for 2 h at 4°C. This was followed by another wash step, five times with TBS/Tween, in order to remove unbound selector. The dishes were filled to the brim with TTDBA and 4ul 10mM biotin was added to block unoccupied biotin-binding sites on the immobilized streptavidin. The dishes were rocked for 10 min at RT. The input phage (f88/4-CysO library for 1st round selection, and 1st and 2nd round eluates for 2nd and 3rd round selection, respectively) was then added and the dishes were rocked at 4°C for 4 h (removal of excess biotin was unnecessary as it won't displace the bound biotinylated selector). After 4 hours, the bound phage was eluted from the dish by adding 400ul elution buffer and rocking it for 10 min. The eluate was then transferred to a microtube and neutralized by mixing it with 50µl 1M Tris-HCL (pH 9.1).

Two-step selection: In two-step selection phage are reacted with biotinylated selector in solution prior to addition to streptavidin-coated plates. Such selectors can serve as an internal indicator of non-specific background yield during affinity selection.

Quantifying yield and amplifying eluates: The entire first round eluate was concentrated and washed once with TBS on a Centricon 30kDa ultrafilter by centrifuging at 5 Krpm in a Sorvall SS34 rotor to give a final volume of ~ 100µl (this step is only applicable in 1st round eluates as eluates from subsequent rounds, in which every clone is represented by many thousands or millions of phage particles, are used without concentrating). 100µl of the eluate (1st and 2nd round) was mixed with 100µl starved K91BluKan cells and incubated for 10-30min at RT. The infected cells were pipetted into a 150ml culture flask containing 40ml NZY medium with 0.2µg/ml tetracycline and left to shake for 30-60 min at 37°C. 200ul portions of appropriate serial dilutions of the culture (10^{-1} - 10^{-4} , diluent = NZY) was spread on NZY plates containing 40µg/ml tetracycline and 100µg/ml kanamycin to enable quantification of the output of affinity selection (a high phage yield is very important in 1st round eluates as the input phage is the whole library and it is thus necessary that each specific phage be represented a few times). 20mg/ml tetracycline was added to the 40ml culture to bring the antibiotic concentration up to 20µg/ml after which the solution was left to shake further overnight at 37°C. The next day the culture was poured into a 50ml tube and cleared of cells by two rounds of centrifugations at 5 and 8 Krpm at 4°C. The doubly-cleared supernatant, at a final volume of ~35ml, was poured into a fresh tube. 5.25ml PEG/NaCl precipitation buffer was added to the cleared culture and mixed by many inversions, allowing the phage to precipitate overnight at 4°C. The precipitated phage was collected the next morning by centrifuging at 12Krpm for 15 min at 4°C. The pellet was dissolved in 1ml TBS and the solution was transferred to a 1.5ml Ep tube. The solution was then centrifuged at 15K rpm to clear insoluble material and the supernatant was transferred to a second 1.5ml Ep tube. 150µl PEG/NaCl was then added and vortexed, and the mixture was left for at least 1 h at 4°C after which it was microfuged for 5 min at 15K rpm . The pellet was once again dissolved in 400µl TBS. This was followed by another microfuge step for 1 min at 15K rpm to clear undissolved material. The supernatant was then transferred to a 500µl Ep tube and stored in the refrigerator. This supernatant is the amplified eluate and the physical partical concentration at this point should be $\sim 5 \times 10^{13}$ virions/ml³. Selection proceeded for 3 rounds after which the 100µl of 1st round eluates

was used as 2nd round “input phage”, and 100µl of 2nd round eluates were used as 3rd round “input phage”. 3rd round eluate (last round) = final eluate.

Propagating clones from final round eluate: Using TBS/*gelatin* (0.1g of gelatine was autoclaved in 100ml 1X TBS) as diluent, serial dilutions was made of the final eluate (dilutions ranged from 10⁻¹ to 10⁻⁵) in 15-ml disposable tubes (tubes were held at an angle and a 10µl droplet of each dilution was deposited on the inner wall of the tube). 10µl starved cells were added to each sample and the mixtures were incubated for 10 min at RT to allow for infection. 1ml of NZY containing 02ug/ml *tetracycline* was added and each mixture was left to incubate while shaking for 40 min at 37°C. The infected cells were spread (200ul/plate) on NZY plates containing 40µg/ml *tetracycline* and 100µg/ml *kanamycine*. Plates were incubated for ~24 h at 37°C. The yield was monitored.

Phage purification: The Wizard® genomic DNA Purification System kit and protocol (Promega) was used. A single, well isolated, phage plaque was picked from the agar plate using a sterile toothpick. The plaque was expelled into a 1.5-ml microcentrifuge tube containing 100µl phage buffer (containing 150mM NaCl, 40mM Tris-HCl (pH 7.4) and 10mM MgSO₄) and left overnight at 4°C. In the meantime a fresh culture was started by inoculating a single colony into 5ml of LB medium containing 50µl 20% maltose and 50µl 1M MgSO₄ and leaving it to shake overnight at 37°C. The next day, 500µl of the overnight culture was added to the tube containing the plaque/phage buffer mixture from the first step and the solution was left to incubate for 20 min at 37°C. 500ul of the infected culture was transferred to a 250-ml Erlenmeyer flask containing 100ml pre-warmed (37°C) LB with 1ml 1M MgSO₄. The solution was left to shake until lysis occurred (for about 5 h). The medium should appear turbid at first, but then clear upon lysis. After cell lysis, 500µl chloroform was added and the mixture was left to shake for a further 15 min. The lysate was centrifuged at 8 000 x g for 10 min to remove cellular debris after which the supernatant was transferred to a sterile tube. 10ml of this lysate was transferred to an appropriate centrifuge tube. The Nuclease Resuspension Solution was added to the lyophilized Nuclease Mixture (both provided by kit), and the solution was resuspended very gently. 40ml of this resuspended Nuclease Mixture was added to

the 10ml of lysate and left to incubate for 15 min at 37°C. 4ml of the provided Phage Precipitant was added, the solution mixed gently, and placed on ice for 30 min. After 30 min the mixture was centrifuged at 10 000 x g for 10 min. The pellet was resuspended in 500µl of phage buffer and transferred to a 1.5-ml microcentrifuge tube. Centrifugation proceeded at 10 000 x g for 10 seconds to remove insoluble particles. The supernatant was transferred to a new tube and 1ml of thoroughly mixed Purification Resin (provided by kit) was added to it and the solution was mixed by inverting the tube. A Wizard® Minicolumn was prepared by attaching the syringe barrel to the Luer-Lok® extension of each minicolumn and inserting the tip of the minicolumn/syringe barrel assembly into each vacuum manifold. The resin/lysate was pipetted into the syringe barrel and a vacuum was applied to draw the mix into the minicolumn. 2ml of 80% isopropanol was added to the syringe barrel to wash the column after which the vacuum was re-applied to draw the solution through the minicolumn. The vacuum was continued for 30 sec to dry the resin after the solution was pulled through. The syringe barrel was removed and the minicolumn was transferred to a 1.5-ml microcentrifuge tube and centrifuged at 10 000 x g for 2 min to remove any residual isopropanol. The minicolumn was transferred to a fresh tube and 100ul pre-warmed (80°C) water was added and the minicolumn was immediately centrifuged at 10 000 x g for 20 sec to elute DNA. The minicolumn was removed and discarded leaving behind the purified DNA.

Alternative phage purification protocol: This protocol was adapted from Wickner *et al.* (1975). A well separated colony from the overnight plates was used to inoculate 1L of NZY containing 20µg/ml *tetracycline* and 1mM IPTG in a Fernbach flask and the solution was left to shake overnight at 37°C. The next day the mixture was cleared by two centrifugations in three 500-ml centrifuge bottles at 5 and 8K rpm for 10 min. The final supernatants were poured into tared 500-ml bottles (volume of each was ~300ml). 0.15 volume PEG/NaCl was added to each and mixed thoroughly by ~100 inversions. The mixture was allowed to precipitate overnight at 4°C. The bottles were centrifuged at 8K rpm for 20 min after which 10ml of 1X TBS was added to each. The bottles were left to shake at RT to resuspend phage. The phage was pooled (30ml altogether) in an Oak Ridge tube and centrifuged at 10K rpm for 15 min to pellet insoluble matter. The

supernatant was poured and pipetted into a fresh Oak Ridge tube. 3.3ml of a 1:9 v/v mixture of triton-X100:water was added and the tube was rocked on its side for 1 h at RT. 5ml PEG/NaCl was added and the solution was mixed by many inversions after which it was immediately centrifuged at 10K rpm for 15 min. The phage pellet was dissolved in 15ml 1X TBS and the centrifuged at 10K rpm for 10 min. The supernatant was poured into a fresh Oak Ridge tube. 15ml 1X TBS containing 2% sarkosyl was added and the solution was mixed gently by inversion. The tube was then rocked on its side for 1 hr at RT. 4.5ml PEG/NaCl was added and the solution was mixed by many inversions. Immediate centrifugation proceeded at 10K rpm for 10 min. The pellet was dissolved in 10ml 1X TBS by pumping and scraping with a 5-ml pipette tip. The mixture was left to shake for 1 h at RT. Centrifugation proceeded at 10 Krpm for 10 min to clear insoluble matter. The supernatant was poured into a 15-ml centrifuge tube (phage was stored at 4°C at this point). 4.83g of CsCl was put into a tared beaker after which the beaker was tared again. The cleared supernatant was added to bring the net weight of aqueous phage to 10.75g. The mixture was stirred gently to dissolve the salt. The final solution was 12ml of a 31% w/w (1.30g/ml) with a density of 1.29-1.31 g/ml. The phage suspension was loaded into a polyallomer SW41 tube and centrifuged for 36-48 h at 37 000 rpm. Using a sterile transfer pipette, the solution above the phage band (a very light, clean, translucent band should be visible towards the middle of the tube) was removed, trying as much as possible to keep the tip at the meniscus. A fresh transfer pipette was the used to remove the phage band into a clean 60Ti bottle. The bottle was filled to shoulder with 1X TBS and centrifuged at 50 Krpm for 4 hours in a 60Ti rotor. RRR. 3ml of 1X TBS was added to the bottle. The top of the bottle was wrapped in parafilm and left to rotate overnight at 4°C to dissolve phage. The next day the solution was re-vortexed and centrifuged briefly to drive solution to the bottom. The dissolved phage was transferred to a 4-ml tube. The mixture was dialyzed in a 3-ml Pierce Slide-A-Lyzer against three changes of ~1L cold 1X TBS. the dialyzed phage was transferred into a clean polyallomer 10-ml Oak Ridge tube and centrifuged at 10 Krpm for 5 min. The supernatant was removed to a clean 4-ml vial. The undiluted physical particle concentration was calculated by making 300µl of a 1/50 dilution and scanning the absorption from 240-320nm.

Sequencing phage: Oligonucleotide primers specific for the phage DNA sequence were purchased (Whitehead Scientific, Cape Town, SA). The primers were specific for the f88-4 vector clones (5' –AGTAGCAGAAGCCTGAAGA-3'). Sequencing was performed by the sequencing facility of the Division of Molecular Biology and Human Genetics, University of Stellenbosch Faculty of Health Sciences. 10µl of f88-4 primer was needed for each sample and the final primer concentration was 1.1pmol. The sample concentration for sequencing had to be 100ng/µl.

2.2.2.2 Micropanning

In order to confirm binding, micropanning was applied. 40µl 10µg/ml streptavidin in 0.1M NaHCO₃ was pipetted into each well of a 96 well polystyrene ELISA dish. The protein was left to absorb to the plastic for at least 1 h at room temperature. The streptavidin solution was aspirated out and the wells were filled to the brim with blocking buffer (~400µl/well). The dish was allowed to sit with the lid off for 2 h at RT. The dish was then washed 5X with TBS/Tween. The desired amount of biotinylated receptor (bAChE, bE8, bC2, b43B4C) was added at about 500ng in 200µl TTDBA and allowed to react for at least 2 h at 4°C in a humidified box. This was followed by another wash step, 5X with TBS/Tween. The wells were filled with 100µl TTDBA. 30µl of the input phage (f88-4/CysO, at a physical particle concentration of up to ~10⁷ virions/ml for qualitative binding conformation) was added and the dish was rocked for 2 h at RT in a humidified box. The wells were washed 10X with TBS/Tween. 20µl elution buffer was pipetted into each well and allowed to sit for ~10 min at room temperature. The eluate in each well was pipetted into the corresponding well of a second microtiter dish already containing 3.75µl 1M Tris.HCL (pH9.1). Into each well starved K91BluKan cells were pipetted and transfection proceeded at RT for 10 min. 200µl NZY medium, containing 0.2µg/ml *tetracycline*, was then pipetted into each well and dishes were put in the 37°C incubator for 30 min. This was the gene expression period, during which the *tetracycline* resistance gene on the incoming phage has a chance to be expressed before the infected cells are challenged with a high concentration of the antibiotic. 20µl portions from each well was spotted onto a NZY plate containing 40µg/ml tetracycline and 100µg/ml kanamycin.

Single standard 100mm petri dishes were able to accommodate 19 spots in a hexagonal array. The colonies were counted after ~12 h at 37°C. Excellent binding (10% yield) corresponds to ~100 colonies/spot. Good binding (~1% yield) correspond to ~10 colonies/spot. Background should be 0.

2.2.2.3 Antibody phage display

In this thesis, two different types of phage libraries were used: peptide and antibody libraries. The principle behind them and the methods of selection, amplification and sequencing are the same.

Antibody phage display has been described by Bradbury and Marks (2004) as “arguably the most successful use of phage display”. The technique involves the use of single-chain Fv (scFv) immunoglobulin fragments rather than the short linear peptides used. ScFvs are approximately 225 residues long and are made up of the single chain variable region of the immunoglobulin molecule. The variable region contains the 6 hypervariable complementarity-determining regions (CDRs), which are primarily responsible for antigen recognition, and therefore vary dramatically in sequence, and the framework regions that occur in between the CDRs. The framework regions are largely a beta-sheet structure that supports the CDRs, and they are far more conserved.

Two kinds of Ab library can be used: naïve or immune. Naïve libraries are derived from natural unimmunised human rearranged V genes (Marks *et al.*, 1991; Vaughan *et al.*, 1996; Sheets *et al.*, 1998; de Haard *et al.*, 1999; Sblattero and Bradbury, 2000), synthetic human genes (Griffiths *et al.*, 1994; Nissim *et al.*, 1994; de Kruif *et al.*, 1995; Knappik *et al.*, 2000) or shuffled V genes (Soderlind *et al.*, 2000). Immune libraries are developed from the V genes of humans (Barbas *et al.*, 1991; Zebedee *et al.*, 1992; Williamson *et al.*, 1993; Amersdorfer and Marks, 2000; Amersdorfer *et al.*, 2002) or mice (Orum *et al.*, 1993; Ames *et al.*, 1994, 1995), and thus are biased towards antibodies of a particular

specificity (Bradbury & Marks, 2004), although their use in selecting antibodies against antigens not used for immunisation has been reported (Williamson *et al.*, 1993).

The Ab phage display was contracted out (Creative Biolabs Inc., NY, USA) for the catalytic MAbs (not for AChE). A naïve human scFv library was used. This approach gives a 3D structure made up of CDRs of the Ab rather than the linear peptide sequences obtained from ordinary phage display. From the sequences obtained from the scFv, homology modelling and docking can be done with AChE in order to identify specific sequences that bind to the PAS and its motifs. The first part of the Ab phage display focused on selecting human scFv binders against rHuAChE (recombinant human AChE) from the HuNSL® naïve ScFv phage display library. Six rounds of selection proceeded. During the first three rounds, the original library as well as the derived sub-libraries was pre-absorbed with pre-blocked panning tube to remove non-specific binders. In the following three rounds, the biotinylated peptide 18 was used as the target. Capturing proceeded using streptavidin conjugated magnetic beads to remove non-specific binders. In order to increase the screening stringency, the subtracted phages from the 1st and 2nd round of screening were incubated with decreased concentrations of rHuAChE protein. At the same time, specifically-bound phages from the first three rounds were eluted using 0.25% Trypsine, while in the last three rounds of screening, specific binders were eluted with high concentrations of the non-biotinylated peptide competitively. Final round clones were amplified and assayed by phage ELISA, among which 23 positive clones were subjected to DNA sequencing.

The top two positive binders obtained from the Ab phage display were subjected to three dimensional modelling using Swiss-Model and RASMOL. The models produced were used to dock with mouse AChE (see 2.2.4.1). The scFv sequences produced were also BLASTed in order to identify additional molecules with which AChE could be redundant.

2.2.3 Peptide array/microarray

Peptide array or microarray is the rapid and quantitative cyclization of multiple peptide loops onto synthetic scaffolds for the structural mimicry of protein surfaces. Structure-based design of synthetic peptides mimicking the functional site of natural proteins, serve as important tools for discovering biochemical interactions, profiling cellular activities, and discovery of novel drugs (Timmerman *et al.*, 2005). Even though a wide variety of structural mimics exist, including mimics for α -helices (Venkatraman *et al.*, 2001; Karl, 1999), β -turns (Venkatraman *et al.*, 2001; Cochran *et al.*, 2001; Burgess, 2001) and β -sheets (Venkatraman *et al.*, 2001; Nowick, 1999), often more complex topologies like four-helix bundles (Hill *et al.*, 2000; Floegel & Mutter, 1992) are needed to adequately mimic protein function (Reineke *et al.*, 1999). The principle involves the immobilization of peptides, previously designed by chemical or by recombinant methods, to a solid surface such as glass chip, paper or monolayers, followed by assaying the bound peptide through protein binding, enzyme activity or cell adhesion. Specific binding can be detected using fluorescence, radioactivity, surface Plasmon resonance or mass spectrometry.

Previous work suggest that the AChE site is clearly conformational (e.g. Johnson & Moore, 2004), involving residues from different loops drawn together by folding as well as the formation of a salt bridge. A precise and detailed mapping of conformational structures is necessary for rational design as well as to compliment results obtained from the phage display which would yield linear as well as conformational binders. A microarray of 500 overlapping peptides of varying length (9-25 amino acids) and residue combinations for the AChE sequence 30-110 was designed in such a way as to represent conformational structure as present in the native protein. Synthesized and execution of the array was done by PepScan Systems (Lelystad, The Netherlands). Using CLiPS™ technology, the microarray was constructed with each peptide containing two cysteine residues. Variation in the position of these residues allows different degrees of constraint and enables reconstruction of conformational epitopes. The immobilization of peptide loops onto a synthetic scaffold is an extremely fast and clean reaction running very well with linear peptides that are 2-30 amino acids long. The reaction is compatible with all

possible side-chain functionalities except for free cysteine. PepScan's CLiPS™ epitope mapping (<http://www.pepscan.com>) used high-throughput synthesis of overlapping peptides on microarrays that completely covered the sequence and structure of the protein. The peptides representing the protein interaction site of interest was identified through antibody binding studies using fully automated ELISA-type read-out. The protein-protein interaction sites were defined at the level of individual amino-acids. For more information on the technique see Timmerman (2007).

2.2.4 Bioinformatics

2.2.4.1 Homology modelling

The three-dimensional structure of a protein is necessary for the understanding and prediction of many of its functions, including ligand interactions. Crystallisation and X-ray diffraction is the gold standard, but is a difficult and time-consuming process. An alternative is nuclear magnetic resonance (NMR), but this is limited to relatively small proteins. Homology modelling is a method that allows the rapid determination of a three-dimensional structure from sequence data, provided a suitable template is available. This technique is sometimes referred to as “comparative modelling” or “knowledge-based modelling”, terms that may be more accurate as “homology” implies a common evolutionary origin of the modelled structure and the template, which may not always be the case.

The first step in the modelling of a protein sequence is the identification of a suitable template. This is done by identifying similar or homologous sequences, and whether they have structures available, on the Basic Local Alignment Search Tool for proteins (BLAST-P; Altschul *et al.*, 1997), National Centre for Biotechnology Information (NCBI), followed by alignment of the sequence to be modelled with that of the proposed template. Following this, the steps in model construction are the identification of structurally conserved and structurally variable regions, the generation of coordinates for the structurally conserved residues of the unknown structure using the coordinates of the known structure, the generation of the conformations of the structurally variable regions

in the unknown structure, building the side-chain conformations, and, finally, the refinement and evaluation of the unknown structure.

In this thesis, modelling was done by the automated web server, Swiss-Model at the Swiss Institute of Bioinformatics (<http://swissmodel.expasy.org>; Arnold *et al.*, 2006) and RASMOL.

2.2.4.2 Protein-protein docking

The goal of protein-protein docking is the prediction of how two individual protein structures may bind and form a complex. There are two different approaches to automated protein-protein docking: rigid-body docking and flexible docking.

In rigid-body docking, both proteins are considered to be completely rigid. This type of docking thus does not consider either conformational changes or interfacial solvation that occur on binding. This reduces the docking problem considerably. Docking is geared towards optimising the geometric and chemical fit of the two surfaces. Flexible docking, on the other hand, takes both conformational changes and solvation into account. This type of docking is therefore much more complex, and tends to be demanding of both time and computing hardware. As a result, it is less frequently used than its rigid-body counterpart.

Docking algorithms use a range of search and scoring methods, including fast Fourier transform correlations, geometric hashing, and Monte Carlo techniques. There are two parts to the docking problem: firstly, developing a scoring/energy function that is able to discriminate between correctly docked orientations and incorrectly docked orientations, and, secondly, developing a method of searching that can pick out a correctly or nearly correctly docked orientation with reasonable accuracy (Ritchie, 2008). The simplest scoring function is shape complementarity, which requires a description of the surface of the protein. Thermodynamic considerations, particularly the free energy change, also

need to be taken into account. Interactions such as electrostatic, Van der Waals and water-mediated interactions are also considered (Ritchie, 2008).

Docking was carried out by using the programs Hex 4.5 (D. Ritchie, University of Aberdeen, Aberdeen, Scotland, U.K) as well as GRAMM-X (Tovchigrechko *et al.*, 2006). This kind of docking gives both a visualization of the receptor-ligand interaction, as well as a detailed analysis of the fit and types of bonding (e.g. hydrogen bonds, Van der Waals interactions, etc.). Hex 4.5 uses rigid-body docking and is distinguished from other docking software by its use of spherical polar Fourier correlations to accelerate docking. Hex also, uniquely, uses an expansion of the molecular surface and electric field in spherical harmonics, which improves the efficiency of docking (Ritchie & Kemp, 2000). It performs a six-dimensional search over the full ranges of both receptor and ligand. The specific parameters used were full rotation plus electrostatics where the contribution of electrostatics to the interaction is calculated during the final search phase. The structures used were: mouse laminin $\alpha 1$ G4-5 domains (PDB code 2JD4); mouse AChE, apo form, chains A and B (PDB code 1J06); mouse AChE dimer-propidium complex (PDB code 1N5R); mouse AChE dimer-gallamine complex (PDB code 1N5M); mouse AChE dimer-fasciculin-2 complex (PDB code 1KU6); *Torpedo* AChE (PDB code 2ACE); human BChE (PDB code 1P0I); and the laminin $\alpha 2$ G4-5 domain pair (PDB code 1DYK). The *Torpedo* AChE (PDB code 2ACE) and human BChE (PDB code 1P0I) are monomers. Analysis of structures, in particular, measurement of distances between residues, was done with DeepView/Swiss PDB Viewer (Guex & Peitsch, 1997). RasMol was used for visualizing structures and for graphics used in illustrations (Sayle & Milner-White, 1995).

2.2.4.3 Identification of Motifs

As mentioned, results from previous studies indicated that laminin-111 binds to AChE through an interaction with the PAS region involving electrostatic mechanisms (Johnson & Moore, 2003). Seeing as the PAS region is anionic, a complementary site would very possibly be cationic. In order to identify such a cationic site, the sequence of the mouse

laminin α 1-chain (Swiss-Prot accession number NP_032506), as well as the β 1 (accession number P02469) and γ 1 (accession number P02468) chains were put under investigation. Potential cationic sites were defined as clusters of three or more basic (Arg, Lys, His) residues. A number of sites promoting cell attachment and spreading on laminin-111 have previously been identified (Nomizu et al., 1995). This information was taken into account when identifying potential interaction sites. In addition, docking of AChE with the LG4-5 domain pair of laminin α 2 (which has 63% identity to laminin α 1) was investigated. This was the only laminin structure available at the time.

For motif searches, both BLAST-P and Prosite were used. Prosite is a protein database curated by the Swiss Institute of Bioinformatics (<http://expasy.org/prosite/>). It contains entries describing protein families, domains and functional sites, as well as information on motifs and signatures. Short amino acid sequences or novel motifs can be scanned against the Swiss-Prot database

2.2.4.4 Other Bioinformatics Methods

Through the use of bioinformatics and *in silico* docking, the possibility of functional redundancy was investigated. The premise behind this analysis was that the MAbs appear to define a site that is critical for neural development, as treatment of developing neural cells with these Abs, blocked cell adhesion and induced apoptosis in neuroblastoma cells *in vitro* (Johnson & Moore, 2000). As the MAbs were raised against AChE, this would suggest that AChE is essential for neural development. However, the AChE knockout mouse does not show the degree of abnormality that the MAbs results would indicate (Xie *et al.*, 2000). The postulation of functional redundancy is a way of reconciling these observations: that the site recognized by the MAbs is present, not only on AChE, but on another molecule or molecules and that these Abs may be cross-reacting. Defining the MAbs epitope and using bioinformatic methods to investigate the presence of a similar epitope in other molecules, could indicate which molecule or molecules might be functionally redundant with AChE.

The analysis was done in two contexts: firstly, the migration and differentiation stages of neural crest cells, outside the CNS, and, secondly, in the CNS and especially in the context of neurodegeneration. The AChE-laminin interaction was used as a template for defining the search. This was done as AChE and laminin were observed to interact *in vitro*, and the MAbs, furthermore, interfere with this interaction (Johnson & Moore, 2003).

2.2.5 Coimmunoprecipitation

Immunoprecipitation is one of the most widely used methods for Ag detection and purification. The process involves allowing an Ab (monoclonal or polyclonal) against a specific target Ag (AChE or laminin in this study) to form an immune complex with that target in sample such as a cell lysate. This is followed by the capturing of this complex on a solid support to which either Protein A or Protein G has been immobilized. Protein A or Protein G is able to bind the Ab which is in turn bound to the Ag, thus extracting or precipitating the complex from the solution. Coimmunoprecipitation (Co-IP) is conducted in the same way; however, the target Ag precipitated by the Ab “co-precipitates” a binding partner/protein complex from a lysate. The components of the bound immune complex can then be analyzed through sodium dodecyl sulphate (SDS) gel electrophoreses, separating the different components according to size/weight. SDS gel electrophoreses is followed by western blot detection, using a secondary Ab, in order to verify the identity of the Ag.

For this study, anti-AChE and anti-laminin Abs were used to extract AChE and laminin, respectively, from cell lysates obtained from neuroblastoma cells. AChE is expressed in primitive neural cells from quite an early stage. In the embryo, the cells are formed in the neural crest where they stay during the early stages of development. At some point these cells start migrating and AChE expression is initiated, limited largely to soluble isoforms. When the cells reach their destinations, after adhering to the ECM, they start to differentiate. It is at this point that expression is very high and the expression form changes to membrane-associated forms. Neuroblastoma cells are, effectively, primitive

neural cells at the proliferation stage. Neuroblastoma is a cancer that shows up in very young children and the general cause seems to be something that goes wrong during the transition from proliferation to differentiation in the embryo. Shifting these cells from proliferation to differentiation can make them benign. There is also the possibility that AChE in undifferentiated cells and AChE in differentiated cells react with different ligands. Therefore both situations of using undifferentiated/proliferating vs. differentiated cells should be taken into account.

Co-IP enabled the investigation of molecules identified by preliminary experiments as possible AChE and laminin ligands (which “co-precipitates” with AChE and laminin), such as heparin sulphate proteoglycans (Battaglia *et al.*, 1992), agrin (Denzer *et al.*, 1997), beta-neurexin (Sugita *et al.*, 2001), etc., as well as enabling the confirmation of the AChE-laminin interaction (Johnson & Moore, 2003; Paroanu & Layer, 2004).

2.2.5.1 Cell culturing

Versene (EDTA in buffered saline): 650mg of Na₂EDTA, 500mg of KCL, 20g of NaCl, 2.85g of Na₂HPO₄ and 500mg of KH₂PO₄ was dissolved in 400ml of dH₂O. The pH was adjusted to 7.2-7.4 after which the volume was increased to 500ml with dH₂O. The solution was autoclaved and stored at 4°C.

Cell line and culture conditions: Neuro-2 α cells (N2 α , neuroblastoma cells) were obtained from the ATCC (The global bioresource center™, Manassas, Virginia, USA). The cells were stored in a liquid nitrogen freezer. The growth medium contained 10% v/v FCS, 1% Penicillin/Streptomycin and 89% v/v Eagle’s Minimum Essential Medium (EMEM) containing L-glutamine. Cells cultured directly from frozen were first grown in a medium containing 20% FCS for two nights after which the media was replaced with the 10% FCS medium. The cell culture media was stored at 4°C. The freezing media contained 8% DMSO in 20% FCS medium. It was important to maintain adequate frozen stocks of cell lines throughout the project.

Subculturing: The culture media was removed and discarded. The cell layer was briefly rinsed with 3ml of Trypsine/versene solution to remove all traces of serum that contains trypsin inhibitor. 5ml of Trypsine/versene solution was added to each flask and the flask was left (occasionally swirling slightly) until the cell layer was dispersed (usually within 5-15 min). The cells/trypsin mixture was pipetted into a 15-ml tube and lightly centrifuged for a few minutes after which the Trypsine/versene solution (supernatant) was removed and discarded. Fresh culture medium was added to new, sterile, culture flasks. 2ml of fresh culture media was added to the cells (pellet) and pipetted up and down to mix the cells into the media. 1ml of each cell solution was added to each new culture flask. The cells were left to grow in the CO₂ incubator until 100% confluency was reached.

Determining the amount of AChE and laminin per cell: Microtitre plates were coated overnight with 1/2000 anti-laminin Ab (L9393) and blocked. Laminin (L2020) was added at various dilutions ranging from 0-50ng. This was followed by secondary Ab-biotin binding. The amount of biotinylated protein bound was probed with streptavidin-peroxidase and H₂O₂/ABTS, and the absorbance was measured at 405nm. The data was used to produce a standard curve with which the cell lysate assay can be compared. For the cell lysate assay, the microtitre plates were coated as above, but instead of using pure laminin, the cell lysate was added in various dilutions (1/10, 1/50, 1/100). The resulting A405 readings, taking the dilution factor into account, were then converted to laminin concentration using the standard curve.

2.2.5.2 Coimmunoprecipitation

Cell lysis buffer: The buffer contained 20mM Tris-HCl (pH 8), 100mM NaCl, 0.5% NP-40, 0.5mM EDTA, 0.5mM PMSF (proteolytic inhibitor) and 0.5% protease inhibitor cocktail. 1ml of a 1M Tris-HCl solution (60.57g Tris dissolved in 500ml dH₂O, pH adjusted to 8 with HCl), 0.29g NaCl, 0.25ml NP-40, 0.007g of EDTA, 0.025ml of a 0.1M PMSF stock solution (1.74g PMSF dissolved in 100ml DMSO) and 0.25ml of protease

inhibitor cocktail was dissolved in dH₂O to give a final volume of 50ml. The buffer was then divided into 2ml aliquots and stored at -20°C. The proteolytic inhibitors contained within the protease inhibitor cocktail had a broad specificity for serine, cysteine, and acid proteases, and aminopeptidases.

NETN buffer: The buffer contained 20mM Tris (pH 8), 1mM EDTA, 900mM NaCl and 0.5% NP-40. 2.42g of Tris (pH 8), 0.29g of EDTA, 52.60g of NaCl and 5ml of NP-40 was dissolved in 1L dH₂O and stored at 4°C. An alternative NETN buffer containing 100mM NaCl was also used.

Precipitating the proteins: N2 α cells were grown in 10% culture medium in four 250-ml culture flasks until 100% confluency was reached for each flask. The cells from each of the four flasks were removed with 5ml of Trypsine/versene solution and pipetted into 15-ml sterile tubes as described above (two flasks worth of cells per tube, thus 10ml per tube). Each of the tubes were lightly centrifuged in order to remove the Trypsine/versene solution. (At this point the cells was either used immediately or stored in 2ml 1X PBS, pH 7.4, per tube, at -20°C). To lyse the cells, 1ml of ice cold lysis buffer was added to each of the two 15-ml tubes (if cells were used from frozen, the tubes were lightly centrifuged first in order to remove the PBS) and pipetted vigorously up and down. The mixture was left to sit on ice for 10 min after which the cells were homogenized as described above. After lysis, the mixture was centrifuged at maximum speed at 4°C for 15 min. The supernatant of each tube was pooled and the antibodies were added to precipitate the proteins: For AChE, 20 μ l of the goat polyclonal anti-AChE (sigma) was added to one tube (sample A); For laminin, 20 μ l of the rabbit polyclonal anti-laminin (sigma) was added to the other tube (sample L). At this point 10 μ g of AChE and 1 μ g of laminin was added to samples A and L, respectively. The immunoprecipitate was left to rock at 4°C for 1-2 h. In the meantime, the protein A-Sepharose slurry was prepared by washing 0.1g of protein-A beads in 1ml 1X PBS for 1 h at RT. The bead-mixture was centrifuged and the PBS discarded. 1ml of PBS/BSA 1% (w/v) was added to the beads and the mixture was left to rock for 1 h at RT. After 1 h the bead-mixture was centrifuged, rinsing twice with 1ml PBS, followed by a final centrifugation step. The last

PBS was discarded and 400 μ l of lysis buffer was added to the beads. The slurry was ready for use. After ~2 h, 100 μ l of the protein-A slurry mixture was added to each of the samples (lysate/antibody solution), and they were left to rock at 4°C for 1 h. The samples were centrifuged and the beads were washed, five times in NETN buffer containing 900mM NaCl), and once with NETN buffer containing 100mM NaCl. The leftover beads contained the precipitated protein.

2.2.5.3 SDS-PAGE

Running buffer for SDS gels: A 10X buffer was made up as a stock solution. The buffer contained 150mM Tris, 1.92M glycine and 1% SDS. 60.4g of Tris base, 288g of glycine and 20g of SDS was dissolved in dH₂O to give a final volume of 2L. A 1X buffer solution was made up prior to running the gels by adding 100ml of the 10X stock solution to 900ml of dH₂O to make up 1L of working buffer.

Sample loading buffer (laemli): 1ml of a 1% bromophenol blue solution was added to 4ml of 1.5M Tris-HCl, pH 6.8. 10ml of glycerol was added to the mix. 2g of SDS was added and left to dissolve. 5ml of β -mercaptoethanol was then added and mixed. The buffer was aliquoted and stored at -20°C.

Preparing and running the gels: SDS-polyacrylamide gel electrophoresis enables the separation of proteins according to their molecular weight. SDS can stop proteins aggregating and precipitating after the thermal denaturing step and provide proteins with a negative charge, irrespective of their isoelectric point. ~20 μ l sample loading buffer, containing SDS and β -mercaptoethanol which breaks disulfide bonds and separates multisubunit proteins to their monomers, was added to each of the samples from the Co-IP and they were boiled for 4 min at 100°C. The SDS gel consists of a separating gel of high concentration and a pH of 8.8, and a stacking gel of lower concentration and a pH of 6.8.

The gel compositions are shown below:

	Separating gel (10%, for 2X 0.75 mini-slab gels)	Stacking gel (3%, X4 gels)
Acrylamide/bisacrylamide, 30%	3.33ml	1.3ml
Tris-HCl	2.5ml (1.5M, pH 8.8)	1.25 (1M, pH 6.8)
10% SDS	0.1ml	0.1ml
dH ₂ O	4ml	7.4ml
TEMED	10µl	20µl
10% ammonium persulfate	50µl	50µl

The separating gel was prepared, loaded into the running cassette and overlaid with butanol. Once the separating gel had set, the butanol was poured off and the stacking gel was prepared and loaded on top of the separating gel. After polymerization, the cassette was placed into the gel chamber and covered with running buffer. Each sample (A and L) was loaded onto a separate 10% gel, along with a protein ladder as well as 3 controls for the AChE sample (C1A, C2A, C3A) and 3 controls for the laminin sample (C1L, C2L, C3L). C1A and C1L represented the cell lysate prior to Ab addition and should contain all the proteins of interest. C2A and C2L represented the supernatants after extraction of precipitated proteins with the protein A-Sepharose slurry and should be free of any AChE or laminin, respectively. C3A and C3L represented the recombinant human AChE (Sigma) and Engelbreth-holm-swarm murine sarcoma laminin (Sigma), respectively, and serve as indicator of successful blotting with antibodies. The gels were run in 1X running buffer for ~1 h at 200V in an SDS tank. Two control gels were also run and subjected to protein staining in order to confirm the presence of the proteins in the gels. Western blotting followed for the two sample gels.

2.2.5.4 Western blotting

When an Ab against an epitope of a particular protein is available, western blotting can enable high sensitivity detection of that specific protein in a protein mixture. The proteins separated by the SDS-PAGE gel are transferred to a nitrocellulose membrane which in turn is subjected to immunodetection. In order to identify optimal concentrations, a dot-blot was performed by directly pipetting the lysate samples from the Co-IP onto a nitrocellulose membrane and then proceeding with the normal western blot detection procedure, description follows.

Blocking buffer: The buffer contained 3% BSA and 0.05% Tween 20 diluted in 1X PBS. 15g of BSA was dissolved in 1X PBS to give a final volume of 500ml. The solution was filter sterilized followed by addition of 250µl Tween 20. The buffer was stored at 4°C. For long term storage, 0.02% NaN₃ was added.

Blotting (transfer) buffer: A 10X stock solution was made up by dissolving 30.3g Tris and 144.1g glycine in 1L of dH₂O. A 1X solution, made up by adding 100ml of the 10X stock solution and 200ml of methanol to dH₂O to a final volume of 1L, was made up prior to blotting each time. The transfer buffer was stored at 4°C.

Transfer of proteins to a nitrocellulose membrane: While the gels were running, the blotting apparatus was prepared. The membranes were soaked in methanol for ~30 min on a rocker at RT. After 30 min, the membranes, along with the fibre pads and blotting filter papers, were pre-soaked in 1X blotting buffer. After SDS-PAGE, the gel was carefully removed from the cassette and assembled into a “sandwich” containing the fibre pads and filter papers on both sides. The gel is placed directly on top of the membrane in the middle of the “sandwich”. The “sandwich” cassette was placed into a western blotting transfer tank and the proteins were transferred electrophoretically at 300 mA for 1-2 h.

Immunodetection: After the proteins were transferred to the membranes, the two membranes (membrane A for the AChE sample, and membrane L for the laminin sample) were incubated overnight at 4°C with blocking buffer. This buffer contained a rich source of natural proteins that allow unspecific binding to all the proteins transferred onto the membrane. The next day, the membranes were washed three times with TBS/Tween wash buffer. Each membrane was incubated with primary Ab: Membrane A with a 1/1000 dilution of the goat anti-AChE Ab (sigma); and membrane L with a 1/1000 dilution of the rabbit anti-laminin Ab (sigma). Abs were diluted in washing buffer. Incubation proceeded on a rocker for 1 h at RT or overnight at 4°C. After incubation, the membranes were washed five times with TBS/Tween. Incubation with secondary Abs followed. Membrane A was incubated with a 1/10 000 dilution of anti-goat IgG (sigma) and membrane L with a 1/10 000 dilution of anti-rabbit IgG (sigma). Incubation proceeded for 1 h at RT. This was followed with another wash step (5X TBS/Tween). The membranes were then incubated with a 1/ 2000 dilution of streptavidin-peroxidase in blocking buffer for 15 min on the rocker at RT followed by another wash step (5X TBS/Tween). After washing, the membranes were sealed in a plastic cover and ~7ml TMB detection fluid containing 1% hydrogen peroxide was added to each sealed “bag”. Detection proceeded for 10-15 min (or once bands become visible) by rocking the membranes at RT. The membranes were then washed five times with purified H₂O. The visible protein bands were analysed.

Stripping and reprobing of blot: Membranes A and L were incubated in preheated stripping buffer at 50°C in a shaking water bath for 30min. The membranes were then washed twice in TBS-tween buffer at RT. This was followed by blocking the membranes in 10% blocking buffer for 1 h at RT. Immunodetection followed.

Immunodetection using opposite Abs: In order to confirm the co-precipitation of AChE with laminin, and laminin with AChE, the membranes A and L were then blotted with opposite Abs: membrane A with anti-laminin primary Ab (followed by incubation with appropriate secondary Ab); and membrane L with anti-AChE Ab (followed by incubation with appropriate secondary Ab). The respected concentrations used were as given above.

Where immunodetection with opposite Abs, following stripping of the membranes, produced weak signals, new samples were run from the start and membranes were blotted with opposite Abs, i.e. where anti-AChE Abs were used in the Co-IP, anti-laminin was used for western detection and vice versa.

3. Results

3.1 Demonstrating the interaction between AChE and laminin-111

In order to demonstrate the binding of AChE with laminin-111, ELISA and Co-IP methods were used. The ELISA demonstrates interaction of the two molecules in a controlled *in vitro* environment, while the Co-IP shows interaction under more physiological conditions. The *in vitro* ELISA experiments are a repeat of previously published work (Johnson & Moore, 2003).

3.1.1 Whole molecule binding: ELISA

Consistent with results previously shown (Johnson & Moore, 2003; Paroanu & Layer, 2004), biotinylated AChE was observed to bind to laminin-111 (Figure 17). The measured K_d value was 4.866 ± 0.3717 nM, and $B_{max} = .5136 \pm 0.008021$ A_{405} units (n = 6). Non-specific binding was measured by using plates that were coated with buffer only. The non-specific binding has been subtracted from the values used for the graph. Purified erythrocyte AChE (Sigma) was used in all assays in preference to the recombinant protein; this was done in order to avoid possible problems with posttranslational modifications, especially glycosylation, that might influence the protein's conformation and binding to ligands.

Neither of the two controls, biotinylated BSA and non-specific anti-human IgG was found to bind laminin-111 (Figure 18). IgG was used because it has a pI value similar to AChE, and BSA was used as a neutral control unlikely to bind. This confirms the specific binding of AChE to laminin-111.

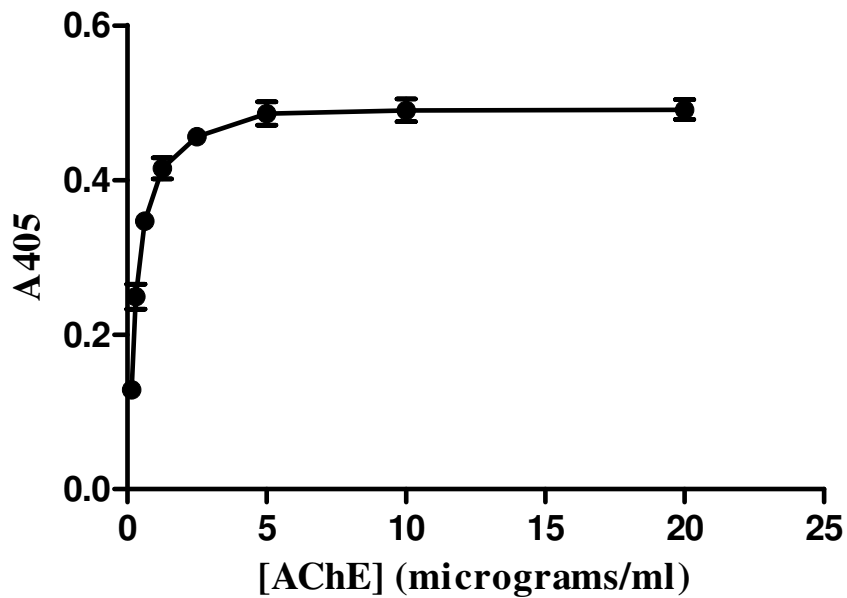


Figure 17. Whole molecule binding between AChE and laminin. Microtitre plates were coated with 10 μ g/ml laminin in 50mM NaHCO₃ buffer (pH 8.0). Biotinylated AChE was added (0.156-20 μ g/ml) and binding was observed at A405. Error bars reflect standard deviation (SD) and an average of 6 replicas was used to produce each data point.

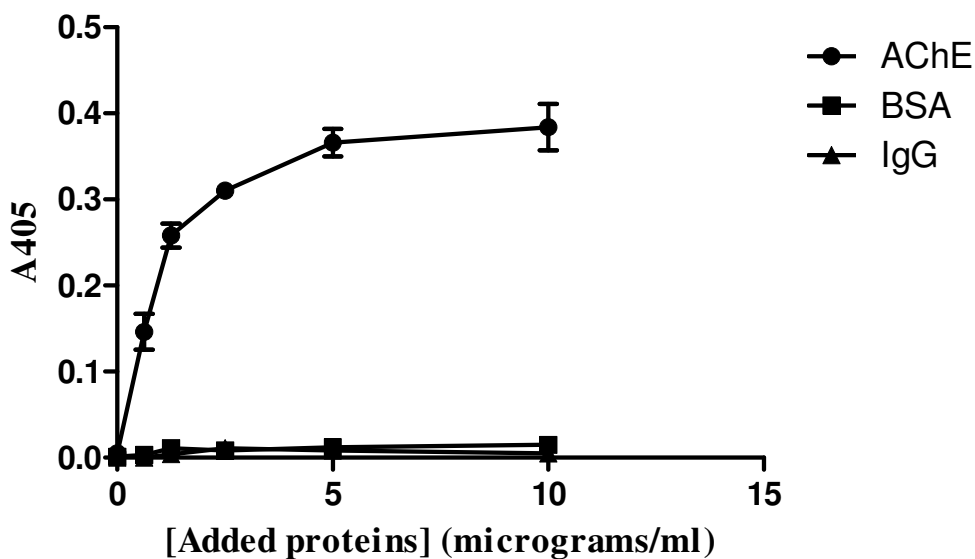


Figure 18. Binding of the controls BSA and IgG to laminin-111. Microtitre plates were coated with 10 μ g/ml laminin in 50mM NaHCO₃ (pH 8.0). Biotinylated AChE, BSA and IgG was added in serial dilutions of 0-10 μ g/ml, and binding was observed at A405. Error bars reflect SD and an average of 5 replicas were used to produce each data point.

In order to investigate the role of electrostatics in the binding between AChE and laminin-111, the NaCl concentration of the buffer was altered and binding was measured as above. It was clear that high concentrations of salt in the buffer disrupted binding (Figure 19), indicating that electrostatics may play a role in the binding of AChE and laminin-111. This was also previously shown (Johnson & Moore, 2003).

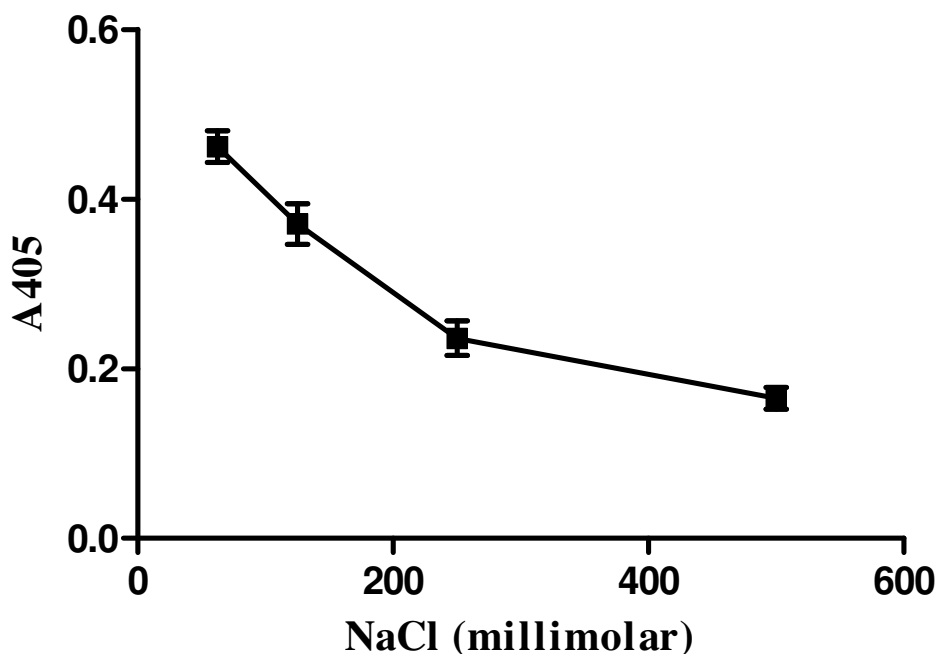


Figure 19. The effects of NaCl on the binding of AChE to laminin. Plates were coated with 10 μ g/ml laminin in 50mM NaHCO₃ (pH 8.0). Biotinylated AChE was added at a concentration of 10 μ g/ml in PBS containing a different concentration of NaCl for each data point (500, 250, 125 and 62.5 mM). n = 6 for each data point.

Pre-incubation of AChE with the PAS-binding inhibitors (BW284c51, propidium, and gallamine), as well as the active site inhibitor, pyridostigmine, was also found to affect AChE-laminin binding (Figure 20), indicating that the PAS as well as the active site may be involved in AChEs binding to laminin.

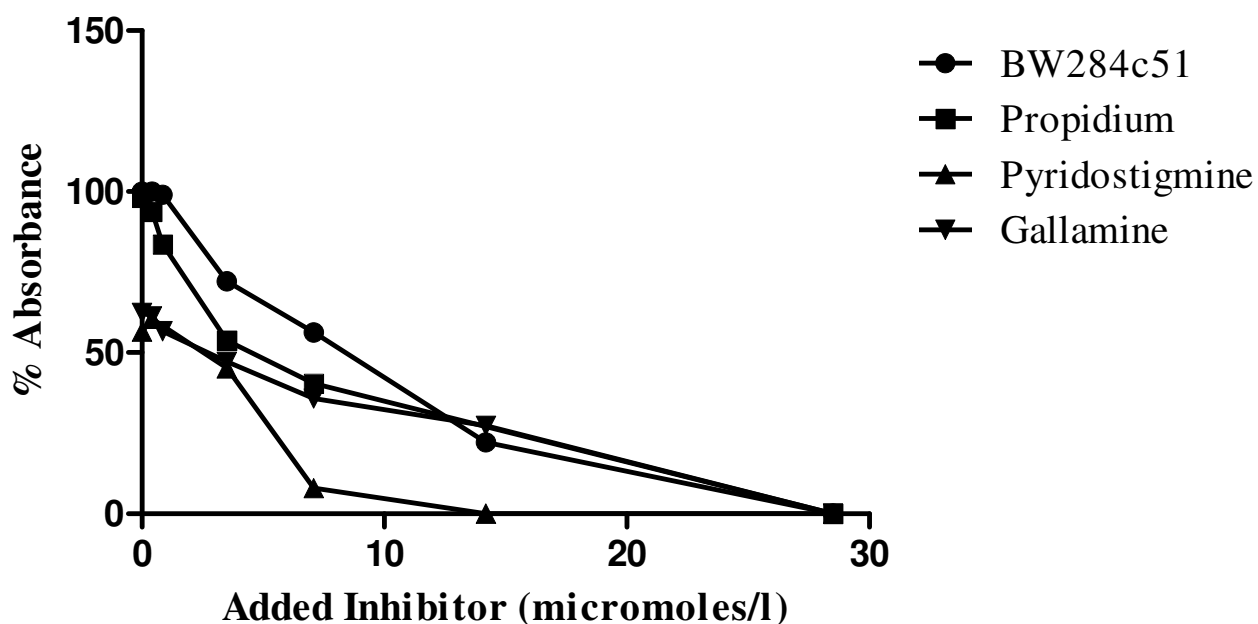


Figure 20. Effects of AChE inhibitors on AChE-laminin binding. Microtitre plates were pre-coated with 10 $\mu\text{g/ml}$ laminin. 20 $\mu\text{g/ml}$ biotinylated AChE was pre-incubated for 1 h in the presence of BW284c51 (●), propidium (■), pyridostigmine (▲) or gallamine (▼), before addition to plates. Inhibitors were used at concentrations of 0-500 μM . Absorbance was calculated as a percentage of total AChE binding at each concentration.

3.1.2 AChE peptides binding to laminin: ELISA

Peptides corresponding to the PAS-associated sequences of human AChE were synthesized. Figure 21 depicts the different positions on mouse AChE (1J06.pdb) of each of the peptides used. Demonstration of the binding of laminin to each of these peptides gives an indication as to the involvement of specific sites on AChE in the binding.

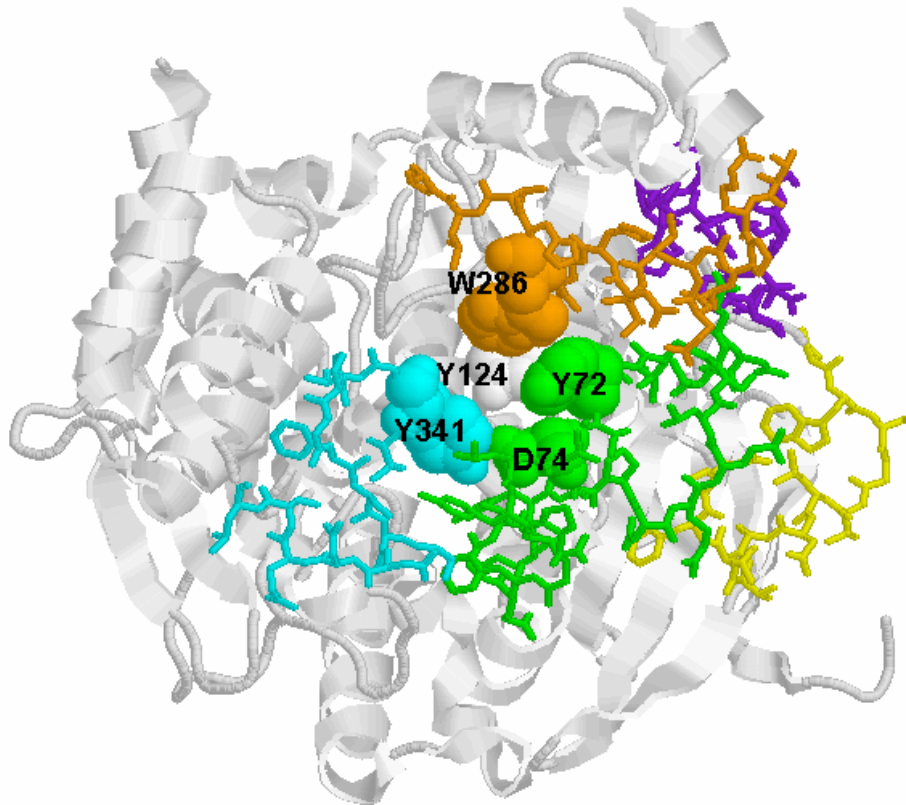


Figure 21. Position on mouse AChE (1J06.pdb) of the peptides used in this study. Residues 39-50 are shown in purple; 55-66 are shown in yellow; 69-96 are shown in green; 275-290 are shown in orange; and 340-353 are shown in cyan. The PAS residues (Y72, D74, Y124, W286 and Y341) are shown in spacefilling mode.

The following peptides showed highest binding to the laminin immobilized on the plates: the omega loop (69-96), 55-66 and the 37-53 peptides (Figure 24). Peptides 275-290 and 340-353 showed lowest binding to laminin. Once again non-specific binding was measured by coating wells with buffer only (without laminin), adding the biotinylated ligands and then subtracting the A405 values from the readings used for representation of the graph in Figure 22.

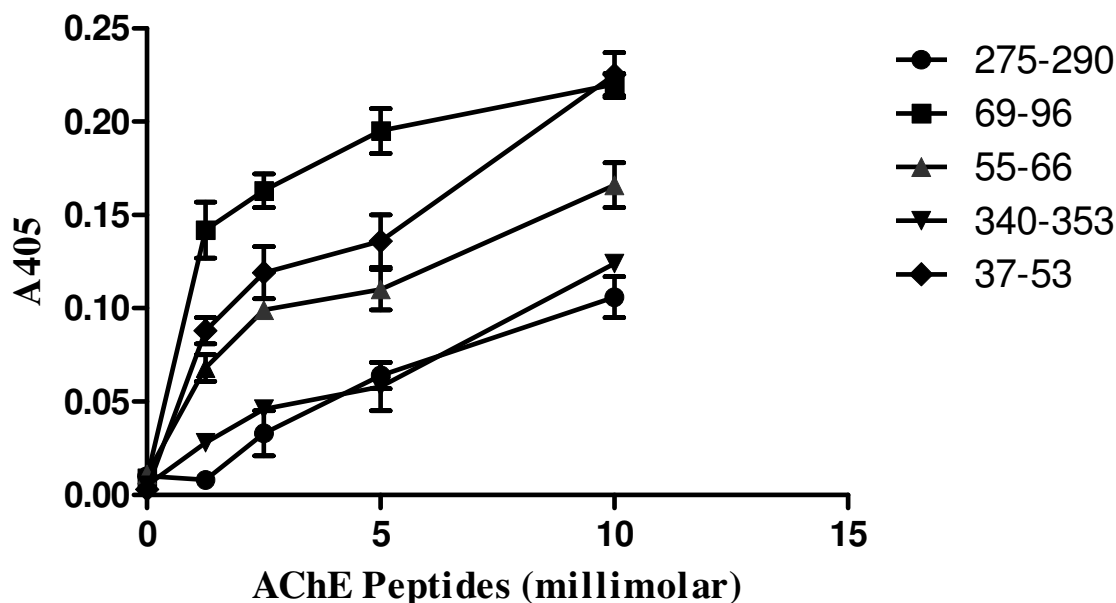


Figure 22. AChE peptides binding to laminin. Microtitre plates were coated with 100 μ g/ml laminin. The biotinylated peptides were added at dilutions of 0-35mM.

3.1.3 Demonstration of the interaction between AChE and laminin: Co-IP

Coimmunoprecipitation was performed in order to investigate the AChE-laminin interaction in a more physiological context as well as to indicate the possibility of other binding partners for AChE. Previous results from the laboratory had shown that the inclusion of proteolytic inhibitors had no effect on Ab recognition of AChE. Seeing as the experiment was not focused on measuring AChE's enzyme activity, using proteolytic inhibitors (such as PMSF, which inhibits AChE), would not matter. Figure 23 shows the basic principle behind the Co-IP method. (Unfortunately some of the protein bands on the immunoblots were less visible after scanning as the resolution of the available scanner was not ideal, and even. The protein bands were also clearer in the electronic copy vs. the printed out hard copy).

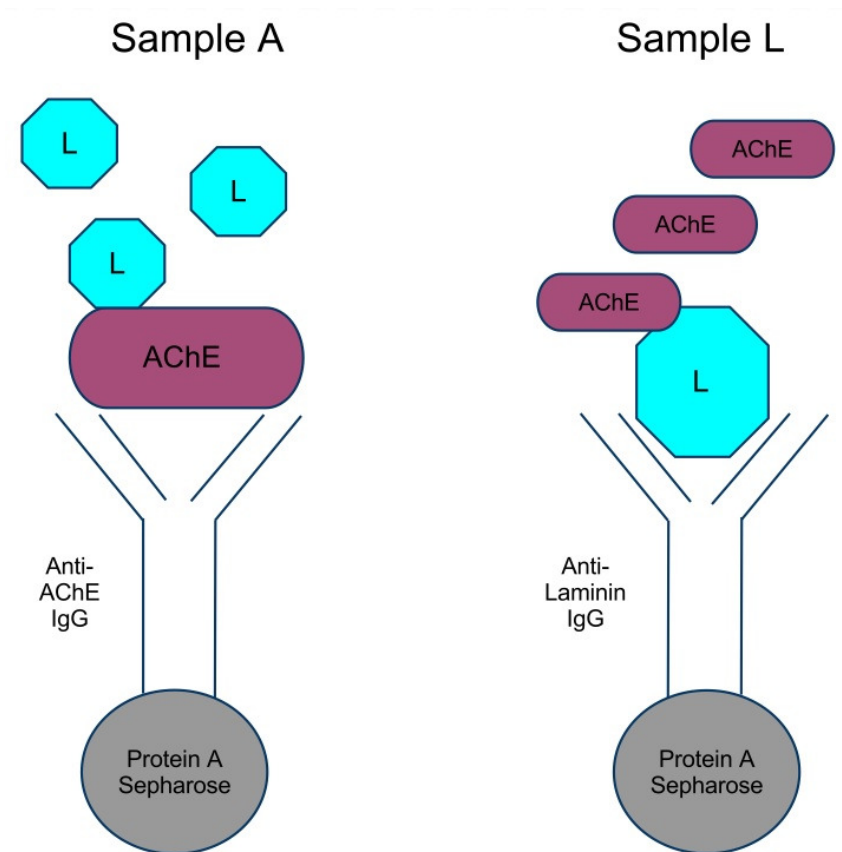


Figure 23. Coimmunoprecipitation. The Ab-protein complex is extracted from the cell lysate using Protein A-Sepharose beads. Any molecules attached to the protein of interest will be extracted along with it.

In Sample A (Figure 24), AChE was extracted from the cell lysates of neuroblastoma cells using goat polyclonal anti-AChE Ab (Sigma). It is important to note that, unlike the MAbs used in the other experiments, this polyclonal Ab did not interfere with the AChE-laminin interaction (results not shown). Immunodetection followed using the same Ab. In theory, only AChE should be visualized here, either on its own, or as part of a complex (with the Ab or another molecule) that did not separate under the denaturing conditions. Results show (lane titled Sample A; Figure 24) that the goat polyclonal anti-AChE Ab was able to successfully extract AChE from the cell lysate (indicated by an arrow in the Sample A lane, represented as a monomer corresponding to the ~70kDa area according to the protein ladder). At around 52kDa, a protein band can be seen. Another light band corresponding to ~30-40kDa can also be seen. These two bands probably represent the IgG light and heavy chains of the Ab molecule. There were no higher molecular weight

bands (possible AChE-complexes) visible in sample A. The first control, C1A, represented the complete neuroblastoma cell lysate prior to precipitation. Protein bands visible in the C1A control corresponded to ~52, 60, 80, 95, 135, and 200Da. The second control, C2A, is the supernatant after extraction of precipitated AChE. No AChE was detected in this lane of the immunoblot indicating successful extraction of protein. The lack of visible bands in this lane also eliminates the possibility of non-specific binding. The final control, C3A, contained the pure AChE and is shown as a light band near the 72kDa mark of the protein ladder (indicated by an arrow in the C3A lane).

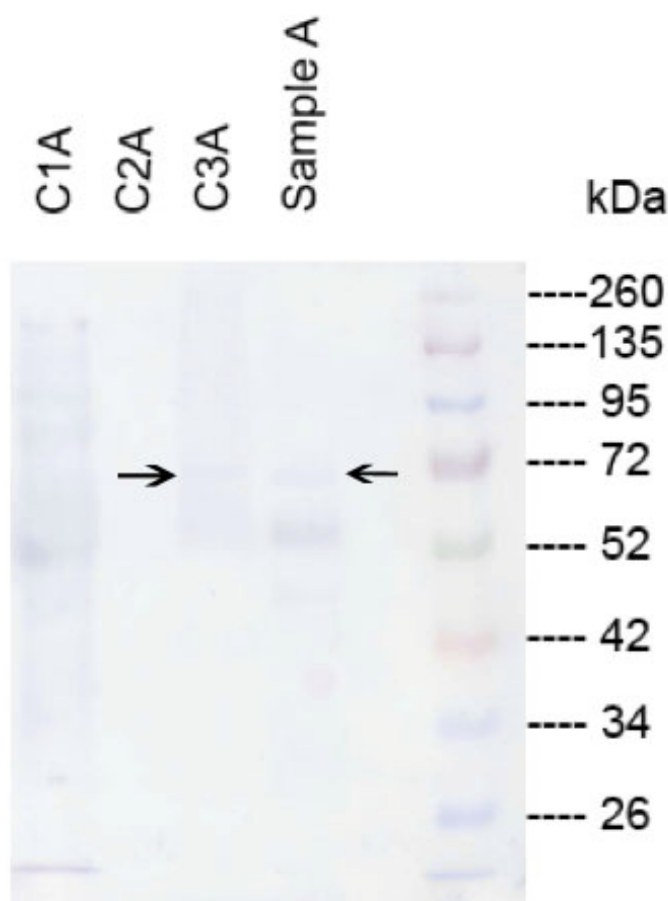


Figure 24. Sample A: Anti-AChE Ab used for detection. Anti-AChE Abs were used for protein extraction as well as for immunodetection. Sample A is the AChE sample from the cell lysate. C1A is the complete lysate control. C2A is the supernatant after AChE extraction control. C3A is the pure AChE.

The visible IgG heavy and light chains could be the result of excess Ab that was left behind from the extraction, i.e. all the Ab may not have been removed from the cell lysate by the protein A. If this was the case, the secondary Ab (anti-goat IgG) would pick it up during immunodetection. This would also happen if the Ab was originally added in

fairly high stoichiometric ratios (compared to AChE). The Ab-AChE complex would probably be split by the SDS, thus showing as separate bands on the membrane, as can be seen in Figure 24.

Although it is likely that the presence of SDS would dissociate complexes, higher molecular weight bands could indicate AChE in complex with a binding partner. It has been shown that certain protein complexes are stable enough to survive SDS degradation (e.g. the investigation of SDS-resistant complexes by Otto *et al.*, 1997). Unfortunately it is not known whether SDS would break up an AChE-complex or if such a complex would survive degradation. However, unless non-specific binding occurred (an absence of non-specific binding is suggested by the lack of protein bands in C2A), anti-AChE immunodetection would only pick up AChE or AChE-associated complexes. Cross-reaction of anti-AChE Abs has been observed (e.g. Mappouras *et al.*, 1995), thus higher molecular weight bands could also be due to the Abs cross-reacting with another, irrelevant entity.

Sample A, containing the precipitated AChE, was also blotted with anti-laminin Ab in order to confirm the AChE-laminin interaction. The sample showed (Figure 25) a protein band once again near the 52kDa region that could represent the IgG heavy chain of the Ab (i.e. Ab left over after Protein A extraction). One or two lighter bands were also visible in the 150-260kDa area (2 very light bands were visible on the membrane, however, these are not as visible on the membrane scan showed in Figure 27; the arrows indicate to where these bands were seen). If visualization of these bands is correct, it may indicate that the laminin molecule separated into its separate chains ($\alpha = 338\text{kDa}$, $\beta = 202\text{kDa}$, $\gamma = 177\text{kDa}$) during electrophoreses. Control C1A showed similar bands in the high molecular region (150-260kDa; indicated by arrows). The higher molecular weight bands seen in this lane could indicate AChE oligomers, AChE complexes, or antibody cross-reaction with other proteins. As a reducing agent, β -mercaptoethanol, was used in the sample buffer, the presence of AChE oligomers, which are linked by disulfide bonds, is unlikely. Complexes are likely to be split by the presence of SDS in the sample buffer and gel, although whether this has occurred in this case is obviously not known.

Similarly, the potential for cross-reaction by the antibody is also not known. Control C2A did not show any protein bands. Seeing as C2A represents the cell lysate after AChE was extracted from it, no bands could indicate that most of the laminin present in the cell lysate may have been extracted along with AChE, thus being in complex with AChE. The control containing the pure AChE (C3A) presented no protein bands indicating no interference of non-specific binding.

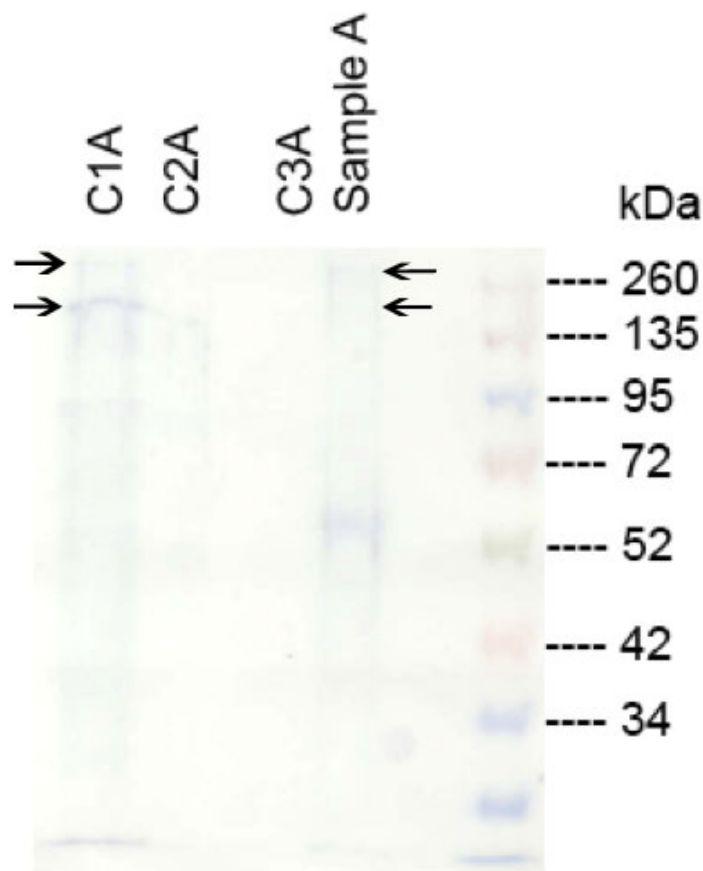


Figure 25. Sample A: Anti-laminin Ab used for detection.

Sample A is the AChE sample from the cell lysate. C1A is the complete cell lysate control. C2A is the cell lysate after extraction of AChE. C3A is the pure AChE control.

In Sample L, laminin was extracted from the cell lysate using a rabbit polyclonal anti-laminin Ab (Sigma). Immunodetection followed using the same Ab. The immunoblot shows (Figure 26) a dark band near the 52kDa region, possibly the IgG heavy chain again. Two lighter bands can be seen in the same area (150-260kDa; once again these bands were quite clear on the original membrane; shown by the two arrows) where the laminin chains could be residing as in Figure 25. Similar two light bands are visible in the

complete cell lysate control, C1L (shown by the arrows in lane C1L). The control containing the pure laminin (C3L) shows a very dark, thick band in the same area. It would appear that the C3L sample was overloaded on the gel, and the consequent lack of definition may obscure minor bands present in the same area. If there is more than one band represented there, it could possibly again indicate the separate chains of the laminin protein. This would suggest that laminin separates into its individual chains during electrophoresis. Control C2L did not show any protein bands, indicating that the protein-Ab extraction was successful.

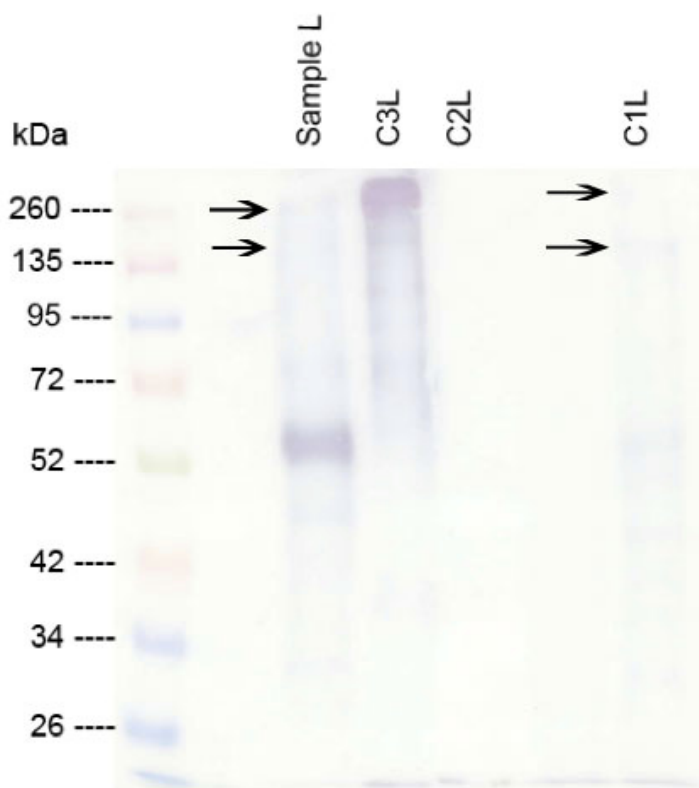


Figure 26.
Sample L:
Anti-laminin
Ab used for
detection.
 Sample L is the laminin sample from the cell lysate. C1L is the complete cell lysate control. C2L is the cell lysate after extraction of laminin. C3L is the pure laminin control.

Sample L was also probed with the anti-AChE Abs for immunodetection to confirm the AChE-laminin binding. Sample L very clearly shows (Figure 27) the presence of AChE corresponding to the 72kDa mark on the protein ladder, as well as two lighter bands near the 45 and 52kDa areas. These two bands again most probably represent the two IgG

chains (heavy and light). C1L showed a similar dark band at 72kDa representing the AChE in the complete cell lysate. C2L also contains the AChE indicating that not all the AChE in the cell lysate was extracted along with the laminin (thus bound to laminin) during the precipitation step. As the pure laminin control, C3L showed no protein bands, it is safe to exclude the possibility of non-specific binding in this experiment. Differences in the intensities of the bands corresponding to AChE on the laminin (Figure 27) and AChE (Figure 24) membranes (although the same anti-AChE was used) could possibly be attributed to differences in experimental conditions as well as differences in cellular concentrations of AChE and laminin (e.g. higher concentrations of laminin extracted would lead to higher concentrations of AChE extracted along with it).

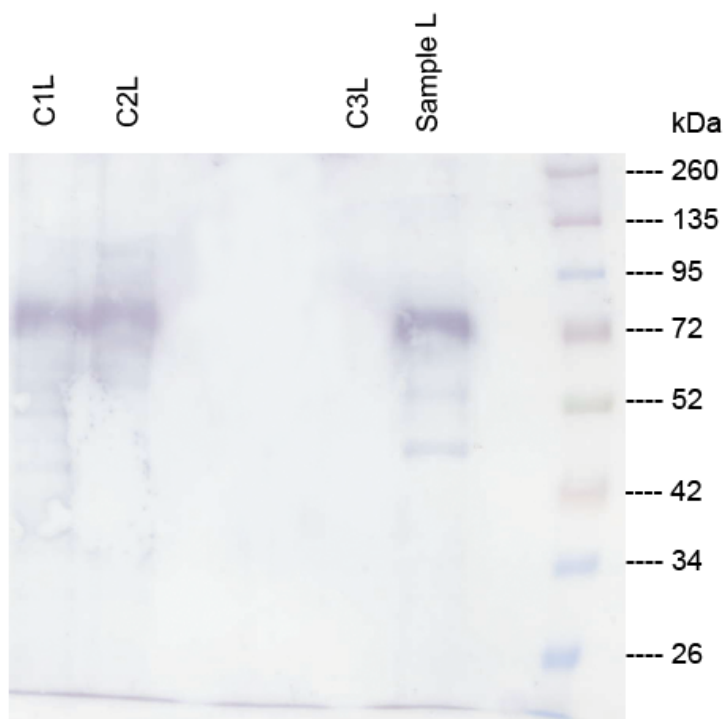


Figure 27. Sample L: Anti-AChE Ab used for detection.

Sample L is the laminin sample extracted from the cell lysate. C1L is the complete cell lysate control. C2L is the cell lysate after laminin extraction. C3L is the pure laminin control.

A few drawbacks need to be taken into account when considering the Co-IP procedure. During the homogenisation and lysis processes, the protein of interest can come into contact with proteins it would not normally come into contact with and these proteins may even bind to each other. A protein expressed on the cell surface may, for example,

meet up with a protein that is always found in the cytosol and discover an affinity for this protein that would not normally happen in the cell, thus creating artefactual results. Lability of protein complexes is also a problem. The complex formed between AChE and laminin may be inherently labile and may split during homogenisation and lysis. It may also split when it encounters SDS. The AChE-laminin complex most probably is a labile one as it is strongly dependant on electrostatic interaction which can very easily be broken by altered ionic conditions. Also, seeing as electrostatics play such a big role in AChEs binding to laminin, the ionic/salt concentrations of the buffers (NETN and wash buffers) used in the experimental procedures could have possibly affected binding.

The use of protein cross-linkers could possibly resolve the issue. Protein cross-linkers are chemical compounds used to covalently bind, or conjugate, biomolecules together. When such cross-linkers are added to the homogenate, they will chemically link two proteins that are bound or close enough to each other. This would increase the likelihood of visualising a complex of interest as well as lead to the formation of complexes that are more stable. However, the issue of the protein of interest reacting with unlikely partners during homogenization and lysis comes into play even more so when cross-linkers are concerned. Normally non-interacting proteins may then be chemically attached to each other by these cross-linkers. This would increase the risk for false positives and high backgrounds, making interpretation of results very difficult. It thus seems to be a trade-off between potentially losing the complex (when excluding the use of cross-linkers), or a false positive and high backgrounds when including cross-linkers. Neither scenario is ideal. The decision to exclude cross-linkers in this study was based on previous findings that demonstrated the interaction between AChE and laminin without the use of cross-linkers (Paraoanu & Layer, 2004).

The findings described in this section confirm the AChE-laminin interaction in the controlled in vitro environment of the ELISA, and also in the more physiological context of the neuroblastoma cell. Interference in AChE-laminin binding by PAS-binding inhibitors confirms previous findings (Johnson & Moore, 2003) of the interaction between the proteins occurring at or near the PAS. The lesser interference with binding

by the carbamate pyridostigmine, which binds to AChE's active site and choline-binding sites, could feasibly be due to conformational changes within the gorge that affect binding at the PAS. The Co-IP results indicate binding of AChE and laminin. It is unfortunate that the resolution of Figure 25, in particular, did not demonstrate the interaction more clearly.

3.2 Definition and characterization of the binding sites involved in the AChE-laminin interaction

3.2.1 Phage display using peptide libraries

The peptide phage display technique appeared to work well. Adequate yields from the selections as well as adequate growth of clones were observed. The DNA yields from the final round of selection also appeared adequate. However, the results of the sequencing were very disappointing. In many cases the sequencing was unsuccessful, due to insufficient DNA, and, where successful, a variety of sequences with little consensus was seen. It is probable that the insufficient amounts of DNA found on the sequencing is a consequence of the apparently large number of sequences present, so that each sequence is encoded by a relatively small proportion of the total DNA. The selection procedure was repeated, with attempts to optimise different parameters, but with the same result. It was concluded that this was a genuine, albeit negative, result, and that, to obtain information about interaction sequences, different techniques would have to be used.

Although the issue will be discussed more thoroughly in the Discussion (section 4), it appeared possible at this stage that the use of peptide libraries could have been the source of the problem. If the AChE site is strongly three-dimensional, these peptides may not be adequate, as they may only bind to a small section of the site. This could also at least partly account for the multiplicity of peptide binders obtained in the sequencing. A solution to the problem would be to use a method that would provide three-dimensional information. A way to do this would be to use the same technology i.e. phage display, but

a library of three-dimensional binders. The only such libraries available are antibody libraries. Antibody libraries, unfortunately, are not readily available; at the time this work was done (2008/2009), no antibody libraries were available for purchase, and the development of a library would not have been feasible in the time frame of research for a degree. The antibody phage display work was thus contracted out to Creative Biolabs Inc., who has a library and do the selections against it.

The different sites on the AChE molecule to which the MAbs bind is shown in Figure 28.

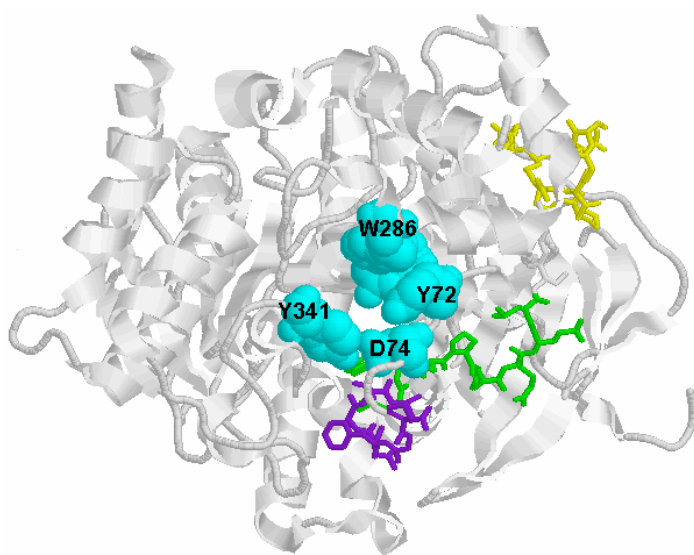


Figure 28. Position on mouse AChE (1J06.pdb) of the principle MAb recognition motifs. Recognition site 40-48 is shown in yellow; 78-85 is shown in purple; and 86-92 is shown in green. The PAS residues (Y72, D74, Y124, W286 and Y341) are coloured cyan and shown in spacefilling mode

3.2.2 Phage display using antibody libraries

Work that was contracted out:

Both AChE whole molecule (rHuAChE) and an AChE peptide (PS18; PPMGPRRFLPPEPKQPWS; corresponding to the human AChE sequence starting at P40) were used. During the first three rounds of panning, rHuAChE was used. The targets were then switched from rHuAChE to biotinylated PS18 in the rounds that followed and these specific binders were eluted by a high concentration of non-

biotinylated PS18. The basic method used in the Ab phage display was the same as that used in the peptide phage display.

Single clones were prepared from the elution of the 6th round screening followed by colony PCR using primers H1 and L1 in order to exclude the clones harbouring the empty vector. For the phage ELISA, the biotinylated target was immobilized indirectly by coated streptavidin. The top 23 positive clones were subjected to DNA sequencing of which a total of 15 clones were sequenced successfully. Sequence analysis showed that these sequences encoded two unique Abs (clone 7 and clone 21; sequences shown in Figure 29) (Table 3). Sequence alignment showed the VL sequences of the two scFv clones to be very similar, although their VH sequences seemed to differ (Figure 30; sequence alignment work was not contracted out). Overall the two clones showed a 95% identity. Phage ELISA with AChE coated plates also demonstrated that the positive clone no. 21 is able to bind AChE as expected. Solid evidence from the Creative Biolabs Inc. laboratory showed that this clone is doubly positive against both the target protein as well as the target peptide.

Table 3. Grouping of the antibody clones based on their amino acid sequences

Sequences	Clone Number	Total
1	7, 18, 25, 39, 52, 60,	6
2	21, 35, 43, 49, 51, 56, 74, 78, 83	9
	Total clone number	15

DNA Sequence of No.7/ [6 clones]: (intact)

ATGGCCGAGGTGCAGCTGTTGGAGTCTGGGGGAGGCTTGGTACAGCCTGGGGGGTCCCTGAGACTCTCCTGTGCAGCCTCTGGATTACCT
 TTAGCAGCTATGCCATGAGCTGGGTCCGCCAGGCTCCAGGGAAGGGGCTGGAGTGGGTCTCAAAGATTCTAGGTAGGGTTATCGTACATG
 GTACGCAGACTCCGTGAAGGGCCGGTTCACCATCTCCAGAGACAATTCCAAGAACACGCTGTATCTGCAAATGAACAGCCTGAGAGCCGAG
 GACACGGCCGTATATTACTGTGCGAAAGTGGGTATAAGTTTGACTACTGGGGCCAGGGAACCCCTGGTCACCGTCTCGAGCGGTTGGAGGCG
GTTTCAGGCGGAGGTGGCAGCGCGGTTGGCGGGTTCGACGGACATCCAGATGACCCAGTCTCCATCCTCCTGTCTGCATCTGTAGGAGACAG
 AGTCACCATCACTTGCCGGGCAAGTCAGAGCATTAGCAGCTATTTAAATTGGTATCAGCAGAAACCAGGGAAAGCCCTAAGCTCCTGATC
 TATGCTGCATCCAGTTTGCAAAGTGGGGTCCCATCAAGGTTTCAGTGGCAGTGGATCTGGGACAGATTTCACTCTCACCATCAGCAGTCTGC
 AACCTGAAGATTTTGCAACTTACTACTGTCAACAGAGTTACAGTACCCTAATACGTTTCGGCCAAGGGACCAAGGTGGAATCAAACGGGC
 GCCCGCA

1 MAEVQLLESG GGLVQPGGSL RLSCAASGFT FSSYAMSWVR QAPGKGLEWV
 51 SKISRZGYRT WYADSVKGRF TISRDNKNT LYLQMNSLRA EDTAVYYCAK
 101 VGHKFDYWQ GTLVTVSSGG GSGGGGGSG GGGSTDIQMTQ SPSSLSASV
 151 DRVTITCRAS QSISYLNWY QQKPGKAPKL LIYAASSLQS GVPSPRFSGS
 201 SGTDFTLTI SLQPEDFATY YCQQSYSTPN TFGQGTKVEI KRAAA

DNA Sequence of No.21/ [9 clones]: (intact)

ATGGCCGAGGTGTAGCTGTTGGAGTCTGGGGGAGGCTTGGTACAGCCTGGGGGGTCCCTGAGACTCTCCTGTGCAGCCTCTGGATTACCT
 TTAGCAGCTATGCCATGAGCTGGGTCCGCCAGGCTCCAGGGAAGGGGCTGGAGTGGGTCTCAAGTATTTCCGCTTCTGGTTCGTAGTACAAA
 GTACGCAGACTCCGTGAAGGGCAGGTTTCACCATCTCCAGAGACAATTCCAAGAACACGCTGTATCTGCAAATGAACAGCCTGAGAGCCGAG
 GACACGGCCGTATATTACTGTGCGAAACGTCGATGAGGTTTGACTACTGGGGCCAGGGAACCCCTGGTCACCGTCTCGAGCGGTTGGAGGCG
GTTTCAGGCGGAGGTGGCAGCGCGGTTGGCGGGTTCGACGGACATCCAGATGACCCAGTCTCCATCCTCCTGTCTGCATCTGTAGGAGACAG
 AGTCACCATCACTTGCCGGGCAAGTCAGAGCATTAGCAGCTATTTAAATTGGTATCAGCAGAAACCAGGGAAAGCCCTAAGCTCCTGATC
 TATGCTGCATCCAGTTTGCAAAGTGGGGTCCCATCAAGGTTTCAGTGGCAGTGGATCTGGGACAGATTTCACTCTCACCATCAGCAGTCTGC
 AACCTGAAGATTTTGCAACTTACTACTGTCAACAGAGTTACAGTACCCTAATACGTTTCGGCCAAGGGACCAAGGTGGAATCAAACGGGC
 GCCCGCA

1 MAEVZLLESG GGLVQPGGSL RLSCAASGFT FSSYAMSWVR QAPGKGLEWV
 51 SSISPSGRST KYADSVKGRF TISRDNKNT LYLQMNSLRA EDTAVYYCAK
 101 RPMRFDYWQ GTLVTVSSGG GSGGGGGSG GGGSTDIQMTQ SPSSLSASV
 151 DRVTITCRAS QSISYLNWY QQKPGKAPKL LIYAASSLQS GVPSPRFSGS
 201 SGTDFTLTI SLQPEDFATY YCQQSYSTPN TFGQGTKVEI KRAAA

Figure 29. Sequences of clone no.7 and clone no. 21

MAEVQLLESG GGLVQPGGSL RLSCAASGFT FSSYAMSWVR QAPGKGLEWV	50
MAEVQLLESG GGLVQPGGSL RLSCAASGFT FSSYAMSWVR QAPGKGLEWV	50
SKISRZGYRT WYADSVKGRF TISRDNKNT LYLQMNSLRA EDTAVYYCAK	100
SSIS PS GRST KYADSVKGRF TISRDNKNT LYLQMNSLRA EDTAVYYCAK	100
VGHKFDYWQ GTLVTVSSGG GSGGGGGSG GGGSTDIQMT QSPSSLSASV	150
RPMRFDYWQ GTLVTVSSGG GSGGGG- SG GGGSTDIQMT QSPSSLSASV	149
GDRVTITCRA QSISYLNW YQKPGKAPK LLIYAASSLQ SGVPSRFSGS	200
GDRVTITCRA QSISYLNW YQKPGKAPK LLIYAASSLQ SGVPSRFSGS	199
GSRTDFTLTI SSLQPEDFAT YCQQSYSTP NTFGQGTKVE IKRAAA	246
GSRTDFTLTI SSLQPEDFAT YCQQSYSTP NTFGQGTKVE IKRAAA	245

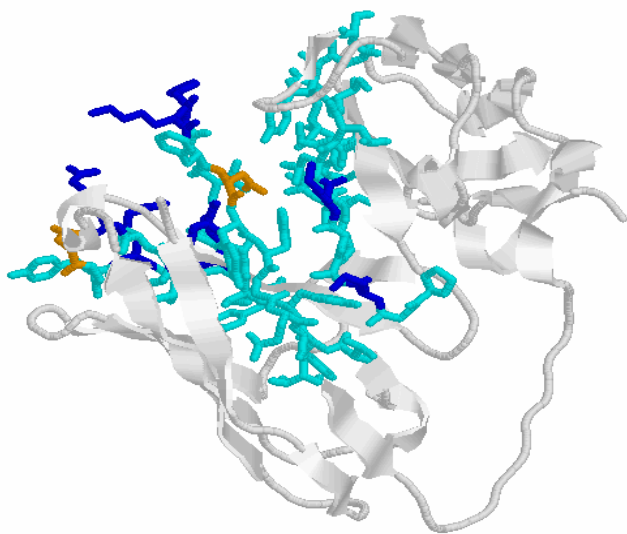
Figure 30. Sequence alignment of clone no. 7 and clone no. 21. Sequence 7 is shown on top of sequence 21. The CDRs are shown in bold and fall between residues 51-61, 95-112, 175-187 and 224-232. Sequence 117-135, containing repeating Gly and Ser residues, is the linker sequence.

It is important to note that there is an amber stop code “TAG” in both of these validated clones. This always occurs in Ab phage display screening (information supplied by Creative Biolabs). This codon does not stop translation in suppressor strains used in this project (i.e. XL-Blue and ER2738 *E. coli* host strain). However, in other protein expression bacterial strains, site-mutation of the amber stop code is necessary to express the soluble scFv fragments.

Work that was not contracted out:

The sequences of the two top binders clone no. 7 and clone no. 21, were used for 3D modelling with Swiss-Model (Figure 31). The models produced were used to dock with mouse AChE (1J06.pdb), using the GRAMM-X webserver. The interaction sites on both clones are shown in Figures 32 and 33. Docking of clone no. 7 with AChE is shown in Figure 34. Docking of clone no. 21 with AChE is shown in Figure 35.

a)



b)

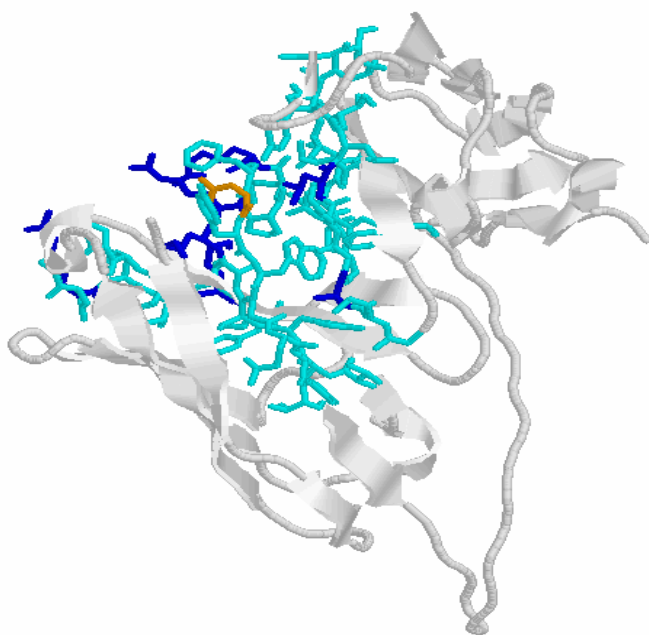


Figure 31. 3D modelling of sequences 7 and 12. Clone no. 7 is shown in a) and clone no. 21 in b). For both sequences: CDRs are shown in cyan; Basic residues (Arg, Lys, His) within the CDRs are shown in blue; Acidic residues (Asp, Glu) within the CDRs are shown in orange.

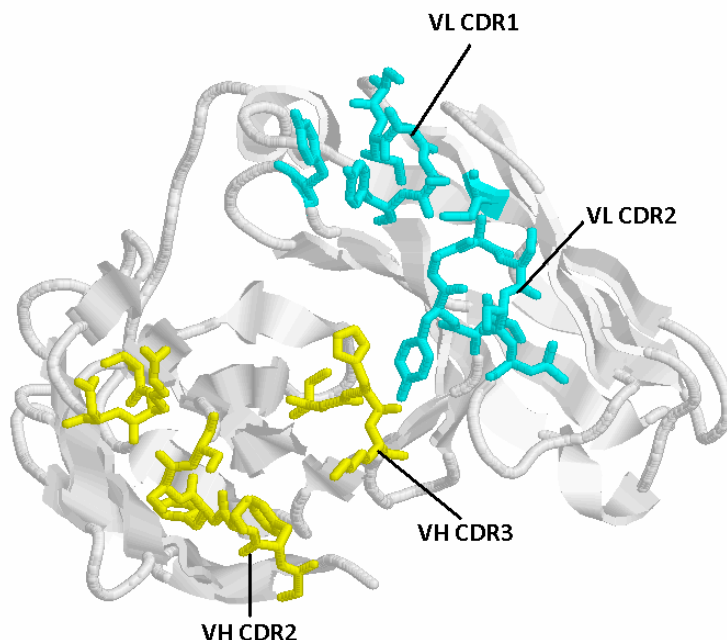


Figure 32. Residues on scFv sequence 7 that interact with AChE in the docking simulations. V_H residues are coloured yellow, and V_L residues are coloured cyan. The residues involved in the interaction are: V_H CDR1 = S32, S33; V_H CDR2 = S54, P55, D56, R58, S59; V_H CDR3 = K100, V101, H103, K104; V_L CDR1 = R158, S163, I164, S165; V_L CDR2 = K177, I183, Y184, A185, A186, S187; V_L CDR3 = Y227.

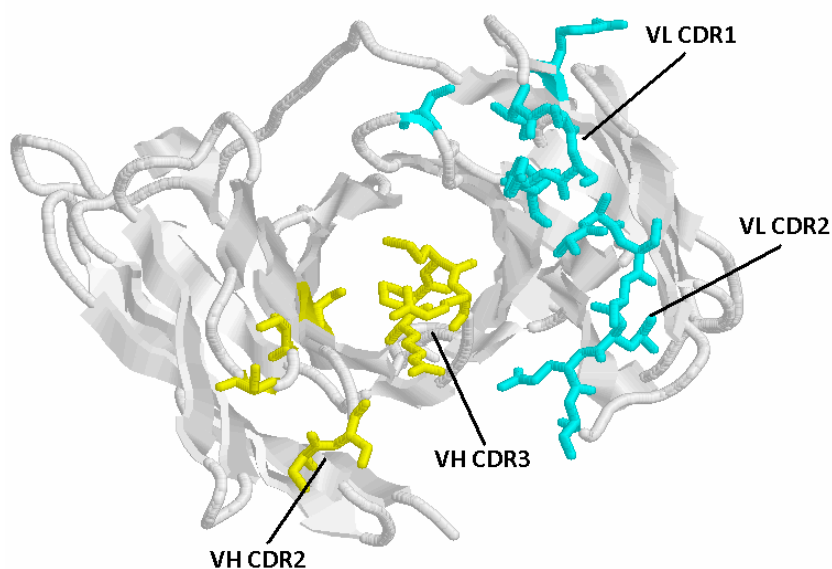


Figure 33. Residues on scFv sequence 21 that interact with AChE in the docking simulations. V_H residues are coloured yellow, and V_L residues are coloured cyan. The residues involved in the interaction are: V_H CDR1 = S32, S33; V_H CDR2 = S54, S56; V_H CDR3 = R101, P102, M103, R104; V_L CDR1 = R158, S163, I164, S165; V_L CDR2 = K177, A178, I183, Y184, A185, A186, S187; V_L CDR3 = Y227.

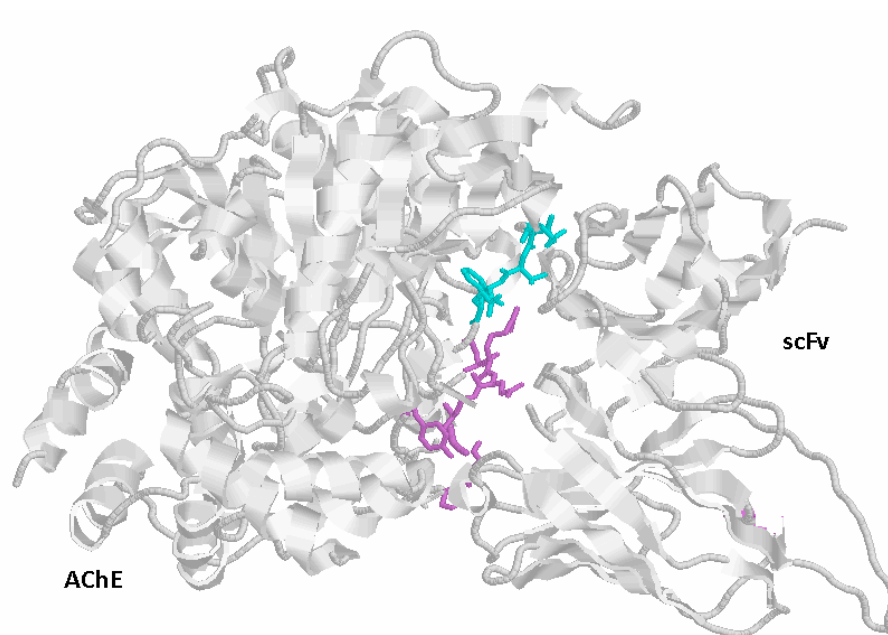


Figure 34. ScFv sequence 7 model docking with AChE (1J06.pdb). The RELSED motif is shown in magenta and the VLDATT motif is shown in cyan.

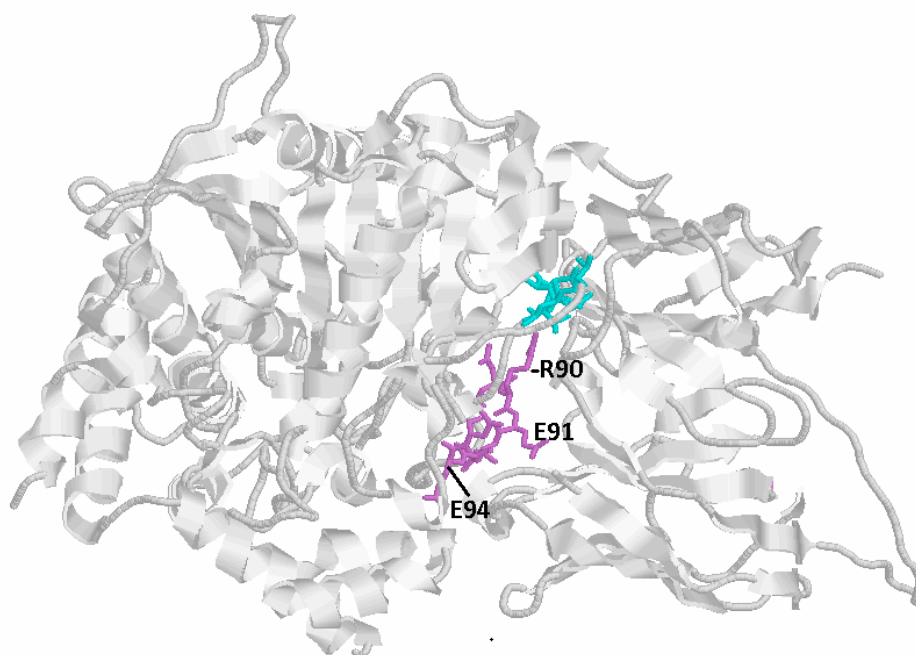


Figure 35. ScFv sequence 21 model docking with AChE (1J06.pdb). The RELSED motif is shown in magenta and the VLDATT motif is shown in cyan. AChE is the molecule in the left and the scFv is shown on the right.

The docking program that was used for generating these docking simulations was the GRAMM-X webserver (Tovchigrechko & Vakser, 2006). The output is given as a protein database (pdb) file containing the multiple simulations (as many as requested; 10 is the minimum). Unfortunately no additional information or confidence in the particular docking poses is provided. It is observed that, using a multiplicity of simulations (minimum of 20), that one particular pose occurs with a significantly greater frequency, and that a number of slight variations on the pose are observed. The poses representing the above docking was selected as being most likely.

The scFv sequences obtained from the Ab phage display were also used to identify other molecules, containing similar epitopes, with which AChE could possibly be functionally redundant (see section 3.3). By applying the BLAST-P alignment tool to the sequences, molecules with similar sequences to AChE, can be identified (Tables 4 & 5).

Table 4. BLAST results for sequence no. 7.

Hit	E value
anti-TREM1	1e-131
anti- α -synuclein	4e-130
anti-laminin	4e-128
anti-factor VIII	4e-116
anti-IFN-G	6e-116
anti-fibronectin	1e-114
anti-tenascin-C	2e-114
anti-tetanus toxin	8e-114
anti-botulinum toxin	3e-100

Table 5. BLAST results for sequence no. 21.

Hit	E value
anti-TREM1	1e-131
anti- α -synuclein	3e-130
anti-laminin	5e-130
anti-IFN-G	6e-118
anti-tenascin-C	2e-117
anti-factor VIII	9e-117
anti-tetanus toxin	2e-116
anti-fibronectin	2e-115
anti-botulinum toxin	2e-99

The E value, in Tables X and Y, refers to the “expected” value, i.e. the chances of a hit occurring by chance alone. The smaller the E value, the smaller the chance of the hit occurring by chance. The hits produced by the BLAST search are other scFvs. Therefore, the population from which the hits were taken is limited to other scFvs that have been developed.

It can be seen from the Tables that many of the E values are extremely low. There are several factors that contribute to this very high similarity. The first is the structure of the scFv itself, which is made up of framework and hypervariable (CDR) regions of the immunoglobulin variable domain. Although part of the variable region, the framework sections are relatively conserved; the hypervariable CDR regions, on the other hand, will differ according to the structures of the individual antigens recognised. Antibody libraries are usually derived from a single individual, immune or non-immune. The antibody library that was used by Creative Biolabs in selecting these scFv is derived from the so-called Tomlinson library (Nissum *et al.*, 1994). scFv derived from the same library, even though they are panned against different antigens, are likely to be highly similar in their framework regions, although not in the CDRs. The BLAST-P algorithm, when assessing similarity, considers the entire sequence of the protein. As the framework regions make

up a relatively large proportion of the scFv compared to the CDRs, the similarity scores will be artificially skewed, resulting in artefactually low E values. Because of this, the hits obtained in Tables 4 and 5 were analysed according to the libraries used in their generation. Table 6 shows the sequence 21 BLAST-hits arranged according to the libraries used in generating the scFvs

Table 6. Sequence 21 BLAST-hits. Only sequence 21 BLAST-hits are shown as the two sequences obtained from the Ab phage display show similar hits, though with different E values. %ID refers to the percentage identity between the scFvs obtained from the Ab phage display and the ones obtained from the BLAST-search.

Hit	Acc. No.	% ID	E value	Library used
anti-TREM1	ABD59020	92	1e-115	human; Tomlinson
anti-laminin	ABS57273	89	4e-114	human; Tomlinson
anti-fibrillar α -synuclein	ACN56324	92	83-114	human; Tomlinson
anti-HSP70	AAM77686	86		human; Tomlinson
anti-IFN-G	CAA06870	80	5e-98	human; other
anti-HCS	CAA06868	80	9e-98	human; other
anti- tenascinC	CAA06867	80	1e-97	human; other
anti-amyloid β	AAS10497	82	1e-97	mouse
anti-tetanus toxin	CAO79114	81	1e-97	human; other
anti-Factor VIII	CAA06869	79	5e-97	human; other
anti- fibronectin	CAA06862	79	2e-96	human; other
anti-rabies glycoprotein	AAY33413	71	2e-85	mouse
anti- botulinum toxin	AAT35553	64	8e-84	mouse
anti-guinea pig C5	CAB60132	68	6e-86	mouse

As expected, the scFvs derived from the Tomlinson libraries show very high similarities to the anti-AChE scFv, with very low E values (Table 6). A second group of scFvs were also derived from the same library, a constructed human library (Pini *et al.*, 1998). These scFvs (against IFN-G, HCS, tenascin-C, fibronectin and Factor VIII) were also very similar to each other in sequence. Hits from several mouse libraries were also produced.

As a control, sequence similarities in random scFvs (where the Ag has no relation to AChE) were investigated (Table 7). It was once again found that the scFv from the Tomlinson library have high similarity to the scFv produced in this study. Those scFvs from human and mouse libraries showed less similarity.

Table 7. ScFv control BLAST. Random scFvs were identified by searching for “scFv” on NCBI Protein. The libraries used in raising the scFv were from the publications describing the scFvs. The random scFv sequences were BLASTed against the anti-AChE scFv sequence 21, and E values and percentage identities determined.

Antigen	scFv Acc. no	%ID to Seq.21	E value	Library
replicase of plant (+) RNA virus	CAG24081	79	1e-108	human; Tomlinson
malonyl CoA decarboxylase	AAQ95595	62	1e-81	human; other
disialoganglioside 2	AAC16042	58	1e-74	mouse
IL-6	CAC69950	47	3e-59	mouse

The antigens against which the “hit” scFv shown in Tables 4 and 5 were aligned with human AChE (P22303), using BLAST-P. The results are shown in Table 8. Sequences and motifs shown in bold are those associated with the PAS, and potentially associated with the AChE-laminin interaction.

Table 8. ScFv antigen alignments with AChE. Sequences and motifs shown in bold are those associated with the PAS, and potentially associated with the AChE-laminin interaction.

BLAST hit	Antigen accession number	Alignment with human AChE	% ID	% pos.
TREM1	Q9NP99	⁷⁹ PGFEGTEMWNPW ³³¹ VKDEGSYFLVYGAP	55 43	55 50
Laminin	P25391	no significant alignment		
Fibrillar α -synuclein	P37840	no significant alignment		
Factor VIII	AAA52484	⁷⁴ DTLY PGFEGTEMWNP NRELS	33	56
IFN-G	NP000610	no significant alignments		
Fibronectin	P02751	⁸⁹ NRELS EDCLYLNWPTYPR ²⁷ GPVSAFGIPFA EPPMGPRR FLPPEPPKQ ⁷² PPMGPRR FLPPEPKQPWSGVVDATTFQSVCYQYVDL	42 29 31	63 50 42
HCS	BAA13332	³⁰⁹ SDTPEALINAGDFHGLQVLVGVVKDEGSYFLVY ⁵²⁹ CAFWNRFLPKLLSATDTLDEA ERQWKA EF	36 28	55 38
Tenascin-C	P24821	279-404 450-479 ⁵³⁹ LLSATDTLDEA ERQWKA EFHRWSSYMMVHWKNQ	24 30 25	39 47 50
Tetanus toxin	AAA23282	⁵⁹ VVDATTFQSVCYQYVDTL YPGFEGTEMWNP NRELS EDC130 ²⁵³ HLVGC PPGG TGGNDTELV ⁵⁰⁶ GAQQYVSLDLRPLEVRR	26 33 32	36 56 44
gp120	AAF69492	100-114 409-438 ⁵⁴⁰ LSATDTLDEA ERQWKA EFHRWSSY MV HWKNQFDH	47 27 24	53 40 50
Botulinum toxin	P10845	⁴⁹ PPEPKQPWSGVVDAT T ²⁸¹ LVNHEWHVLPQESVFRFSFVPVVD 454-463	47 25 40	53 67 90
Amyloid β -peptide	1IYT	²⁵⁴ LVGC PPGG ⁵⁵⁵ AEFHRWSSY MVH	38 58	63 58

It is clear that several of these antigens, in particular, laminin and α -synuclein, although their scFv generated very low E values compared to the anti-AChE scFv, bear no significant resemblance to AChE. Both these scFv were derived from the Tomlinson libraries, and it is therefore concluded that these hits are false positives. The remaining hits, however, do align with AChE, and an examination of the alignments shows a preponderance of four sequences: the PGFEGTE motif; the PPMGPRRF motif; the short omega loop, especially the PPMG motif; and the C-terminal peptide. These results tie in very strongly with the peptide array results (section 3.2.3), and will be discussed in depth in the discussion (section 4).

3.2.3 Conformational epitope mapping of adhesion-inhibiting anti-AChE MAb: Peptide Arrays

Not only have the anti-AChE MAb been shown to block cell adhesion and neurite outgrowth to varying degrees, they also interfere with the binding of laminin-111 to AChE *in vitro*. For these reasons, it appeared probable that the common epitope of the MAbs and the site on AChE to which laminin binds may be one and the same. Thus, the epitope mapping was undertaken to identify this common epitope and, hopefully, as a consequence, to identify the laminin-binding site on AChE. Table 9 show the different recognition motifs of the MAbs.

The results of the conformational epitope mapping showed that the MAbs did, indeed, recognise a common epitope, and, furthermore, that this epitope was associated with the PAS. Table 6 shows the MAbs' major recognition sites, ranked in order of reactivity.

It was found that the MAbs that most effectively inhibit cell adhesion recognize the ⁴⁰PPMGPRRFL motif. This motif is linked by a salt bridge to the omega loop; the residues involved in the salt bridge are ⁴⁶Arg and ⁹⁴Glu on the omega loop. Because of this linkage, the ⁴⁰PPMGPRRFL sequence is brought into close proximity to both the omega loop and the PAS (Figure 36). These Abs however, also showed a strong recognition of the motifs ⁸⁵WNPNRE and ⁷⁸PGFEGTE, both situated on the omega loop

(Figure 36). It was found that the reactivity of the Ab towards a specific peptide in the array was immediately increased following addition of a proline residue to that peptide sequence. This not only indicates that the primary epitope of these Abs is the proline-rich ⁴⁰PPMGPRRFL sequence, but that these Abs also respond to other proline-containing sequences. As stated, the MAb E12C8 was raised against *Torpedo* AChE. Here the equivalent sequence is PPVGNMRFR (Figure 37). E12C8 was found to also respond strongly to the presence of proline and also inhibit cell adhesion. All the MAbs that recognize the WNPnRE motif inhibit cell adhesion effectively. MAbs AE-2 and 29H, which do not react with WNPnRE, do not inhibit cell adhesion.

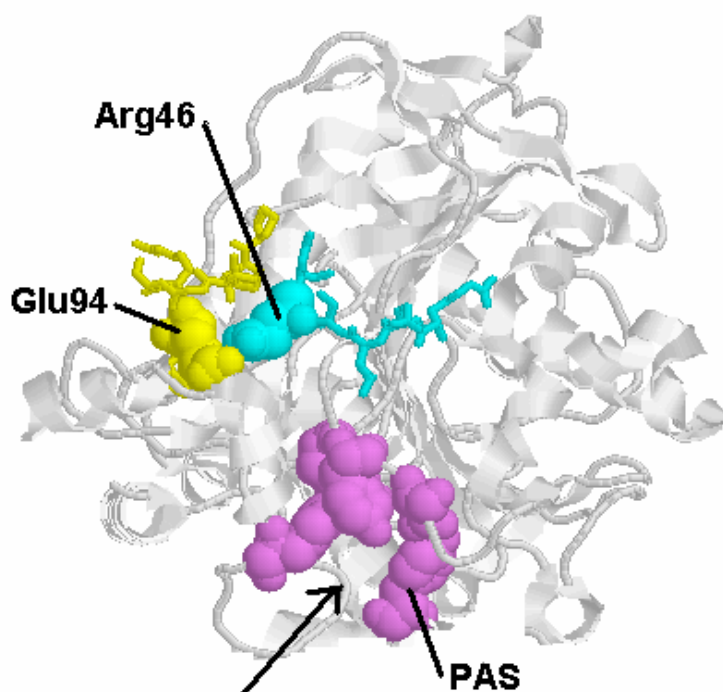


Figure 36. AChE structure (1J06.pdb) showing the position of the Arg 46-Glu 94 salt bridge. The ⁹⁰RELS motif is shown in yellow. The ⁴⁰PPMGPRR motif is shown in cyan. The PAS residues (Y72, D74, W286 and Y341) are shown in violet. The arrow indicates the direction of the active site gorge. The two residues comprising the salt bridge (Arg 46 and Glu 94) are shown in spacefilling mode.

Table 9. Recognition of motifs by MAb. Inhibition of cell adhesion is a measure of the effects of the MAbs (at 40µg/ml) on neuroblastoma cells *in vitro* after 48h. Motifs are

ranked in order of their recognition by MAb. Cell adhesion data are from Johnson and Moore (2000).

MAB	Inhibition of adhesion	Motif 1	Motif 2	Motif 3
C2	94.0	PPMGPRRFL	WNP NREL	PGFEGTE
E8	92.0	PPMGPRRRFL	PGFEGTE	WNP NREL
43B4C	87.2	VVDATT	PPMGPRRFL	YQYVD
13B9F	85.0	PPMGPRRFL	PGFEGTE	WNP NREL
E12C8	81.4	PPMGPRRFL	WNP NREL	PGFEGTE
13B9C	49.0	PPMGPRRFL	YQYVD	WNP NREL
9H	0.0	VVDATT	PPMGPRRFL	-
AE-2	0.0	VVDATT	PPMGPRRFL	YQYVD

Mouse	P P V G S R R F M	P P E P K R P W S G V L	60
Human	P P M G P R R F L	P P E P K Q P W S G V V	60
Torpedo	P P V G N M R F R	R P E P K K P W S G V W	58
BChE	P P L G R L R F K	K P Q S L T K W S D I W	56
Mouse	D A T T F Q N V C	Y Q Y V D T L Y	77
Human	D A T T F Q S V C	Y Q Y V D T L Y	77
Torpedo	N A S T Y P N N C	Q Q Y V D E Q F	75
BChE	N A T K Y A N S C	C Q N I D Q S F	73
Mouse	P G F E G T E	M W N P N R E L S E D C	96
Human	P G F E G T E	M W N P N R E L S E D C	96
Torpedo	P G F S G S E	M W N P N R E M S E D C	94
BChE	P G F H G S E	M W N P N T D L S E D C	92

Figure 37. Comparison of mouse and human AChE (residues 40-96), *Torpedo* AChE (residues 38-94), and the human BChE sequence (residues 36-92). The two disulfide-linked cysteine residues (69 and 96 in mouse and human; 67 and 94 in *Torpedo*; 65 and 92 in BChE) at the ends of the omega loop, along with the PAS residues Y72 and D74 (mouse and human AChE), Y70 and D72 (*Torpedo* AChE) and D70 (BChE), are shown in boldface. The shaded parts represent motifs recognized by the adhesion-inhibiting MAbs (Johnson *et al.*, 2008a).

These results, therefore, indicate that the epitope of the MAbs is the ⁴⁰PPMGPRFFFL motif adjacent to the omega loop, and that they also recognize the Pro-containing sequences ⁸⁵WNPNRE and ⁷⁸PGFEGTE on the omega loop itself. It is possible that the site on AChE that binds laminin and promotes cell adhesion and neurite outgrowth is identical to this epitope. It is also possible, however, that the site is not identical, but close by with perhaps common features. The observation that the MAbs prevent AChE-laminin binding is compatible with both possibilities: Abs are large molecules (the molecular weight of IgG is approximately 150 kDa), and steric hindrance could play a significant role. The specific identification of the site on laminin that interacts with AChE is addressed in the following sections.

It is interesting that the epitope/s identified by the peptide array agree very closely with the common sequences identified by the BLAST alignments of AChE with the scFv antigens (Table 8). The scFv antigen alignments produced four common motifs:

1. the ⁴⁰PPMGPRRFL motif
2. the large (69-96) omega loop, containing the ⁷⁸PGFEGTE and ⁸⁵WNPNRE motifs
3. the short omega loop 257-272.
4. the C-terminal T-peptide.

Common features of points 1-3 are the high concentrations of Pro and Gly residues. As discussed above, cross-recognition of Pro-Gly motifs on the 69-96 omega loop and its immediate surrounds (such as the ⁴⁰PPMGPRRFL motif) was observed with the MAbs. Thus, it would appear that these motifs are structurally very similar.

There is likewise structural similarity between the ⁷⁸PGFEGTE motif and the Pro and Gly-containing initial section of the short omega loop (257-272). Structural overlay of these two motifs was shown (Johnson & Moore, 2009). This short omega loop is also of interest because of its interaction with the PAS: in the crystal structure of the mouse AChE tetramer (Bourne *et al.*, 1999), it was observed that the 257-272 omega loop interacts with the PAS of an adjacent AChE subunit. This interaction appears to be useful

in stabilising the tetrameric assembly. Bourne *et al.* (1999) furthermore demonstrated a structural similarity between the short omega loop and both the amyloid beta-peptide and the prion protein. Both the beta-peptide and the prion protein have been shown to interact with the PAS: the beta-peptide at the hydrophobic 274-308 sequence on AChE, which contains the PAS residue W286 (De Ferrari *et al.*, 2001); and the prion protein at an unspecified site at the PAS (Clos *et al.*, 2006).

Yet more structural similarities emerge. The amyloid beta-peptide, apart from being an AChE ligand, also aligns with a part of the AChE sequence: part of the C-terminal T-peptide (Greenfield & Vaux, 2002). Cottingham *et al.* (2002; 2003), furthermore, showed this AChE peptide to be capable of assuming beta-sheet conformation and assembling into amyloid-like fibrils, as does the beta-peptide.

Thus, it is possible to say that the four sites – the ⁴⁰PPMGPRRFL motif, the ⁷⁸PGFEGTE/⁸⁵WNPNRE motif, the ²⁵³PPGGTGG motif and the C-terminal T-peptide – are structurally similar, and that they appear to be recognized as such by the hybridoma-derived MAbs as well as the scFv. It should be noted that the docking of the scFv with AChE produced only docking at the large omega loop region: the adjacent ⁷⁸PGFEGTE/⁸⁵WNPNRE motifs (W84 lies within the gorge, forming the major component of the choline-binding site), and the ⁴⁰PPMGPRRFL (or ⁴⁰PPVGPRRFL in the mouse pdb structure 1J06.pdb) which is linked to the ⁹⁰RELSER motif by a salt bridge between Arg46 and Glu94. Docking did not occur at either the short omega loop or the C-terminal peptide: neither of these structures is present in the crystal structure.

3.2.4 Identification of potential binding sites on laminin α 1 through sequence analysis.

Previous results show binding of AChE to laminin-111 (Johnson & Moore, 2003), which is the isoform expressed during development. These results had shown that PAS-binding inhibitors and PAS-binding Abs interfered with the AChE-laminin binding, suggesting that the AChE PAS was involved in the interaction. It was also demonstrated that binding

occurred through an electrostatic mechanism, indicating that the anionic PAS, theoretically, should attract a cationic complimentary site. Identification of such a site called, first of all, for the investigation of the mouse laminin α 1-chain (Swiss-Prot accession number NP_032506) sequence. Nomizu et al. (1995) have previously identified a number of sites involved in cell attachment and spreading, many of which are cationic. Five of the laminin peptides showed cell attachment activities with cell-type specificities: AG-10, AG-22, AG-32, AG-56 and AG-73 (Nomizu et al., 1995).

Potential cationic sites on the mouse laminin α 1 chain (accession number P19137):

144 RYKITPRRGPPTYR
204 RYIRLRLQRIRT
364 RPHK
1719 RFQKPQEKLK
1844 KRRAR
1942 RRKQ
1988 REKGRKAR
2086 KLLISRAKAR
2155 RRGK
2378 RNRK
2426 KAVRKGVSSR
2718 RKRLQVQ (AG-73)
2764 KGRTK
2790 KRKAFMDKDR

Cationic sites in laminin β 1 and γ 1 chains:

Laminin β 1 (mouse laminin, accession number P02469)

213 RIKFVK
1175 RTHK
1554 KRASK
1695 RRK

Laminin γ 1 (mouse laminin, accession number P02468):

¹²⁹KRTR
²⁹¹RPWRR
⁵⁵⁰RRDTR
¹⁰⁹⁸RARSR
¹⁴⁴¹KRK
¹⁴⁶⁹RKAK

3.2.5 Docking with laminin α 2, and identification of AG-73 as likely site.

At the time when this aspect of the study was commenced, the structure of the laminin α 1 chain (the component of laminin-111 which was used in the binding assays) was not available. The only laminin structure available was the laminin α 2 G4 and G5 domain pair, the component of laminin-211 (merosin). The α 1 and α 2 chains are, however, strongly homologous (45% identity; Figure 38), and the G4 and G5 domain pair – the region of the laminin molecule where most ligands, including heparin and integrins, bind – show 63% identity between the α 1 and α 2 chains. Thus, the initial docking studies were done with the laminin α 2 G4 and G5 domains (1DYK.pdb).

Docking of AChE with laminin α 2 G4/G5 domain pair was found to take place between regions of the AChE PAS and the ²⁷⁶⁹KVKNRLTIELEVRT sequence (Figure 39). This sequence was found to correspond to AG-73 (²⁷¹⁸RKRLQVQLSIRT) of the laminin α 1-chain (in the nomenclature of Nomizu et al. (1995)), making this site a top candidate. Docking was done by GRAMM webserver, producing 10 docked simulations. These were visualised and analysed on DeepView. Residues within 5Å of each other on the two molecules were determined. On AChE these were: the PAS containing sequences 72-78, 279-293 and 340-347. On laminin these were: 2769-2782 (incorporates part of the AG-73 sequence equivalent) I2880, Y2882, P2887, I2888.

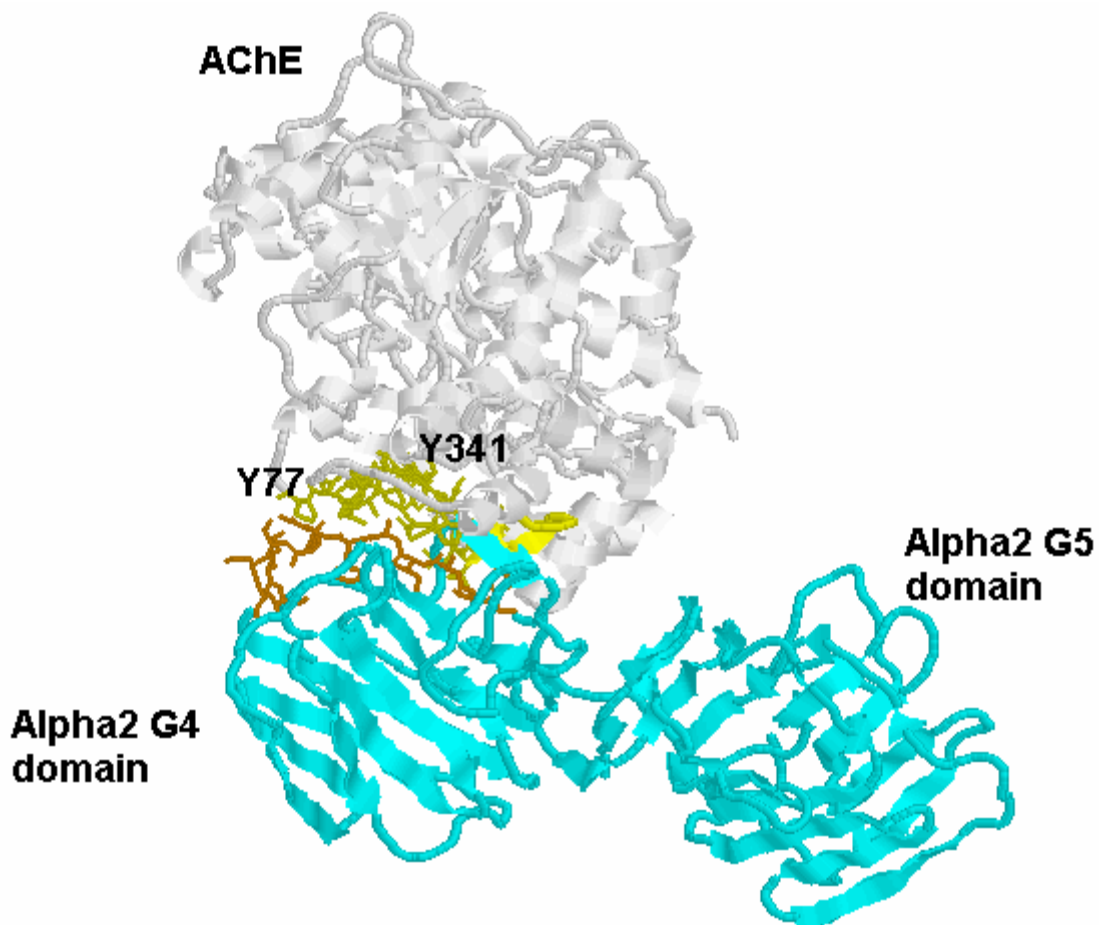


Figure 39. Docking of mouse AChE (1J06.pdb) with mouse laminin $\alpha 2$ G4 and G5 domains (1DYK.pdb). AChE is shown in grey and laminin is shown in cyan. Interaction sites (Y72-78, 279-293, 340-347 on AChE and 2769-2782 on laminin) are coloured yellow and orange, respectively.

3.2.5 In vitro binding of the PAS of AChE to AG-73

Binding of biotinylated AChE to the AG-73 peptide occurred with a K_d value of 276.9 ± 38.77 nM and a B_{max} of 1.371 ± 0.2326 (A405 absorbance units) (Figure 41a). Figure 40 shows the AG-73-associated interaction on the laminin molecule. AChE did not bind to the scrambled version of AG-73. Neither of the two controls, biotinylated BSA and non-specific mouse IgG (with a similar pI value as AChE), was found to bind to any of the two peptides (normal and scrambled version). In the reverse situation, biotinylated AG-

73 was observed to bind to AChE. Here, no binding occurred with either of the controls. The biotinylated scrambled version of the AG-73 peptide did not bind. The AG-73 peptide was also found to have a significant interfering effect on the binding of AChE and laminin (Figure 41b).

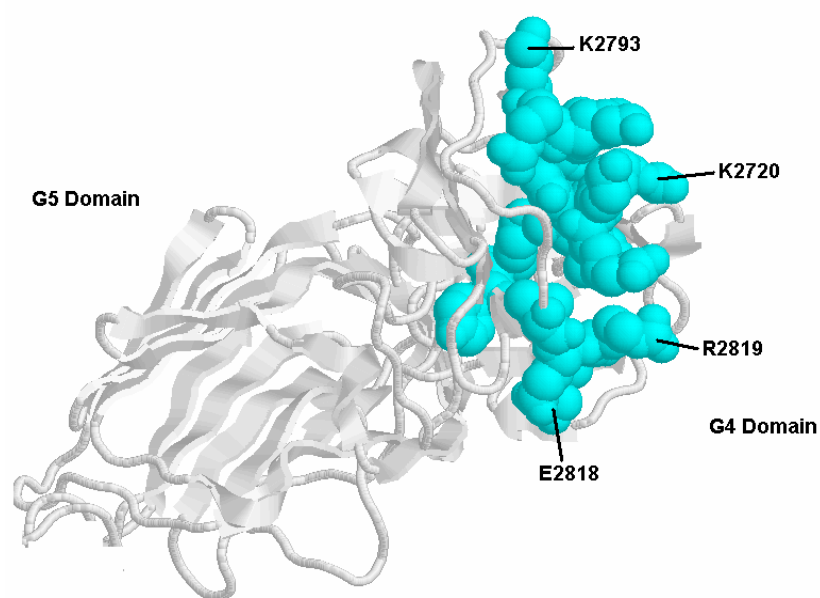


Figure 40. The G4 and G5 domains of the laminin molecule showing the AG-73 interaction site. The site on laminin G4 that was found to interact with AChE is shown in cyan and spacefilling mode. The interaction residues are ²⁷¹⁸VRKRL, ²⁷³⁸YY, ²⁷⁸⁹YIKRK and ²⁸¹⁷VERK. Structure is 2JD4.pdb.

The presence of salt in the buffers once again disrupted binding (Figure 42), indicating the electrostatic significance in the reaction. Pre-incubation of AChE with inhibitors showed varying results (Figure 43). Propidium (PAS-binding inhibitor) showed to have a strong effect, significantly reducing binding ($P < 0.001$). The effects of gallamine were somewhat less, but still significant ($P < 0.001$). The binding of AChE to AG-73 was unaffected by the active-site inhibitor pyridostigmine. The role of the PAS in this binding is once again highlighted.

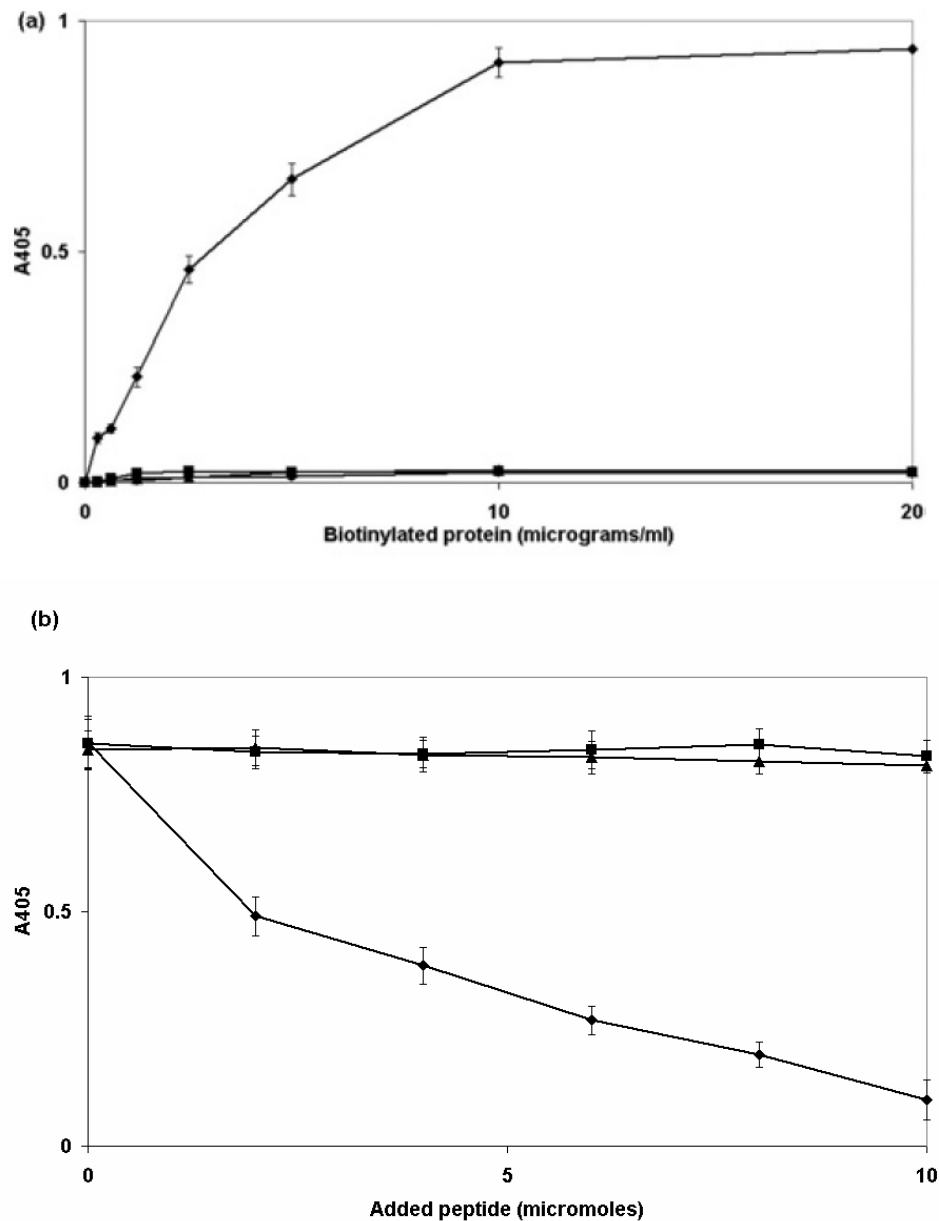


Figure 41. Binding of AChE to the AG-73 laminin peptide. (a) Binding of biotinylated AChE to AG-73. Microtitre plates were coated with either 20 μ g/ml AG-73, or the scrambled version. Biotinylated proteins included AChE, BSA and IgG. \diamond = Biotinylated AChE; AG-73 as plate-coating. \blacksquare = Biotinylated AChE; scrambled version of peptide AG-73 as plate-coating. \blacktriangle = Biotinylated BSA; AG-73 as plate-coating. \bullet = Biotinylated IgG; AG-73 as plate-coating. (b) Interference with AChE-laminin binding by AG-73. Microtitre plates were coated with 10 μ g/ml laminin-111. Biotinylated AChE (20 μ g/ml or 286 nM) was pre-incubated with various concentrations (0-10 μ M) of either AG-73 or its scrambled version. \diamond = Pre-incubated with AG-73. \blacksquare = Pre-incubated with scrambled version of AG-73. \blacktriangle = AChE only, no added peptide (Johnson *et al.*, 2008a).

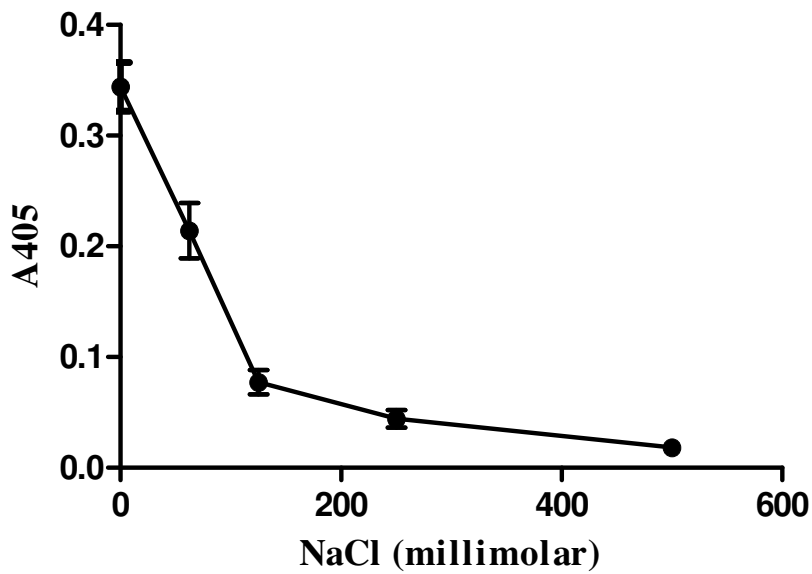


Figure 42. Effects of NaCl on AChE-AG-73 binding. The different buffer NaCl concentrations used were: 500, 250, 125, 62.5 mM.

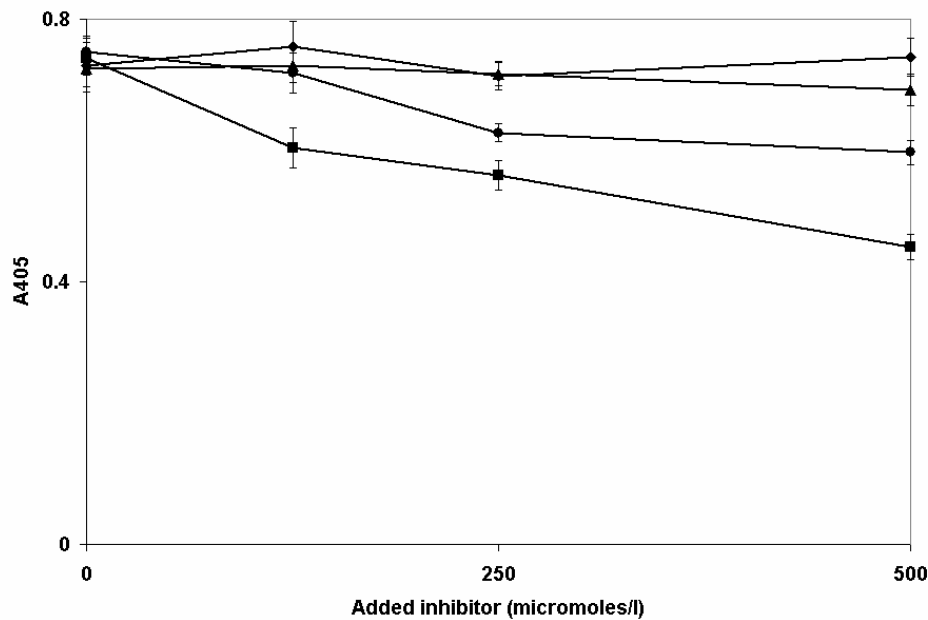


Figure 43. Effects of AChE inhibitors on AChE binding to AG-73. The microtitre plates were coated with 20 μ g/ml AG-73. Biotinylated AChE (20 μ g/ml) was pre-incubated for 1 h in the presence of propidium (■), gallamine (●), or pyridostigmine (▲) inhibitor. Absence of inhibitor is shown as = ◆ (Johnson *et al.*, 2008a).

3.2.7 AChE competing with heparan sulfate for binding to laminin-111 and AG-73

The site on laminin that binds AChE has much in common with the heparin-binding site. The AG-73 peptide was initially identified as a heparin-binding site (Hoffman *et al.*, 1998). Competition ELISA was performed in order to investigate whether AChE competes with this molecule for binding to laminin. The presence of heparan sulfate was found to significantly reduced the binding of biotinylated AChE to laminin ($P < 0.001$) (Figure 44). Pre-coating the microtitre plates with AChE or heparan sulfate showed similar results (results not shown).

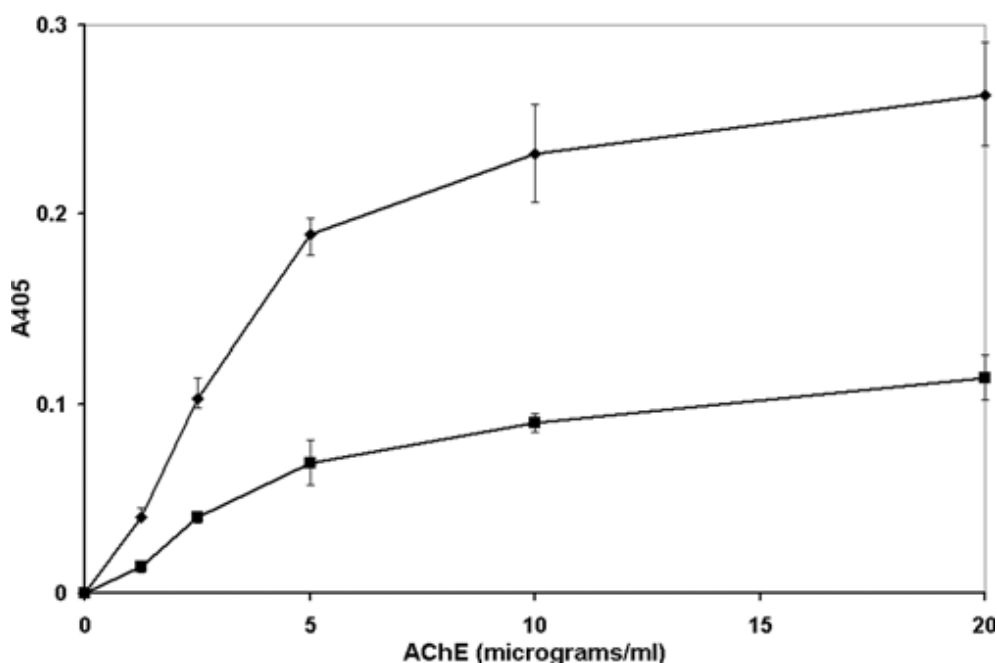


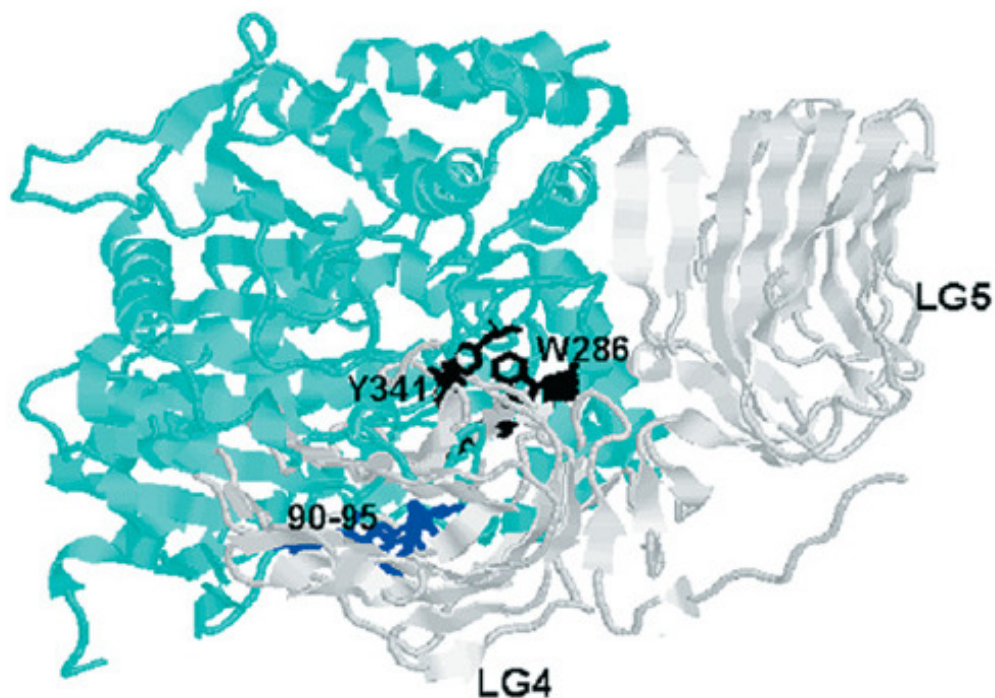
Figure 44. Competition between AChE and heparan sulfate for binding laminin-111. Microtitre plates were coated with 10µg/ml laminin-111. Serial dilutions of biotinylated AChE (0-20µg/ml; 0-286nM) were added in the presence (■), or absence (♦) of 10µg/ml heparan sulfate (Johnson *et al.*, 2008a).

Competition ELISA confirmed the involvement of the AG-73 site on laminin in its binding with AChE. Seeing as AChE and heparin compete for binding to laminin, this could indicate the possibility of functional redundancy between AChE and heparin (see section 3.3 on functional redundancy).

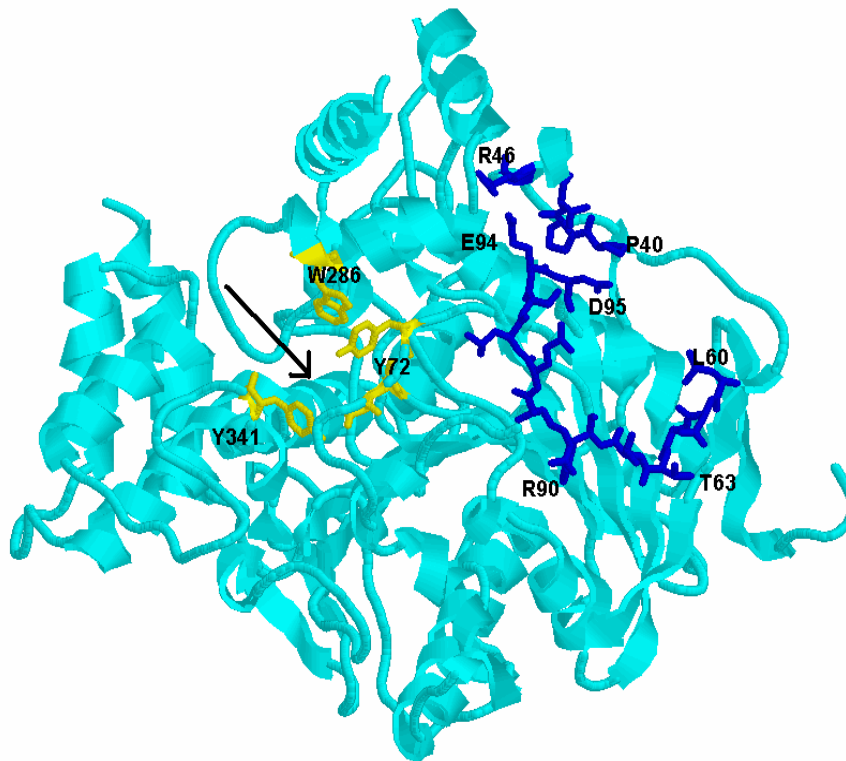
3.2.8 Docking of AChE and laminin $\alpha 1$: Identification of interaction sites on both AChE and laminin.

The laminin $\alpha 1$ G4-5 domain structure only became available towards the end of this aspect of the study (Harrison et al., 2007). The docking results are shown in Figure 45 (a-d). One of the catalytic subunits of the AChE dimer was shown to dock with the G4 domain of laminin where the laminin contribution to the docking was observed to come from four clusters of the residues: ²⁷¹⁸VRKRL, ²⁷³⁸YY, ²⁷⁸⁹YIKRK and ²⁸¹⁷VERK. The first group of residues, 2718-2722, form part of the AG-73 sequence. These residues seem to interact closely with R90 and E91 as well as the N61-Q66 sequence of AChE. The acidic sequence, ⁹⁰RELSED, was found to be the major interaction site on AChE. Parts of this acidic sequence appear to interact with all three of the laminin basic sequences.

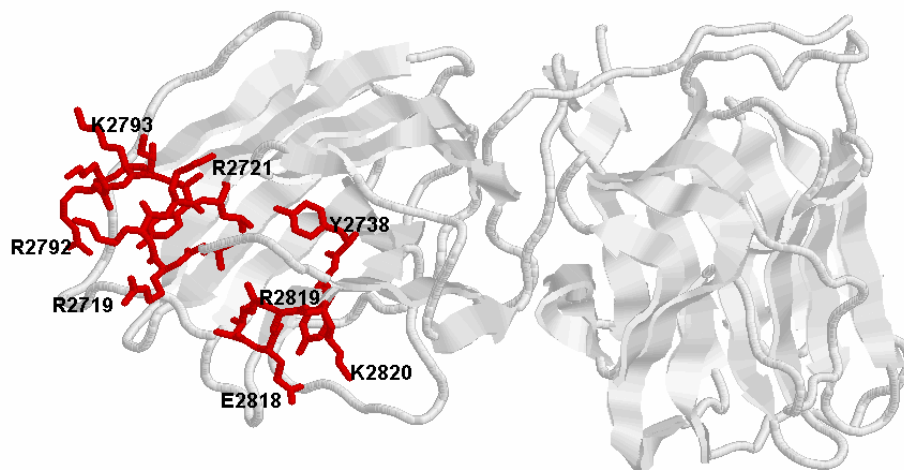
a) The docked structures:



b) Interacting residues on AChE:



c) Interacting residues on laminin:



d) Stereo view of the interacting structures:

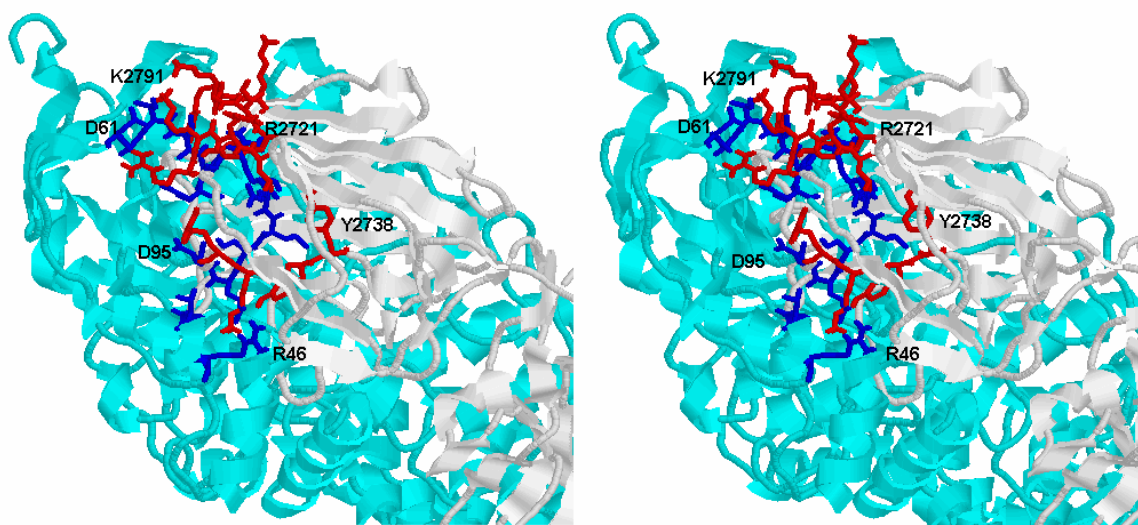


Figure 45. Docking of AChE (PDB code 1JO6) and laminin (PDB code 2JD4). (a) The docked structures: AChE (single catalytic subunit) is shown in cyan; the LG4 and LG5 domains (one domain of each) of laminin are shown in grey; the PAS residues (Y72, D74, Y124, W286 and Y341) are shown in black; and ⁹⁰RELS is in blue. (b) Interacting residues on the AChE molecule: the PAS residues on AChE are shown in yellow, and the interacting residues in blue. (c) Interacting residues on the laminin molecule (LG4 and LG5 domain): shown in red. (d) Stereo view of the interacting structures: the AChE molecule is shown in cyan and the laminin molecule in grey; the interacting structures on AChE are shown in blue and the interacting structures on laminin in red (Johnson *et al.*, 2008a).

In the docked structure, as illustrated in Figure 45 (a-d), R90 is observed to lie within 4 Å (1 Å = 0.1nm) of R2719, K2720, F2760, F2762 and K2793 and within 2 Å of L2722 and Y2789. E91 was found to lie within 4 Å of L2722, as does L92 with Y2738 and Y2739, and S93 with E2818, R2819 and V2740. E94 approaches E2818 and K2820, and D95 approaches V2817, E2818 and R2819. Due to its salt bridge linkage with E94, R46 also interacts with this sequence, and lies within 4 Å of K2820, as well as L2862 and S2863 on the laminin chain. P40, P41 and V42 and Y70 were also observed to associate V2817,

E2818, R2819 and K2820. Other laminin residues that appear to interact with AChE are ²⁷³⁷¹YY. These residues lie close to P88 and L92, as well as both Q71 and V72.

Torpedo AChE did not dock with the mouse laminin G4 domain (results not shown). Sequence differences occur between mouse/human and *Torpedo* AChE (see Figure 37). These differences include: in the RELSED motif, L92 is replaced by methionine residue in *Torpedo*, a conservative replacement. The DATTFQ sequence, however, show even more variation: in *Torpedo*, the equivalent sequence is NASTT. The replacement of the acidic A61 with the uncharged N59 could thus possibly have a negative effect on the interaction.

No docking was observed between the mouse AChE-inhibitor complexes (with propidium, gallamine and fasciculin-2) and laminin $\alpha 1$ (results not shown). Human BChE also did not dock (results not shown). In BChE, R90 is replaced by a threonine residue. The BChE sequence also contains a replacement of the non-polar T64 with a positively charged lysine residue (Figure 37).

3.3 Functional Redundancy

3.3.1 In neural development

3.3.1.1 Clues from the laminin site

On laminin, the AChE binding site overlaps the heparin-binding site (Harrison *et al*, 2007). This site has previously been identified showing that the AG-73 peptide forms part of it (Hoffman *et al.*, 2001). From the results it is evident that AChE competes with heparan sulfate for binding to laminin, suggesting heparin-containing molecules could possibly be functionally redundant with AChE.

An array of proteoglycans is expressed during neural development. This expression occurs both in the ECM and on the surfaces of cells (Hartmann & Maurer, 2001). Not a lot is known about proteoglycan expression patterns and function, but accumulating evidence show that these molecules portray important roles in development. They have been found to promote cell adhesion, cell-cell interactions as well as growth factor (GF) signalling (Bandtlow & Zimmerman, 2000; Selleck, 2000). The proteoglycan protein core can contain heparan, chondroitin, or less frequently, dermatan sulfate, alone or in combination. Intermolecular interactions have been shown to be a common occurrence both by the sugars and protein core (Hartmann & Maurer, 2001; Bandtlow & Zimmerman, 2000). A multiplicity of potential binding and signalling structures could result from the different variations in sugar composition and length together with the diversity of proteins to which they attach. In the developing nervous system, heparan sulfate containing proteoglycans (HSPGs) have been observed to bind a heterogeneous group of molecules. These include proteins such as NCAM, slit proteins, fibronectin and the thrombospondins; as well as GFs such as members of the fibroblast growth factor (FGF), Wnt, transforming growth factor β as well as the hedgehog families and pleiotrophin (Bandtlow & Zimmerman, 2000). Bindings like these may occur exclusively by the HS chains or alongside contributions from the protein core. HSPGs showing similar spatiotemporal expression to AChE include: the membrane-associated syndecans, glypicans and testicans; and the extracellular molecules perlecan, agrin and collagen XVIII (Table 10).

Syndecans, a family of four transmembrane receptors, are expressed in a variety of tissues portraying multiple biological functions (Tkachenko *et al.*, 2005). These HSPGs are capable of carrying both heparan and chondroitin sulfate chains. The extracellular domain of syndecans may be shed into the matrix as functional molecules (Kim *et al.*, 1994). Even though all four of these transmembrane receptors are expressed in the developing nervous system, they have different spatiotemporal distributions. It is thus likely that they also have different functions. Binding of syndecans with various GFs, ECM molecules, as well as with LDL, have been previously demonstrated (Bernfield & Sanderson, 1994). The syndecan knockout mouse showed no obvious phenotypes

(Hartmann & Maurer, 2001). Syndecan-1, a prototype HSPG first identified as a developmentally regulated type-1 transmembrane protein that bound ECM components to epithelial cells (Rapraeger & Bernfield, 1983; Koda & Bernfield, 1984; Saunders & Bernfield, 1988), has been shown to bind laminin-111. Interestingly, this binding occurs through an interaction of the heparan sulfate with AG-73 site in the LG4 domain of the laminin molecule (Hoffman *et al.*, 1998).

Table 10. HSPGs in the developing nervous system (the majority of the data from: Hartmann & Maurer, 2001; Bandtlow & Zimmerman, 2000; Selleck, 2000). Notes ^{a-f} indicate the other relevant references (see below). (Johnson *et al.*, 2008b)

Family	HSPG	Expression	Ligands	
			Growth factors	Proteins
Syndecans	Syndecan-1	Cell surface	FGF family transforming growth factor β family pleiotrophin	Laminin, fibronectin, tenascin-C ^a , LDL ^b
	Syndecan-2	Cell surface	FGF2	Laminin, synbindin ^c , fibronectin
	Syndecan-3	Cell surface	FGF2, midkine, pleiotrophin	Laminin, EGFR ^d
	Syndecan-4	Cell surface	FGF family	Laminin, synbindin ^c , fibronectin
Glypicans	GLP-1	Cell surface	FGF family	Laminin, slit-1 slit-2
	GLP-2	Cell surface	FGF2	Laminin, thrombospondin
	GLP-3	Cell surface	IGFII ^e	
	GLP-4	Cell surface	FGF2	
	GLP-5	Cell surface	FGF family	
	GLP-6	Cell surface		
Testicans	Testican-1	Cell surface		
	Testican-2	Cell surface		
	Testican-3	Cell surface		
	Perlecan	ECM		Laminin, collagen, fibronectin, tenascin, amyloid precursor protein ^f
	Aggrin	ECM	FGF family	Laminin, NCAM, tenascin-C, thrombospondin
	Collagen XVIII	ECM		Laminin, heparan sulfate

a= Bernfield *et al.*, 1999; b= Fuki *et al.*, 1997; c= Ethell *et al.*, 2000; d= Hienola *et al.*, 2006; e= Song *et al.*, 2005; f= Anderson *et al.*, 2007

The glypicans are distinctive cell surface HSPGs linked directly to membrane phospholipid (David *et al.*, 1990). These glycosylphosphatidylinositol-linked (GPI-linked) HSPGs appear to play important roles in cell growth and differentiation (Bernfield *et al.*, 1999). Several additional structurally related glypicans have been identified. Like the syndecans, glypican gene products bear HS chains as a permanent

feature and individual glypicans have been known to show differences in their developmental expression patterns. These expression pattern variations once again suggest distinct functions. Glypicans also modulate GF signaling through their HS chains. Glypican-2, a HSPG exclusive to the nervous system, along with glypican-1, have been shown to bind laminin-111 *in vitro* (Stipp *et al.*, 1994). None of the other members of the glypican family have been demonstrated to bind laminin.

As a subgroup of the BM-40/SPARC/osteonectin family of modular proteins, the testicans have yet to demonstrate laminin binding. These proteins also seem to have an inhibitory effect on neurite outgrowth (Schnepp *et al.*, 2005). These findings suggest the testicans are unlikely to show redundancy with AChE.

Perlecan, a large multifunctional HSPG, is well known for its role in the formation of the BM by cross-linking many cell-surface and ECM molecules. In addition to its structural role, both the protein core and the HS constituents of perlecan have been shown to support various biological activities. These functions include cell adhesion, GF binding, as well as apoptosis (Farach-Carson & Carson, 2007). Perlecan expression occurs from very early stages of development and the molecule consists of five domains. Domain I contains the HS attachment site and domain II the LDL receptor repeats. Domain V is found to be homologous to the laminin G domains and laminin binding through the AG-73 site have been demonstrated (Brown *et al.*, 1997). *In vitro* and *in culture* binding studies, along with studies using genetically modified mice have indicated that perlecan is responsible for localizing AChE on the synaptic basal lamina (reviewed in Inestrosa & Perelman, 1989). Through interactions with the ColQ collagen-like tail associated with the asymmetric forms, perlecan has been shown to bind AChE in the NMJ (Kimbell *et al.*, 2004). Unlike perlecan, these asymmetric isoforms of AChE are not expressed during early neural developmental stages. In a recent study, colocalization of AChE and perlecan was observed near membrane protrusion sites in fibroblasts and astrocytes (Anderson *et al.*, 2007). Results from this study also indicated possible interactions of perlecan with amyloid precursor protein. Colocalization may indicate the presence of redundancy.

The multidomain HSPG, Agrin, is well known for its role in AChR clustering during synaptogenesis. Binding of agrin with various molecules, including laminin-111, have been demonstrated. Such binding can occur by both HS-dependant and HS-independent means (Hartmann & Maurer, 2001; Bandtlow & Zimmerman, 2000). The laminin interaction site does not, however, correspond to the heparin-binding site AG-73 in the G4 domain (Denzer *et al.*, 1998). These findings, along with the demonstration that agrin inhibits rather than enhances neurite outgrowth; indicate that this molecule is unlikely to show redundancy with AChE.

Collagens XVIII, along with its cleavage product endostatin, are both components of the BM. These molecules share structural characteristics with both proteoglycans and collagen. Collagen XVIII have been shown to play a physiological role in modulating axonal growth by acting as a ligand for neural receptor tyrosine phosphatase. Even though collagen XVIII binds laminin, the site does not correspond to the heparin-binding site. Binding of collagen XVIII with heparan sulfate on the cell surface have also been demonstrated (Marneros & Olsen, 2005). These findings suggest collagen XVIII unlikely to be functionally redundant with AChE.

3.3.1.2 Clues from the AChE site

3.3.1.2.1 Homologous proteins

The ⁹⁰RELSED site on AChE falls partly within the carboxylesterase type b signature 2 (signature sequence EDCLYLNVWTP; prosite pattern PS00941), a signature strongly conserved throughout the α/β hydrolase fold family of proteins. As mentioned, the hydrolase fold family includes the cholinesterases (AChE and BChE), the cholinesterases-domain proteins (the neuroligins, neurotactin, glutactin, gliotactin, thyroglobulin and the Dictyolstelium crystal protein), the carboxylesterases and the lipases (Holmquist, 2000). The signature sequence occurs in the sequence surrounding a cysteine residue involved in a disulfide bond. Sequence conservation implies that at least

part of the ⁹⁰RELSED site is conserved in the cholinesterase-domain proteins as well. Additional conserved residues are found in the ⁴⁰PPMGPRRFL sequence where R46, which forms a salt bridge with E94, is conserved. Pro 40 and 41 are also conserved (Figure 37).

BChE, although very closely homologous to AChE, does not promote cell adhesion nor does it bind laminin *in vitro* (Johnson & Moore, 2000, 2003; Mack & Robitzki, 2000). The two molecules were also unable to dock.

As mentioned, the neuroligins are a group of four transmembrane proteins able to form adhesion complexes with β -neurexins in the presynaptic membrane where they promote synapse formation (Chubykin *et al.*, 2005). The neuroligin-1 extracellular domain shares 34% identity with AChE. Here a clear resemblance is seen in both the ⁹⁰RELSED (¹⁴⁷QDQSED) and the ⁴⁰PPMGPRRFL (⁸⁸PPTFERRFQ) sequences (Figure 46). Seeing as both AChE and neuroligin-1 bind to β -neurexin, functional redundancy between these two molecules has previously been proposed (Grifman *et al.*, 1998). This redundancy was not confirmed in a subsequent study (Comoletti *et al.*, 2003). Given that the neurexins show considerable alternative splicing, it is possible that isoforms other than those tested bind. Functional redundancy during early stages of development is unlikely as the neuroligins appear to be expressed only after synaptogenesis.

```

NL-1      KIRGIKKELNNEILGPVIQFLGVPYAAPPTGERRFQPEPPSPWSDIRNATQFAPVCPQN 120
NL-2      RVRGVRRELNNEILGPVVQFLGVPYATPPLGARRFQPEAPASWPGVRNATLLPPACPQN 109
NL-3      KLRGARVPLPSEILGPVDQYLGVPYAAPIGEKRFLPPEPPSPWSGIRNATHFPPVCPQN 109
NL-4      KIRGLRTPLENEILGPVEQYLGVPYASPPTGERRFQPEPPSSWTGIRNTTQFAAVCPQH 113

AChE     RLRGIRLKTTP---GGPVSAFLGIPFAEPPMGPRRFLPPEPKQPWSGVVDATTFQSVCYQY 103
BChE     KVRGMNLTVF---GGTVTAFLGIPYAQPLGRLRFKKPQSLTKWSDIWNATKYANSCCQN 96
          ::* .      *.* :**:* * * * * * * * * * * * * * * * * * * * * * *

NL-1      IIDGRLPEVMLPVWFTNNDLVVSSYVQDQSEDCLYLNIYVPTED-----DIRDSGG 171
NL-2      LHG-ALPAIMLPVWFTDNLEAAATYVQNQSEDCLYLNLVYPTEDGPLTKKR--DEATLNP 166
NL-3      IHT-AVPEVMLPVWFTANLDIVATYIQEPNEDCLYLNVYVPTEDGSGAKKQGEDLADNDG 168
NL-4      LDERSLLHDMLPIWFTANLDTLMTYVQDQNEDCLYLNIYVPTED-----DIHDQNS 164

AChE     VDTLYPGFEGTEMWNP-----RELSEDCLYLNWVTPYPR-----PTSPT 143
BChE     IDQSFPGFHGSEMWNPN-----TDLSEDCLYLNWVWPAPK-----PKNAT 136
          :          :* .          : .***** : : *

```

Figure 46. Sequence alignment of neuroligins 1-4, AChE and BChE. Asterisks indicate conserved residues. Dots indicate conservative replacements. The residues (and their equivalents) forming the laminin-binding site in AChE are shown in bold. Alignment was performed by using CLUSTALW (Johnson *et al.*, 2008b).

3.3.1.2.2 Searches for similar motifs in other proteins

Searches were performed for the ⁴⁰PPMGPRRFL and the ⁹⁰RELSED sequences, along with equivalents and conservative replacements for both. ⁴⁰PPMGPRRFL sequence searches only showed various AChEs and neuroligins from a number of species. Searches for the ⁹⁰RELSED sequence in neural molecules yielded the syntaxins, ligatin, proto-oncogene receptor tyrosine kinase Mer, perlecan and the LDL receptor. Of these, the only molecules expressed during migration and differentiation is Mer, perlecan and the LDL receptor. It is important to note that the motif search was not done for the exact sequence, but allowed for conservative replacements. The motif search on ProSite was [RK]-[ED]-[LAIM]-[ST]-[ED]-[ED]. The hit on Mer was residue 428-433 KELSEE (mouse receptor tyrosine kinase Mer, accession number NP 032613). This sequence is found in the extracellular domain of Mer, in a fibronectin type 3 domain.

Searches for the subsidiary ⁶⁰VDATT sequence also involved in the AChE-laminin interaction, yielded a number of candidates. When the search was narrowed to developmentally-associated neural proteins containing both the ⁹⁰RELSED and ⁴⁰VDATT

motifs, the yielded subset was considerably smaller. This subset seems to consist of perlecan and Mer. In perlecan, it would appear from the position of the two motifs that they may be situated far apart. As the structure of perlecan has yet to be solved, this speculation could not be confirmed. For Mer the VDAT motif search was [VLI]-[DE]-[LAIM]-[TS]-[TS], and the hit was residues 652-656. This falls within the tyrosine kinase domain, so is unlikely to associate with the KELSEE motif mentioned above. The structure of the relevant part of Mer has also not been solved. It appears, however, from the sequence that the motifs in Mer may be relatively close. Mer, belonging to the Ax1/Sky/Mer family of receptor tyrosine kinases, is expressed in both embryonic and mature nervous tissue (Graham *et al.*, 1995). Reports show that Mer is able to induce cell adhesion and flattening. It has also been found to, in combination with interleukin-3, promote differentiation. In contrast with many receptor tyrosine kinases, Mer does not appear to stimulate proliferation (Guttridge *et al.*, 2002).

The receptor tyrosine kinases Mer, Sky and Ax1 are activated through binding with Gas6. Gas6 is the product of the growth arrest-specific gene 6 and belongs to the vitamin K-dependant protein family characterized by the presence of γ -carboxyglutamic acid residues that mediate calcium-dependant phospholipid membrane binding. The receptor binding site is situated in two domains that are very similar to the laminin-G domains (Sasaki *et al.*, 2002). When the docking of Gas6 with AChE was investigated, it was observed that docking occurs at the same position as laminin (Figure 47). The ⁹⁰RELSED motif on AChE seems to lie within 2Å of the Gas6 residues 296-298 (YLG) and 306-309 (VIRL). Interestingly, this site is identical to the site described for Gas6 binding to Ax1 (Sasaki *et al.*, 2002). It was also found that the ⁴⁰PPMGPRRFL peptide lies within 2Å of Gas6 residues 339-345 (GMQDSW) along with F428 and D432. The ⁶⁰VDAT motif lies within 2Å of G298 and R299, as well as 329-332 (DPEG), 350-351 (LR) and 437-440 (IPR). However, the exact positions of the Gas6 binding site are unknown. This analysis is an indication only of molecules that may be similar to AChE in critical motifs. Mer came up as a hit. This does not necessarily suggest that it is definitely functionally redundant with AChE, but only that it is a possibility. Mer ligand binding would,

presumably, trigger a signaling event of cascade; which of course is a major difference between it and AChE, which cannot do this.

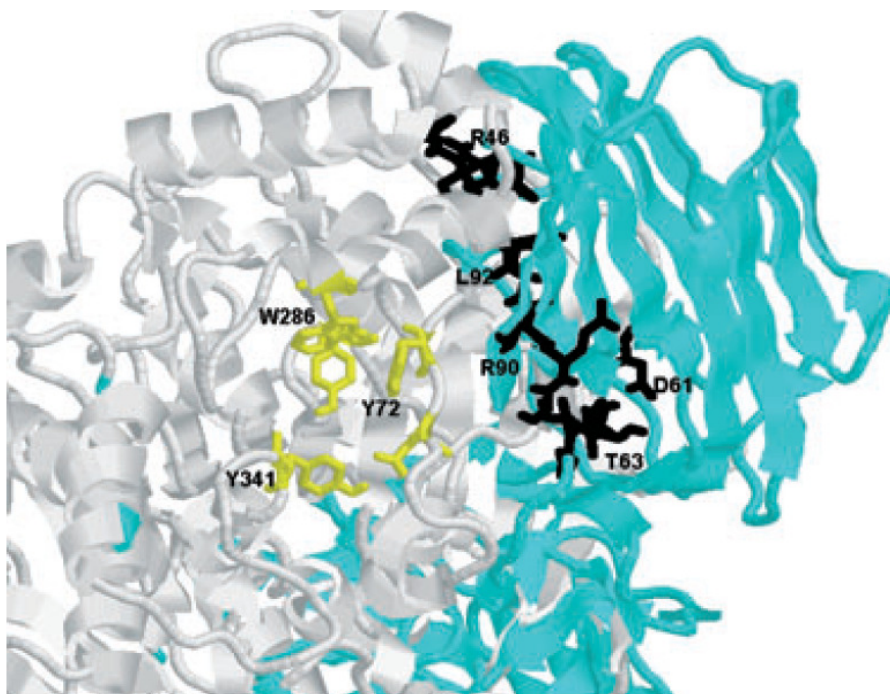


Figure 47. Docking of AChE with Gas6. Details of the docking of the mouse AChE dimer (1J06.pdb; shown in grey) with human Gas6 (1H30.pdb; shown in cyan). The PAS residues on AChE are shown in yellow. Residues 40-42, 46, 60-64 and 90-95 are represented in black (Johnson *et al.*, 2008b).

3.3.1.2.3 The LDL receptor pentapeptide DGSDE

Although their function is unknown, a number of molecules, including perlecan, contain low-density lipoprotein repeats (LDLR). In the LDL receptor, these repeats play a role in the binding of LDL. The conserved pentapeptide DGSDE sequence has been found to be especially important (Noonan *et al.*, 1991). Interestingly, this sequence is very similar to the AChE⁹⁰RELSED sequence. The LDL ligand that binds to DGSDE is also known to bind heparin. It appears that the AChE site resembles heparin as both these molecules

bind to the same site on laminin. Reports show that LDL is also able to bind syndecan-1 (Fuki *et al.*, 1997).

As mentioned, lipoproteins are known to play roles in neurite outgrowth and plasticity. The role of the apoE4 allele in AD has also been discussed in previous sections (Strittmatter *et al.*, 1993). Even though the specific mechanisms are still unclear, apoE3 seem to promote neurite outgrowth where apoE4 inhibits it (Beffert *et al.*, 2004). Both isoforms have been shown to bind amyloid β -peptide, apoE4 binds with greater avidity than apoE3.

The docking of apoE isoforms with AChE was investigated (1LPE.pdb and 1LPE4.pdb; apoE3 and apoE4, respectively). It was found that AChE docked with apoE3 (Figure 48) again via the same site that laminin binding occurs. Residues of apoE lying within 2\AA of the AChE $^{90}\text{RELSED}$ motif were R142, K143, R145 and K146. Residues lying within 2\AA of the $^{40}\text{PPMGPRR}$ sequence were W34, R38, R145 and K146. Residues of apoE lying 2\AA of the $^{60}\text{VDATT}$ motif were L43, Q48, W118, E131, L133, R134, V135 and R136. The receptor-binding region has previously been identified to lay between residues 135 and 151 (Datta *et al.*, 2000). This receptor-binding site is the same region that docks with the AChE site (many of these residues are basic). ApoE4 does not dock with AChE.

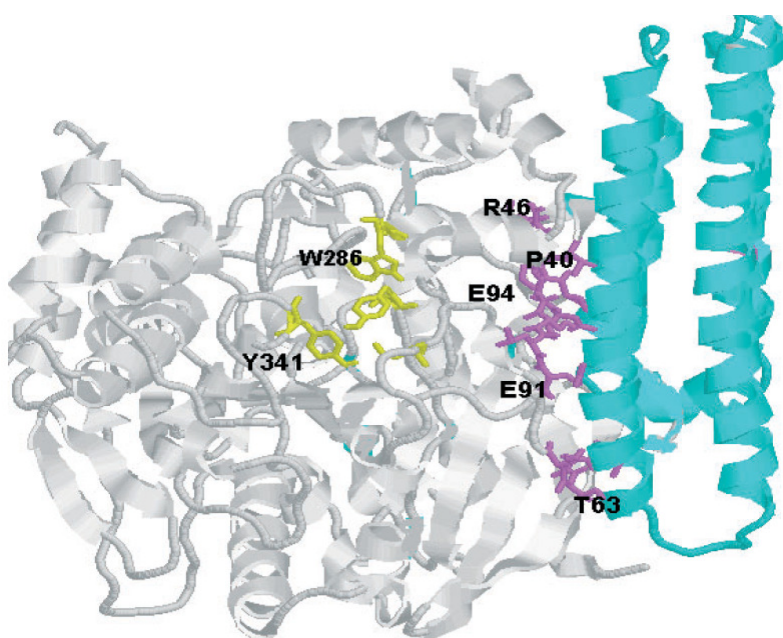


Figure 48. Docking of AChE with apolipoprotein E3. Detailed docking of the mouse AChE dimer (1J06.pdb; represented in grey) with human apoE3 (1LPE.pdb; represented in cyan). The PAS residues are shown in yellow, and residues 40-42, 46, 60-64 and 90-95 are shown in magenta (Johnson *et al.*, 2008b).

3.3.2 Potentially redundant molecules in Neurodegeneration: Alzheimer's disease

The REISED (ELSESED instead of REISED in order to minimize restriction) and DGSDE motifs were also used to BLAST-search candidates for redundancy in neurodegeneration. This time around the focus was strictly on molecules associated with brain function and also molecules that have previously been connected to Alzheimer's disease. The BLAST-search was restricted to the *Mus musculus* genome.

3.3.2.1 Searches for the ELSESED motif

The first BLAST-hit was for sickle tail protein. Sickle tail protein is involved in skeletal development, in particular, the development of the intervertebral disc (Semba *et al.*, 2006). This is a non-neuronal protein that is not connected to neurodegeneration and thus unlikely to be redundant.

Another unlikely hit was for the guanine nucleotide factor, Son of sevenless (SOS). SOS proteins act on Ras and Rho subfamilies of small GTPases and functions downstream of many growth factors and adhesion receptors (Wing *et al.*, 2003). Although they are expressed in neural cells, SOS proteins are not cell surface proteins.

Integrin $\beta 7$, also produced from the ELSESED-motif search, is a protein involved in adhesive interactions in leukocytes. Here integrin $\beta 7$ ($\alpha 4\beta 7$ integrin) acts as a receptor for fibronectin, MADCAM1, VCAM1 and E-cadherin (see Higgens *et al.*, 2000 for review). Even though integrin $\beta 7$ is found on cell surfaces, it does not appear to be involved in neural cell adhesion.

Several proteasome proteins, such as Psm2 and mCG49710, were also produced from the search, but none of these are involved in cell adhesion. In conclusion, searches for the ELSESED motif did not produce any molecules with potential for functional redundancy with AChE.

3.3.2.2 Searches for the DGSDE motif

As mentioned, the REISED motif resembles the DGSDE motif that binds apolipoproteins on LDL receptors (see section 3.3.1.2.3). It was also shown that AChE is capable of docking with apoE at the REISED site (Figure 48). ApoE, as well as LDL receptors and LDLR-containing molecules, have all been previously implicated in Alzheimer's disease (AD). For these reasons, proteins involved in neurodegeneration containing the DGSDE motif, was also investigated.

A number of significant hits were produced for the DGSDE motif:

SCO-spondin, a member of the thrombospondin family, is secreted by the sub commissural organ. It is a multidomain protein expressed in the brain and is conserved in all mammals (Meiniel & Meiniel, 2007). SCO-spondin contains 8 LDLR domain repeats (Accession number NP_775604) and has been shown to be involved in the modulation of neural aggregation (Gobron *et al.*, 1996). No specific involvement of SCO-spondin in AD has been documented making it an unlikely candidate for redundancy with AChE in neurodegeneration.

The structurally-related LDL receptors are the main class of apoE receptors expressed in the CNS (reviewed in Strittmatter *et al.*, 1993; Schmechel *et al.*, 1993). These receptors themselves, along with their variations, are candidates for functional redundancy. All members of this family of receptors are able to bind and internalize apoE-containing lipoproteins and are specifically expressed in the brain, particularly in regions prone to amyloid deposition and AD-associated neuronal cell loss (Andersen & Willnow, 2006). For these reasons, much attention has focused on a possible role of LDLR-related receptors in AD. Seeing as these receptors are components of the cellular machinery that supplies cholesterol to neurons, their activities might be crucial for the regulation of cellular cholesterol homeostasis, thus affecting the rate of APP processing. This concept is supported by association of disorders of cholesterol metabolism with high risk of AD (Shobab *et al.*, 2005). It is also possible that these receptors clear apoE or apoE-A β

complexes from the extraneuronal space, thereby modulating the extent of A β oligomerization and neurodegeneration (Kang *et al.*, 2000).

α -2 macroglobulin is a serum pan-protease inhibitor and its receptor also contains LDLR domain repeats (Borth, 1992; Strickland *et al.*, 1990). α -2 macroglobulin is upregulated in the brain during injury and has been localized to senile plaques in AD (Rebeck *et al.*, 1995). α -2 macroglobulin seem to mediate A β degradation and clearance thereof via endocytosis (Narita *et al.*, 1997). A common variant (29.5%) polymorphism in α -2 macroglobulin has also been associated with an increased risk of AD (Saunders & Tanzi, 2003).

The ECM molecule perlecan (HSPG2), also containing LDLRs, has been shown to be associated with amyloid plaques and tau aggregation. Polymorphisms in this molecule, however, do not appear to confer risk for AD (Rosenmann *et al.*, 2004). This indicates that perlecan is unlikely to be a candidate for redundancy with AChE in the prevalence of neurodegeneration.

Sortilin-related receptor (SORL1) is a mosaic protein expressed predominantly in the CNS. SORL1 consists of an N-terminal portion resembling the vacuolar protein sorting-10 (Vps110) receptor family and a C-terminal portion that has attributes of the LDLR family. This protein is capable of binding ligands ranging from receptor-associated protein (RAP) to apoE (Jakobsen *et al.*, 2001) and has been termed a neuronal receptor. SORL1 has been associated with AD in that it was found to interact with APP in the Golgi and endosomes to reduce production of A β (Anderson *et al.*, 2005; Offe *et al.*, 2006; Dodson *et al.*, 2008). SORL1 expression was found to be decreased in the neurons of sporadic AD patients (Scherzer *et al.*, 2004; Sager *et al.*, 2007). It seems that SORL1 variants that reduce SORL1 expression may increase risk for developing AD by increasing A β production (Gear *et al.*, 2009). The many associations of SORL1 with neurodegeneration suggest that this protein could be functionally redundant with AChE.

It is important to note that a five amino acid motif will possibly produce random matches. However, by starting an investigation with a specific motif (DGSDE) that is known to be involved in a specific interaction, simply extends the exploration to a slightly different context and suggests an intriguing possibility. These findings thus do not provide a definite case for redundancy, but are purely suggestive and might be interesting to follow up on in future studies.

4. Discussion

Apart from its primary function in the synaptic hydrolysis of acetylcholine, AChE has been shown through *in vitro* demonstrations to be able to promote various non-cholinergic functions, including cell adhesion and neurite outgrowth. AChE was also shown to interact with laminin-111 *in vitro* (Johnson & Moore, 2003). As this interaction was blocked by both PAS-binding inhibitors and PAS-binding MAbs, it was concluded that laminin binding by AChE occurred at the PAS. Furthermore, the abrogation of cell adhesion, resulting in apoptotic cell death or anoikis, by the same PAS-binding inhibitors and MAbs strongly suggested that the AChE-laminin interaction promoted cell adhesion. The involvement of the PAS in cell adhesion and neurite outgrowth is supported by similar findings in neural cells from a variety of tissues and species (see section 1.6.2.4). The anionic nature of the PAS itself and of the area surrounding the gorge (Ripoll *et al.* 1993; Porschke *et al.* 1996; Antosiewicz *et al.*, 1996) contributes to the attraction of the cationic acetylcholine molecule, and may also, as suggested by the annular motif of negative charge seen in the adhesion-mediating AChE and the CLAMS, but not in BChE (Botti *et al.*, 1998) be involved in mediating cell adhesion as well. Observations (Johnson & Moore, 2003; Bigbee & Sharma, 2004) that electrostatics play an important part in AChE-mediated cell adhesion support this. The project described in this thesis took these findings – the involvement of the PAS and electrostatic interactions – as its premise, and used as tools the PAS-reacting MAbs and inhibitors that had been used before.

Selection pressure on the PAS (the five residues constituting the substrate-binding site) has undoubtedly been directed towards catalysis and, specifically, acetylcholine hydrolysis, resulting in strong phylogenetic conservation of the structure. However, apart from this, there are several other features that contribute to structural conservation of its surrounds. One of these is the carboxylesterase type B signature 2 motif that surrounds Cys 96 of the omega loop (the ⁹⁴EDCLYLN motif). The other is the salt bridge between Arg 46 and Glu 94. Both of these features are involved in maintaining AChE's tertiary structure, and are very strongly conserved in all cholinesterases as well as the carboxylesterases from which they evolved. It is interesting that all these conserved

features – the anionic charge, the ⁹⁴EDCLYLN motif and the Arg-Glu salt bridge – are implicated in the interaction site with laminin: anionic charge through the electrostatic nature of the interaction, the principal interaction motif, ⁹⁰RELSER, forms part of the ⁹⁴EDCLYLN motif, as does the salt bridge, through Glu 94 and the Arg 46-associated ⁴⁰PPMGPRR motif.

Not all PAS ligands, however, are cationic. Small inhibitors, such as propidium, BW284c51 and gallamine, are cationic. These compounds interact directly with the PAS residues. On the other hand, fasciculin 2, a 61 amino acid peptide from green mamba venom, is not cationic. Its interaction with AChE covers a relatively large surface area, involving non-electrostatic interactions with residues of the Cys69-Cys96 omega loop, and insertion into the gorge itself (e.g. Radic *et al.*, 1994). In terms of ligands binding at the PAS, the amyloid beta peptide is hydrophobic. The beta peptide, however, does not bind on the 69-96 omega loop, or to the anionic regions of the PAS and its surrounds, but to the hydrophobic 274-308 sequence on the opposite side of the gorge (De Ferrari *et al.*, 2001). The prion protein has also been shown to bind AChE at the PAS, and, because of its structural similarity to the amyloid beta peptide (Bourne *et al.*, 1999), it is likely that it binds to the same sequence.

Paroanu and Layer (2004) observed binding of AChE to laminin-111, and, using a yeast 2 hybrid technique, identified an interaction between the laminin β 1 chain and an unidentified site in the C-terminal domain (between residues 240 and 503) of AChE. They confirmed their results using Co-IP, using mouse brain extracts as their tissue source. Bigbee and Sharma (2004) also observed binding of AChE to laminin, but in this case, the γ 1 chain (it was observed that the AChE binding partner ran in the laminin γ 1 position on the gel, but the identity of the band was not specifically confirmed). These authors used dorsal root ganglion cells; these cells extend axons into the central nervous system. The project described in this thesis used neuroblastoma cells, a tumour that is derived from the peripheral nervous system. There are distinct differences in the composition of the extracellular matrix between the central and peripheral nervous systems. In the peripheral nervous system, laminin and collagen IV are major constituents

of the extracellular matrix surrounding the neurons and neural precursors, but this is not the case in the central nervous system. These differences in tissue and extracellular matrix composition may play a significant role in the results obtained in the different studies. In this project, Co-IP, using whole molecule laminin was used, with no attempt to identify binding to the different laminin chains.

The localisation by Paraoanu and Layer of the AChE interaction site to the C-terminal domain may represent, to reconcile with the findings here, binding to C-terminal domain parts of the PAS itself (W286, Y341 and associated sequences), mimicry of PAS-associated structures (such as the short omega loop), part of the C-terminal T-peptide (findings by Greenfield's group - e.g. Day and Greenfield, (2002) - implicate this in cell adhesion) or, most likely, and especially taking into account the different laminin chains involved, an entirely different interaction site. Again, this may be a consequence of the different tissue source used.

The proteins and proteoglycans of the extracellular matrix (including the basement membrane) are frequently large and are characterised by an ability to interact with a variety of molecules. Many, like perlecan and fibronectin, are modular, and may be made up of multiple repeating domains. These multiple interactions serve a variety of functions, but a major one is the formation of a strong and stable network supporting the cells. During the development of the peripheral nervous system, AChE (as a hydrophilic tetramer) is secreted by the cell into the matrix (Layer & Willbold, 1995). The function of this secreted form is not known. At a later stage, AChE expression shifts to the PRiMA anchored form in the cell membrane. Greenfield (e.g. Day & Greenfield, 2002) has suggested that the secreted AChE is of primary importance in developmental non-classical functions. AChE appears to be capable of using different sites to interact with a variety of protein partners. It interacts, firstly, via the charged REISED motif near the PAS with laminin $\alpha 1$ (this thesis), secondly, via the hydrophobic PAS sequence with the amyloid β -peptide (De Ferrari *et al.*, 2001) and very likely with the prion protein also (Bourne *et al.*, 1999; Clos *et al.*, 2006), thirdly, with collagen IV (Johnson & Moore, 2003) and fibronectin (Giordano *et al.*, 2006) by as yet identified PAS-associated sites,

fourthly, with laminin $\beta 1$ via an unidentified site in the C-terminal domain (Paraoanu and Layer, 2004), very likely with laminin $\gamma 1$ by an unidentified site (Bigbee and Sharma, 2004) and, fifthly via its C-terminal T-peptide with nAChR (Day & Greenfield, 2002) as well as the anchoring proteins ColQ and PRiMA. It also appears to interact with perlecan (Anderson *et al.*, 2008) by an unidentified site. The overlay technique used by Bigbee and Sharma (2004) has suggested a number of additional binding partners of MW 200, 110, 35 and 33 kDa, respectively (the 200 kDa protein is probably laminin $\gamma 1$). These are all documented interactions. The investigations into possible functional redundancy open up the field still further. With the caveat that neural cells from different tissue sources (peripheral or central nervous system) were used in these studies, and these tissues have different compositions and physiological requirements, a degree of promiscuity is evident, suggesting that AChE could possibly be functioning in stabilising the matrix and basement membrane through these multiple interactions.

4.1 Defining the interaction between AChE and laminin

The first aim of this study was to demonstrate the interaction between AChE and laminin, and to identify and describe the interaction sites of AChE and laminin involved in this binding. Unlike AChE, where preliminary results showed the site involved to be PAS-associated, no specifications concerning the associated laminin site had been made. The only clue came from the assays which showed that laminin-111 interacts with AChE (Johnson & Moore, 2003; Figure 17). An additional problem is that laminin is a very big molecule (400-900kDa), and is known to interact with a large number of ligands and receptors such as integrins, heparin, dystroglycan, collagen IV, etc. (e.g. Tzu & Marinkovich, 2008; Chen *et al.*, 1999; Schneider *et al.*, 2006; Mecham, 1991). This makes working with this molecule, to identify a particular binding site, quite difficult. The interference of NaCl, which alters the ionic conditions, on the binding of AChE with laminin, supported the notion that the binding involves electrostatics (Johnson & Moore, 2003; Figure 19). Seeing as the MAbs interfered with both the AChE-laminin interaction

and cell adhesion, it appeared likely that the epitope on AChE that they recognised was the same as the laminin-binding site.

Peptides and binders identified through phage display would represent ligands, or rather, parts of ligands, for AChE. The identified binders could then be BLASTed in order to determine where they came from, thus possibly identifying a protein ligand for AChE. Sequences obtained from phage display could also contribute towards identifying the particular sites involved in the interaction. Unfortunately no consensus sequences were produced with the peptide phage display. The site on AChE was previously shown to be a highly conformational structure (Johnson & Moore, 2003). A possible explanation for the negative results could be that the peptides may not adequately define the site, possibly binding to only a small section of it. The results obtained in the microarray suggest that the MAbs may show cross-recognition of different proline-containing sequences on AChE; it is possible that an analogous recognition of multiple proline-containing sequences by the phage-displayed peptides may have complicated the issue and affected the enrichment of a single binder. Proline is almost always found on the surfaces of proteins due to its ability to destabilise and prevent ordered folding (Levitt, 1980). Proline is also very strongly antigenic (partly due to its own ring structure and partly because of the characteristic kink it induces in the polypeptide chain), and Abs tend to prefer proline and proline-rich regions.

Ab display, using three dimensional binders, could possibly make up for where the peptide phage display was lacking. The Ab phage display work was contracted out as the Ab libraries used were not commercially available at the time. The basic technique is the same as peptide phage display. The Ab phage display provides information on both the sequences that bind the AChE site, as well as the three dimensional structure of the site (from modelling). The panning process was completed with success and two specific binders were identified. In particular, among the 23 DNA-sequences clones, 15 shared two homologous sequences (clone no. 7 & clone no. 21). Sequence alignment of the two identified binders showed them to share 95% sequence identity (Figure 30). The CDRs of the scFv sequences both showed a relatively large number of basic residues (sequence 7:

6 basic & 1 acidic; sequence 21: 4 basic & 0 acidic). This would agree with the findings on the the laminin site that interacts with AChE, which also has a predominance of basic residues, and also supports the overall supposition that electrostatic interactions play a major role in the interaction of AChE with binding partners and with laminin in particular.

The models of the sequences of the two clones produced from the Ab phage display were used to dock with AChE (Figure 34 & 35). The docking results indicate recognition of the 69-96 omega loop, including the ⁸⁸PNRELEASED motif and the VVDATT (human) motif. These results agree closely with the laminin interaction, but with some differences. While the laminin interaction appears to be centred on the ⁹⁰RELEASED motif itself, with contributions from ⁴⁰PPVG (mouse) and ⁵⁹VLDATT (mouse), the sequences recognised by the scFv, as well as by the MAbs, as shown by the microarray epitope analysis (see below), is skewed slightly to include Pro 88 and Asn 89 just before. These results indicate that the epitope recognised by both the scFv and the MAbs is the same. Although this project was begun with the premise that the epitope recognised by these MAbs, which inhibit both cell adhesion and the AChE-laminin interaction, is the same as the adhesion-mediating and laminin-binding site, this appears not to be the case. The site is very close and has much in common, but is not precisely the same. The inclusion of part of the site in the MAbs' epitope, together with steric hindrance, would account for both the interference with cell adhesion and the AChE-laminin interaction.

Previous studies (Johnson & Moore, 2004) had suggested, based on epitope analysis of the adhesion-inhibiting MAbs using long synthetic peptides, that the adhesion-mediating site was located primarily on the 37-53 sequence along with contributions from residues on the omega loop and the 55-66 sequence. This is structurally feasible as these sequences lie very close to one another in the tertiary structure. In this study, a peptide microarray using 500 peptides varying in length from 9 to 15 residues as well as different degrees of constraint, were used to define the binding site on AChE. Results confirmed the previous findings and showed the primary epitope to be the proline-rich motif ⁴⁰PPMGPRRFL (human) of the 37-53 peptide. Proline is not the only antigenic amino

acid found in this motif, arginine and phenylalanine residues are also known to attract Abs. This motif was identified as one of the most antigenic regions of the AChE surface by the Antigenicity Plot program (JaMBW) which computes and plots antigenicity along a polypeptide chain as predicted by the algorithm of Hopp and Woods (1983). In *Torpedo* AChE, the analogous peptide has also been identified as an epitope (Wasserman *et al.*, 1993). In contrast with the long peptide results, the microarray was able to show that the MAbs' reactivity increased on addition of proline to a peptide. Possible interpretations of these findings have been described above.

The α -chain of the laminin-111 molecule contains most of the receptor-binding sites. Here, these sites are located predominantly in the G domains (Suzuki *et al.*, 2005; Figure 15). Due to the evident involvement of electrostatics in the binding between AChE and laminin, the search for potential sites on laminin was focussed on cationic sites. Analysis of the laminin α 1 chain showed this chain to have 14 potential cationic sites that could, theoretically, be attracted to the anionic PAS-region of the AChE molecule. Among them was the laminin AG-73 site, a site that had previously been described as being involved in cell attachment and spreading (Nomizu *et al.*, 1995). The initial observation that AChE is able to dock with the equivalent of this site in laminin-211 (the sequence identity between laminin α 1 and α 2 is 63%; Figures 38 & 39), suggests that it is possible that AChE interacts with laminin-211 (merosin) *in vivo*. Merosin is expressed in peripheral nerves, striated muscle and placenta. Deficiency of merosin is associated with congenital muscular dystrophy (Wewer & Engvall, 1996). These docking results also led to the *in vitro* examination of this sequence by using binding assays. The binding assays confirmed the docking results and indicated that the AG-73 site plays an important role in the AChE-laminin interaction (Figure 41). Docking of AChE with the laminin α 1 chain (Figure 45), confirmed the importance of AG-73. The docking performed was rigid-body, and thus did not take into account conformational changes that might occur during the interaction.

Docking of AChE with the laminin α 1 G4-5 domain pair showed that AChE interacts with laminin primarily by the ⁹⁰RELSED motif. Part of this motif is recognized by the

adhesion-inhibiting MAbs. This strongly suggests that the motif is involved in cell adhesion, which, in turn, involves the AChE-laminin interaction. The observation that the MAbs that recognized the ⁹⁰RELSED motif were able to block cell adhesion, while those that do not recognize the ⁹⁰RELSED have no effect, supports the significance of this motif for cell adhesion. The slight offset in the recognition sequence of the the MAbs and scFv (⁸⁸PNRELS) and the laminin-binding motif (⁹⁰RELSED) may be explained by steric hindrance: binding of the antibody molecule prevents binding by laminin, even though they do not compete for exactly the same site. The highly antigenic ⁴⁰PPMGPRRFL motif also appears to be involved in the laminin interaction; because of the salt bridge link between Arg 46 and Glu 94 (Figure 36), it lies closely apposed to this section of the omega loop. Along with disulfide bonds, the salt bridge acts in stabilizing the tertiary structure of the AChE molecule. Residues involved in these bonds, as well as residues in their vicinity, also have a strong propensity towards conservation. This is evident when comparing the AChE and BChE sequences (Figure 37). As mentioned, this part of the sequence forms part of the carboxylesterase type 2 signature B, conserved around a cysteine residue involved in a disulfide bond, and is strongly conserved throughout the α/β hydrolase fold family. The ⁹⁰RELSED motif also falls within the conserved area as it lies very close to Cys 96 (Cys 94 in *Torpedo* AChE and Cys 92 in BChE). The inability of *Torpedo* AChE and BChE to dock with laminin could possibly be due to sequence differences between *Torpedo* AChE and mouse AChE, and BChE and mouse AChE (Figure 37). Although the mouse structure (1J06.pdb) used in the docking is dimeric and both the *Torpedo* (2ACE.pdb) and BChE (1P0I.pdb) structures are monomeric, it is unlikely that conformational differences are responsible, as such differences are not observed in the crystallography. Another possible explanation could be the important role that the charge distribution over the entire PAS plays in cell adhesion, as BChE does not have the same concentration of charge in this area (Botti *et al.*, 1998). BChE has not been observed to be able to bind laminin *in vitro* or to promote cell adhesion (Johnson & Moore, 2000).

The sequence data obtained from the Ab phage display is empirical experimental data as the two sequences of the scFvs are definite and the positions of the CDRs are also fact.

The same cannot be said for results obtained from molecular modelling and protein docking. In silico simulation and modelled structures are not in the same category as data obtained in a laboratory and structures obtained through crystallography. Another important implication is that both the scFvs and MAbs were raised against human AChE and the conformational site mapping was also done against human AChE. The docking, however, was performed with mouse AChE (due to availability of the structure). Sequence identity between mouse and human AChE is 92% and that for the laminin α 1 chain, 86%. Although the sequences for human and mouse AChE differ, they are still strongly conserved in critical regions, in particular, the catalytic apparatus, including the PAS and its surrounds, that have specific functions (see Figure 37). Comparison of these AChE sequences shows that conservative replacements of Val 42 and Met 48 in the mouse with Met 42 and Leu 48 in the human occur, respectively. These differences could have had an effect on the reported results. The results obtained for both the MAbs and conformational site mapping, as well as for the scFvs and docking with AChE, largely agree, but there are some subtle differences. These differences may be due to the limitations of the docking technology; they may simply be due to the differences in the experimental approach.

Overall, both the MAbs and the scFvs were found to recognize aspects associated with the PAS of AChE. The conformational site mapping indicated the strongest recognition by the Abs was to the ⁴⁰PPMGPRR motif. Other proline-containing motifs were also recognized, especially ⁷⁸PGFEGTE and ⁸⁸PNRELSSED on the omega loop. The peptide arrays suggested that the Abs responded strongly to the presence of proline. Here the ⁵⁹VVDATT did not seem to play a significant role in the Ab recognition. The scFv docking results, however, show a reaction/recognition pattern very similar to the site that laminin interacts with. This suggests direct competition between laminin and the Abs, which correlates with the adhesion experiments on the N2 α cells (Johnson & Moore, 2000). The findings from the conformational epitope mapping, indicating the primary Ab recognition sequence as being the ⁴⁰PPMGPRR motif, suggest that the competition is not 1:1. One explanation of this is steric hindrance, in other words, that the Abs, which are fairly substantial molecules, while binding to the ⁴⁰PPMGPRR motif, prevent laminin, an

even more substantial molecule, from binding to the ⁹⁰RELSSED motif. Another explanation is that the peptide array effectively “dissects” the epitope, quantitating the recognition of individual components. As already discussed, the highly antigenic amino acid proline forms a major recognition component of the epitope. It could be that the strength of recognition of the ⁴⁰PPMGPRR motif is primarily a response to its proline content, and that the adjacent ⁹⁰RELSSED motif, although not showing as strong a recognition, is nevertheless a critical, even a primary, part of the epitope. The docking results with the scFv and mouse AChE indicate a recognition of the ⁹⁰RELSSED motif, the PPMG (PPVG in mouse) sequence, as well as a recognition of the ⁵⁹VVDATT (VLDATT in mouse), which agrees with the laminin interaction.

4.2 The question of redundancy

The term “functional redundancy” suggests the possibility of a formal backup system, with AChE standing in the wings as an understudy in the event of the principal's failure. This may not necessarily be the case, and the less restrictive term “functional compensation” may, in many cases, be preferable. However, in this thesis, the term “functional redundancy” has been used to cover both the more formal and the less formal applications.

The AG-73 site on laminin, that binds AChE, was initially identified as a heparin-binding site (Hoffman *et al.*, 1998). Through site-directed mutagenesis, Harrison *et al.* (2007) showed that heparin was bound largely by two clusters of basic residues: ²⁷¹⁹RKR (AG-73) and ²⁷⁹¹KRK. Andac *et al.* (1999), using the same method, found contributions by three basic regions: 2766–2770, 2791–2793 and 2819–2820. The same basic clusters with some additional basic residues were also found to contribute to the binding of α -dystroglycan and sulfatides. AChE was observed to interact with ²⁷¹⁸VRKR, ²⁷³⁸YYIKRK, ²⁷⁸⁹YIKRK as well as ²⁸¹⁷VERK. These residues are all either charged, hydrophobic or, in the case of tyrosine, aromatic.

From these findings it would thus appear that AChE is able to compete with other molecules for binding to laminin. The competition ELISA performed in this study, confirmed this by showing competition between AChE and heparan sulfate (Figure 44). Both heparin and the AChE surface (in the vicinity of the PAS) are anionic. This is not the first demonstration that both a protein and carbohydrate is able to bind to a single polypeptide site (Ma *et al.*, 2002). The PAS thus appears to promote an array of functions involving molecular binding. These functions range from binding ACh and promoting catalysis to binding laminin. This agrees with Wyman's principle of linked functions (Wyman, 1964). The principle considers the likelihood of an interdependence of several functions of a molecule.

These findings, that AChE binds to a heparin-binding site and is able to compete with heparin for binding to laminin, indicate the possibility of functional redundancy between AChE and heparin, *in vivo*. Functional redundancy would explain the apparent inconsistency between the *in vitro* experimental findings detailing non-cholinergic functions (the importance of AChE for neural cell survival and differentiation), and the evidence from the knockout models (Xie *et al.*, 2000). Survival of the AChE knockout led to the questioning of the non-cholinergic structural involvement of AChE in neural differentiation (Cousin *et al.*, 2005). The well documented evidence of ACh's inhibition of neurite outgrowth (Biagioni *et al.*, 2000), indicate that at least part of AChE's neurite-promoting ability may be due to the hydrolysis, and thus removal, of ACh, allowing neurite outgrowth to proceed. However, there is clear evidence indicating non-cholinergic involvement: De Jaco *et al.* (2002) observed AChE-mediated neurite outgrowth in a cell line lacking acetylcholine, and there are also several studies using both inhibitory and non-inhibitory anti-AChE MAbs (Johnson & Moore, 2000; Sharma & Bigbee, 1998). The possibility that the adhesion-inhibiting Abs react with a particular site, whether on AChE or another molecule, should be considered.

This raises some interesting speculative questions, perhaps the most challenging being whether the adhesion-mediating ability of AChE is purely fortuitous and perhaps even irrelevant. It could be argued that the AChE-laminin interaction is of no functional

significance at all, arising by chance and surviving because there is no selective pressure to remove it. Although, against this is the demonstrated importance of the interaction site on AChE, i.e. the importance of the PAS site. The AG-73 site on laminin has been previously shown to play a role in mediating cell adhesion, neurite outgrowth, as well as metastasis (Nomizu *et al.*, 1995; Richard *et al.*, 1996). Blocking the complementary site whether on AChE or some other molecule, also showed to abrogate cell adhesion and result in cell death (Johnson & Moore, 2000).

Although the specific signaling mechanisms involved have yet to be determined, the possibility that AChE (or another molecule) may bind synergistically with, for example, an integrin or α -dystroglycan, should be considered. Integrins and α -dystroglycans are molecules capable of transducing a signal to the cell's interior. Although PRiMA-linked AChE does have a small cytoplasmic domain, details of its ability to transduce information from the cell surface to the interior remain unknown. The presumption that it relies on complexation with other molecules for signal transduction, is thus feasible.

Neural development is an extremely complex process. Development of peripheral neurons involves the migration of neural crest cells, their settling and differentiation at the required destinations, followed by the development of the synaptic pathways. Cellular signals in this process are mediated by cell surface receptors, ECM and BM molecules, growth factors and cytokines, governed by a complex array of transcriptional switches. Functional redundancy is known to occur. From a 'design' point of view, redundancy could be a fail-safe mechanism in view of the complexity of these processes and potential for error. Carbohydrates, due to their microheterogeneity, have the potential for subtle changes in signaling.

Molecules on the cell surfaces that could possibly be functionally redundant with AChE are the syndecans and glypicans. It has been shown that AG-73 binds syndecan-1, through heparan sulfate chains (Hoffman *et al.*, 1998). Syndecan-1, however, is not expressed to any significant extent in neural cells (Kim *et al.*, 1994). An unusually high number of proteoglycans are expressed during nervous system development (Hartmann &

Maurer, 2001). The lack of comprehensive information on the developmental expression and interactions of HSPGs makes it difficult to narrow the field of possibilities. The neuroligins are also possible candidates. Functional redundancy of AChE with neuroligin-1 has been reported as both molecules seem to interact with the cell surface receptor β -neurexin (Grifman *et al.*, 1998). Unfortunately there is no documented evidence that neuroligins are expressed prior to synaptogenesis. Findings from this study show, however, that it is unlikely that AChE and neuroligin could function with laminin as the neuroligin sequence of the omega loop is not conserved and is very different. Sequence conservation of the latter part of the omega loop does occur, but this is probably because it is in the region of the disulfide-forming Cys 96, and functions in stabilization of the molecule's tertiary structure. The cell surface receptor tyrosine kinase Mer, is another cell surface candidate for redundancy. Together with the LDL receptor, Mer seem to have similar peptide motifs to AChE.

In the ECM, perlecan could be a possible candidate due to the double virtue of its heparan sulfate chains and the speculation of it containing motifs similar to both AChE and the LDL receptor. Perlecan has also been shown to bind laminin through the AG-73 site (Brown *et al.*, 1997), as well as the asymmetric AChE forms through interactions with ColQ (Kimbell *et al.*, 2004). It also appears that PRiMA-linked AChE may bind perlecan through an unknown mechanism (Anderson *et al.*, 2008). ECM molecules characteristically demonstrate multiple interactions, by means of various sites. Many of these molecules are modular containing several types of domains. A number of ECM cells, including agrin, pentraxin, slit protein, serum amyloid P component, Gas6 and β -neurexin, have domains resembling the laminin G domains, thus resembling the laminin site with which AChE interacts *in vitro*. Docking results from this study indicate that AChE may bind Gas6 (Figure 47). Interactions of AChE with a number of ECM molecules have been described: laminin (evidence from this study; Johnson & Moore, 2003; Paraoanu & Layer, 2004), collagen IV (Johnson & Moore, 2003), fibronectin (Giordano *et al.*, 2007), nAChR (Greenfield *et al.*, 2004), prion protein (Pera *et al.*, 2006), as well as amyloid- β peptide (De Ferrari *et al.*, 2001). AChE also appears to have a number of interaction sites itself. It would seem that AChE, in its potential for multiple

interactions, thus resembles ECM molecules. Interestingly a number of ECM cells with which AChE interacts, are found in amyloid deposits. These include: amyloid- β peptide, laminin, collagen, fibronectin, perlecan, various HSPGs, apoE, agrin, and serum amyloid P component.

Results from the scFv BLAST also produced a number of ECM molecules (laminin, fibronectin, tenascin-c), along with TREM1, α -synuclein and tetanus and botulinium toxins. Although the resemblance between AChE and laminin appeared to be an artefactual consequence of using a similar antibody library, and thus can be discounted, there are distinct resemblances between fibronectin and tenascin-C and AChE. The observation that fibronectin, as well as the amyloid β -peptide, which have been shown to be AChE ligands, are included in the list raises some questions. A possible explanation for this is the apparent presence of complementary sites at or associated with the PAS (Johnson & Moore, 2009): structural resemblances between the ⁷⁸PGFEGTE motif on the 69-96 omega loop, the 257-272 short omega loop, and the C-terminal peptide, and their (demonstrated or presumed) interaction with the PAS itself. This suggests that AChE may have more than one site of interaction with ECM molecules, acting as both receptor and ligand. Apart from the PAS and its interaction sites, AChE interacts with the basal lamina through ColQ, attached to the C-terminal T-peptide. A multiplicity of interactions is characteristic of ECM molecules, and this would support the view that AChE's function in cell adhesion is related to strengthening the ECM, providing support for the cell and the developing neurites, rather than a specific receptor-ligand interaction.

TREM1 also appears to resemble AChE, TREM is involved in the haematopoietic system, and AChE has long been associated with the haematopoietic system. AChE is expressed in significant quantities in erythrocyte membranes and deletions of the ACHE locus at 7q22 are associated with the myelodysplastic syndrome and acute myeloid leukemia (Stephenson *et al.*, 1996). AChE has also been implicated, enzymatically and non-enzymatically, in haematopoiesis (Soreq *et al.*, 1994; Grisaru *et al.*, 2006), and numerous epidemiological studies have linked exposure to anti-cholinesterase pesticides

to leukemia (reviewed in Merhi *et al.*, 2007). The link to the haematopoietic system, suggested by the scFv, warrants further investigation.

The structurally related *Clostridium* toxins, the tetanus and botulinum toxins, both interact with neurons and, indirectly, alter acetylcholine levels. This also warrants further investigation.

BLAST-searches for potentially redundant molecules in neurodegeneration were limited to the (R)ELSEED and DGSDE (which is very similar to the AChE ⁹⁰RELSED sequence). The focus was on molecules specifically associated with brain function and AD. Searches for the RELSED motif did not deliver any molecules with potential for redundancy with AChE. The conserved LDL receptor pentapeptide DGSDE has previously been shown to be very important (Noonan *et al.*, 1991) and the LDL ligand that binds to this motif is also known to bind heparin. LDL receptors are the main class of apoE receptors found in the CNS (reviewed in Strittmatter *et al.*, 1993). Members of the LDLR family themselves have been implicated in Alzheimer's disease; the LDL receptor-related protein (LRP), in particular, has been shown to be involved in APP endocytic trafficking and its processing to the A β -peptide (Bu *et al.*, 2006). Human apoE receptors are known to bind soluble A β (Koudinov *et al.*, 1998). The cholesterol transporter, apoE4 is a risk factor in late-onset AD (Chalmers *et al.*, 2003; Fagan & Holtzman, 2000) and was found to bind A β more rapidly than other apolipoproteins (Sanan *et al.*, 1994; Beffert *et al.*, 2004). However, the exact influence of apoE-4 on AD is not known. ApoE is a major constituent of amyloid plaques (Namda *et al.*, 1991). The role of LDL receptors in cholesterol homeostasis, along with their ability to clear apoE and apoE-A β from the extracellular space, as well as their role in APP processing, indicates a strong association of these receptors with the pathogenesis of AD. The LDL receptors and their variations are all candidates for functional redundancy with AChE in neurodegeneration. Although these findings are based on a number of presumptions and suppositions (that AChE is functionally redundant with LDL receptors and LDL receptor domain-containing molecules, specifically), they do offer intriguing suggestions for future hypotheses.

SORL1, a neuronal apoE receptor, has also been linked to APP processing and AD. SORL1 has been shown to, through its interaction with APP; reduce the production of A β (Anderson *et al.*, 2005; Offe *et al.*, 2006; Dodson *et al.*, 2008). Studies show that variations in the SORL1 gene are associated with an increased rate of late-onset AD (Kimura *et al.*, 2009). The strong apparent association of SORL1 with the pathology of AD suggests the possibility for redundancy with AChE in neurodegeneration.

The BLAST-search once again indicated perlecan as a possible candidate. Perlecan contains LDL repeats, and although this molecule has been associated with amyloid plaques and tau aggregation, polymorphisms do not appear to confer risk for AD. Perlecan thus seems an unlikely candidate for redundancy with AChE in reemergence to neurodegeneration.

From an evolutionary perspective, the ChEs, CLAMs and ACh appear to have been around for a very long time. AChE and ACh, for example, are found in bacteria, algae and protozoa as well as, as far as is known, throughout the plant and animal kingdoms. CLAMs have been described not only in mammals and insects, but also in the slime mould *Dictyostelium*. This suggests that the split between enzymes and non-enzymes may have occurred in the earliest of life-forms. It seems that the common ancestor probably had both enzymatic and adhesive characteristics, and the cholinesterase-domain protein branch of the family specialized in cell adhesion and signaling, losing their catalytic function. AChE, on the other hand, retained and perfected its enzymatic ability and along with it, apparently its adhesive capabilities. Interestingly, early organisms did not have nervous systems, it is thus possible that AChE, along with ACh, may have obtained morphogenetic functions and that these functions (both enzymatic and non-enzymatic) may be more ancient than its synaptic capabilities. Such presumed antiquity suggests there may have been a distinct selective advantage in retaining these functions, that they fulfill a definite role and are neither trivial nor fortuitous.

4.3 Conclusions

In conclusion, it was observed that AChE is able to interact with laminin $\alpha 1$ through its G4 domain. The sites of interaction on both AChE and laminin have also been defined. It is strongly suggested that the AChE-laminin interaction is involved in cell adhesion as is seen from the adhesion-inhibiting MAbs that recognize the associated AChE site. While it is possible that the AChE and laminin interaction sites may have evolved specifically for this interaction, this is probably unlikely due to a number of different factors. The structure of the interaction site on AChE appears to be a consequence of the conservation of structural features involved in stabilisation of the tertiary structure of the protein (the carboxylesterase signature 2 motif and the Arg46-Glu94 salt bridge) together with the evolution of structures enhancing catalysis (the PAS and the negative charge surrounding it). Nevertheless, the presence of these features in the non-enzymatic CLAMS as well suggests an adaptation to cell adhesion, and that present-day mammalian AChE is a dual-purpose enzyme and adhesion molecule. The interaction site on laminin, however, is not specifically directed towards AChE; it is well-documented adhesion-mediating site and binds heparan sulfate proteoglycans. Furthermore, the apparently promiscuous interactions of AChE, not only with the laminin $\beta 1$ and $\gamma 1$ chains as well, but with other matrix molecules, suggests that AChE's role in this respect may be in enhancing the structure and stability of the extracellular matrix or basement membrane. This is a structural, rather than a signalling role, and, although it is possible that PRiMA-linked AChE, through the small cytoplasmic domain, may be capable of signal transduction, the proposed structural role fits the expression data showing the secretion of the hydrophilic tetramer into the matrix, and the later presence of the amphiphilic tetramer in the cell membrane. This relatively non-specific role also fits the evidence of the knockout mouse; although there are some instances (particularly in the development of the retina) where non-enzymatic roles of AChE cannot be compensated for.

The search for proteins that could compensate for AChE loss in the non-enzymatic context, or for which AChE could compensate in the reverse situation, has shown some intriguing possibilities. Heparan sulfate proteoglycans are ubiquitous and important

components of the extracellular matrix, as well as the basal lamina. They are also closely associated with amyloid deposits in Alzheimer's disease. Similarly, LDL receptor domains are found in a variety of proteins, and apolipoprotein E is also associated with Alzheimer's disease. These apparent structural similarities offer interesting possibilities for future research, particularly in view of the close association of AChE with Alzheimer's pathology.

In conclusion, therefore, the interaction sites between AChE and the G4 domain of the laminin $\alpha 1$ chain have been identified and investigated by *in vitro* and *in silico* techniques. Coimmunoprecipitation evidence suggests that this interaction occurs in the *in vivo* situation as well. Using the interaction sites as a template, various molecules that could compensate for the AChE-laminin interaction in the absence of AChE, as in the knockout, or for which AChE could possibly function as a backup device, have been identified or suggested.

5. Bibliography

- Abramson SN, Ellisman MH, Deerinck TJ, Maulet Y, Gentry MK, Doctor BP *et al* (1989). Differences in structure and distribution of the molecular forms of acetylcholinesterase. *J Cell Biol* **108**: 2301-2311.
- Aldridge WN, Reiner E (1969). Acetylcholinesterase. Two types of inhibition by an organophosphorus compound: one the formation of phosphorylated enzyme and the other analogous to inhibition by substrate. *Biochem J* **115**: 147-162.
- Alexander SP, Mathie A, Peters JA (2006). Guide to receptors and channels, 2nd edition. *Br J Pharmacol* **147 Suppl 3**: S1-168.
- Altschul SF, Madden TL, Schaffer AA, Zhang J, Zhang Z, Miller W *et al* (1997). Gapped BLAST and PSI-BLAST: a new generation of protein database search programs. *Nucleic Acids Res* **25**: 3389-3402.
- Alvarez A, Opazo C, Alarcon R, Garrido J, Inestrosa NC (1997). Acetylcholinesterase promotes the aggregation of amyloid-beta-peptide fragments by forming a complex with the growing fibrils. *J Mol Biol* **272**: 348-361.
- Amersdorfer P, Marks JD (2000). Phage libraries for generation of anti-botulinum scFv antibodies. *Methods Mol Biol* **145**: 219-240.
- Amersdorfer P, Wong C, Smith T, Chen S, Deshpande S, Sheridan R *et al* (2002). Genetic and immunological comparison of anti-botulinum type A antibodies from immune and non-immune human phage libraries. *Vaccine* **20**: 1640-1648.
- Ames RS, Tornetta MA, Jones CS, Tsui P (1994). Isolation of neutralizing anti-C5a monoclonal antibodies from a filamentous phage monovalent Fab display library. *J Immunol* **153**: 910.
- Ames RS, Tornetta MA, Deen K, Jones CS, Swift AM, Ganguly S (1995). Conversion of murine Fabs isolated from a combinatorial phage display library to full length immunoglobulins. *J Immunol Methods* **184**: 177-186.
- Ancsin JB, Kisilevsky R (1999). The heparin/heparan sulfate-binding site on apo-serum amyloid A. Implications for the therapeutic intervention of amyloidosis. *J Biol Chem* **274**: 7172-7181.
- Andac Z, Sasaki T, Mann K, Brancaccio A, Deutzmann R, Timpl R (1999). Analysis of heparin, alpha-dystroglycan and sulfatide binding to the G domain of the laminin alpha1 chain by site-directed mutagenesis. *J Mol Biol* **287**: 253-264.
- Andersen OM, Reiche J, Schmidt V, Gotthardt M, Spoelgen R, Behlke J *et al* (2005). Neuronal sorting protein-related receptor sorLA/LR11 regulates processing of the amyloid precursor protein. *Proc Natl Acad Sci U S A* **102**: 13461-13466.
- Andersen OM, Willnow TE (2006). Lipoprotein receptors in Alzheimer's disease. *Trends Neurosci* **29**: 687-694.
- Anderson AA, Ushakov DS, Ferenczi MA, Mori R, Martin P, Saffell JL (2007). Morphoregulation by acetylcholinesterase in fibroblasts and astrocytes. *J Cell Physiol* **215**: 82-100.
- Anderson AA, Ushakov DS, Ferenczi MA, Mori R, Martin P, Saffell JL (2008). Morphoregulation by acetylcholinesterase in fibroblasts and astrocytes. *J Cell Physiol* **215**: 82-100.

- Anderson RB, Key B (1999). Role of acetylcholinesterase in the development of axon tracts within the embryonic vertebrate brain. *Int J Dev Neurosci* **17**: 787-793.
- Andres C, Beeri R, Friedman A, Lev-Lehman E, Henis S, Timberg R *et al* (1997). Acetylcholinesterase-transgenic mice display embryonic modulations in spinal cord choline acetyltransferase and neurexin Ibeta gene expression followed by late-onset neuromotor deterioration. *Proc Natl Acad Sci U S A* **94**: 8173-8178.
- Angus LM, Chan RY, Jasmin BJ (2001). Role of intronic E- and N-box motifs in the transcriptional induction of the acetylcholinesterase gene during myogenic differentiation. *J Biol Chem* **276**: 17603-17609.
- Annaert WG, Levesque L, Craessaerts K, Dierinck I, Snellings G, Westaway D *et al* (1999). Presenilin 1 controls gamma-secretase processing of amyloid precursor protein in pre-golgi compartments of hippocampal neurons. *J Cell Biol* **147**: 277-294.
- Antosiewicz J, Gilson MK, Lee IH, McCammon JA (1995). Acetylcholinesterase: diffusional encounter rate constants for dumbbell models of ligand. *Biophys J* **68**: 62-68.
- Antosiewicz J, Wlodek ST, McCammon JA (1996). Acetylcholinesterase: role of the enzyme's charge distribution in steering charged ligands toward the active site. *Biopolymers* **39**: 85-94.
- Appleyard ME, McDonald B (1991). Reduced adrenal gland acetylcholinesterase activity in Alzheimer's disease. *Lancet* **338**: 1085-1086.
- Arendt T, Bruckner MK, Lange M, Bigl V (1992). Changes in acetylcholinesterase and butyrylcholinesterase in Alzheimer's disease resemble embryonic development--a study of molecular forms. *Neurochem Int* **21**: 381-396.
- Armstrong RA (2009). The molecular biology of senile plaques and neurofibrillary tangles in Alzheimer's disease. *Folia Neuropathol* **47**: 289-299.
- Arnold K, Bordoli L, Kopp J, Schwede T (2006). The SWISS-MODEL workspace: a web-based environment for protein structure homology modelling. *Bioinformatics* **22**: 195-201.
- Arpagaus M, Kott M, Vatsis KP, Bartels CF, La Du BN, Lockridge O (1990). Structure of the gene for human butyrylcholinesterase. Evidence for a single copy. *Biochemistry* **29**: 124-131.
- Arredondo J, Nguyen VT, Chernyavsky AI, Bercovich D, Orr-Urtreger A, Kummer W *et al* (2002). Central role of alpha7 nicotinic receptor in differentiation of the stratified squamous epithelium. *J Cell Biol* **159**: 325-336.
- Atack JR, Perry EK, Bonham JR, Perry RH, Tomlinson BE, Blessed G *et al* (1983). Molecular forms of acetylcholinesterase in senile dementia of Alzheimer type: selective loss of the intermediate (10S) form. *Neurosci Lett* **40**: 199-204.
- Auld VJ, Fetter RD, Broadie K, Goodman CS (1995). Gliotactin, a novel transmembrane protein on peripheral glia, is required to form the blood-nerve barrier in *Drosophila*. *Cell* **81**: 757-767.
- Aumailley M, Krieg T (1996). Laminins: a family of diverse multifunctional molecules of basement membranes. *J Invest Dermatol* **106**: 209-214.
- Aumailley M, Gayraud B (1998). Structure and biological activity of the extracellular matrix. *J Mol Med (Berl)* **76**: 253-265.

- Aumailley M, Pesch M, Tunggal L, Gaill F, Fassler R (2000). Altered synthesis of laminin 1 and absence of basement membrane component deposition in (beta)1 integrin-deficient embryoid bodies. *J Cell Sci* **113 Pt 2**: 259-268.
- Aumailley M, Bruckner-Tuderman L, Carter WG, Deutzmann R, Edgar D, Ekblom P *et al* (2005). A simplified laminin nomenclature. *Matrix Biol* **24**: 326-332.
- Bandtlow CE, Zimmermann DR (2000). Proteoglycans in the developing brain: new conceptual insights for old proteins. *Physiol Rev* **80**: 1267-1290.
- Barak D, Kronman C, Ordentlich A, Ariel N, Bromberg A, Marcus D *et al* (1994). Acetylcholinesterase peripheral anionic site degeneracy conferred by amino acid arrays sharing a common core. *J Biol Chem* **269**: 6296-6305.
- Barak D, Ordentlich A, Bromberg A, Kronman C, Marcus D, Lazar A *et al* (1995). Allosteric modulation of acetylcholinesterase activity by peripheral ligands involves a conformational transition of the anionic subsite. *Biochemistry* **34**: 15444-15452.
- Barbas CF, 3rd, Kang AS, Lerner RA, Benkovic SJ (1991). Assembly of combinatorial antibody libraries on phage surfaces: the gene III site. *Proc Natl Acad Sci U S A* **88**: 7978-7982.
- Bartus RT, Dean RL, 3rd, Beer B, Lippa AS (1982). The cholinergic hypothesis of geriatric memory dysfunction. *Science* **217**: 408-414.
- Bassols A, Massague J (1988). Transforming growth factor beta regulates the expression and structure of extracellular matrix chondroitin/dermatan sulfate proteoglycans. *J Biol Chem* **263**: 3039-3045.
- Bataille S, Portalier P, Coulon P, Ternaux JP (1998). Influence of acetylcholinesterase on embryonic spinal rat motoneurons growth in culture: a quantitative morphometric study. *Eur J Neurosci* **10**: 560-572.
- Battaglia C, Mayer U, Aumailley M, Timpl R (1992). Basement-membrane heparan sulfate proteoglycan binds to laminin by its heparan sulfate chains and to nidogen by sites in the protein core. *Eur J Biochem* **208**: 359-366.
- Becker RE, Giacobini E (1988). Mechanism of cholinesterase inhibition in senile dementia of the Alzheimer's type: Clinical pharmacological and therapeutic aspects. *Drug Dev Res* **12**.
- Becker RE, Moriearty P, Unni L (1991). The second generation of cholinesterase inhibitors: clinical and pharmacological effects. In: Becker R, Giacobini E (eds). *Cholinergic basis for Alzheimer therapy*. . Birkhauser: Boston. pp 263-296.
- Beeri R, Andres C, Lev-Lehman E, Timberg R, Huberman T, Shani M *et al* (1995). Transgenic expression of human acetylcholinesterase induces progressive cognitive deterioration in mice. *Curr Biol* **5**: 1063-1071.
- Beffert U, Stolt PC, Herz J (2004). Functions of lipoprotein receptors in neurons. *J Lipid Res* **45**: 403-409.
- Behra M, Cousin X, Bertrand C, Vonesch JL, Biellmann D, Chatonnet A *et al* (2002). Acetylcholinesterase is required for neuronal and muscular development in the zebrafish embryo. *Nat Neurosci* **5**: 111-118.
- Belbeoc'h S, Falasca C, Leroy J, Ayon A, Massoulie J, Bon S (2004). Elements of the C-terminal peptide of acetylcholinesterase that determine amphiphilicity, homomeric and heteromeric associations, secretion and degradation. *Eur J Biochem* **271**: 1476-1487.
- Ben Aziz-Aloya R, Seidman S, Timberg R, Sternfeld M, Zakut H, Soreq H (1993). Expression of a human acetylcholinesterase promoter-reporter construct in developing neuromuscular junctions of *Xenopus* embryos. *Proc Natl Acad Sci U S A* **90**: 2471-2475.

- Benjamins JA, McKhann GM (1981). Development, regeneration, and aging of the brain. In: Siegel GJ, Albers RW, Agranoff BW, Katzman R (eds). *Basic Neurochemistry*. Little-Brown: Boston, MA. pp 445-469.
- Benke GM, Murphy SD (1975). The influence of age on the toxicity and metabolism of methyl parathion and parathion in male and female rats. *Toxicol Appl Pharmacol* **31**: 254-269.
- Berman HA, Nowak MW (1992). In: Shafferman A, Velan B (eds). *Multidisciplinary Approaches to Cholinesterase Functions* Plenum Publishing Corp: New York. pp 149-156.
- Bernardi CC, Ribeiro Ede S, Cavalli IJ, Chautard-Freire-Maia EA, Souza RL (2010). Amplification and deletion of the AChE and BCHE cholinesterase genes in sporadic breast cancer. *Cancer Genet Cytogenet* **197**: 158-165.
- Bernfield M, Sanderson RD (1990). Syndecan, a developmentally regulated cell surface proteoglycan that binds extracellular matrix and growth factors. *Philos Trans R Soc Lond B Biol Sci* **327**: 171-186.
- Bernfield M, Gotte M, Park PW, Reizes O, Fitzgerald ML, Lincecum J *et al* (1999). Functions of cell surface heparan sulfate proteoglycans. *Annu Rev Biochem* **68**: 729-777.
- Betz W, Sakmann B (1973). Effects of proteolytic enzymes on function and structure of frog neuromuscular junctions. *J Physiol* **230**: 673-688.
- Bhakdi S, Roth M, Hugo F (1989). Biotinylation: a simple method for labelling complement component C8 with preservation of functional activity. *J Immunol Methods* **121**: 61-66.
- Biagioni S, Tata AM, De Jaco A, Augusti-Tocco G (2000). Acetylcholine synthesis and neuron differentiation. *Int J Dev Biol* **44**: 689-697.
- Biederer TSM (2009). Signalling by synaptogenic molecules. *Biophysics* **18**: 261-269.
- Bigbee JW, DeVries GH (1987). Inhibition of acetylcholinesterase retards neurite outgrowth in vitro. *J Neurochem* **48**: 558.
- Bigbee JW, Sharma KV, Chan EL, Bogler O (2000). Evidence for the direct role of acetylcholinesterase in neurite outgrowth in primary dorsal root ganglion neurons. *Brain Res* **861**: 354-362.
- Bird RE, Hardman KD, Jacobson JW, Johnson S, Kaufman BM, Lee SM *et al* (1988). Single-chain antigen-binding proteins. *Science* **242**: 423-426.
- Blake C, Serpell L (1996). Synchrotron X-ray studies suggest that the core of the transthyretin amyloid fibril is a continuous beta-sheet helix. *Structure* **4**: 989-998.
- Bon S, Toutant JP, Meflah K, Massoulie J (1988a). Amphiphilic and nonamphiphilic forms of Torpedo cholinesterases: I. Solubility and aggregation properties. *J Neurochem* **51**: 776-785.
- Bon S, Toutant JP, Meflah K, Massoulie J (1988b). Amphiphilic and nonamphiphilic forms of Torpedo cholinesterases: II. Electrophoretic variants and phosphatidylinositol phospholipase C-sensitive and -insensitive forms. *J Neurochem* **51**: 786-794.
- Bon S, Rosenberry TL, Massoulie J (1991). Amphiphilic, glycoposphatidylinositol-specific phospholipase C (PI-PLC)-insensitive monomers and dimers of acetylcholinesterase. *Cell Mol Neurobiol* **11**: 157-172.
- Bon S, Coussen F, Massoulie J (1997). Quaternary associations of acetylcholinesterase. II. The polyproline attachment domain of the collagen tail. *J Biol Chem* **272**: 3016-3021.

Bon S, Dufourcq J, Leroy J, Cornut I, Massoulie J (2004). The C-terminal t peptide of acetylcholinesterase forms an alpha helix that supports homomeric and heteromeric interactions. *Eur J Biochem* **271**: 33-47.

Bondi MW, Salmon DP, Butlers NM (1994). Neuropsychological features of memory disorders in Alzheimer's disease. In: Terry AD, Katzman R, Bick KL (eds). *Alzheimer's Disease*. Raven Press: New York. pp 41-63.

Boopathy R, Layer PG (2004). Aryl acylamidase activity on acetylcholinesterase is high during early chicken brain development. *Protein J* **23**: 325-333.

Borth W (1992). Alpha 2-macroglobulin, a multifunctional binding protein with targeting characteristics. *FASEB J* **6**: 3345-3353.

Bossy-Wetzel E, Schwarzenbacher R, Lipton SA (2004). Molecular pathways to neurodegeneration. *Nat Med* **10 Suppl**: S2-9.

Botti SA, Felder CE, Sussman JL, Silman I (1998). Electrotactins: a class of adhesion proteins with conserved electrostatic and structural motifs. *Protein Eng* **11**: 415-420.

Boudreau N, Sympson CJ, Werb Z, Bissell MJ (1995). Suppression of ICE and apoptosis in mammary epithelial cells by extracellular matrix. *Science* **267**: 891-893.

Bourne Y, Taylor P, Marchot P (1995). Acetylcholinesterase inhibition by fasciculin: crystal structure of the complex. *Cell* **83**: 503-512.

Bourne Y, Taylor P, Bougis PE, Marchot P (1999). Crystal structure of mouse acetylcholinesterase. A peripheral site-occluding loop in a tetrameric assembly. *J Biol Chem* **274**: 2963-2970.

Bourne Y, Taylor P, Radic Z, Marchot P (2003). Structural insights into ligand interactions at the acetylcholinesterase peripheral anionic site. *EMBO J* **22**: 1-12.

Bradbury AR, Marks JD (2004). Antibodies from phage antibody libraries. *J Immunol Methods* **290**: 29-49.

Brandan E, Inestrosa NC (1984). Binding of the asymmetric forms of acetylcholinesterase to heparin. *Biochem J* **221**: 415-422.

Brandan E, Inestrosa NC (1993). Extracellular matrix components and amyloid in neuritic plaques of Alzheimer's disease. *Gen Pharmacol* **24**: 1063-1068.

Branduardi D, Gervasio FL, Cavalli A, Recanatini M, Parrinello M (2005). The role of the peripheral anionic site and cation-pi interactions in the ligand penetration of the human AChE gorge. *J Am Chem Soc* **127**: 9147-9155.

Brann MR, Ellis J, Jorgensen H, Hill-Eubanks D, Jones SV (1993). Muscarinic acetylcholine receptor subtypes: localization and structure/function. *Prog Brain Res* **98**: 121-127.

Breen KC, Bruce M, Anderton BH (1991). Beta amyloid precursor protein mediates neuronal cell-cell and cell-surface adhesion. *J Neurosci Res* **28**: 90-100.

Brodeur J, Dubois KP (1963). Comparison of Acute Toxicity of Anticholinesterase Insecticides to Weanling and Adult Male Rats. *Proc Soc Exp Biol Med* **114**: 509-511.

Bronfman FC, Garrido J, Alvarez A, Morgan C, Inestrosa NC (1996). Laminin inhibits amyloid-beta-peptide fibrillation. *Neurosci Lett* **218**: 201-203.

Brown JC, Sasaki T, Gohring W, Yamada Y, Timpl R (1997). The C-terminal domain V of perlecan promotes beta1 integrin-mediated cell adhesion, binds heparin, nidogen and fibulin-2 and can be modified by glycosaminoglycans. *Eur J Biochem* **250**: 39-46.

Brown LM, Dosemeci M, Blair A, Burmeister L (1991). Comparability of data obtained from farmers and surrogate respondents on use of agricultural pesticides. *Am J Epidemiol* **134**: 348-355.

Bu G, Cam J, Zerbinatti C (2006). LRP in amyloid-beta production and metabolism. *Ann N Y Acad Sci* **1086**: 35-53.

Burgess K (2001). Solid-phase syntheses of beta-turn analogues to mimic or disrupt protein-protein interactions. *Acc Chem Res* **34**: 826-835.

Burton MD, Nouri K, Baichoo S, Samuels-Toyloy N, Kazemi H (1994). Ventilatory output and acetylcholine: perturbations in release and muscarinic receptor activation. *J Appl Physiol* **77**: 2275-2284.

Butcher LL (1978). Recent advances in histochemical techniques for the study of central cholinergic mechanisms. In: Jenden DJ (ed). *Cholinergic Mechanisms and Psychopharmacology*. Plenum Press: New York. pp 93-124.

Bytyqi AH, Lockridge O, Duysen E, Wang Y, Wolfrum U, Layer PG (2004). Impaired formation of the inner retina in an AChE knockout mouse results in degeneration of all photoreceptors. *Eur J Neurosci* **20**: 2953-2962.

Cadigan KM, Nusse R (1997). Wnt signaling: a common theme in animal development. *Genes Dev* **11**: 3286-3305.

Cai XD, Golde TE, Younkin SG (1993). Release of excess amyloid beta protein from a mutant amyloid beta protein precursor. *Science* **259**: 514-516.

Calne DB, Eisen A, McGeer E, Spencer P (1986). Alzheimer's disease, Parkinson's disease, and motoneuron disease: abiotrophic interaction between ageing and environment? *Lancet* **2**: 1067-1070.

Camps P, Formosa X, Galdeano C, Gomez T, Munoz-Torrero D, Scarpellini M *et al* (2008). Novel donepezil-based inhibitors of acetyl- and butyrylcholinesterase and acetylcholinesterase-induced beta-amyloid aggregation. *J Med Chem* **51**: 3588-3598.

Caricasole A, Copani A, Caruso A, Caraci F, Iacovelli L, Sortino MA *et al* (2003). The Wnt pathway, cell-cycle activation and beta-amyloid: novel therapeutic strategies in Alzheimer's disease? *Trends Pharmacol Sci* **24**: 233-238.

Caricasole A, Copani A, Caraci F, Aronica E, Rozemuller AJ, Caruso A *et al* (2004). Induction of Dickkopf-1, a negative modulator of the Wnt pathway, is associated with neuronal degeneration in Alzheimer's brain. *J Neurosci* **24**: 6021-6027.

Cartaud A, Strohlic L, Guerra M, Blanchard B, Lambergeon M, Krejci E *et al* (2004). MuSK is required for anchoring acetylcholinesterase at the neuromuscular junction. *J Cell Biol* **165**: 505-515.

Carvalho FA, Graca LM, Martins-Silva J, Saldanha C (2005). Biochemical characterization of human umbilical vein endothelial cell membrane bound acetylcholinesterase. *FEBS J* **272**: 5584-5594.

Castillo GM, Ngo C, Cummings J, Wight TN, Snow AD (1997). Perlecan binds to the beta-amyloid proteins (A beta) of Alzheimer's disease, accelerates A beta fibril formation, and maintains A beta fibril stability. *J Neurochem* **69**: 2452-2465.

- Castillo GM, Lukito W, Wight TN, Snow AD (1999). The sulfate moieties of glycosaminoglycans are critical for the enhancement of beta-amyloid protein fibril formation. *J Neurochem* **72**: 1681-1687.
- Castillo GM, Lukito W, Peskind E, Raskind M, Kirschner DA, Yee AG *et al* (2000). Laminin inhibition of beta-amyloid protein (Abeta) fibrillogenesis and identification of an Abeta binding site localized to the globular domain repeats on the laminin a chain. *J Neurosci Res* **62**: 451-462.
- Castro A, Martinez A (2006). Targeting beta-amyloid pathogenesis through acetylcholinesterase inhibitors. *Curr Pharm Des* **12**: 4377-4387.
- Caughey B, Lansbury PT (2003). Protofibrils, pores, fibrils, and neurodegeneration: separating the responsible protein aggregates from the innocent bystanders. *Annu Rev Neurosci* **26**: 267-298.
- Chalmers K, Wilcock GK, Love S (2003). APOE epsilon 4 influences the pathological phenotype of Alzheimer's disease by favouring cerebrovascular over parenchymal accumulation of A beta protein. *Neuropathol Appl Neurobiol* **29**: 231-238.
- Chan RY, Adatia FA, Krupa AM, Jasmin BJ (1998). Increased expression of acetylcholinesterase T and R transcripts during hematopoietic differentiation is accompanied by parallel elevations in the levels of their respective molecular forms. *J Biol Chem* **273**: 9727-9733.
- Chan RY, Boudreau-Lariviere C, Angus LM, Mankal FA, Jasmin BJ (1999). An intronic enhancer containing an N-box motif is required for synapse- and tissue-specific expression of the acetylcholinesterase gene in skeletal muscle fibers. *Proc Natl Acad Sci U S A* **96**: 4627-4632.
- Changeux JP (1966). Responses of acetylcholinesterase from *Torpedo marmorata* to salts and curarizing drugs. *Mol Pharmacol* **2**: 369-392.
- Changeux JP, Edelstein SJ (2005). Nicotinic Acetylcholine Receptors: From Molecular Biology to Cognition. Editions Odile Jacob/Johns Hopkins University Press. pp 1-6.
- Chatonnet A, Lockridge O (1989). Comparison of butyrylcholinesterase and acetylcholinesterase. *Biochem J* **260**: 625-634.
- Checler F, Vincent J-P (1989). Peptidase activities associated with acetylcholinesterase are due to contaminating enzymes. *J Neurochem* **53**: 924-928.
- Chen MS, Almeida EA, Huovila AP, Takahashi Y, Shaw LM, Mercurio AM *et al* (1999). Evidence that distinct states of the integrin alpha6beta1 interact with laminin and an ADAM. *J Cell Biol* **144**: 549-561.
- Chernyavsky AI, Nguyen VT, Arredondo J, Ndoye A, Zia S, Wess J *et al* (2003). The M4 muscarinic receptor-selective effects on keratinocyte crawling locomotion. *Life Sci* **72**: 2069-2073.
- Chernyavsky AI, Arredondo J, Marubio LM, Grando SA (2004). Differential regulation of keratinocyte chemokinesis and chemotaxis through distinct nicotinic receptor subtypes. *J Cell Sci* **117**: 5665-5679.
- Chernyavsky AI, Arredondo J, Karlsson E, Wessler I, Grando SA (2005). The Ras/Raf-1/MEK1/ERK signaling pathway coupled to integrin expression mediates cholinergic regulation of keratinocyte directional migration. *J Biol Chem* **280**: 39220-39228.
- Choi RC, Siow NL, Cheng AW, Ling KK, Tung EK, Simon J *et al* (2003). ATP acts via P2Y1 receptors to stimulate acetylcholinesterase and acetylcholine receptor expression: transduction and transcription control. *J Neurosci* **23**: 4445-4456.
- Chu FK, Trimble RB, Maley F (1978). The effect of carbohydrate depletion on the properties of yeast external invertase. *J Biol Chem* **253**: 8691-8693.

- Chubb IW, Smith t (1975). Release of acetylcholinesterase into the perfusate from the ox adrenal gland. *Proc R Soc Lond B Biol Sci* **191**: 263-269.
- Chubb IW, Goodman S, Smith AD (1976). Is acetylcholinesterase secreted from central neurons into the cerebral fluid? *Neuroscience* **1**: 57-62.
- Chubykin AA, Liu X, Comoletti D, Tsigelny I, Taylor P, Sudhof TC (2005). Dissection of synapse induction by neuroligins: effect of a neuroligin mutation associated with autism. *J Biol Chem* **280**: 22365-22374.
- Citron M, Oltersdorf T, Haass C, McConlogue L, Hung AY, Seubert P *et al* (1992). Mutation of the beta-amyloid precursor protein in familial Alzheimer's disease increases beta-protein production. *Nature* **360**: 672-674.
- Clos MV, Pera M, Ratia M, Roman S, Camps P, Munoz-Torrero D *et al* (2006). Effect of acetylcholinesterase inhibitors on AChE-induced PrP106-126 aggregation. *J Mol Neurosci* **30**: 89-90.
- Coates PM, Simpson NE (1972). Genetic variation in human erythrocyte acetylcholinesterase. *Science* **175**: 1466-1477.
- Cochran AG, Tong RT, Starovasnik MA, Park EJ, McDowell RS, Theaker JE *et al* (2001). A minimal peptide scaffold for beta-turn display: optimizing a strand position in disulfide-cyclized beta-hairpins. *J Am Chem Soc* **123**: 625-632.
- Cohen O, Reichenberg A, Perry C, Ginzberg D, Pollmacher T, Soreq H *et al* (2003). Endotoxin-induced changes in human working and declarative memory associate with cleavage of plasma "readthrough" acetylcholinesterase. *J Mol Neurosci* **21**: 199-212.
- Coleman BA, Taylor P (1996). Regulation of acetylcholinesterase expression during neuronal differentiation. *J Biol Chem* **271**: 4410-4416.
- Colletier JP, Fournier D, Greenblatt HM, Stojan J, Sussman JL, Zaccai G *et al* (2006). Structural insights into substrate traffic and inhibition in acetylcholinesterase. *EMBO J* **25**: 2746-2756.
- Colognato H, Yurchenco PD (2000). Form and function: the laminin family of heterotrimers. *Dev Dyn* **218**: 213-234.
- Colombres M, Henriquez JP, Reig GF, Scheu J, Calderon R, Alvarez A *et al* (2008). Heparin activates Wnt signaling for neuronal morphogenesis. *J Cell Physiol* **216**: 805-815.
- Comoletti D, Flynn R, Jennings LL, Chubykin A, Matsumura T, Hasegawa H *et al* (2003). Characterization of the interaction of a recombinant soluble neuroligin-1 with neurexin-1beta. *J Biol Chem* **278**: 50497-50505.
- Comoletti D, Miller MT, Jeffries CM, Wilson J, Demeler B, Taylor P *et al* (2010). The macromolecular architecture of extracellular domain of alphaNRXN1: domain organization, flexibility, and insights into trans-synaptic disposition. *Structure* **18**: 1044-1053.
- Corder EH, Saunders AM, Strittmatter WJ, Schmechel DE, Gaskell PC, Small GW *et al* (1993). Gene dose of apolipoprotein E type 4 allele and the risk of Alzheimer's disease in late onset families. *Science* **261**: 921-923.
- Corey S, Krapivinsky G, Krapivinsky L, Clapham DE (1998). Number and stoichiometry of subunits in the native atrial G-protein-gated K⁺ channel, IKACH. *J Biol Chem* **273**: 5271-5278.

- Corrado MUD, Politi H, Trielli F, Angelini C, Falugi C (1999). Evidence for the presence of a mammalian-like cholinesterase in paramecium primaurelia (Protista, Ciliophora) developmental cycle. *J Exp Zool* **283**: 102-105.
- Cottingham MG, Voskuil JL, Vaux DJ (2003). The intact human acetylcholinesterase C-terminal oligomerization domain is alpha-helical in situ and in isolation, but a shorter fragment forms beta-sheet-rich amyloid fibrils and protofibrillar oligomers. *Biochemistry* **42**: 10863-10873.
- Couchman JR, Woods A (1993). Structure and biology of pericellular proteoglycans. In: Roberts DD, Mecham RR (eds). *Cell Surface and Extracellular Glycoconjugates*. Academic Press: San Diego. pp 33–82.
- Cousin X, Creminon C, Grassi J, Meflah K, Cornu G, Saliou B *et al* (1996). Acetylcholinesterase from Bungarus venom: a monomeric species. *FEBS Lett* **387**: 196-200.
- Cousin X, Bon S, Massoulie J, Bon C (1998). Identification of a novel type of alternatively spliced exon from the acetylcholinesterase gene of Bungarus fasciatus. Molecular forms of acetylcholinesterase in the snake liver and muscle. *J Biol Chem* **273**: 9812-9820.
- Cousin X, Strahle U, Chatonnet A (2005). Are there non-catalytic functions of acetylcholinesterases? Lessons from mutant animal models. *Bioessays* **27**: 189-200.
- Crossin KL, Krushel LA (2000). Cellular signaling by neural cell adhesion molecules of the immunoglobulin superfamily. *Dev Dyn* **218**: 260-279.
- Cuello AC, Sofroniew MV (1985). The anatomy of the CNS cholinergic neurons. In: Bousfield D (ed). *Neurotransmitters in Action*. Elsevier: Amsterdam. pp 309-318.
- Cygler M, Schrag J, Sussman JL, Harel M, Silman I, Gentry MK *et al* (1993). Relationship between sequence conservation and three-dimensional structure in a large family of esterases, lipases, and related proteins. *Protein Sci* **2**: 366-382.
- Dahlgren KN, Manelli AM, Stine WB, Jr., Baker LK, Krafft GA, LaDu MJ (2002). Oligomeric and fibrillar species of amyloid-beta peptides differentially affect neuronal viability. *J Biol Chem* **277**: 32046-32053.
- Dale HH (1914). The action of certain esters of choline and their relation to muscarine. *J Pharmacol Exp Ther* **6**: 147-190.
- Darboux I, Barthalay Y, Piovant M, Hipeau-Jacquotte R (1996). The structure-function relationships in Drosophila neurotactin show that cholinesterasic domains may have adhesive properties. *EMBO J* **15**: 4835-4843.
- Darvesh S, MacDonald SE, Losier AM, Martin E, Hopkins DA, Armour JA (1998). Cholinesterases in cardiac ganglia and modulation of canine intrinsic cardiac neuronal activity. *J Auton Nerv Syst* **71**: 75-84.
- Darvesh S, Hopkins DA, Geula C (2003). Neurobiology of butyrylcholinesterase. *Nat Rev Neurosci* **4**: 131-138.
- Datta G, Chaddha M, Garber DW, Chung BH, Tytler EM, Dashti N *et al* (2000). The receptor binding domain of apolipoprotein E, linked to a model class A amphipathic helix, enhances internalization and degradation of LDL by fibroblasts. *Biochemistry* **39**: 213-220.
- David G, Lories V, Decock B, Marynen P, Cassiman JJ, Van den Berghe H (1990). Molecular cloning of a phosphatidylinositol-anchored membrane heparan sulfate proteoglycan from human lung fibroblasts. *J Cell Biol* **111**: 3165-3176.

- Day T, Greenfield SA (2002). A non-cholinergic, trophic action of acetylcholinesterase on hippocampal neurones in vitro: molecular mechanisms. *Neuroscience* **111**: 649-656.
- Day T, Greenfield SA (2004). Bioactivity of a peptide derived from acetylcholinesterase in hippocampal organotypic cultures. *Exp Brain Res* **155**: 500-508.
- De Ferrari GV, Inestrosa NC (2000). Wnt signaling function in Alzheimer's disease. *Brain Res Rev* **33**: 1-12.
- De Ferrari GV, Mallender WD, Inestrosa NC, Rosenberry TL (2001a). Thioflavin T Is a fluorescent probe of the acetylcholinesterase peripheral site that reveals conformational interactions between the peripheral and acylation sites. *J Biol Chem* **276**: 23282-23287.
- De Ferrari GV, Canales MA, Shin I, Weiner LM, Silman I, Inestrosa NC (2001b). A structural motif of acetylcholinesterase that promotes amyloid β -peptide fibril formation. *Biochemistry* **40**.
- De Ferrari GV, Chacon MA, Barria MI, Garrido JL, Godoy JA, Olivares G *et al* (2003). Activation of Wnt signaling rescues neurodegeneration and behavioral impairments induced by β -amyloid fibrils. *Mol Psychiatry* **8**: 195-208.
- De Ferrari GV, Papassotiropoulos A, Biechele T, Wavrant De-Vrieze F, Avila ME, Major MB *et al* (2007). Common genetic variation within the low-density lipoprotein receptor-related protein 6 and late-onset Alzheimer's disease. *Proc Natl Acad Sci USA* **104**: 9434-9439.
- de Haard HJ, van Neer N, Reurs A, Hufton SE, Roovers RC, Henderikx P *et al* (1999). A large non-immunized human Fab fragment phage library that permits rapid isolation and kinetic analysis of high affinity antibodies. *J Biol Chem* **274**: 18218-18230.
- De Jaco A, Augusti-Tocco G, Biagioni S (2002). Alternative acetylcholinesterase molecular forms exhibit similar ability to induce neurite outgrowth. *J Neurosci Res* **70**: 756765.
- de Kruij J, Boel E, Logtenberg T (1995). Selection and application of human single chain Fv antibody fragments from a semi-synthetic phage antibody display library with designed CDR3 regions. *J Mol Biol* **248**: 97-105.
- de la Escalera S, Bockamp EO, Moya F, Piovant M, Jimenez F (1990). Characterization and gene cloning of neurotactin, a Drosophila transmembrane protein related to cholinesterases. *EMBO J* **9**: 3593-3601.
- Dellon ES, Dellon AL (1993). The first nerve graft, Vulpian, and the nineteenth century neural regeneration controversy. *J Hand Surg Am* **18**: 369-372.
- Demaurex N, Distelhorst C (2003). Cell biology. Apoptosis--the calcium connection. *Science* **300**: 65-67.
- Denzer AJ, Brandenberger R, Gesemann M, Chiquet M, Ruegg MA (1997). Agrin binds to the nerve-muscle basal lamina via laminin. *J Cell Biol* **137**: 671-683.
- Denzer AJ, Schulthess T, Fauser C, Schumacher B, Kammerer RA, Engel J *et al* (1998). Electron microscopic structure of agrin and mapping of its binding site in laminin-1. *EMBO J* **17**: 335-343.
- Desban N, Duband JL (1997). Avian neural crest cell migration on laminin: interaction of the $\alpha 1 \beta 1$ integrin with distinct laminin-1 domains mediates different adhesive responses. *J Cell Sci* **110** (Pt 21): 2729-2744.

Deschenes-Furry J, Belanger G, Perrone-Bizzozero N, Jasmin BJ (2003). Post-transcriptional regulation of acetylcholinesterase mRNAs in nerve growth factor-treated PC12 cells by the RNA-binding protein HuD. *J Biol Chem* **278**: 5710-5717.

Destexhe A, Sejnowski TJ (1995). G protein activation kinetics and spillover of gamma-aminobutyric acid may account for differences between inhibitory responses in the hippocampus and thalamus. *Proc Natl Acad Sci U S A* **92**: 9515-9519.

Deutsch VR, Pick M, Perry C, Grisaru D, Hemo Y, Golan-Hadari D *et al* (2002). The stress-associated acetylcholinesterase variant AChE-R is expressed in human CD34(+) hematopoietic progenitors and its C-terminal peptide ARP promotes their proliferation. *Exp Hematol* **30**: 1153-1161.

Dinamarca MC, Weinstein D, Monasterio O, Inestrosa NC (2011). The Synaptic Protein Neuroligin-1 Interacts with the Amyloid beta-Peptide. Is There a Role in Alzheimer's Disease? *Biochemistry* **50**: 8127-8137.

Dodson G, Wlodawer A (1998). Catalytic triads and their relatives. *Trends Biochem Sci* **23**: 347-352.

Dodson SE, Andersen OM, Karmali V, Fritz JJ, Cheng D, Peng J *et al* (2008). Loss of LR11/SORLA enhances early pathology in a mouse model of amyloidosis: evidence for a proximal role in Alzheimer's disease. *J Neurosci* **28**: 12877-12886.

Dransfield I, Stocks SC, Haslett C (1995). Regulation of cell adhesion molecule expression and function associated with neutrophil apoptosis. *Blood* **85**: 3264-3273.

Drews U (1975). Cholinesterase in embryonic development. *Prog Histochem Cytochem* **7**: 1-52.

Dube S, Fisher JW, Powell JS (1988). Glycosylation at specific sites of erythropoietin is essential for biosynthesis, secretion, and biological function. *J Biol Chem* **263**: 17516-17521.

Dubovy P, Haninec P (1990). Non-specific cholinesterase activity of the developing peripheral nerves and its possible function in cells in intimate contact with growing axons of chick embryo. *Int J Dev Neurosci* **8**: 589-602.

Dunnett SB, Everitt BJ, Robbins TW (1991). The basal forebrain-cortical cholinergic system: interpreting the functional consequences of excitotoxic lesions. *Trends Neurosci* **14**: 494-501.

Dunnett SB, Fibiger HC (1993). Role of forebrain cholinergic systems in learning and memory: relevance to the cognitive deficits of aging and Alzheimer's dementia. *Prog Brain Res* **98**: 413-420.

Dvir H, Jiang HL, Wong DM, Harel M, Chetrit M, He XC *et al* (2002). X-ray structures of Torpedo californica acetylcholinesterase complexed with (+)-huperzine A and (-)-huperzine B: structural evidence for an active site rearrangement. *Biochemistry* **41**: 10810-10818.

Eagleson GW, Ubink R, Jenks BG, Roubos EW (1998). Forebrain differentiation and axonogenesis in amphibians: I. Differentiation of the suprachiasmatic nucleus in relation to background adaptation behavior. *Brain Behav Evol* **52**: 23-36.

Eastman J, Wilson EJ, Cervenansky C, Rosenberry TL (1995). Fasciculin 2 binds to the peripheral site on acetylcholinesterase and inhibits substrate hydrolysis by slowing a step involving proton transfer during enzyme acylation. *J Biol Chem* **270**: 19694-19701.

Eckenstein F, Sofroniew MV (1983). Identification of central cholinergic neurons containing both choline acetyltransferase and acetylcholinesterase and of central neurons containing only acetylcholinesterase. *J Neurosci* **3**: 2286-2291.

- Ecobichon DJ (1991). Toxic effects of pesticides. In: Amdur MO, Doull J, Klaassen CD (eds). *Cassarett and Doull's Toxicology*, 4th edn. Pergamon: New York. pp 565-622.
- Eggers C, Herholz K, Kalbe E, Heiss WD (2006). Cortical acetylcholine esterase activity and ApoE4-genotype in Alzheimer disease. *Neurosci Lett* **408**: 46-50.
- Eglen RM (2006). Muscarinic receptor subtypes in neuronal and non-neuronal cholinergic function. *Auton Autacoid Pharmacol* **26**: 219-233.
- Ehrlich G, Viegas-Pequignot E, Ginzberg D, Sindel L, Soreq H, Zakut H (1992). Mapping the human acetylcholinesterase gene to chromosome 7q22 by fluorescent in situ hybridization coupled with selective PCR amplification from a somatic hybrid cell panel and chromosome-sorted DNA libraries. *Genomics* **13**: 1192-1197.
- Ekstrom TJ, Klump WM, Getman D, Karin M, Taylor P (1993). Promoter elements and transcriptional regulation of the acetylcholinesterase gene. *DNA Cell Biol* **12**: 63-72.
- Elliott TR (1904). On the action of adrenaline. *J Physiol* **31**: xx-xxi.
- Endo T, Tamiya N (1987). Current view on the structure-function relationship of postsynaptic neurotoxins from snake venoms. *Pharmacol Ther* **34**: 403-451.
- Engel PA, Gelber J (1992). Does computed tomographic brain imaging have a place in the diagnosis of dementia? *Arch Intern Med* **152**: 1437-1440.
- Erickson JD, Varoqui H (2000). Molecular analysis of vesicular amine transporter function and targeting to secretory organelles. *FASEB J* **14**: 2450-2458.
- Esler WP, Wolfe MS (2001). A portrait of Alzheimer secretases--new features and familiar faces. *Science* **293**: 1449-1454.
- Ethell IM, Hagihara K, Miura Y, Irie F, Yamaguchi Y (2000). Synbindin, A novel syndecan-2-binding protein in neuronal dendritic spines. *J Cell Biol* **151**: 53-68.
- Evin G, Beyreuther K, Masters CL (1994). Alzheimer's disease amyloid precursor protein (A β PP): proteolytic processing, secretases and β A4 amyloid production. *Amyloid* **1**: 263-280.
- Fagan AM, Holtzman DM (2000). Astrocyte lipoproteins, effects of apoE on neuronal function, and role of apoE in amyloid-beta deposition in vivo. *Microsc Res Tech* **50**: 297-304.
- Fan YY, Yu TS, Wang T, Liu WW, Zhao R, Zhang ST *et al* (2011). Nicotinic acetylcholine receptor alpha7 subunit is time-dependently expressed in distinct cell types during skin wound healing in mice. *Histochem Cell Biol* **135**: 375-387.
- Farach-Carson MC, Carson DD (2007). Perlecan--a multifunctional extracellular proteoglycan scaffold. *Glycobiology* **17**: 897-905.
- Felder CE, Botti SA, Lifson S, Silman I, Sussman JL (1997). External and internal electrostatic potentials of cholinesterase models. *J Mol Graph Model* **15**: 318-327, 335-317.
- Felder CE, Harel M, Silman I, Sussman JL (2002). Structure of a complex of the potent and specific inhibitor BW284C51 with *Torpedo californica* acetylcholinesterase. *Acta Crystallogr D Biol Crystallogr* **58**: 1765-1771.

- Feng G, Krejci E, Molgo J, Cunningham JM, Massoulie J, Sanes JR (1999). Genetic analysis of collagen Q: roles in acetylcholinesterase and butyrylcholinesterase assembly and in synaptic structure and function. *J Cell Biol* **144**: 1349-1360.
- Fernandez-Vidal A, Ysebaert L, Didier C, Betous R, De Toni F, Prade-Houdellier N *et al* (2006). Cell adhesion regulates CDC25A expression and proliferation in acute myeloid leukemia. *Cancer Res* **66**: 7128-7135.
- Fersht AR (1985). *Enzyme Structure and Mechanism*, 2nd edn. Freeman: New York. pp 150-154.
- Fersht AR (1999). Folding pathways and energy landscapes. In: Julet MR, Hadler GL (eds). *Structure and mechanism in protein science: A guide to enzyme catalysis and protein folding*. W H Freeman and Co.: New York. pp 573-614.
- Fertuck HC, Salpeter MM (1976). Quantitation of junctional and extrajunctional acetylcholine receptors by electron microscope autoradiography after ¹²⁵I-alpha-bungarotoxin binding at mouse neuromuscular junctions. *J Cell Biol* **69**: 144-158.
- Fetrow JS (1995). Omega loops: nonregular secondary structures significant in protein function and stability. *FASEB J* **9**: 708-717.
- Fibiger HC (1982). The organization and some projections of cholinergic neurons of the mammalian forebrain. *Brain Res* **257**: 327-388.
- Fibiger HC (1991). Cholinergic mechanisms in learning, memory and dementia: a review of recent evidence. *Trends Neurosci* **14**: 220-223.
- Fink AL (1998). Protein aggregation: folding aggregates, inclusion bodies and amyloid. *Fold Des* **3**: R9-23.
- Fishman EB, Siek GC, MacCallum RD, Bird ED, Volicer L, Marquis JK (1986). Distribution of the molecular forms of acetylcholinesterase in human brain: alterations in dementia of the Alzheimer type. *Ann Neurol* **19**: 246-252.
- Fitch JM, Lisenmayer TR (1994). Interstitial basement membrane components in development. In: Yurchenco PD, Birk DE, Mecham RP (eds). *Extracellular Matrix Assembly and Structure*. Academic Press: San Diego. pp 441-462.
- Flaskos J, Nikolaidis E, Harris W, Sachana M, Hargreaves AJ (2011). Effects of sub-lethal neurite outgrowth inhibitory concentrations of chlorpyrifos oxon on cytoskeletal proteins and acetylcholinesterase in differentiating N2a cells. *Toxicol Appl Pharmacol*.
- Floegel R, Mutter M (1992). Molecular dynamics conformational search of six cyclic peptides used in the template assembled synthetic protein approach for protein de novo design. *Biopolymers* **32**: 1283-1310.
- Fodero LR, Saez-Valero J, McLean CA, Martins RN, Beyreuther K, Masters CL *et al* (2002). Altered glycosylation of acetylcholinesterase in APP (SW) Tg2576 transgenic mice occurs prior to amyloid plaque deposition. *J Neurochem* **81**: 441-448.
- Forrest DL, Lee CL (2002). Constitutional rearrangements of 7q22 in hematologic malignancies. a new case report. *Cancer Genet Cytogenet* **139**: 75-77.
- Foutz AS, Boudinot E, Denavit-Saubie M (1987). Central respiratory depression induced by acetylcholinesterase inhibition: involvement of anaesthesia. *Eur J Pharmacol* **142**: 207-213.
- Francis PT, Palmer AM, Snape M, Wilcock GK (1999). The cholinergic hypothesis of Alzheimer's disease: a review of progress. *J Neurol Neurosurg Psychiatry* **66**: 137-147.

- Fredriksson R, Lagerstrom MC, Lundin LG, Schioth HB (2003). The G-protein-coupled receptors in the human genome form five main families. Phylogenetic analysis, paralogon groups, and fingerprints. *Mol Pharmacol* **63**: 1256-1272.
- Friede RL (1967). A comparative histochemical mapping of the distribution of butyryl cholinesterase in the brains of four species of mammals, including man. *Acta Anat (Basel)* **66**: 161-177.
- Frolow F, Harel M, Sussman JL, Mevarech M, Shoham M (1996). Insights into protein adaptation to a saturated salt environment from the crystal structure of a halophilic 2Fe-2S ferredoxin. *Nat Struct Biol* **3**: 452-458.
- Fuki IV, Kuhn KM, Lomazov IR, Rothman VL, Tuszynski GP, Iozzo RV *et al* (1997). The syndecan family of proteoglycans. Novel receptors mediating internalization of atherogenic lipoproteins in vitro. *J Clin Invest* **100**: 1611-1622.
- Furchgott RF, Zawadzki JV (1980). The obligatory role of endothelial cells in the relaxation of arterial smooth muscle by acetylcholine. *Nature* **288**: 373-376.
- Furukawa Y, Iwase S, Kikuchi J, Terui Y, Nakamura M, Yamada H *et al* (2000). Phosphorylation of Bcl-2 protein by CDC2 kinase during G2/M phases and its role in cell cycle regulation. *J Biol Chem* **275**: 21661-21667.
- Gagne J, Brodeur J (1972). Metabolic studies on the mechanisms of increased susceptibility of weaning rats to parathion. *Can J Physiol Pharmacol* **50**: 902-915.
- Gamat G (2007). NF-kB inhibitors: New class of drugs potentially anti-Alzheimer's disease. *Pharma Gazette*. http://www.pharmagazette.com/2007/01/nfkb_inhibitors_new_class_of_d.html.
- Garcia-Ayllon MS, Small DH, Avila J, Saez-Valero J (2011). Revisiting the Role of Acetylcholinesterase in Alzheimer's Disease: Cross-Talk with P-tau and beta-Amyloid. *Front Mol Neurosci* **4**: 22.
- Garrido JL, Godoy JA, Alvarez A, Bronfman M, Inestrosa NC (2002). Protein kinase C inhibits amyloid beta peptide neurotoxicity by acting on members of the Wnt pathway. *FASEB J* **16**: 1982-1984.
- Gearing M, Mori H, Mirra SS (1996). Abeta-peptide length and apolipoprotein E genotype in Alzheimer's disease. *Ann Neurol* **39**: 395-399.
- Genever PG, Birch MA, Brown E, Skerry TM (1999). Osteoblast-derived acetylcholinesterase: a novel mediator of cell-matrix interactions in bone? *Bone* **24**: 297-303.
- Gennari K, Brunner J, Brodbeck U (1987). Tetrameric detergent-soluble acetylcholinesterase from human caudate nucleus: subunit composition and number of active sites. *J Neurochem* **49**: 12-18.
- Gentry MK, Doctor BP (1991). In: Massoulie J, Bacou F, Barnard EA, Doctor BP, Quinn DM (eds). *Cholinesterases: Structure, Function, Mechanism, Genetics and Cell Biology*. American Chemical Society: Washington. pp 394-398.
- Getman DK, Eubanks JH, Camp S, Evans GA, Taylor P (1992). The human gene encoding acetylcholinesterase is located on the long arm of chromosome 7. *Am J Hum Genet* **51**: 170-177.
- Geula C, Mesulam MM (1989). Cortical cholinergic fibers in aging and Alzheimer's disease: a morphometric study. *Neuroscience* **33**: 469-481.

- Geula C, Mesulam MM, Tokuno H, Kuo CC (1993). Developmentally transient expression of acetylcholinesterase within cortical pyramidal neurons of the rat brain. *Brain Res Dev Brain Res* **76**: 23-31.
- Geula C, Mesulam MM (1995). Cholinesterases and the pathology of Alzheimer disease. *Alzheimer Dis Assoc Disord* **9 Suppl 2**: 23-28.
- Geula C, Mesulam MM, Kuo CC, Tokuno H (1995). Postnatal development of cortical acetylcholinesterase-rich neurons in the rat brain: permanent and transient patterns. *Exp Neurol* **134**: 157-178.
- Ghohestani RF, Li K, Rousselle P, Uitto J (2001). Molecular organization of the cutaneous basement membrane zone. *Clin Dermatol* **19**: 551-562.
- Gibot S (2004). [TREM, new receptors mediating innate immunity]. *Med Sci (Paris)* **20**: 503-505.
- Gibson R, Schlesinger S, Kornfeld S (1979). The nonglycosylated glycoprotein of vesicular stomatitis virus is temperature-sensitive and undergoes intracellular aggregation at elevated temperatures. *J Biol Chem* **254**: 3600-3607.
- Gilbert MM, Auld VJ (2005). Evolution of clams (cholinesterase-like adhesion molecules): structure and function during development. *Front Biosci* **10**: 2177-2192.
- Gillis RA, Walton DP, Quest JA, Namath IJ, Hamosh P, Dretchen KL (1988). Cardiorespiratory effects produced by activation of cholinergic muscarinic receptors on the ventral surface of the medulla. *J Pharmacol Exp Ther* **247**: 765-773.
- Giordano C, Poiana G, Augusti-Tocco G, Biagioni S (2007). Acetylcholinesterase modulates neurite outgrowth on fibronectin. *Biochem Biophys Res Commun* **356**: 398-404.
- Giordano G, White CC, McConnachie LA, Fernandez C, Kavanagh TJ, Costa LG (2006). Neurotoxicity of domoic Acid in cerebellar granule neurons in a genetic model of glutathione deficiency. *Mol Pharmacol* **70**: 2116-2126.
- Gobron S, Monnerie H, Meiniel R, Creveaux I, Lehmann W, Lamalle D *et al* (1996). SCO-spondin: a new member of the thrombospondin family secreted by the subcommissural organ is a candidate in the modulation of neuronal aggregation. *J Cell Sci* **109 (Pt 5)**: 1053-1061.
- Goedert M (2001). Alpha-synuclein and neurodegenerative diseases. *Nat Rev Neurosci* **2**: 492-501.
- Gong Y, Chang L, Viola KL, Lacor PN, Lambert MP, Finch CE *et al* (2003). Alzheimer's disease-affected brain: presence of oligomeric A beta ligands (ADDLs) suggests a molecular basis for reversible memory loss. *Proc Natl Acad Sci U S A* **100**: 10417-10422.
- Goodman CS, Tessier-Lavigne M (1997). In: Cowan WM, Jessell TM, Zipursky SL (eds). *Molecular and Cellular Approaches to Neural Development*. Oxford Univ Press: Oxford. pp 108-178.
- Graham A, Francis-West P, Brickell P, A. L (2002). The signalling molecule BMP4 mediates apoptosis in the rhombencephalic neural crest. *Nature* **372**: 684-686.
- Graham DK, Bowman GW, Dawson TL, Stanford WL, Earp HS, Snodgrass HR (1995). Cloning and developmental expression analysis of the murine c-mer tyrosine kinase. *Oncogene* **10**: 2349-2359.
- Grando SA, Horton RM, Pereira EF, Diethelm-Okita BM, George PM, Albuquerque EX *et al* (1995). A nicotinic acetylcholine receptor regulating cell adhesion and motility is expressed in human keratinocytes. *J Invest Dermatol* **105**: 774-781.

- Grando SA (1997). Biological functions of keratinocyte cholinergic receptors. *J Invest Dermatol Symp Proc* **2**: 41-48.
- Grando SA, Horton RM, Pereira EF, Diethelm-Okita BM, George PM, Albuquerque EX *et al* (1995). A nicotinic acetylcholine receptor regulating cell adhesion and motility is expressed in human keratinocytes. *J Invest Dermatol* **105**: 774-781.
- Grando SA, Kawashima K, Wessler I (2003). Introduction: the non-neuronal cholinergic system in humans. *Life Sci* **72**: 2009-2012.
- Grando SA, Pittelkow MR, Schallreuter KU (2006). Adrenergic and cholinergic control in the biology of epidermis: physiological and clinical significance. *J Invest Dermatol* **126**: 1948-1965.
- Grando SA, Kawashima K, Kirkpatrick CJ, Wessler I (2007). Recent progress in understanding the non-neuronal cholinergic system in humans. *Life Sci* **80**: 2181-2185.
- Grear KE, Ling IF, Simpson JF, Furman JL, Simmons CR, Peterson SL *et al* (2009). Expression of SORL1 and a novel SORL1 splice variant in normal and Alzheimers disease brain. *Mol Neurodegener* **4**: 46.
- Greenberg SM, Rebeck GW, Vonsattel JP, Gomez-Isla T, Hyman BT (1995). Apolipoprotein E epsilon 4 and cerebral hemorrhage associated with amyloid angiopathy. *Ann Neurol* **38**: 254-259.
- Greenfield S (1996). Non-classical actions of cholinesterases: role in cellular differentiation, tumorigenesis and Alzheimer's disease. *Neurochem Int* **28**: 485-490.
- Greenfield S, Vaux DJ (2002). Parkinson's disease, Alzheimer's disease and motor neurone disease: identifying a common mechanism. *Neuroscience* **113**: 485-492.
- Greenfield SA, Smith AD (1979). The influence of electrical stimulation of certain brain regions on the concentration of acetylcholinesterase in rabbit cerebrospinal fluid. *Brain Res* **177**: 445-459.
- Greenfield SA (1991a). A non-cholinergic function for AChE in the substantia nigra. In: Massoule J, Doctor B, Bacou F (eds). *Cholinesterases, Structure, Function, Mechanism, Genetics and Cell Biology*. Plenum: Dordrecht. pp 366-370.
- Greenfield SA (1991b). A noncholinergic action of acetylcholinesterase (AChE) in the brain: from neuronal secretion to the generation of movement. *Cell Mol Neurobiol* **11**: 55-77.
- Greenfield SA, Day T, Mann EO, Bermudez I (2004). A novel peptide modulates alpha7 nicotinic receptor responses: implications for a possible trophic-toxic mechanism within the brain. *J Neurochem* **90**: 325-331.
- Griffin WS, Stanley LC, Ling C, White L, MacLeod V, Perrot LJ *et al* (1989). Brain interleukin 1 and S-100 immunoreactivity are elevated in Down syndrome and Alzheimer disease. *Proc Natl Acad Sci U S A* **86**: 7611-7615.
- Griffiths AD, Williams SC, Hartley O, Tomlinson IM, Waterhouse P, Crosby WL *et al* (1994). Isolation of high affinity human antibodies directly from large synthetic repertoires. *EMBO J* **13**: 3245-3260.
- Grifman M, Arbel A, Ginzberg D, Glick D, Elgavish S, Shaanan B *et al* (1997). In vitro phosphorylation of acetylcholinesterase at non-consensus protein kinase A sites enhances the rate of acetylcholine hydrolysis. *Brain Res Mol Brain Res* **51**: 179-187.
- Grifman M, Galyam N, Seidman S, Soreq H (1998). Functional redundancy of acetylcholinesterase and neuroigin in mammalian neuritogenesis. *Proc Natl Acad Sci U S A* **95**: 13935-13940.

Grisaru D, Sternfeld M, Eldor A, Glick D, Soreq H (1999). Structural roles of acetylcholinesterase variants in biology and pathology. *Eur J Biochem* **264**: 672-686.

Grisaru D, Deutsch V, Shapira M, Pick M, Sternfeld M, Melamed-Book N *et al* (2001). ARP, a peptide derived from the stress-associated acetylcholinesterase variant, has hematopoietic growth promoting activities. *Mol Med* **7**: 93-105.

Grisaru D, Pick M, Perry C, Sklan EH, Almog R, Goldberg I *et al* (2006). Hydrolytic and nonenzymatic functions of acetylcholinesterase comodulate hemopoietic stress responses. *J Immunol* **176**: 27-35.

Guex N, Peitsch MC (1997). SWISS-MODEL and the Swiss-PdbViewer: an environment for comparative protein modeling. *Electrophoresis* **18**: 2714-2723.

Guillozet AL, Smiley JF, Mash DC, Mesulam MM (1997). Butyrylcholinesterase in the life cycle of amyloid plaques. *Ann Neurol* **42**: 909-918.

Guimond S, Maccarana M, Olwin BB, Lindahl U, Rapraeger AC (1993). Activating and inhibitory heparin sequences for FGF-2 (basic FGF). Distinct requirements for FGF-1, FGF-2, and FGF-4. *J Biol Chem* **268**: 23906-23914.

Guo L, Groenendyk J, Papp S, Dabrowska M, Knoblach B, Kay C *et al* (2003). Identification of an N-domain histidine essential for chaperone function in calreticulin. *J Biol Chem* **278**: 50645-50653.

Guo Q, Sebastian L, Sopher BL, Miller MW, Glazner GW, Ware CB *et al* (1999). Neurotrophic factors [activity-dependent neurotrophic factor (ADNF) and basic fibroblast growth factor (bFGF)] interrupt excitotoxic neurodegenerative cascades promoted by a PS1 mutation. *Proc Natl Acad Sci U S A* **96**: 4125-4130.

Gurwitz D, Razon N, Sokolovsky M, Soreq H (1984). Expression of muscarinic binding sites in primary human brain tumors. *Brain Res* **316**: 61-70.

Guttridge KL, Luft JC, Dawson TL, Kozłowska E, Mahajan NP, Varnum B *et al* (2002). Mer receptor tyrosine kinase signaling: prevention of apoptosis and alteration of cytoskeletal architecture without stimulation or proliferation. *J Biol Chem* **277**: 24057-24066.

Hall ZW, Kelly RB (1971). Enzymatic detachment of endplate acetylcholinesterase from muscle. *Nat New Biol* **232**: 62-63.

Hanneman E, Westerfield M (1989). Early expression of acetylcholinesterase activity in functionally distinct neurons of the zebrafish. *J Comp Neurol* **284**: 350-361.

Harbison RD (1975). Comparative toxicity of some selected pesticides in neonatal and adult rats. *Toxicol Appl Pharmacol* **32**: 443-446.

Hardman JG, Limbird LE, Goodman Gilman A (2001). Neurotransmission. *Goodman and Gilman's the pharmacological basis of therapeutics*, 10th edn. The McGraw-Hill Companies Inc: USA. pp 115-154.

Harel M, Sussman JL, Krejci E, Bon S, Chanal P, Massoulie J *et al* (1992). Conversion of acetylcholinesterase to butyrylcholinesterase: modeling and mutagenesis. *Proc Natl Acad Sci U S A* **89**: 10827-10831.

Harel M, Kleywegt GJ, Ravelli RB, Silman I, Sussman JL (1995). Crystal structure of an acetylcholinesterase-fasciculin complex: interaction of a three-fingered toxin from snake venom with its target. *Structure* **3**: 1355-1366.

- Harkany T, Abraham I, Konya C, Nyakas C, Zarandi M, Penke B *et al* (2000). Mechanisms of beta-amyloid neurotoxicity: perspectives of pharmacotherapy. *Rev Neurosci* **11**: 329-382.
- Harlow E, Lane D (1988). *Antibodies: a Laboratory Manual*. . Cold Spring Harbor Laboratory.: Cold Spring Harbor.
- Harrison D, Hussain SA, Combs AC, Ervasti JM, Yurchenco PD, Hohenester E (2007). Crystal structure and cell surface anchorage sites of laminin alpha1LG4-5. *J Biol Chem* **282**: 11573-11581.
- Hartley DM, Walsh DM, Ye CP, Diehl T, Vasquez S, Vassilev PM *et al* (1999). Protofibrillar intermediates of amyloid beta-protein induce acute electrophysiological changes and progressive neurotoxicity in cortical neurons. *J Neurosci* **19**: 8876-8884.
- Hartmann E, Kilbinger H (1974a). Occurrence of light-dependent acetylcholine concentrations in higher plants. *Experientia* **30**: 1397-1398.
- Hartmann E, Kilbinger H (1974b). Gas-liquid-chromatographic determination of light-dependent acetylcholine concentrations in moss callus. *Biochem J* **137**: 249-252.
- Hartmann U, Maurer P (2001). Proteoglycans in the nervous system--the quest for functional roles in vivo. *Matrix Biol* **20**: 23-35.
- Hatten ME (1999). Central nervous system neuronal migration. *Annu Rev Neurosci* **22**: 511-539.
- Heckers S, Geula C, Mesulam MM (1992). Acetylcholinesterase-rich pyramidal neurons in Alzheimer's disease. *Neurobiol Aging* **13**: 455-460.
- Heston LL (1977). Alzheimer's disease, trisomy 21, and myeloproliferative disorders: associations suggesting a genetic diathesis. *Science* **196**: 322-323.
- Heston LL, Mastri AR, Anderson VE, White J (1981). Dementia of the Alzheimer type. Clinical genetics, natural history, and associated conditions. *Arch Gen Psychiatry* **38**: 1085-1090.
- Hevron E, David G, Arnon A, Yaari Y (1986). Acetylcholine modulates two types of presynaptic potassium channels in vertebrate motor nerve terminals. *Neurosci Lett* **72**: 87-92.
- Heyman A, Wilkinson WE, Hurwitz BJ, Schmechel D, Sigmon AH, Weinberg T *et al* (1983). Alzheimer's disease: genetic aspects and associated clinical disorders. *Ann Neurol* **14**: 507-515.
- Hienola A, Tumova S, Kuleskiy E, Rauvala H (2006). N-syndecan deficiency impairs neural migration in brain. *J Cell Biol* **174**: 569-580.
- Hill BT, Perrin D, Kruczynski A (2000). Inhibition of RAS-targeted prenylation: protein farnesyl transferase inhibitors revisited. *Crit Rev Oncol Hematol* **33**: 7-23.
- Hirano A, Zimmerman HM (1962). Alzheimer's neurofibrillary changes. A topographic study. *Arch Neurol* **7**: 227-242.
- Hobmayer B, Rentzsch F, Kuhn K, Happel CM, von Laue CC, Snyder P *et al* (2000). WNT signalling molecules act in axis formation in the diploblastic metazoan Hydra. *Nature* **407**: 186-189.
- Hoffman MP, Nomizu M, Roque E, Lee S, Jung DW, Yamada Y *et al* (1998). Laminin-1 and laminin-2 G-domain synthetic peptides bind syndecan-1 and are involved in acinar formation of a human submandibular gland cell line. *J Biol Chem* **273**: 28633-28641.

- Hoffman MP, Engbring JA, Nielsen PK, Vargas J, Steinberg Z, Karmand AJ *et al* (2001). Cell type-specific differences in glycosaminoglycans modulate the biological activity of a heparin-binding peptide (RKRLQVQLSIRT) from the G domain of the laminin alpha1 chain. *J Biol Chem* **276**: 22077-22085.
- Holmes C, Jones SA, Greenfield SA (1995). The influence of target and non-target brain regions on the development of mid-brain dopaminergic neurons in organotypic slice culture. *Brain Res Dev Brain Res* **88**: 212-219.
- Holmes C, Jones SA, Budd TC, Greenfield SA (1997). Non-cholinergic, trophic action of recombinant acetylcholinesterase on mid-brain dopaminergic neurons. *J Neurosci Res* **49**: 207-218.
- Holmquist M (2000). Alpha/Beta-hydrolase fold enzymes: structures, functions and mechanisms. *Curr Protein Pept Sci* **1**: 209-235.
- Hopp TP, Woods KR (1983). A computer program for predicting protein antigenic determinants. *Mol Immunol* **20**: 483-489.
- Horiuchi Y, Kimura R, Kato N, Fujii T, Seki M, Endo T *et al* (2003). Evolutional study on acetylcholine expression. *Life Sci* **72**: 1745-1756.
- Hortsch M, Patel NH, Bieber AJ, Traquina ZR, Goodman CS (1990). Drosophila neurotactin, a surface glycoprotein with homology to serine esterases, is dynamically expressed during embryogenesis. *Development* **110**: 1327-1340.
- Horwich AL, Weissman JS (1997). Deadly conformations - Protein misfolding in prion disease. *Cell Press* **89**: 499-510.
- Hosea NA, Radic Z, Tsigelny I, Berman HA, Quinn DM, Taylor P (1996). Aspartate 74 as a primary determinant in acetylcholinesterase governing specificity to cationic organophosphonates. *Biochemistry* **35**: 10995-11004.
- Hosoya H, Komatsu S, Shimizu T, Inagaki M, Ikegami M, Yazaki K (1994). Phosphorylation of dynamin by cdc2 kinase. *Biochem Biophys Res Commun* **202**: 1127-1133.
- Houshmand H, Froman G, Magnusson G (1999). Use of bacteriophage T7 displayed peptides for determination of monoclonal antibody specificity and biosensor analysis of the binding reaction. *Anal Biochem* **268**: 363-370.
- Howlett DR, Jennings KH, Lee DC, Clark MS, Brown F, Wetzel R *et al* (1995). Aggregation state and neurotoxic properties of Alzheimer beta-amyloid peptide. *Neurodegeneration* **4**: 23-32.
- Hu L, Wong TP, Cote SL, Bell KF, Cuellar AC (2003). The impact of Abeta-plaques on cortical cholinergic and non-cholinergic presynaptic boutons in alzheimer's disease-like transgenic mice. *Neuroscience* **121**: 421-432.
- Huang Y (2010). Abeta-independent roles of apolipoprotein E4 in the pathogenesis of Alzheimer's disease. *Trends Mol Med* **16**: 287-294.
- Hucho F, Jarv J, Weise C (1991). Substrate-binding sites in acetylcholinesterase. *Trends Pharmacol Sci* **12**: 422-426.
- Hurwitz L, Von Hagen S, Joiner PD (1967). Acetylcholine and calcium on membrane permeability and contraction of intestinal smooth muscle. *J Gen Physiol* **50**: 1157-1172.
- Huveneers S, Danen EH (2009). Adhesion signaling - crosstalk between integrins, Src and Rho. *J Cell Sci* **122**: 1059-1069.

Hyman BT, West HL, Rebeck GW, Buldyrev SV, Mantegna RN, Ukleja M *et al* (1995). Quantitative analysis of senile plaques in Alzheimer disease: observation of log-normal size distribution and molecular epidemiology of differences associated with apolipoprotein E genotype and trisomy 21 (Down syndrome). *Proc Natl Acad Sci U S A* **92**: 3586-3590.

Ichtchenko K, Nguyen T, Sudhof TC (1996). Structures, alternative splicing, and neurexin binding of multiple neuroligins. *J Biol Chem* **271**: 2676-2682.

Inagaki J, Matsuura E, Nomizu M, Sugiura-Ogasawara M, Katano K, Kaihara K *et al* (2001). IgG anti-laminin-1 autoantibody and recurrent miscarriages. *Am J Reprod Immunol* **45**: 232-238.

Inagaki J, Kondo A, Lopez LR, Shoenfeld Y, Matsuura E (2005). Pregnancy loss and endometriosis: pathogenic role of anti-laminin-1 autoantibodies. *Ann N Y Acad Sci* **1051**: 174-184.

Inestrosa C (1988). Trophic roles of neuromuscular junction extracellular matrix constituents. In: Fernandez HL (ed). *Nerve-muscle cell trophic communication*. CRC Press: Boca Raton FL. pp 147-172

Inestrosa N, De Ferrari GV, Garrido JL, Alvarez A, Olivares GH, Barria MI *et al* (2002). Wnt signaling involvement in beta-amyloid-dependent neurodegeneration. *Neurochem Int* **41**: 341-344.

Inestrosa NC, Roberts WL, Marshall TL, Rosenberry TL (1987). Acetylcholinesterase from bovine caudate nucleus is attached to membranes by a novel subunit distinct from those of acetylcholinesterases in other tissues. *J Biol Chem* **262**: 4441-4444.

Inestrosa NC, Perelman A (1989). Distribution and anchoring of molecular forms of acetylcholinesterase. *Trends Pharmacol Sci* **10**: 325-329.

Inestrosa NC, Alvarez A, Calderon F (1996). Acetylcholinesterase is a senile plaque component that promotes assembly of amyloid beta-peptide into Alzheimer's filaments. *Mol Psychiatry* **1**: 359-361.

Inestrosa NC, Alarcon R (1998). Molecular interactions of acetylcholinesterase with senile plaques. *J Physiol Paris* **92**: 341-344.

Inestrosa NC, Toledo EM (2008). The role of Wnt signaling in neuronal dysfunction in Alzheimer's Disease. *Mol Neurodegener* **3**: 9.

Ishii T (1966). Distribution of Alzheimer's neurofibrillary changes in the brain stem and hypothalamus of senile dementia. *Acta Neuropathol* **6**: 181-187.

Ishino H, Otsuki S (1975). Frequency of Alzheimer's neurofibrillary tangles in the basal ganglia and brain-stem in Alzheimer's disease, senile dementia and the aged. *Folia Psychiatr Neurol Jpn* **29**: 279-287.

Jacobsen L, Madsen P, Jacobsen C, Nielsen MS, Gliemann J, Petersen CM (2001). Activation and functional characterization of the mosaic receptor SorLA/LR11. *J Biol Chem* **276**: 22788-22796.

Jaffe MJ (1970). Evidence for the regulation of phytochrome-mediated processes in bean roots by the neurohumor, acetylcholine. *Plant Physiol* **46**: 768-777.

Jamain S, Quach H, Betancur C, Rastam M, Colineaux C, Gillberg IC *et al* (2003). Mutations of the X-linked genes encoding neuroligins NLGN3 and NLGN4 are associated with autism. *Nat Genet* **34**: 27-29.

Jayanthi LD, Balasubramanian N, Balasubramanian AS (1992). Cholinesterases exhibiting aryl acylamidase activity in human amniotic fluid. *Clin Chim Acta* **205**: 157-166.

- Jbilo O, L'Hermite Y, Talesa V, Toutant JP, Chatonnet A (1994). Acetylcholinesterase and butyrylcholinesterase expression in adult rabbit tissues and during development. *Eur J Biochem* **225**: 115-124.
- Jedrzejczyk J, Silman I, Lai J, Barnard EA (1984). Molecular forms of acetylcholinesterase in synaptic and extrasynaptic regions of avian tonic muscle. *Neurosci Lett* **46**: 283-289.
- Jin HY, Katori M, Majima M, Sunahara N (1992). Increased secretion of glandular-kallikrein in the bronchial washings induced by intravenous injection of leukotriene C4 in guinea-pigs. *Br J Pharmacol* **105**: 632-638.
- Jin K, Peel AL, Mao XO, Xie L, Cottrell BA, Henshall DC *et al* (2004). Increased hippocampal neurogenesis in Alzheimer's disease. *Proc Natl Acad Sci U S A* **101**: 343-347.
- Johnson G, Moore SW (1999). The adhesion function on acetylcholinesterase is located at the peripheral anionic site. *Biochem Biophys Res Commun* **258**: 758-762.
- Johnson G, Moore SW (2000). Cholinesterases modulate cell adhesion in human neuroblastoma cells in vitro. *Int J Dev Neurosci* **18**: 781-790.
- Johnson G, Moore SW (2002). Catalytic antibodies with acetylcholinesterase activity. *J Immunol Methods* **269**: 13-28.
- Johnson G, Moore SW (2003). Human acetylcholinesterase binds to mouse laminin-1 and human collagen IV by an electrostatic mechanism at the peripheral anionic site. *Neurosci Lett* **337**: 37-40.
- Johnson G, Moore SW (2004). Functional idiotypic mimicry of an adhesion- and differentiation-promoting site on acetylcholinesterase. *J Cell Biochem* **91**: 999-1009.
- Johnson G, Moore SW (2006). The peripheral anionic site of acetylcholinesterase: structure, functions and potential role in rational drug design. *Curr Pharm Des* **12**: 217-225.
- Johnson G, Swart C, Moore SW (2008a). Interaction of acetylcholinesterase with the G4 domain of the laminin alpha1-chain. *Biochem J* **411**: 507-514.
- Johnson G, Swart C, Moore SW (2008b). Non-enzymatic developmental functions of acetylcholinesterase--the question of redundancy. *FEBS J* **275**: 5129-5138.
- Johnson G, Moore SW (2009). Investigations into the development of catalytic activity in anti-acetylcholinesterase idiotypic and anti-idiotypic antibodies. *J Mol Recognit* **22**: 188-196.
- Johnson JA, Wallace KB (1987). Species-related differences in the inhibition of brain acetylcholinesterase by paraoxon and malaaxon. *Toxicol Appl Pharmacol* **88**: 234-241.
- Jones SA, Holmes C, Budd TC, Greenfield SA (1995). The effect of acetylcholinesterase on outgrowth of dopaminergic neurons in organotypic slice culture of rat mid-brain. *Cell Tissue Res* **279**: 323-330.
- Kakio A, Nishimoto S, Yanagisawa K, Kozutsumi Y, Matsuzaki K (2002). Interactions of amyloid beta-protein with various gangliosides in raft-like membranes: importance of GM1 ganglioside-bound form as an endogenous seed for Alzheimer amyloid. *Biochemistry* **41**: 7385-7390.
- Kalaria RN, Kroon SN, Grahovac I, Perry G (1992). Acetylcholinesterase and its association with heparan sulphate proteoglycans in cortical amyloid deposits of Alzheimer's disease. *Neuroscience* **51**: 177-184.
- Kandel E, Schwartz J, Jessel TM (2000). *Principles of Neural Sciences*, 4th edn. McGraw-Hill: New York.

- Kaplan D, Ordentlich A, Barak D, Ariel N, Kronman C, Velan B *et al* (2001). Does "butyrylization" of acetylcholinesterase through substitution of the six divergent aromatic amino acids in the active center gorge generate an enzyme mimic of butyrylcholinesterase? *Biochemistry* **40**: 7433-7445.
- Karczmar AG (1969). Is the central cholinergic nervous system overexploited? *Fed Proc* **28**: 147-159.
- Karl F (1999). [Letter to the editor on the editorial: "Social work with the aged--Balance, crisis and prospectives" by T. Kllie and R. Schmidt: *Gerontologie und Geriatrie*, 31:301-303 (1998)]. *Z Gerontol Geriatr* **32**: 473-474.
- Karlin A (1993). Structure of nicotinic acetylcholine receptors. *Curr Opin Neurobiol* **3**: 299-309.
- Karpel R, Ben Aziz-Aloya R, Sternfeld M, Ehrlich G, Ginzberg D, Tarroni P *et al* (1994). Expression of three alternative acetylcholinesterase messenger RNAs in human tumor cell lines of different tissue origins. *Exp Cell Res* **210**: 268-277.
- Karpel R, Sternfeld M, Ginzberg D, Guhl E, Graessmann A, Soreq H (1996). Overexpression of alternative human acetylcholinesterase forms modulates process extensions in cultured glioma cells. *J Neurochem* **66**: 114-123.
- Karu AE, Bell CW, Chin TE (1995). Recombinant antibody technology. *ILAR J* 37(3). http://dels-old.nas.edu/ilar_n/ilarjournal/37_3/37_3Recombinant.shtml.
- Kasa P, Papp H, Zombori J, Mayer P, Checler F (2003). C-terminal fragments of amyloid-beta peptide cause cholinergic axonal degeneration by a toxic effect rather than by physical injury in the nondemented human brain. *Neurochem Res* **28**: 493-498.
- Kasprzak H, Salpeter MM (1985). Recovery of acetylcholinesterase at intact neuromuscular junctions after in vivo inactivation with di-isopropylfluorophosphate. *J Neurosci* **5**: 951-955.
- Kato M, Wang H, Bernfield M, Gallagher JT, Turnbull JE (1994). Cell surface syndecan-1 on distinct cell types differs in fine structure and ligand binding of its heparan sulfate chains. *J Biol Chem* **269**: 18881-18890.
- Kato T, Sasaki H, Katagiri T, Koiwai K, Youki H, Totsuka S *et al* (1991). The binding of basic fibroblast growth factor to Alzheimer's neurofibrillary tangles and senile plaques. *Neurosci Lett* **122**: 33-36.
- Katzung BG (2001). Introduction to autonomic pharmacology. *Basic and clinical pharmacology*, 8th edn. The McGraw Hill Companies, Inc: USA. pp 75-91.
- Kawashima K, Fujii T (2000). Extraneuronal cholinergic system in lymphocytes. *Pharmacol Ther* **86**: 29-48.
- Kawashima K, Fujii T (2003a). The lymphocytic cholinergic system and its biological function. *Life Sci* **72**: 2101-2109.
- Kawashima K, Fujii T (2003b). The lymphocytic cholinergic system and its contribution to the regulation of immune activity. *Life Sci* **74**: 675-696.
- Kawashima K, Fujii T (2004). Expression of non-neuronal acetylcholine in lymphocytes and its contribution to the regulation of immune function. *Front Biosci* **9**: 2063-2085.
- Kayed R, Head E, Thompson JL, McIntire TM, Milton SC, Cotman CW *et al* (2003). Common structure of soluble amyloid oligomers implies common mechanism of pathogenesis. *Science* **300**: 486-489.

- Kelly JW (1996). Alternative conformations of amyloidogenic proteins govern their behavior. *Curr Opin Struct Biol* **6**: 11-17.
- Kelly JW (1998). The alternative conformations of amyloidogenic proteins and their multi-step assembly pathways. *Curr Opin Struct Biol* **8**: 101-106.
- Kemper T (1984). Neuroanatomical and neuropathological changes in normal aging and dementia. . In: Albert ML (ed). *Clinical neurology of aging*. . Oxford University Press: New York. pp 9-52.
- Kere J (1989). Chromosome 7 long arm deletion breakpoints in preleukemia: mapping by pulsed field gel electrophoresis. *Nucleic Acids Res* **17**: 1511-1520.
- Kere J, Donis-Keller H, Ruutu T, de la Chapelle A (1989a). Chromosome 7 long-arm deletions in myeloid disorders: terminal DNA sequences are commonly conserved and breakpoints vary. *Cytogenet Cell Genet* **50**: 226-229.
- Kere J, Ruutu T, Davies KA, Roninson IB, Watkins PC, Winqvist R *et al* (1989b). Chromosome 7 long arm deletion in myeloid disorders: a narrow breakpoint region in 7q22 defined by molecular mapping. *Blood* **73**: 230-234.
- Kidokoro Y, Brass B (1985). Redistribution of acetylcholine receptors during neuromuscular junction formation in *Xenopus* cultures. *J Physiol (Paris)* **80**: 212-220.
- Kim CW, Goldberger OA, Gallo RL, Bernfield M (1994). Members of the syndecan family of heparan sulfate proteoglycans are expressed in distinct cell-, tissue-, and development-specific patterns. *Mol Biol Cell* **5**: 797-805.
- Kimbell LM, Ohno K, Engel AG, Rotundo RL (2004). C-terminal and heparin-binding domains of collagenic tail subunit are both essential for anchoring acetylcholinesterase at the synapse. *J Biol Chem* **279**: 10997-11005.
- Kimura R, Yamamoto M, Morihara T, Akatsu H, Kudo T, Kamino K *et al* (2009). SORL1 is genetically associated with Alzheimer disease in a Japanese population. *Neurosci Lett* **461**: 177-180.
- King N, Hittinger CT, Carroll SB (2003). Evolution of key cell signaling and adhesion protein families predates animal origins. *Science* **301**: 361-363.
- Kisilevsky R, Lemieux LJ, Fraser PE, Kong X, Hultin PG, Szarek WA (1995). Arresting amyloidosis in vivo using small-molecule anionic sulphonates or sulphates: implications for Alzheimer's disease. *Nat Med* **1**: 143-148.
- Klapproth H, Reinheimer T, Metzen J, Munch M, Bittinger F, Kirkpatrick CJ *et al* (1997). Non-neuronal acetylcholine, a signalling molecule synthesized by surface cells of rat and man. *Naunyn Schmiedeberg's Arch Pharmacol* **355**: 515-523.
- Knappik A, Ge L, Honegger A, Pack P, Fischer M, Wellnhofer G *et al* (2000). Fully synthetic human combinatorial antibody libraries (HuCAL) based on modular consensus frameworks and CDRs randomized with trinucleotides. *J Mol Biol* **296**: 57-86.
- Koda JE, Bernfield M (1984). Heparan sulfate proteoglycans from mouse mammary epithelial cells. Basal extracellular proteoglycan binds specifically to native type I collagen fibrils. *J Biol Chem* **259**: 11763-11770.
- Koelle WA, Koelle GB, Smyrl EG (1976). Effects of persistent selective suppression of ganglionic butyrylcholinesterase on steady state and regenerating levels of acetylcholinesterase: implications regarding

function of butyrylcholinesterase and regulation of protein synthesis. *Proc Natl Acad Sci U S A* **73**: 2936-2938.

Koenigsberger C, Chiappa S, Brimijoin S (1997). Neurite differentiation is modulated in neuroblastoma cells engineered for altered acetylcholinesterase expression. *J Neurochem* **69**: 1389-1397.

Kokenyesi R, Bernfield M (1994). Core protein structure and sequence determine the site and presence of heparan sulfate and chondroitin sulfate on syndecan-1. *J Biol Chem* **269**: 12304-12309.

Koo EH, Park L, Selkoe DJ (1993). Amyloid beta-protein as a substrate interacts with extracellular matrix to promote neurite outgrowth. *Proc Natl Acad Sci U S A* **90**: 4748-4752.

Koo EH, Squazzo SL (1994). Evidence that production and release of amyloid beta-protein involves the endocytic pathway. *J Biol Chem* **269**: 17386-17389.

Kosik KS (1992). Alzheimer's disease: a cell biological perspective. *Science* **256**: 780-783.

Kostovic I, Goldman-Rakic PS (1983). Transient cholinesterase staining in the mediodorsal nucleus of the thalamus and its connections in the developing human and monkey brain. *J Comp Neurol* **219**: 431-447.

Koudinov AR, Berezov TT, Kumar A, Koudinova NV (1998). Alzheimer's amyloid beta interaction with normal human plasma high density lipoprotein: association with apolipoprotein and lipids. *Clin Chim Acta* **270**: 75-84.

Krejci E, Duval N, Chatonnet A, Vincens P, Massoulie J (1991). Cholinesterase-like domains in enzymes and structural proteins: functional and evolutionary relationships and identification of a catalytically essential aspartic acid. *Proc Natl Acad Sci U S A* **88**: 6647-6651.

Krejci E, Thomine S, Boschetti N, Legay C, Sketelj J, Massoulie J (1997). The mammalian gene of acetylcholinesterase-associated collagen. *J Biol Chem* **272**: 22840-22847.

Krejci E (1998). The building of acetylcholinesterase collagen-tailed forms: a model. In: Doctor BP, Quinn DM, Rotundo RL, Taylor P (eds). *Cholinesterases '98'*. Plenum Publishing Corporation: New York.

Kristt DA (1979). Somatosensory cortex: acetylcholinesterase staining of barrel neuropil in the rat. *Neurosci Lett* **12**: 177-182.

Kristt DA, JV WA (1981). The origin of the acetylcholinesterase-rich afferents to layer IV of infant somatosensory cortex. A histochemical analysis following lesions. *Anat Embryol (Berl)* **163**: 31-41.

Kristt DA, Waldman JV (1982). Developmental reorganization of acetylcholinesterase-rich inputs to somatosensory cortex of the mouse. *Anat Embryol (Berl)* **164**: 331-342.

Kristt DA (1983). Acetylcholinesterase in the ventrobasal thalamus: transience and patterning during ontogenesis. *Neuroscience* **10**: 923-939.

Kristt DA (1989). Acetylcholinesterase in immature thalamic neurons: relation to afferentation, development, regulation and cellular distribution. *Neuroscience* **29**: 27-43.

Krnjevic K (2004). Synaptic mechanisms modulated by acetylcholine in cerebral cortex. *Prog Brain Res* **145**: 81-93.

Kroeze WK, Sheffler DJ, Roth BL (2003). G-protein-coupled receptors at a glance. *J Cell Sci* **116**: 4867-4869.

- Kronman C, Velan B, Marcus D, Ordentlich A, Reuveny S, Shafferman A (1995). Involvement of oligomerization, N-glycosylation and sialylation in the clearance of cholinesterases from the circulation. *Biochem J* **311** (Pt 3): 959-967.
- Kurzen H, Berger H, Jager C, Hartschuh W, Naher H, Gratchev A *et al* (2004). Phenotypical and molecular profiling of the extraneuronal cholinergic system of the skin. *J Invest Dermatol* **123**: 937-949.
- Kurzen H, Wessler I, Kirkpatrick CJ, Kawashima K, Grando SA (2007). The non-neuronal cholinergic system of human skin. *Horm Metab Res* **39**: 125-135.
- Lambert MP, Barlow AK, Chromy BA, Edwards C, Freed R, Liosatos M *et al* (1998). Diffusible, nonfibrillar ligands derived from Abeta1-42 are potent central nervous system neurotoxins. *Proc Natl Acad Sci U S A* **95**: 6448-6453.
- Lansbury PT, Jr. (1999). Evolution of amyloid: what normal protein folding may tell us about fibrillogenesis and disease. *Proc Natl Acad Sci U S A* **96**: 3342-3344.
- Lapidot-Lifson Y, Prody CA, Ginzberg D, Meytes D, Zakut H, Soreq H (1989). Coamplification of human acetylcholinesterase and butyrylcholinesterase genes in blood cells: correlation with various leukemias and abnormal megakaryocytopoiesis. *Proc Natl Acad Sci U S A* **86**: 4715-4719.
- Layer PG (1983). Comparative localization of acetylcholinesterase and pseudocholinesterase during morphogenesis of the chicken brain. *Proc Natl Acad Sci U S A* **80**: 6413-6417.
- Layer PG, Sporns O (1987). Spatiotemporal relationship of embryonic cholinesterases with cell proliferation in chicken brain and eye. *Proc Natl Acad Sci U S A* **84**: 284-288.
- Layer PG (1990). Cholinesterases preceding major tracts in vertebrate neurogenesis. *Bioessays* **12**: 415-420.
- Layer PG (1991). Cholinesterases during development of the avian nervous system. *Cell Mol Neurobiol* **11**: 7-33.
- Layer PG, Kaulich S (1991). Cranial nerve growth in birds is preceded by cholinesterase expression during neural crest cell migration and the formation of an HNK-1 scaffold. *Cell Tissue Res* **265**: 393-407.
- Layer PG, Weikert T, Willbold E (1992). Chicken retinospheroids as developmental and pharmacological in vitro models: acetylcholinesterase is regulated by its own and by butyrylcholinesterase activity. *Cell Tissue Res* **268**: 409-418.
- Layer PG, Weikert T, Alber R (1993). Cholinesterases regulate neurite growth of chick nerve cells in vitro by means of a non-enzymatic mechanism. *Cell Tissue Res* **273**: 219-226.
- Layer PG (1995). Nonclassical roles of cholinesterases in the embryonic brain and possible links to Alzheimer disease. *Alzheimer Dis Assoc Disord* **9 Suppl 2**: 29-36.
- Layer PG, Willbold E (1995). Novel functions of cholinesterases in development, physiology and disease. *Prog Histochem Cytochem* **29**: 1-94.
- Lazar M, Vigny M (1980). Modulation of the distribution of acetylcholinesterase molecular forms in a murine neuroblastoma x sympathetic ganglion cell hybrid cell line. *J Neurochem* **35**: 1067-1079.
- Le Douarin NM, Hallonet ME, Pourquie O (1994). Cell migrations and establishment of neuronal connections in the developing brain: a study using the quail-chick chimera system. *Prog Brain Res* **100**: 3-18.

- Lee E, Taussig R, Gilman AG (1992). The G226A mutant of Gs alpha highlights the requirement for dissociation of G protein subunits. *J Biol Chem* **267**: 1212-1218.
- Legay C, Bon S, Vernier P, Coussen F, Massoulie J (1993). Cloning and expression of a rat acetylcholinesterase subunit: generation of multiple molecular forms and complementarity with a Torpedo collagenic subunit. *J Neurochem* **60**: 337-346.
- Legay C (2000). Why So Many Forms of Acetylcholinesterase? *Microsc Res Tech* **49**: 56-72.
- Lemere CA, Lopera F, Kosik KS, Lendon CL, Ossa J, Saido TC *et al* (1996). The E280A presenilin 1 Alzheimer mutation produces increased A beta 42 deposition and severe cerebellar pathology. *Nat Med* **2**: 1146-1150.
- Leveugle B, Scanameo A, Ding W, Fillit H (1994). Binding of heparan sulfate glycosaminoglycan to beta-amyloid peptide: inhibition by potentially therapeutic polysulfated compounds. *Neuroreport* **5**: 1389-1392.
- Levey AI, Wainer BH, Mufson EJ, Mesulam MM (1983). Co-localization of acetylcholinesterase and choline acetyltransferase in the rat cerebrum. *Neuroscience* **9**: 9-22.
- Levitt M (1980). Effect of proline residues on protein folding. *J Mol Biol* **145**: 251-263.
- Li JP, Galvis ML, Gong F, Zhang X, Zcharia E, Metzger S *et al* (2005). In vivo fragmentation of heparan sulfate by heparanase overexpression renders mice resistant to amyloid protein A amyloidosis. *Proc Natl Acad Sci U S A* **102**: 6473-6477.
- Li Y, Camp S, Rachinsky TL, Getman D, Taylor P (1991). Gene structure of mammalian acetylcholinesterase. *J Biol Chem* **266**: 23083-23090.
- Liesi P, Kaakkola S, Dahl D, Vaheri A (1984). Laminin is induced in astrocytes of adult brain by injury. *EMBO J* **3**: 683-686.
- Liesi P, Narvanen A, Soos J, Sariola H, Snounou G (1989). Identification of a neurite outgrowth-promoting domain of laminin using synthetic peptides. *FEBS Lett* **244**: 141-148.
- Lin MT, Beal MF (2006). Mitochondrial dysfunction and oxidative stress in neurodegenerative diseases. *Nature* **443**: 787-795.
- Lindahl B, Westling C, Gimenez-Gallego G, Lindahl U, Salmivirta M (1999). Common binding sites for beta-amyloid fibrils and fibroblast growth factor-2 in heparan sulfate from human cerebral cortex. *J Biol Chem* **274**: 30631-30635.
- Linhardt RJ, Loganathan D (1990). Heparin, heparinoids and heparin oligosaccharides. In: Gebelein G (ed). *Structure and biological activities*. Plenum Press: New York. pp 135-173.
- Lipton SA, Kater SB (1989). Neurotransmitter regulation of neuronal outgrowth, plasticity and survival. *Trends Neurosci* **12**: 265-270.
- Llinas RR, Greenfield SA (1987). On-line visualization of dendritic release of acetylcholinesterase from mammalian substantia nigra neurons. *Proc Natl Acad Sci U S A* **84**: 3047-3050.
- Lockridge O, Bartels CF, Vaughan TA, Wong CK, Norton SE, Johnson LL (1987). Complete amino acid sequence of human serum cholinesterase. *J Biol Chem* **262**: 549-557.
- Lockridge O (1990). Genetic variants of human serum cholinesterase influence metabolism of the muscle relaxant succinylcholine. *Pharmacol Ther* **47**: 35-60.

- Loewi O, Navratil E (1926). Über humorale Übertragbarkeit der Herznervenwirkung. X. Mitteilung: Über das Schicksal des Vagusstoffes. *Pflug Arch ges Physiol* **214**: 678-688.
- Lotem J, Sachs L (1999). Cytokines as suppressors of apoptosis. *Apoptosis* **4**: 187-196.
- Lotti M (1991). Treatment of acute organophosphate poisoning. *Med J Aust* **154**: 51-55.
- Lowman HB, Wells JA (1993). Affinity maturation of human growth hormone by monovalent phage display. *J Mol Biol* **234**: 564-578.
- Lu FC, Jessup DC, Lavalley A (1965). Toxicity of pesticides in young versus adult rats. *Food Cosmet Toxicol* **3**: 591-596.
- Luo W, Yu QS, Kulkarni SS, Parrish DA, Holloway HW, Tweedie D *et al* (2006). Inhibition of human acetyl- and butyrylcholinesterase by novel carbamates of (-)- and (+)-tetrahydrofurobenzofuran and methanobenzodioxepine. *J Med Chem* **49**: 2174-2185.
- Luo Z, Fuentes ME, Taylor P (1994). Regulation of acetylcholinesterase mRNA stability by calcium during differentiation from myoblasts to myotubes. *J Biol Chem* **269**: 27216-27223.
- Lydic R, Baghdoyan HA (2005). Sleep, anesthesiology, and the neurobiology of arousal state control. *Anesthesiology* **103**: 1268-1295.
- Lydic R, Baghdoyan HA (2008). Acetylcholine modulates sleep and wakefulness: a synaptic perspective. In: Monti JM, Pandi-Perumal SR, Sinton CM (eds). *Neurochemistry of sleep and wakefulness*. Cambridge UP: New York. pp 109-143.
- Lyles JM, Silman I, Barnard EA (1979). Developmental changes in levels and forms of cholinesterases in muscles of normal and dystrophic chickens. *J Neurochem* **33**: 727-738.
- Ma B, Shatsky M, Wolfson HJ, Nussinov R (2002). Multiple diverse ligands binding at a single protein site: a matter of pre-existing populations. *Protein Sci* **11**: 184-197.
- Mack A, Robitzki A (2000). The key role of butyrylcholinesterase during neurogenesis and neural disorders: an antisense-5'butyrylcholinesterase-DNA study. *Prog Neurobiol* **60**: 607-628.
- MacPhee-Quigley K, Vedvick TS, Taylor P, Taylor SS (1986). Profile of the disulfide bonds in acetylcholinesterase. *J Biol Chem* **261**: 13565-13570.
- Magdesian MH, Carvalho MM, Mendes FA, Saraiva LM, Juliano MA, Juliano L *et al* (2008). Amyloid-beta binds to the extracellular cysteine-rich domain of Frizzled and inhibits Wnt/beta-catenin signaling. *J Biol Chem* **283**: 9359-9368.
- Mahoney TS, Weyrich AS, Dixon DA, McIntyre T, Prescott SM, Zimmerman GA (2001). Cell adhesion regulates gene expression at translational checkpoints in human myeloid leukocytes. *Proc Natl Acad Sci U S A* **98**: 10284-10289.
- Malany S, Baker N, Verweyst M, Medhekar R, Quinn DM, Velan B *et al* (1999). Theoretical and experimental investigations of electrostatic effects on acetylcholinesterase catalysis and inhibition. *Chem Biol Interact* **119-120**: 99-110.
- Malinger G, Zakut H, Soreq H (1989). Cholinoceptive properties of human primordial, preantral, and antral oocytes: in situ hybridization and biochemical evidence for expression of cholinesterase genes. *J Mol Neurosci* **1**: 77-84.

Mallender WD, Szegletes T, Rosenberry TL (2000). Acetylthiocholine binds to asp74 at the peripheral site of human acetylcholinesterase as the first step in the catalytic pathway. *Biochemistry* **39**: 7753-7763.

Mappouras DG, Philippou G, Haralambous S, Tzartos SJ, Balafas A, Souvatzoglou A *et al* (1995). Antibodies to acetylcholinesterase cross-reacting with thyroglobulin in myasthenia gravis and Graves's disease. *Clin Exp Immunol* **100**: 336-343.

Marchot P, Khelif A, Ji YH, Mansuelle P, Bougis PE (1993). Binding of 125I-fasciculin to rat brain acetylcholinesterase. The complex still binds diisopropyl fluorophosphate. *J Biol Chem* **268**: 12458-12467.

Mark RJ, Keller JN, Kruman I, Mattson MP (1997). Basic FGF attenuates amyloid beta-peptide-induced oxidative stress, mitochondrial dysfunction, and impairment of Na⁺/K⁺-ATPase activity in hippocampal neurons. *Brain Res* **756**: 205-214.

Marks JD, Hoogenboom HR, Bonnert TP, McCafferty J, Griffiths AD, Winter G (1991). By-passing immunization. Human antibodies from V-gene libraries displayed on phage. *J Mol Biol* **222**: 581-597.

Marneros AG, Olsen BR (2005). Physiological role of collagen XVIII and endostatin. *FASEB J* **19**: 716-728.

Martins-Green M, Erickson CA (1988). Patterns of cholinesterase staining during neural crest cell morphogenesis in mouse and chick embryos. *J Exp Zool* **247**: 62-68.

Masson P, Xie W, Froment MT, Levitsky V, Fortier PL, Albaret C *et al* (1999). Interaction between the peripheral site residues of human butyrylcholinesterase, D70 and Y332, in binding and hydrolysis of substrates. *Biochim Biophys Acta* **1433**: 281-293.

Massoulie J, Bon S (1982). The molecular forms of cholinesterase and acetylcholinesterase in vertebrates. *Annu Rev Neurosci* **5**: 57-106.

Massoulie J, Bon S (2006). The C-terminal T peptide of cholinesterases: structure, interactions, and influence on protein folding and secretion. *J Mol Neurosci* **30**: 233-236.

Massoulié J, Bon S, Anselmet A, Chatel JM, Coussen F, Duval N *et al* (199b). In: Shafferman A, Velan B (eds). *Multidisciplinary Approaches to Cholinesterase Functions*. Plenum Press: New York. pp 17-24.

Massoulié J, Toutant JP (1988). Vertebrate cholinesterases: structure and types of interaction. *Handb Exp Pharmac* **86**: 167-224.

Massoulié J, Sussman JL, Doctor BP, Soreq H, Velan B, Cygler M *et al* (1992a). Recommendations for nomenclature in cholinesterases. In: Shafferman A, Velan B (eds). *Multidisciplinary Approaches to Cholinesterase Functions*. Plenum Press: New York. pp 285-288.

Massoulié J, Pezzementi L, Bon S, Krejci E, Vallette FM (1993). Molecular and cellular biology of cholinesterases. *Prog Neurobiol* **41**: 31-91.

Massoulié J, Anselmet A, Bon S, Krejci E, Legay C, Morel N *et al* (1999). The polymorphism of acetylcholinesterase: post-translational processing, quaternary associations and localization. *Chem Biol Interact* **119-120**: 29-42.

Massoulié J (2002). The origin of the molecular diversity and functional anchoring of cholinesterases. *Neurosignals* **11**: 130-143.

Massoulié J, Bon S, Perrier N, Falasca C (2005). The C-terminal peptides of acetylcholinesterase: cellular trafficking, oligomerization and functional anchoring. *Chem Biol Interact* **157-158**: 3-14.

- Mattson MP (1988). Neurotransmitters in the regulation of neuronal cytoarchitecture. *Brain Res* **472**: 179-212.
- Mattson MP (1992). Calcium as sculptor and destroyer of neural circuitry. *Exp Gerontol* **27**: 29-49.
- Matzuk MM, Keene JL, Boime I (1989). Site specificity of the chorionic gonadotropin N-linked oligosaccharides in signal transduction. *J Biol Chem* **264**: 2409-2414.
- McClellan JS, Coblenz WB, Sapp M, Rulewicz G, Gaines DI, Hawkins A *et al* (1998). cDNA cloning, in vitro expression, and biochemical characterization of cholinesterase 1 and cholinesterase 2 from amphioxus--comparison with cholinesterase 1 and cholinesterase 2 produced in vivo. *Eur J Biochem* **258**: 419-429.
- McCubbin WD, Kay CM, Narindrasorasak S, Kisilevsky R (1988). Circular-dichroism studies on two murine serum amyloid A proteins. *Biochem J* **256**: 775-783.
- McDuff T, Sumi SM (1985). Subcortical degeneration in Alzheimer's disease. *Neurology* **35**: 123-126.
- McLaurin J, Franklin T, Zhang X, Deng J, Fraser PE (1999). Interactions of Alzheimer amyloid-beta peptides with glycosaminoglycans effects on fibril nucleation and growth. *Eur J Biochem* **266**: 1101-1110.
- McMahan UJ, Sanes JR, Marshall LM (1978). Cholinesterase is associated with the basal lamina at the neuromuscular junction. *Nature* **271**: 172-174.
- Mecham RP (1991). Laminin receptors. *Annu Rev Cell Biol* **7**: 71-91.
- Meinzel O, Meinzel A (2007). The complex multidomain organization of SCO-spondin protein is highly conserved in mammals. *Brain Res Rev* **53**: 321-327.
- Meir A, Ginsburg S, Butkevich A, Kachalsky SG, Kaiserman I, Ahdut R *et al* (1999). Ion channels in presynaptic nerve terminals and control of transmitter release. *Physiol Rev* **79**: 1019-1088.
- Melo JB, Agostinho P, Oliveira CR (2003). Involvement of oxidative stress in the enhancement of acetylcholinesterase activity induced by amyloid beta-peptide. *Neurosci Res* **45**: 117-127.
- Mendel B, Mundell DB, Rudney H (1943). Studies on cholinesterase: 3. Specific tests for true cholinesterase and pseudo-cholinesterase. *Biochem J* **37**: 473-476.
- Menez A (1991). In: Harvey AL (ed). *Snake Toxins*. Pergamon Press: New York. pp 35-90.
- Merhi M, Raynal H, Cahuzac E, Vinson F, Cravedi JP, Gamet-Payrastré L (2007). Occupational exposure to pesticides and risk of hematopoietic cancers: meta-analysis of case-control studies. *Cancer Causes Control* **18**: 1209-1226.
- Merlini G, Bellotti V (2003). Molecular mechanisms of amyloidosis. *N Engl J Med* **349**: 583-596.
- Mesulam M (1995). Cholinesterases in Alzheimer's disease. In: Balasubramanian AS, Doctror BP, Massoulie J, Shafferman A, Silman I, Taylor P (eds). *Enzymes of the cholinesterase family*. . Plenum Press: New York.
- Mesulam MM, Mufson EJ, Levey AI, Wainer BH (1984). Atlas of cholinergic neurons in the forebrain and upper brainstem of the macaque based on monoclonal choline acetyltransferase immunohistochemistry and acetylcholinesterase histochemistry. *Neuroscience* **12**: 669-686.
- Mesulam MM, Asuncion Moran M (1987). Cholinesterases within neurofibrillary tangles related to age and Alzheimer's disease. *Ann Neurol* **22**: 223-228.

Mesulam MM, Geula C (1988a). Nucleus basalis (Ch4) and cortical cholinergic innervation in the human brain: observations based on the distribution of acetylcholinesterase and choline acetyltransferase. *J Comp Neurol* **275**: 216-240.

Mesulam MM, Geula C (1988b). Acetylcholinesterase-rich pyramidal neurons in the human neocortex and hippocampus: absence at birth, development during the life span, and dissolution in Alzheimer's disease. *Ann Neurol* **24**: 765-773.

Mesulam MM, Guillozet A, Shaw P, Levey A, Duysen EG, Lockridge O (2002). Acetylcholinesterase knockouts establish central cholinergic pathways and can use butyrylcholinesterase to hydrolyze acetylcholine. *Neuroscience* **110**: 627-639.

Metz B (1958). Brain acetylcholinesterase and a respiratory reflex. *Am J Physiol* **192**: 101-105.

Metz CN, Tracey KJ (2005). It takes nerve to dampen inflammation. *Nat Immunol* **6**: 756-757.

Mikawa YG, Maruyama IN, Brenner S (1996). Surface display of proteins on bacteriophage lambda heads. *J Mol Biol* **262**: 21-30.

Miner JH, Patton BL, Lentz SI, Gilbert DJ, Snider WD, Jenkins NA *et al* (1997). The laminin alpha chains: expression, developmental transitions, and chromosomal locations of alpha1-5, identification of heterotrimeric laminins 8-11, and cloning of a novel alpha3 isoform. *J Cell Biol* **137**: 685-701.

Miner JH, Yurchenco PD (2004). Laminin functions in tissue morphogenesis. *Annu Rev Cell Dev Biol* **20**: 255-284.

Misery L (2004). Nicotine effects on skin: are they positive or negative? *Exp Dermatol* **13**: 665-670.

Mohammadi M, Olsen SK, Ibrahim OA (2005). Structural basis for fibroblast growth factor receptor activation. *Cytokine Growth Factor Rev* **16**: 107-137.

Moller HJ (1999). Reappraising neurotransmitter-based strategies. *Eur Neuropsychopharmacol* **9 Suppl 2**: S53-59.

Monji A, Tashiro K, Yoshida I, Tashiro N (1998). Laminin inhibits Abeta42 fibril formation in vitro. *Brain Res* **788**: 187-190.

Monteau R, Morin D, Hilaire G (1990). Acetylcholine and central chemosensitivity: in vitro study in the newborn rat. *Respir Physiol* **81**: 241-253.

Montenegro MF, Nieto-Ceron S, Ruiz-Espejo F, Paez de la Cadena M, Rodriguez-Berrocal FJ, Vidal CJ (2005). Cholinesterase activity and enzyme components in healthy and cancerous human colorectal sections. *Chem Biol Interact* **157-158**: 429-430.

Montenegro MF, Moral-Naranjo MT, Paez de la Cadena M, Campoy FJ, Munoz-Delgado E, Vidal CJ (2008). The level of aryl acylamidase activity displayed by human butyrylcholinesterase depends on its molecular distribution. *Chem Biol Interact* **175**: 336-339.

Moon RT, Kohn AD, De Ferrari GV, Kaykas A (2004). WNT and beta-catenin signalling: diseases and therapies. *Nat Rev Genet* **5**: 691-701.

Moreno NP, Tharp BZ (2007). Message in a neuron. *Baylor College of Medicine: Brain Chemistry Teacher's Guide*. www.BioEdOnline.org.

- Mori F, Lai CC, Fusi F, Giacobini E (1995). Cholinesterase inhibitors increase secretion of APPs in rat brain cortex. *Neuroreport* **6**: 633-636.
- Morris AJ, Malbon CC (1999). Physiological regulation of G protein-linked signaling. *Physiol Rev* **79**: 1373-1430.
- Morrison RS, Kinoshita Y, Johnson MD, Ghatan S (2000). Neuronal Survival and Cell Death Signaling Pathways. Madame Curie Bioscience Database: Austin TX.
- Mortensen SR, Hooper MJ, Padilla S (1998). Rat brain acetylcholinesterase activity: developmental profile and maturational sensitivity to carbamate and organophosphorus inhibitors. *Toxicology* **125**: 13-19.
- Mueller BK (1999). Growth cone guidance: first steps towards a deeper understanding. *Annu Rev Neurosci* **22**: 351-388.
- Munoz-Torrero D (2008). Acetylcholinesterase inhibitors as disease-modifying therapies for Alzheimer's disease. *Curr Med Chem* **15**: 2433-2455.
- Munoz FJ, Aldunate R, Inestrosa NC (1999). Peripheral binding site is involved in the neurotrophic activity of acetylcholinesterase. *Neuroreport* **10**: 3621-3625.
- Murakoshi T, Otsuka M (1985). Respiratory reflexes in an isolated brainstem-lung preparation of the newborn rat: possible involvement of gamma-aminobutyric acid and glycine. *Neurosci Lett* **62**: 63-68.
- Murtomaki S, Risteli J, Risteli L, Koivisto UM, Johansson S, Liesi P (1992). Laminin and its neurite outgrowth-promoting domain in the brain in Alzheimer's disease and Down's syndrome patients. *J Neurosci Res* **32**: 261-273.
- Mutero A, Camp S, Taylor P (1995). Promoter elements of the mouse acetylcholinesterase gene. Transcriptional regulation during muscle differentiation. *J Biol Chem* **270**: 1866-1872.
- Nakamura S, Kawashima S, Nakano S, Tsuji T, Araki W (1990). Subcellular distribution of acetylcholinesterase in Alzheimer's disease: abnormal localization and solubilization. *J Neural Transm Suppl* **30**: 13-23.
- Namba Y, Tomonaga M, Kawasaki H, Otomo E, Ikeda K (1991). Apolipoprotein E immunoreactivity in cerebral amyloid deposits and neurofibrillary tangles in Alzheimer's disease and kuru plaque amyloid in Creutzfeldt-Jakob disease. *Brain Res* **541**: 163-166.
- Naslund J, Haroutunian V, Mohs R, Davis KL, Davies P, Greengard P *et al* (2000). Correlation between elevated levels of amyloid beta-peptide in the brain and cognitive decline. *JAMA* **283**: 1571-1577.
- Nattie EE, Li AH (1990). Ventral medulla sites of muscarinic receptor subtypes involved in cardiorespiratory control. *J Appl Physiol* **69**: 33-41.
- Navaratnam DS, Priddle JD, McDonald B, Esiri MM, Robinson JR, Smith AD (1991). Anomalous molecular form of acetylcholinesterase in cerebrospinal fluid in histologically diagnosed Alzheimer's disease. *Lancet* **337**: 447-450.
- Neary D, Snowden JS, Mann DM, Bowen DM, Sims NR, Northen B *et al* (1986). Alzheimer's disease: a correlative study. *J Neurol Neurosurg Psychiatry* **49**: 229-237.
- Nicolet Y, Lockridge O, Masson P, Fontecilla-Camps JC, Nachon F (2003). Crystal structure of human butyrylcholinesterase and of its complexes with substrate and products. *J Biol Chem* **278**: 41141-41147.

- Nissim A, Hoogenboom HR, Tomlinson IM, Flynn G, Midgley C, Lane D *et al* (1994). Antibody fragments from a 'single pot' phage display library as immunochemical reagents. *EMBO J* **13**: 692-698.
- Nitsch RM, Slack BE, Wurtman RJ, Growdon JH (1992). Release of Alzheimer amyloid precursor derivatives stimulated by activation of muscarinic acetylcholine receptors. *Science* **258**: 304-307.
- Nitsch RM, Rossner S, Albrecht C, Mayhaus M, Enderich J, Schliebs R *et al* (1998). Muscarinic acetylcholine receptors activate the acetylcholinesterase gene promoter. *J Physiol Paris* **92**: 257-264.
- Nolte HJ, Rosenberry TL, Neumann E (1980). Effective charge on acetylcholinesterase active sites determined from the ionic strength dependence of association rate constants with cationic ligands. *Biochemistry* **19**: 3705-3711.
- Nomizu M, Kim WH, Yamamura K, Utani A, Song SY, Otaka A *et al* (1995). Identification of cell binding sites in the laminin alpha 1 chain carboxyl-terminal globular domain by systematic screening of synthetic peptides. *J Biol Chem* **270**: 20583-20590.
- Noonan DM, Fulle A, Valente P, Cai S, Horigan E, Sasaki M *et al* (1991). The complete sequence of perlecan, a basement membrane heparan sulfate proteoglycan, reveals extensive similarity with laminin A chain, low density lipoprotein-receptor, and the neural cell adhesion molecule. *J Biol Chem* **266**: 22939-22947.
- Noureddine H, Schmitt C, Liu W, Garbay C, Massoulie J, Bon S (2007). Assembly of acetylcholinesterase tetramers by peptidic motifs from the proline-rich membrane anchor, PRiMA: competition between degradation and secretion pathways of heteromeric complexes. *J Biol Chem* **282**: 3487-3497.
- Nurcombe V, Aumailley M, Timpl R, Edgar D (1989). The high-affinity binding of laminin to cells. Assignment of a major cell-binding site to the long arm of laminin and of a latent cell-binding site to its short arms. *Eur J Biochem* **180**: 9-14.
- Offe K, Dodson SE, Shoemaker JT, Fritz JJ, Gearing M, Levey AI *et al* (2006). The lipoprotein receptor LR11 regulates amyloid beta production and amyloid precursor protein traffic in endosomal compartments. *J Neurosci* **26**: 1596-1603.
- Olivera S, Rodriguez-Ithurralde D, Henley JM (2003). Acetylcholinesterase promotes neurite elongation, synapse formation, and surface expression of AMPA receptors in hippocampal neurones. *Mol Cell Neurosci* **23**: 96-106.
- Ollis DL, Cheah E, Cygler M, Dijkstra B, Frolov F, Franken SM *et al* (1992). The alpha/beta hydrolase fold. *Protein Eng* **5**: 197-211.
- Olson PF, Fessler LI, Nelson RE, Sterne RE, Campbell AG, Fessler JH (1990). Glutactin, a novel Drosophila basement membrane-related glycoprotein with sequence similarity to serine esterases. *EMBO J* **9**: 1219-1227.
- Ordentlich A, Barak D, Kronman C, Flashner Y, Leitner M, Segall Y *et al* (1993). Dissection of the human acetylcholinesterase active center determinants of substrate specificity. Identification of residues constituting the anionic site, the hydrophobic site, and the acyl pocket. *J Biol Chem* **268**: 17083-17095.
- Ordentlich A, Barak D, Kronman C, Ariel N, Segall Y, Velan B *et al* (1998). Functional characteristics of the oxyanion hole in human acetylcholinesterase. *J Biol Chem* **273**: 19509-19517.
- Orum H, Andersen PS, Oster A, Johansen LK, Riise E, Bjornvad M *et al* (1993). Efficient method for constructing comprehensive murine Fab antibody libraries displayed on phage. *Nucleic Acids Res* **21**: 4491-4498.

- Ott P, Lustig A, Brodbeck U, Rosenbusch JP (1982). Acetylcholinesterase from human erythrocytes membranes: dimers as functional units. *FEBS Lett* **138**: 187-189.
- Otto CM, Niagro F, McGraw RA, Rawlings CA (1997). Production of polyclonal antibodies to feline tumor necrosis factor. *Clin Diagn Lab Immunol* **4**: 487-490.
- Oudega M, Marani E (1990). Acetylcholinesterase in the developing rat spinal cord: an enzyme histochemical study. *Eur J Morphol* **28**: 379-393.
- Pakaski M, Kasa P (2003). Role of acetylcholinesterase inhibitors in the metabolism of amyloid precursor protein. *Curr Drug Targets CNS Neurol Disord* **2**: 163-171.
- Pang YP (2006). Novel acetylcholinesterase target site for malaria mosquito control. *PLoS One* **1**: e58.
- Pang YP, Ekstrom F, Polsinelli GA, Gao Y, Rana S, Hua DH *et al* (2009). Selective and irreversible inhibitors of mosquito acetylcholinesterases for controlling malaria and other mosquito-borne diseases. *PLoS One* **4**: e6851.
- Paraoanu LE (2004). Binding partners for mouse acetylcholinesterase in the central nervous system. Doctor thesis, Technische Universität Darmstadt, Darmstadt
- Paraoanu LE, Layer PG (2008). Acetylcholinesterase in cell adhesion, neurite growth and network formation. *FEBS J* **275**: 618-624.
- Paulus JM, Maigne J, Keyhani E (1981). Mouse megakaryocytes secrete acetylcholinesterase. *Blood* **58**: 1100-1106.
- Peifer M, Polakis P (2000). Wnt signaling in oncogenesis and embryogenesis--a look outside the nucleus. *Science* **287**: 1606-1609.
- Peng HB, Xie H, Rossi SG, Rotundo RL (1999). Acetylcholinesterase clustering at the neuromuscular junction involves perlecan and dystroglycan. *J Cell Biol* **145**: 911-921.
- Pera M, Roman S, Ratia M, Camps P, Munoz-Torrero D, Colombo L *et al* (2006). Acetylcholinesterase triggers the aggregation of PrP 106-126. *Biochem Biophys Res Commun* **346**: 89-94.
- Perrier AL, Massoulie J, Krejci E (2002). PRiMA: the membrane anchor of acetylcholinesterase in the brain. *Neuron* **33**: 275-285.
- Perry C, Sklan EH, Birikh K, Shapira M, Trejo L, Eldor A *et al* (2002). Complex regulation of acetylcholinesterase gene expression in human brain tumors. *Oncogene* **21**: 8428-8441.
- Perry C, Soreq H (2004). Organophosphate risk of leukemogenesis. *Leuk Res* **28**: 905-906.
- Perry EK, Tomlinson BE, Blessed G, Bergmann K, Gibson PH, Perry RH (1978). Correlation of cholinergic abnormalities with senile plaques and mental test scores in senile dementia. *Br Med J* **2**: 1457-1459.
- Perry EK (1980). The cholinergic system in old age and Alzheimer's disease. *Age Ageing* **9**: 1-8.
- Perry EK (1986). The cholinergic hypothesis--ten years on. *Br Med Bull* **42**: 63-69.
- Perry G, Siedlak SL, Richey P, Kawai M, Cras P, Kaloria RN *et al* (1991). Association of heparan sulfate proteoglycan with the neurofibrillary tangles of Alzheimer's disease. *J Neurosci* **11**: 3679-3683.

Perutz MF (1999). Glutamine repeats and neurodegenerative diseases: molecular aspects. *Trends Biochem Sci* **24**: 58-63.

Pezzementi L, Sutherland D, Sanders M, Soong W, Milner D, McClellan JS *et al* (1998). In: B.P. D, P. T, D.M. Q, R.L. R, M.K. G (eds). *Structure and Function of Cholinesterases and Related Proteins*. Plenum Press: New York. pp 105-110.

Pezzementi L, Chatonnet A (2010). Evolution of cholinesterases in the animal kingdom. *Chem Biol Interact* **187**: 27-33.

Pike CJ, Walencewicz AJ, Glabe CG, Cotman CW (1991). In vitro aging of beta-amyloid protein causes peptide aggregation and neurotoxicity. *Brain Res* **563**: 311-314.

Pini A, Viti F, Santucci A, Carnemolla B, Zardi L, Neri P *et al* (1998). Design and use of a phage display library. Human antibodies with subnanomolar affinity against a marker of angiogenesis eluted from a two-dimensional gel. *J Biol Chem* **273**: 21769-21776.

Podlisny MB, Walsh DM, Amarante P, Ostaszewski BL, Stimson ER, Maggio JE *et al* (1998). Oligomerization of endogenous and synthetic amyloid beta-protein at nanomolar levels in cell culture and stabilization of monomer by Congo red. *Biochemistry* **37**: 3602-3611.

Polsinelli GA, Singh SK, Mishra RK, Suranyi R, Ragsdale DW, Pang YP *et al* (2010). Insect-specific irreversible inhibitors of acetylcholinesterase in pests including the bed bug, the eastern yellowjacket, German and American cockroaches, and the confused flour beetle. *Chem Biol Interact* **187**: 142-147.

Polvikoski T, Sulkava R, Haltia M, Kainulainen K, Vuorio A, Verkkoniemi A *et al* (1995). Apolipoprotein E, dementia, and cortical deposition of beta-amyloid protein. *N Engl J Med* **333**: 1242-1247.

Pope C, Karanth S, Liu J (2005). Pharmacology and toxicology of cholinesterase inhibitors: uses and misuses of a common mechanism of action. *Env Toxicol Pharm* **19**: 433-446.

Porschke D, Creminon C, Cousin X, Bon C, Sussman J, Silman I (1996). Electrooptical measurements demonstrate a large permanent dipole moment associated with acetylcholinesterase. *Biophys J* **70**: 1603-1608.

Povlsen GK, Ditlevsen DK, Berezin V, Bock E (2003). Intracellular signaling by the neural cell adhesion molecule. *Neurochem Res* **28**: 127-141.

Price DL, Whitehouse PJ, Struble RG, Coyle JT, Clark AW, DeLong MR *et al* (1982). Alzheimer's disease and Down's syndrome. *Ann N Y Acad Sci* **396**: 145-164.

Prody CA, Zevin-Sonkin D, Gnatt A, Goldberg O, Soreq H (1987). Isolation and characterization of full-length cDNA clones coding for cholinesterase from fetal human tissues. *Proc Natl Acad Sci U S A* **84**: 3555-3559.

Quinn DM (1987). Acetylcholinesterase: Enzyme structure, reaction dynamics, and virtual transition states. *Chem Rev* **87**: 955-979.

Quon D, Catalano R, Cordell B (1990). Fibroblast growth factor induces beta-amyloid precursor mRNA in glial but not neuronal cultured cells. *Biochem Biophys Res Commun* **167**: 96-102.

Racchi M, Mazzucchelli M, Porrello E, Lanni C, Govoni S (2004). Acetylcholinesterase inhibitors: novel activities of old molecules. *Pharmacol Res* **50**: 441-451.

- Rachinsky TL, Camp S, Li Y, Ekstrom TJ, Newton M, Taylor P (1990). Molecular cloning of mouse acetylcholinesterase: tissue distribution of alternatively spliced mRNA species. *Neuron* **5**: 317-327.
- Radic Z, Reiner E, Taylor P (1991). Role of the peripheral anionic site on acetylcholinesterase: inhibition by substrates and coumarin derivatives. *Mol Pharmacol* **39**: 98-104.
- Radic Z, Gibney G, Kawamoto S, MacPhee-Quigley K, Bongiorno C, Taylor P (1992). Expression of recombinant acetylcholinesterase in a baculovirus system: kinetic properties of glutamate 199 mutants. *Biochemistry* **31**: 9760-9767.
- Radic Z, Duran R, Vellom DC, Li Y, Cervenansky C, Taylor P (1994). Site of fasciculin interaction with acetylcholinesterase. *J Biol Chem* **269**: 11233-11239.
- Raineri M, P. M (1986). Preliminary evidence for a cholinergic-like system in lichen morphogenesis. *Histochem J* **18**: 647-657.
- Rajendran L, Honsho M, Zahn TR, Keller P, Geiger KD, Verkade P *et al* (2006). Alzheimer's disease beta-amyloid peptides are released in association with exosomes. *Proc Natl Acad Sci U S A* **103**: 11172-11177.
- Rao A, Harms KJ, Craig AM (2000). Neuroligation: building synapses around the neurexin-neuroigin link. *Nat Neurosci* **3**: 747-749.
- Rapraeger AC, Bernfield M (1983). Heparan sulfate proteoglycans from mouse mammary epithelial cells. A putative membrane proteoglycan associates quantitatively with lipid vesicles. *J Biol Chem* **258**: 3632-3636.
- Raufman JP, Cheng K, Zimniak P (2003). Activation of muscarinic receptor signaling by bile acids: physiological and medical implications. *Dig Dis Sci* **48**: 1431-1444.
- Razon N, Soreq H, Roth E, Bartal A, Silman I (1984). Characterization of activities and forms of cholinesterases in human primary brain tumors. *Exp Neurol* **84**: 681-695.
- Rebeck GW, Reiter JS, Strickland DK, Hyman BT (1993). Apolipoprotein E in sporadic Alzheimer's disease: allelic variation and receptor interactions. *Neuron* **11**: 575-580.
- Rebeck GW, Harr SD, Strickland DK, Hyman BT (1995). Multiple, diverse senile plaque-associated proteins are ligands of an apolipoprotein E receptor, the alpha 2-macroglobulin receptor/low-density-lipoprotein receptor-related protein. *Ann Neurol* **37**: 211-217.
- Reineke U, Sabat R, Misselwitz R, Welfle H, Volk HD, Schneider-Mergener J (1999). A synthetic mimic of a discontinuous binding site on interleukin-10. *Nat Biotechnol* **17**: 271-275.
- Renaudon B, Bois P, Bescond J, Lenfant J (1997). Acetylcholine modulates I(f) and IK(ACh) via different pathways in rabbit sino-atrial node cells. *J Mol Cell Cardiol* **29**: 969-975.
- Richard BL, Nomizu M, Yamada Y, Kleinman HK (1996). Identification of synthetic peptides derived from laminin alpha1 and alpha2 chains with cell type specificity for neurite outgrowth. *Exp Cell Res* **228**: 98-105.
- Ripoll DR, Faerman CH, Axelsen PH, Silman I, Sussman JL (1993). An electrostatic mechanism for substrate guidance down the aromatic gorge of acetylcholinesterase. *Proc Natl Acad Sci U S A* **90**: 5128-5132.
- Ritchie DW, Kemp GJ (2000). Protein docking using spherical polar Fourier correlations. *Proteins* **39**: 178-194.

Ritchie DW (2008). Recent progress and future directions in protein-protein docking. *Curr Protein Pept Sci* **9**: 1-15.

Rizzuto R, Pinton P, Ferrari D, Chami M, Szabadkai G, Magalhaes PJ *et al* (2003). Calcium and apoptosis: facts and hypotheses. *Oncogene* **22**: 8619-8627.

Robertson RT, Tijerina AA, Gallivan ME (1985). Transient patterns of acetylcholinesterase activity in visual cortex of the rat: normal development and the effects of neonatal monocular enucleation. *Brain Res* **353**: 203-214.

Robertson RT (1987). A morphogenic role for transiently expressed acetylcholinesterase in developing thalamocortical systems? *Neurosci Lett* **75**: 259-264.

Robertson RT, Mostamand F (1988). Development of 'non-specific' cholinesterase-containing neurons in the dorsal thalamus of the rat. *Brain Res* **469**: 43-60.

Robertson RT, Mostamand F, Kageyama GH, Gallardo KA, Yu J (1991). Primary auditory cortex in the rat: transient expression of acetylcholinesterase activity in developing geniculocortical projections. *Brain Res Dev Brain Res* **58**: 81-95.

Robertson RT, Yu J (1993). Acetylcholinesterase and Neural Development: New Tricks for an Old Dog? *News Physiol Sci* **8**: 266-272.

Rosenberry TL (1975). Catalysis by acetylcholinesterase: evidence that the rate-limiting step for acylation with certain substrates precedes general acid-base catalysis. *Proc Natl Acad Sci U S A* **72**: 3834-3838.

Rosenmann H, Meiner Z, Kahana E, Aladjem Z, Friedman G, Ben-Yehuda A *et al* (2004). An association study of a polymorphism in the heparan sulfate proteoglycan gene (perlecan, HSPG2) and Alzheimer's disease. *Am J Med Genet B Neuropsychiatr Genet* **128B**: 123-125.

Ross LS, Parrett T, Easter SS, Jr. (1992). Axonogenesis and morphogenesis in the embryonic zebrafish brain. *J Neurosci* **12**: 467-482.

Rossi SG, Rotundo RL (1993). Localization of "non-extracTable" acetylcholinesterase to the vertebrate neuromuscular junction. *J Biol Chem* **268**: 19152-19159.

Rossi SG, Rotundo RL (1996). Transient interactions between collagen-tailed acetylcholinesterase and sulfated proteoglycans prior to immobilization on the extracellular matrix. *J Biol Chem* **271**: 1979-1987.

Rossier J (1977). Choline acetyltransferase: a review with special reference to its cellular and subcellular localization. *Int Rev Neurobiol* **20**: 283-337.

Rotundo RL, Rossi SG, Anglister L (1997). Transplantation of quail collagen-tailed acetylcholinesterase molecules onto the frog neuromuscular synapse. *J Cell Biol* **136**: 367-374.

Rubino S, Mann SKO, Hori RT, Pinko C, Firtel RA (1989). Molecular analysis of a developmentally regulated gene required for dictyostelium aggregation. *Dev Biol* **131**: 27-36.

Saez-Valero J, Sberna G, McLean CA, Masters CL, Small DH (1997). Glycosylation of acetylcholinesterase as diagnostic marker for Alzheimer's disease. *Lancet* **350**: 929.

Saez-Valero J, Sberna G, McLean CA, Small DH (1999). Molecular isoform distribution and glycosylation of acetylcholinesterase are altered in brain and cerebrospinal fluid of patients with Alzheimer's disease. *J Neurochem* **72**: 1600-1608.

- Saffell JL, Walsh FS, Doherty P (1992). Direct activation of second messenger pathways mimics cell adhesion molecule-dependent neurite outgrowth. *J Cell Biol* **118**: 663-670.
- Sanan DA, Weisgraber KH, Russell SJ, Mahley RW, Huang D, Saunders A *et al* (1994). Apolipoprotein E associates with beta amyloid peptide of Alzheimer's disease to form novel monofibrils. Isoform apoE4 associates more efficiently than apoE3. *J Clin Invest* **94**: 860-869.
- Sane DH, Reh TA, Harris WA (2000). *Development of the Nervous System* Academic: San Diego.
- Sargent MS, Weremowicz S, Rein MS, Morton CC (1994). Translocations in 7q22 define a critical region in uterine leiomyomata. *Cancer Genet Cytogenet* **77**: 65-68.
- Sasaki T, Knyazev PG, Cheburkin Y, Gohring W, Tisi D, Ullrich A *et al* (2002). Crystal structure of a C-terminal fragment of growth arrest-specific protein Gas6. Receptor tyrosine kinase activation by laminin G-like domains. *J Biol Chem* **277**: 44164-44170.
- Sastry BV, Sadavongvivad C (1978). Cholinergic systems in non-nervous tissues. *Pharmacol Rev* **30**: 65-132.
- Sastry BV, Janson VE, Chaturvedi AK (1981). Inhibition of human sperm motility by inhibitors of choline acetyltransferase. *J Pharmacol Exp Ther* **216**: 378-384.
- Sastry PB, Krishnamurty A (1978). Acetylcholine synthesis and release in isolated and perfused single cotyledon of human placenta. *Indian J Med Res* **68**: 867-879.
- Saunders AJ, Tanzi RE (2003). Welcome to the complex disease world. Alpha2-macroglobulin and Alzheimer's disease. *Exp Neurol* **184**: 50-53.
- Saunders S, Bernfield M (1988). Cell surface proteoglycan binds mouse mammary epithelial cells to fibronectin and behaves as a receptor for interstitial matrix. *J Cell Biol* **106**: 423-430.
- Sayle RA, Milner-White EJ (1995). RASMOL: biomolecular graphics for all. *Trends Biochem Sci* **20**: 374.
- Sberna G, Saez-Valero J, Beyreuther K, Masters CL, Small DH (1997). The amyloid beta-protein of Alzheimer's disease increases acetylcholinesterase expression by increasing intracellular calcium in embryonal carcinoma P19 cells. *J Neurochem* **69**: 1177-1184.
- Sberna G, Saez-Valero J, Li QX, Czech C, Beyreuther K, Masters CL *et al* (1998). Acetylcholinesterase is increased in the brains of transgenic mice expressing the C-terminal fragment (CT100) of the beta-amyloid protein precursor of Alzheimer's disease. *J Neurochem* **71**: 723-731.
- Sblattero D, Bradbury A (2000). Exploiting recombination in single bacteria to make large phage antibody libraries. *Nat Biotechnol* **18**: 75-80.
- Schapiro MB, Kumar A, White B (1989). Alzheimer's disease (AD) in mosaic/translocation Down's syndrome (DS) without mental retardation. *Neurology* **39**: 169.
- Schatz CR, Geula C, Mesulam M (1990). Competitive substrate inhibition in the histochemistry of cholinesterase activity in Alzheimer's disease. *Neurosci Lett* **117**: 56-61.
- Scheiffele P, Fan J, Choih J, Fetter R, Serafini T (2000). Neuroligin expressed in nonneuronal cells triggers presynaptic development in contacting axons. *Cell* **101**: 657-669.
- Scherzer CR, Offe K, Gearing M, Rees HD, Fang G, Heilman CJ *et al* (2004). Loss of apolipoprotein E receptor LR11 in Alzheimer disease. *Arch Neurol* **61**: 1200-1205.

Scheuner D, Eckman C, Jensen M, Song X, Citron M, Suzuki N *et al* (1996). Secreted amyloid beta-protein similar to that in the senile plaques of Alzheimer's disease is increased in vivo by the presenilin 1 and 2 and APP mutations linked to familial Alzheimer's disease. *Nat Med* **2**: 864-870.

Schlaggar BL, De Carlos JA, O'Leary DD (1993). Acetylcholinesterase as an early marker of the differentiation of dorsal thalamus in embryonic rats. *Brain Res Dev Brain Res* **75**: 19-30.

Schlereth T, Birklein F, an Haack K, Schiffmann S, Kilbinger H, Kirkpatrick CJ *et al* (2006). In vivo release of non-neuronal acetylcholine from the human skin as measured by dermal microdialysis: effect of botulinum toxin. *Br J Pharmacol* **147**: 183-187.

Schmechel DE, Saunders AM, Strittmatter WJ, Crain BJ, Hulette CM, Joo SH *et al* (1993). Increased amyloid beta-peptide deposition in cerebral cortex as a consequence of apolipoprotein E genotype in late-onset Alzheimer disease. *Proc Natl Acad Sci U S A* **90**: 9649-9653.

Schneider H, Muhle C, Pacho F (2007). Biological function of laminin-5 and pathogenic impact of its deficiency. *Eur J Cell Biol* **86**: 701-717.

Schnepf A, Komp Lindgren P, Hulsmann H, Kroger S, Paulsson M, Hartmann U (2005). Mouse testican-2. Expression, glycosylation, and effects on neurite outgrowth. *J Biol Chem* **280**: 11274-11280.

Scholl FG, Scheiffele P (2003). Making connections: cholinesterase-domain proteins in the CNS. *Trends Neurosci* **26**: 618-624.

Schroeder CE, Steinschneider M, Javitt DC, Tenke CE, Givre SJ, Mehta AD *et al* (1995). Localization of ERP generators and identification of underlying neural processes. *Electroencephalogr Clin Neurophysiol Suppl* **44**: 55-75.

Schumacher M, Camp S, Maulet Y, Newton M, MacPhee-Quigley K, Taylor SS *et al* (1986). Primary structure of Torpedo californica acetylcholinesterase deduced from its cDNA sequence. *Nature* **319**: 407-409.

Schupf N, Kapell D, Lee JH, Ottman R, Mayeux R (1994). Increased risk of Alzheimer's disease in mothers of adults with Down's syndrome. *Lancet* **344**: 353-356.

Scott JK, Smith GP (1990). Searching for peptide ligands with an epitope library. *Science* **249**: 386-390.

Seidman S, Sternfeld M, Ben Aziz-Aloya R, Timberg R, Kaufer-Nachum D, Soreq H (1995). Synaptic and epidermal accumulations of human acetylcholinesterase are encoded by alternative 3'-terminal exons. *Mol Cell Biol* **15**: 2993-3002.

Seilheimer B, Bohrmann B, Bondolfi L, Muller F, Stuber D, Dobeli H (1997). The toxicity of the Alzheimer's beta-amyloid peptide correlates with a distinct fiber morphology. *J Struct Biol* **119**: 59-71.

Selkoe DJ (1995). The Swedish mutation causes early-onset Alzheimer's disease by beta-secretase cleavage within the secretory pathway. *Nat Med* **1**: 1291-1296.

Selkoe DJ (1996). Amyloid beta-protein and the genetics of Alzheimer's disease. *J Biol Chem* **271**: 18295-18298.

Selkoe DJ (2001). Alzheimer's disease: genes, proteins, and therapy. *Physiol Rev* **81**: 741-766.

Selkoe DJ (2002). Alzheimer's disease is a synaptic failure. *Science* **298**: 789-791.

Selleck SB (2000). Proteoglycans and pattern formation: sugar biochemistry meets developmental genetics. *Trends Genet* **16**: 206-212.

- Semba K, Araki K, Li Z, Matsumoto K, Suzuki M, Nakagata N *et al* (2006). A novel murine gene, Sickletail, linked to the Danforth's short tail locus, is required for normal development of the intervertebral disc. *Genetics* **172**: 445-456.
- Semenkovich CF, Luo CC, Nakanishi MK, Chen SH, Smith LC, Chan L (1990). In vitro expression and site-specific mutagenesis of the cloned human lipoprotein lipase gene. Potential N-linked glycosylation site asparagine 43 is important for both enzyme activity and secretion. *J Biol Chem* **265**: 5429-5433.
- Shafferman A, Kronman C, Flashner Y, Leitner M, Grosfeld H, Ordentlich A *et al* (1992). Mutagenesis of human acetylcholinesterase. Identification of residues involved in catalytic activity and in polypeptide folding. *J Biol Chem* **267**: 17640-17648.
- Shafferman A, Ordentlich A, Barak D, Kronman C, Ber R, Bino T *et al* (1994). Electrostatic attraction by surface charge does not contribute to the catalytic efficiency of acetylcholinesterase. *EMBO J* **13**: 3448-3455.
- Shafferman A, Barak D, Kaplan D, Ordentlich A, Kronman C, Velan B (2005). Functional requirements for the optimal catalytic configuration of the AChE active center. *Chem Biol Interact* **157-158**: 123-131.
- Shao XM, Feldman JL (2000). Acetylcholine modulates respiratory pattern: effects mediated by M3-like receptors in preBotzinger complex inspiratory neurons. *J Neurophysiol* **83**: 1243-1252.
- Sharma KV, Bigbee JW (1998). Acetylcholinesterase antibody treatment results in neurite detachment and reduced outgrowth from cultured neurons: further evidence for a cell adhesive role for neuronal acetylcholinesterase. *J Neurosci Res* **53**: 454-464.
- Sharma KV, Koenigsberger C, Brimijoin S, Bigbee JW (2001). Direct evidence for an adhesive function in the noncholinergic role of acetylcholinesterase in neurite outgrowth. *J Neurosci Res* **63**: 165-175.
- Sheets MD, Amersdorfer P, Finnern R, Sargent P, Lindquist E, Schier R *et al* (1998). Efficient construction of a large nonimmune phage antibody library: the production of high-affinity human single-chain antibodies to protein antigens. *Proc Natl Acad Sci U S A* **95**: 6157-6162.
- Sherrington R, Rogaev EI, Liang Y, Rogaeva EA, Levesque G, Ikeda M *et al* (1995). Cloning of a gene bearing missense mutations in early-onset familial Alzheimer's disease. *Nature* **375**: 754-760.
- Shi J, Tai K, McCammon JA, Taylor P, Johnson DA (2003). Nanosecond dynamics of the mouse acetylcholinesterase cys69-cys96 omega loop. *J Biol Chem* **278**: 30905-30911.
- Shibata F, Takagi Y, Kitajima M, Kuroda T, Omura T (1993). Molecular cloning and characterization of a human carboxylesterase gene. *Genomics* **17**: 76-82.
- Shin MH, Lee EG, Lee SH, Lee YS, Son H (2002). Neural cell adhesion molecule (NCAM) promotes the differentiation of hippocampal precursor cells to a neuronal lineage, especially to a glutamatergic neural cell type. *Exp Mol Med* **34**: 401-410.
- Shivers BD, Hilbich C, Multhaup G, Salbaum M, Beyreuther K, Seeburg PH (1988). Alzheimer's disease amyloidogenic glycoprotein: expression pattern in rat brain suggests a role in cell contact. *EMBO J* **7**: 1365-1370.
- Shobab LA, Hsiung GY, Feldman HH (2005). Cholesterol in Alzheimer's disease. *Lancet Neurol* **4**: 841-852.
- Sidiropoulou E, Sachana M, Flaskos J, Harris W, Hargreaves AJ, Woldehiwet Z (2009). Diazinon oxon affects the differentiation of mouse N2a neuroblastoma cells. *Arch Toxicol* **83**: 373-380.

Sigrist CJ, Cerutti L, de Castro E, Langendijk-Genevaux PS, Bulliard V, Bairoch A *et al* (2010). PROSITE, a protein domain database for functional characterization and annotation. *Nucleic Acids Res* **38**: D161-166.

Silman I, Sussman JL (2008). Acetylcholinesterase: How is structure related to function? *Chem Biol Interact* **175**: 3-10.

Silow M, Oliveberg M (1997). Transient aggregates in protein folding are easily mistaken for folding intermediates. *Proc Natl Acad Sci U S A* **94**: 6084-6086.

Silver A (1974). *The Biology of Cholinesterases*. North Holland Publishing Company: Amsterdam.

Simmons LK, May PC, Tomaselli KJ, Rydel RE, Fuson KS, Brigham EF *et al* (1994). Secondary structure of amyloid beta peptide correlates with neurotoxic activity in vitro. *Mol Pharmacol* **45**: 373-379.

Sims NR, Bowen DM, Smith CC, Flack RH, Davison AN, Snowden JS *et al* (1980). Glucose metabolism and acetylcholine synthesis in relation to neuronal activity in Alzheimer's disease. *Lancet* **1**: 333-336.

Siow NL, Choi RC, Cheng AW, Jiang JX, Wan DC, Zhu SQ *et al* (2002). A cyclic AMP-dependent pathway regulates the expression of acetylcholinesterase during myogenic differentiation of C2C12 cells. *J Biol Chem* **277**: 36129-36136.

Sipe JD (1994). Amyloidosis. *Crit Rev Clin Lab Sci* **31**: 325-354.

Sirvio J (1999). Strategies that support declining cholinergic neurotransmission in Alzheimer's disease patients. *Gerontology* **45 Suppl 1**: 3-14.

Small DH, Ismael Z, Chubb IW (1987). Acetylcholinesterase exhibits trypsin-like and metalloexopeptidase-like activity in cleaving a model peptide. *Neuroscience* **21**: 991-995.

Small DH (1988). Serum acetylcholinesterase possesses trypsin-like and carboxypeptidase B-like activity. *Neurosci Lett* **95**: 307-312.

Small DH (1990). Non-cholinergic actions of acetylcholinesterases: proteases regulating cell growth and development? *Trends Biochem Sci* **15**: 213-216.

Small DH, Nurcombe V, Moir R, Michaelson S, Monard D, Beyreuther K *et al* (1992). Association and release of the amyloid protein precursor of Alzheimer's disease from chick brain extracellular matrix. *J Neurosci* **12**: 4143-4150.

Small DH, Reed G, Whitefield B, Nurcombe V (1995). Cholinergic regulation of neurite outgrowth from isolated chick sympathetic neurons in culture. *J Neurosci* **15**: 144-151.

Small DH, Michaelson S, Sberna G (1996). Non-classical actions of cholinesterases: role in cellular differentiation, tumorigenesis and Alzheimer's disease. *Neurochem Int* **28**: 453-483.

Smallman BN, Maneckjee A (1981). The synthesis of acetylcholine by plants. *Biochem J* **194**: 361-364.

Smith AD, Cuello AC (1984). Alzheimer's disease and acetylcholinesterase-containing neurons. *Lancet* **1**: 513.

Smith GP (1985). Filamentous fusion phage: novel expression vectors that display cloned antigens on the virion surface. *Science* **228**: 1315-1317.

Snow AD, Kisilevsky R (1985). Temporal relationship between glycosaminoglycan accumulation and amyloid deposition during experimental amyloidosis. A histochemical study. *Lab Invest* **53**: 37-44.

- Snow AD, Mar H, Nochlin D, Kimata K, Kato M, Suzuki S *et al* (1988). The presence of heparan sulfate proteoglycans in the neuritic plaques and congophilic angiopathy in Alzheimer's disease. *Am J Pathol* **133**: 456-463.
- Snow AD, Mar H, Nochlin D, Kresse H, Wight TN (1992). Peripheral distribution of dermatan sulfate proteoglycans (decorin) in amyloid-containing plaques and their presence in neurofibrillary tangles of Alzheimer's disease. *J Histochem Cytochem* **40**: 105-113.
- Snyder SW, Ladror US, Wade WS, Wang GT, Barrett LW, Matayoshi ED *et al* (1994). Amyloid-beta aggregation: selective inhibition of aggregation in mixtures of amyloid with different chain lengths. *Biophys J* **67**: 1216-1228.
- Soderlind E, Strandberg L, Jirholt P, Kobayashi N, Alexeiva V, Aberg AM *et al* (2000). Recombining germline-derived CDR sequences for creating diverse single-framework antibody libraries. *Nat Biotechnol* **18**: 852-856.
- Song H, Poo M (2001). The cell biology of neuronal navigation. *Nat Cell Biol* **3**: E81-88.
- Song HH, Shi W, Xiang YY, Filmus J (2005). The loss of glypican-3 induces alterations in Wnt signaling. *J Biol Chem* **280**: 2116-2125.
- Song P, Sekhon HS, Jia Y, Keller JA, Blusztajn JK, Mark GP *et al* (2003). Acetylcholine is synthesized by and acts as an autocrine growth factor for small cell lung carcinoma. *Cancer Res* **63**: 214-221.
- Sorensen K, Gentinetta R, Brodbeck U (1982). An amphiphile-dependent form of human brain caudate nucleus acetylcholinesterase: purification and properties. *J Neurochem* **39**: 1050-1060.
- Soreq H, Malinger G, Zakut H (1987). Expression of cholinesterase genes in human oocytes revealed by in-situ hybridization. *Hum Reprod* **2**: 689-693.
- Soreq H, Ben-Aziz R, Prody CA, Seidman S, Gnat A, Neville L *et al* (1990). Molecular cloning and construction of the coding region for human acetylcholinesterase reveals a G + C-rich attenuating structure. *Proc Natl Acad Sci U S A* **87**: 9688-9692.
- Soreq H, Zakut H (1993). *Human Cholinesterases and Anticholinesterases*. Academic Press: San Diego, USA.
- Soreq H, Patinkin D, Lev-Lehman E, Grifman M, Ginzberg D, Eckstein F *et al* (1994). Antisense oligonucleotide inhibition of acetylcholinesterase gene expression induces progenitor cell expansion and suppresses hematopoietic apoptosis ex vivo. *Proc Natl Acad Sci U S A* **91**: 7907-7911.
- Soreq H, Seidman S (2001). Acetylcholinesterase — new roles for an old actor. *Nat Rev Neuro* **2**: 294-302.
- Soreq H, Yirmiya R, Cohen O, Glick D (2005). Acetylcholinesterase as a window onto stress responses. In: Steckler T, Kalin NH, Reul JM (eds). *Handbook of Stress and the Brain*. Elsevier: Amsterdam. pp 585–608.
- Sorrentino G, Bonavita V (2007). Neurodegeneration and Alzheimer's disease: the lesson from tauopathies. *Neurol Sci* **28**: 63-71.
- Spring J, Goldberger OA, Jenkins NA, Gilbert DJ, Copeland NG, Bernfield M (1994a). Mapping of the syndecan genes in the mouse: linkage with members of the myc gene family. *Genomics* **21**: 597-601.
- Spring J, Paine-Saunders SE, Hynes RO, Bernfield M (1994b). Drosophila syndecan: conservation of a cell-surface heparan sulfate proteoglycan. *Proc Natl Acad Sci U S A* **91**: 3334-3338.

- Srivatsan M, Peretz B (1997). Acetylcholinesterase promotes regeneration of neurites in cultured adult neurons of Aplysia. *Neuroscience* **77**: 921-931.
- Stedman E, Easson LH (1932). Choline-esterase. An enzyme present in the blood-serum of the horse. *Biochem J* **26**: 2056-2066.
- Stephenson J, Czepulkowski B, Hirst W, Mufti GJ (1996). Deletion of the acetylcholinesterase locus at 7q22 associated with myelodysplastic syndromes (MDS) and acute myeloid leukaemia (AML). *Leuk Res* **20**: 235-241.
- Steriade M, McCarley RW (2005). *Brain control of wakefulness and sleep, Ed 2*. Plenum Press: New York.
- Sternfeld M, Ming G, Song H, Sela K, Timberg R, Poo M *et al* (1998). Acetylcholinesterase enhances neurite growth and synapse development through alternative contributions of its hydrolytic capacity, core protein, and variable C termini. *J Neurosci* **18**: 1240-1249.
- Stipp CS, Litwack ED, Lander AD (1994). Cerebroglycan: an integral membrane heparan sulfate proteoglycan that is unique to the developing nervous system and expressed specifically during neuronal differentiation. *J Cell Biol* **124**: 149-160.
- Strickland DK, Ashcom JD, Williams S, Burgess WH, Migliorini M, Argraves WS (1990). Sequence identity between the alpha 2-macroglobulin receptor and low density lipoprotein receptor-related protein suggests that this molecule is a multifunctional receptor. *J Biol Chem* **265**: 17401-17404.
- Strittmatter WJ, Saunders AM, Schmechel D, Pericak-Vance M, Enghild J, Salvesen GS *et al* (1993). Apolipoprotein E: high-avidity binding to beta-amyloid and increased frequency of type 4 allele in late-onset familial Alzheimer disease. *Proc Natl Acad Sci U S A* **90**: 1977-1981.
- Struble RG, Cork LC, Whitehouse PJ, Price DL (1982). Cholinergic innervation in neuritic plaques. *Science* **216**: 413-415.
- Sugita S, Saito F, Tang J, Satz J, Campbell K, Sudhof TC (2001). A stoichiometric complex of neuexins and dystroglycan in brain. *J Cell Biol* **154**: 435-445.
- Sugiyama JE, Glass DJ, Yancopoulos GD, Hall ZW (1997). Laminin-induced acetylcholine receptor clustering: an alternative pathway. *J Cell Biol* **139**: 181-191.
- Sussman JL, Harel M, Frolov F, Oefner C, Goldman A, Toker L *et al* (1991). Atomic structure of acetylcholinesterase from *Torpedo californica*: a prototypic acetylcholine-binding protein. *Science* **253**: 872-879.
- Sussman JL, Silman I (1992). Acetylcholinesterase: structure and use as a model for specific cation-protein interactions. *Curr Opin Struct Biol* **2**: 729-721.
- Suzuki N, Cheung TT, Cai XD, Odaka A, Otvos L, Jr., Eckman C *et al* (1994). An increased percentage of long amyloid beta protein secreted by familial amyloid beta protein precursor (beta APP717) mutants. *Science* **264**: 1336-1340.
- Suzuki N, Yokoyama F, Nomizu M (2005). Functional sites in the laminin alpha chains. *Connect Tissue Res* **46**: 142-152.
- Swillens S, Ludgate M, Mercken L, Dumont JE, Vassart G (1986). Analysis of sequence and structure homologies between thyroglobulin and acetylcholinesterase: possible functional and clinical significance. *Biochem Biophys Res Commun* **137**: 142-148.

- Tago H, Maeda T, McGeer PL, Kimura H (1992). Butyrylcholinesterase-rich neurons in rat brain demonstrated by a sensitive histochemical method. *J Comp Neurol* **325**: 301-312.
- Takacs Z, Wilhelmsen KC (2001). Snake alpha-neurotoxin binding site on the Egyptian cobra (*Naja haje*) nicotinic acetylcholine receptor is conserved. *Mol Biol Evol* **18**: 1800-1809.
- Takashima A, Murayama M, Murayama O, Kohno T, Honda T, Yasutake K *et al* (1998). Presenilin 1 associates with glycogen synthase kinase-3beta and its substrate tau. *Proc Natl Acad Sci U S A* **95**: 9637-9641.
- Talesa VN (2001). Acetylcholinesterase in Alzheimer's disease. *Mech Ageing Dev* **122**: 1961-1969.
- Tan RC, Truong TN, McCammon JA, Sussman JL (1993). Acetylcholinesterase: electrostatic steering increases the rate of ligand binding. *Biochemistry* **32**: 401-403.
- Tan SY, Pepys MB (1994). Amyloidosis. *Histopathology* **25**: 403-414.
- Taylor P (1991). The cholinesterases. *J Biol Chem* **266**: 4025-4028.
- Taylor P, Radic Z (1994). The cholinesterases: from genes to proteins. *Annu Rev Pharmacol Toxicol* **34**: 281-320.
- Tennyson VM, Brzin M (1970). The appearance of acetylcholinesterase in the dorsal root neuroblast of the rabbit embryo. A study by electron microscope cytochemistry and microgasometric analysis with the magnetic diver. *J Cell Biol* **46**: 64-80.
- Terzi E, Holzemann G, Seelig J (1997). Interaction of Alzheimer beta-amyloid peptide(1-40) with lipid membranes. *Biochemistry* **36**: 14845-14852.
- Tessier-Lavigne M, Goodman CS (1996). The molecular biology of axon guidance. *Science* **274**: 1123-1133.
- Timmerman P, Beld J, Puijk WC, Meloen RH (2005). Rapid and quantitative cyclization of multiple peptide loops onto synthetic scaffolds for structural mimicry of protein surfaces. *Chembiochem* **6**: 821-824.
- Timmerman P, Puijk WC, Meloen RH (2007). Functional reconstruction and synthetic mimicry of a conformational epitope using CLIPS technology. *J Mol Recognit* **20**: 283-299.
- Timpl R (1996). Macromolecular organization of basement membranes. *Curr Opin Cell Biol* **8**: 618-624.
- Timpl R, Brown JC (1996). Supramolecular assembly of basement membranes. *Bioessays* **18**: 123-132.
- Tkachenko E, Rhodes JM, Simons M (2005). Syndecans: new kids on the signaling block. *Circ Res* **96**: 488-500.
- Toutant JP, Massoulie J (1987). Acetylcholinesterase. In mammalian ectoenzymes. . In: J. TAJaKA (ed). *Acetylcholinesterase. In mammalian ectoenzymes*. . Elsevier: Amsterdam. pp 289-328.
- Tovchigrechko A, Vakser IA (2006). GRAMM-X public web server for protein-protein docking. *Nucleic Acids Res* **34**: W310-314.
- Tsai JH, Waldman AS, Nowick JS (1999). Two new beta-strand mimics. *Bioorg Med Chem* **7**: 29-38.
- Tsim KW, Randall WR, Barnard EA (1988). Synaptic acetylcholinesterase of chicken muscle changes during development from a hybrid to a homogeneous enzyme. *EMBO J* **7**: 2451-2456.

- Tsutsui-Kimura I, Ohmura Y, Izumi T, Yamaguchi T, Yoshida T, Yoshioka M (2010). Endogenous acetylcholine modulates impulsive action via alpha4beta2 nicotinic acetylcholine receptors in rats. *Eur J Pharmacol* **641**: 148-153.
- Tung EK, Choi RC, Siow NL, Jiang JX, Ling KK, Simon J *et al* (2004). P2Y2 receptor activation regulates the expression of acetylcholinesterase and acetylcholine receptor genes at vertebrate neuromuscular junctions. *Mol Pharmacol* **66**: 794-806.
- Tzu J, Marinkovich MP (2008). Bridging structure with function: structural, regulatory, and developmental role of laminins. *Int J Biochem Cell Biol* **40**: 199-214.
- Valera S, Ballivet M, Bertrand D (1992). Progesterone modulates a neuronal nicotinic acetylcholine receptor. *Proc Natl Acad Sci U S A* **89**: 9949-9953.
- Van Crielinge W, Beyaert R (1999). Yeast two-hybrid: State of the art. *Biological Procedures Online* 2(1). www.biologicalprocedures.com.
- Varner JA, Cheresch DA (1996). Integrins and cancer. *Curr Opin Cell Biol* **8**: 724-730.
- Vaughan TJ, Williams AJ, Pritchard K, Osbourn JK, Pope AR, Earnshaw JC *et al* (1996). Human antibodies with sub-nanomolar affinities isolated from a large non-immunized phage display library. *Nat Biotechnol* **14**: 309-314.
- Velan B, Kronman C, Ordentlich A, Flashner Y, Leitner M, Cohen S *et al* (1993). N-glycosylation of human acetylcholinesterase: effects on activity, stability and biosynthesis. *Biochem J* **296** (Pt 3): 649-656.
- Vellom DC, Radic Z, Li Y, Pickering NA, Camp S, Taylor P (1993). Amino acid residues controlling acetylcholinesterase and butyrylcholinesterase specificity. *Biochemistry* **32**: 12-17.
- Venkatraman J, Shankaramma SC, Balaram P (2001). Design of folded peptides. *Chem Rev* **101**: 3131-3152.
- Vickers JC, Dickson TC, Adlard PA, Saunders HL, King CE, McCormack G (2000). The cause of neuronal degeneration in Alzheimer's disease. *Prog Neurobiol* **60**: 139-165.
- Vidal CJ (2005). Expression of cholinesterases in brain and non-brain tumours. *Chem Biol Interact* **157-158**: 227-232.
- Vignaud A, Fougerousse F, Mouisel E, Bertrand C, Bonafos B, Molgo J *et al* (2008). Genetic ablation of acetylcholinesterase alters muscle function in mice. *Chem Biol Interact* **175**: 129-130.
- Vlodavsky I, Friedmann Y (2001). Molecular properties and involvement of heparanase in cancer metastasis and angiogenesis. *J Clin Invest* **108**: 341-347.
- Wallace BG (1986). Aggregating factor from Torpedo electric organ induces patches containing acetylcholine receptors, acetylcholinesterase, and butyrylcholinesterase on cultured myotubes. *J Cell Biol* **102**: 783-794.

